OBTENÇÃO E ANÁLISE DE METABOLITOS E INTERMEDIÁRIOS DE SÍNTESE

ESTUDOS DE CORRELAÇÃO ENTRE ESTRUTURA, PROPRIEDADES FÍSICO-QUÍMICAS E ACTIVIDADE BIOLÓGICA

Nuno Jorge da Silva Pereira Milhazes

Faculdade de Farmácia da Universidade do Porto

2006

OBTENÇÃO E ANÁLISE DE METABOLITOS E INTERMEDIÁRIOS DE SÍNTESE

ESTUDOS DE CORRELAÇÃO ENTRE ESTRUTURA, PROPRIEDADES FÍSICO-QUÍMICAS E ACTIVIDADE BIOLÓGICA

FACULDADE DE FARMACIA
U. P.
BIBLIOTECA
Data 04/04/2007
Reg. 4945
Cota

FFD
MIL
4945

Nuno Jorge da Silva Pereira Milhazes

Faculdade de Farmácia da Universidade do Porto

2006

U.PORTO
FACULDADE DE FARMÁCIA
UNIVERSIDADE DO PORTO

Dissertação de candidatura à obtenção do grau de Doutor em Química Farmacêutica submetida à Faculdade de Farmácia da Universidade do Porto

Os estudos efectuados no âmbito desta dissertação tiveram lugar, em sua grande parte, no Centro de Estudos de Química Orgânica, Fitoquímica e Farmacologia (CEQOFFUP)/Serviço de Química Orgânica da Faculdade de Farmácia da Universidade do Porto. Outros estudos, não menos importantes, foram realizados nos Serviços de Microbiologia e de Toxicologia da Faculdade de Farmácia da Universidade do Porto, nos Departamentos de Química da Faculdade de Ciências da Universidade do Porto e da Universidade de Aveiro e nos Departamentos de Bioquímica das Faculdades de Ciências e Tecnologia e de Medicina da Universidade de Coimbra.

Alguns trabalhos foram ainda realizados em estreita colaboração com o Departamento de Farmacologia e Toxicologia da Universidade do Texas em Austin, nos Estados Unidos da América, e com o Departamento de Química Orgânica da Universidade de Santiago de Compostela.

Esta dissertação teve o apoio financeiro da Fundação para a Ciência e a Tecnologia (Programa PRAXIS XXI/BD/18520/98).

Os resultados apresentados nesta dissertação fazem parte das seguintes publicações, resumos e comunicações (ao abrigo do artigo 8º do decreto-lei nº 388/70):

Publicações

1. Remião, F.; Milhazes, N.; Borges, F.; Carvalho, F.; Bastos, M.L.; Lemos-Amado, F.; Domingues, P.; Ferrer-Correia, A. (2003) Synthesis and analysis of aminochromes by HPLC-photodiode array. Adrenochrome evaluation in rat blood. *Biomed. Chromatogr.* 17: 6-13.
2. Calheiros, R.; Milhazes, N.; Borges, F.; Marques, M.P.M. (2004) β-Nitrostyrene derivatives – a conformational study by combined Raman spectroscopy and ab initio MO calculations. *J. Mol. Struct.* 692: 91-106.
3. Carvalho, M.; Milhazes, N.; Remião, F.; Borges, F.; Fernandes, E.; Amado, F.; Monks, T.J.; Carvalho, F.; Bastos, M.L. (2004) Hepatotoxicity of 3,4-methylenedioxyamphetamine and α-methyldopamine in isolated rat hepatocytes: formation of glutathione conjugates. *Arch. Toxicol.* 78: 16-24.
4. Milhazes, N.; Borges, F.; Calheiros, R.; Marques, M.P.M. (2004) Identification of synthetic precursors of amphetamine-like drugs using Raman spectroscopy and *ab initio* calculations: β-methyl-β-nitrostyrene derivatives. *Analyst* 129: 1106-1117.
5. Milhazes, N.; Calheiros, R.; Marques, M.P.M.; Garrido, J.; Cordeiro, M.N.D.S.; Rodrigues, C.; Quinteira, S.; Novais, C.; Peixe, L.; Borges, F. (2006) β-Nitrostyrene derivatives as potential antibacterial agents: a structure–property–activity relationship study. *Bioorg. Med. Chem.* 14: 4078-4088.
6. Milhazes, N.; Cunha-Oliveira, T.; Martins, P.; Garrido, J.; Oliveira, C.; Rego, A.C.; Borges, F. (2006) Synthesis and cytotoxic profile of 3,4-methylenedioxymethamphetamine ("ecstasy") and its metabolites on undifferentiated PC12 cells: a putative structure–toxicity relationship. *Chem Res. Toxicol.* 19: 1294-1304.
7. Milhazes, N.; Martins, P.; Uriarte, E.; Garrido, J.; Calheiros, R.; Marques, M.P.M.; Borges, F. (2007) Electrochemical and spectroscopic characterisation of amphetamine-like drugs: application to the screening of 3,4-methylenedioxymethamphetamine (MDMA) and its synthetic precursors (submetido para publicação).

Resumos

1. Lemos-Amado, F.; Domingues, P.; Remião, F.; Milhazes, N.; Carvalho, F.; Borges, F.; Ferrer-Correia, A.; Bastos, M.L. (2001) Aminochromes: synthesis, HPLC separation, ESI-MS characterization and *in vitro* studies in freshly isolated cardiomyocytes. *Eur. J. Biochem.* 268 (Suppl. 1): 124.

   Trabalho apresentado no 27th Meeting of the Federation of European Biochemical Societies em Lisboa, Portugal, 30 de Junho a 5 de Julho de 2001.

2. Milhazes, N.; Borges, F.; Silva, A.M.S.; Lemos-Amado, F.; Carvalho, F.D.; Fernandes, E. (2002) Synthesis and structural elucidation of polyphenolic-glutathione conjugates for the screening of their toxicological profile. *Drugs Fut.* 27 (Suppl. A): 453.

   Trabalho apresentado no XVII International Symposium on Medicinal Chemistry em Barcelona, Espanha, 1 a de 5 Setembro de 2002.

3. Carvalho, M.; Milhazes, N.; Remião, F.; Borges, F.; Fernandes, E.; Monks, T.J.; Carvalho, F.; Bastos, M.L. (2003) Hepatotoxic effects of 3,4-methylenedioxymethamphetamine and α-methyldopamine in freshly isolated rat hepatocytes. *Toxicol. Lett.* 144 (Suppl. 1): 98.

   Trabalho apresentado no Eurotox 2003, 41st European Congress of Toxicology em Florença, Itália, 28 de Setembro a 1 de Outubro de 2003.

4. Carvalho, M.; Milhazes, N.; Remião, F.; Borges, F.; Fernandes, E.; Monks, T.J.; Carvalho, F.; Bastos, M.L. (2003) The metabolism of 3,4-methylenedioxymethamphetamine (ecstasy) into *N*-methyl-α-methyldopamine drastically increases its *in vitro* toxicity. *Toxicol. Lett.* 144 (Suppl. 1): 99.

   Trabalho apresentado no Eurotox 2003, 41st European Congress of Toxicology em Florença, Itália, 28 de Setembro a 1 de Outubro de 2003.

5. Remião, F.; Milhazes, N.; Borges, F.; Carvalho, F.; Bastos, M.L.; Lemos-Amado, F.; Domingues, P.; Ferrer-Correia, A. (2003) Analysis of aminochromes by HPLC-photodiode array. Adrenochrome evaluation in rat blood. *Toxicol. Lett.* 144 (Suppl. 1): 117.

   Trabalho apresentado no Eurotox 2003, 41st European Congress of Toxicology em Florença, Itália, 28 de Setembro a 1 de Outubro de 2003.

6. Carvalho, M.; Remião, F.; Fernandes, E.; Carvalho, F.; Bastos, M.L.; Milhazes, N.; Borges, F.; Amado, F. (2004) Hepatotoxicity of 3,4-methylenedioxymethamphetamine (ecstasy) and its major metabolites in isolated rat hepatocytes. *Fundam. Clin. Pharmacol.* 18 (Suppl. 1): 97.
   Trabalho apresentado no 4th Congress of the Federation of the European Pharmacological Societies (EPHAR) no Porto, Portugal, 17 a 19 de Julho de 2004.
7. Carvalho, M.; Remião, F.; Milhazes, N.; Borges, F.; Fernandes, E.; Carvalho, F.; Bastos, M.L. (2004) In vitro hepatotoxicity of N-methyl-α-methyldopamine. Protective effect by antioxidants. *Toxicol. Appl. Pharm.* 197: 333-334.
   Trabalho apresentado no 10th International Congress of Toxicology (ICT X) em Tampere, Finlândia, 11 a 15 de Julho de 2004.

Comunicações

1. Milhazes, N.; Remião, F.; Carmo, H.; Borges, F.; Carvalho, F.; Bastos, M.L. (2000) Oxidation of adrenaline and isoprenaline into their aminochromes using enzymatic and non-enzymatic systems: a comparative study. *XIX European Colloquium on Heterocyclic Chemistry*, Aveiro, Portugal, 19 a 22 de Julho.
2. Milhazes, N.; Remião, F.; Carmo, H.; Borges, F.; Carvalho, F.; Bastos, M.L. (2000) Desenvolvimento de uma metodologia analítica para a monitorização da oxidação de catecolaminas. *XIV Encontro Luso-Galego de Química*, Braga, Portugal, 22 a 24 de Novembro.
3. Milhazes, N.; Martins, P.; Borges, F.; Uriarte, E.; Carvalho, M.; Carvalho, F.; Fernandes, E.; Bastos, M.L. (2001) Synthesis of putative metabolites of 3,4-methylenedioxymethamphetamine ("ecstasy"). *12th European Symposium on Organic Chemistry*, Groningen, Holanda, 13 a 18 de Julho.
4. Martins, P.; Milhazes, N.; Borges, F.; Uriarte, E. (2001) Studies on the *N*-methylation of 3,4-methylenedioxyamphetamine (MDA). *8th European Symposium on Organic Reactivity*, Cavtav, Croácia, 1 a 6 de Setembro.

5. Remião, F.; Milhazes, N.; Borges, F.; Carvalho, F.; Carmo, H.; Bastos, M.L.; Amado, F.; Domingues, P.; Ferrer-Correia, A. (2001) Synthesis and mass spectrometry characterization of aminochromes. Extraction and quantification of isoprenochrome and adrenochrome in biological samples. *5º Congresso de Radicais Livres em Química, Biologia e Medicina*, Porto, Portugal, 13 a 15 de Dezembro.
6. Milhazes, N.; Borges, F.; Gomes, C.A.; Marques, M.P.M. (2002) Spectroscopic and conformational studies on β-nitrostyrene and β-methyl-β-nitrostyrene derivatives. *II Congresso Ibérico de Espectroscopia/XVIII Reunión Española de Espectroscopía*, Coimbra, Portugal, 16 a 21 de Setembro.
7. Milhazes, N.; Borges, F.; Calheiros, R.; Marques, M.P.M. (2003) Spectroscopic and conformational studies on the synthetic precursors of abuse drugs: β-methyl-β-nitrostyrene derivatives. *13th European Symposium on Organic Chemistry*, Cavtat, Dubrovnik, Croácia, 10 a 15 de Setembro.
8. Carvalho, M.; Remião, F.; Milhazes, N.; Borges, F.; Fernandes, E.; Monks, T.J.; Amado, F.; Carvalho, F.; Bastos, M.L. (2004) Formation of glutathione conjugates in rat hepatocytes incubated with 3,4-methylenedioxyamphetamine (MDA) and α-methyldopamine. *1st Luso-Spanish Congress on Free Radicals – 6º Congresso de Radicais Livres em Química, Biologia e Medicina*, Coimbra, Portugal, 4 a 6 Dezembro.
9. Calheiros , R.; Milhazes, N.; Rodrigues, C.; Novais, C.; Quinteira, S.; Antunes, P.; Peixe, L.; Borges, F.; Marques, M.P.M (2004) Structure-activity study of β-nitrostyrene and β-methyl-β-nitrostyrene derivatives – synthesis, antibacterial activity and conformational analysis. *XIX Encontro Nacional da Sociedade Portuguesa de Química*, Coimbra, Portugal, 14 a 17 de Abril.
10. Milhazes, N.; Calheiros, R.; Marques, M.P.M.; Borges, F. (2004) Synthetic precursors of amphetamine-like drugs: a Raman spectroscopy and *ab initio* study. *III Congresso Ibérico de Espectroscopia/XIX Reunión Española de Espectroscopía*, Las Palmas de Gran Canaria, Espanha, 4 a 9 Julho.
11. Milhazes, N.; Rodrigues, C.; Novais, C.; Quinteira, S.; Antunes, P.; Peixe, L.; Borges, F. (2004) β-nitrostyrene and β-methyl-β-nitrostyrene derivatives as potential antibacterial agents – a structure–activity relationship study. *International Symposium on Advances in Synthetic, Combinatorial and Medicinal Chemistry (ASCMC)*, Moscovo, Rússia, 5 a 8 de Maio.

12. Garrido, E.M.P.J.; Garrido, J.M.P.J.; Borges, F.; Milhazes, N.; Oliveira-Brett, A.M. (2005) Voltammetric behaviour of 3,4-methylenedioxymethamphetamine (*ecstasy*). *Joint Meeting Bioelectrochemistry-2005*, Coimbra, Portugal, 19 a 24 de Junho.
13. Garrido, J.M.P.J.; Borges, F.; Milhazes, N.; Rodrigues, C.; Peixe, L. (2005) Inhibitory effects of substituted β-nitrostyrenes towards bacteria: correlation with redox potentials. *Joint Meeting Bioelectrochemistry-2005*, Coimbra, Portugal, 19 a 24 de Junho.

Agradecimentos

Este trabalho não teria sido possível sem a ajuda, a nível pessoal e profissional, de muitas pessoas que acreditaram em mim...

À Professora Doutora Fernanda Borges, orientadora desta dissertação, agradeço todo o apoio e toda a amizade e incentivo que foram fundamentais para a sua conclusão. Se este trabalho tem pontos meritórios devo-os, quase em exclusivo, à dedicação e ao acompanhamento com que seguiu todos os estudos desta dissertação.

A todos os co-autores das publicações e comunicações apresentadas neste trabalho quero expressar o meu profundo reconhecimento, principalmente (mas não só...) pelo valor científico que imprimiram a esta dissertação e o empenho que sempre demonstraram.

A todos os membros do Centro de Estudos de Química Orgânica Fitoquímica e Farmacologia da Universidade do Porto e do Serviço de Química Orgânica da Faculdade de Farmácia da Universidade do Porto, e em particular à Professora Doutora Madalena Pinto, agradeço o acolhimento caloroso e toda a disponibilidade com que me receberam ao longo da execução deste trabalho.
O meu muito obrigado também ao Instituto Superior de Ciências da Saúde – Norte por me ter proporcionado a experiência, gratificante e extremamente valiosa, do contacto com alunos e colegas. O seu contributo foi precioso para enfrentar os momentos mais complicados!

A todos aqueles (e foram muitos...) que estiveram presentes nas mais variadas fases deste trabalho e que me escuso de nomear, com o receio de me esquecer de alguém, o meu mais sincero agradecimento, sem a sua inestimável ajuda o sucesso desta dissertação não seria, de todo, possível. Obrigado por estarem por aí sempre que precisei!

À minha família e amigos por tudo...
Para os meus pais e para a Filipa, palavras para quê? A minha gratidão é imensa!!!

ÍNDICE

Resumo/Abstract/Résumé 3

Abreviaturas 9

PARTE I – INTRODUÇÃO

1. OBJECTIVOS E ESTRUTURA DA DISSERTAÇÃO 13

2. PREÂMBULO 16

2.1 A Química Farmacêutica e os estudos de relação estrutura – actividade 16

2.2 O metabolismo e os estudos de relação estrutura – toxicidade e estrutura – metabolismo 18

3. OBTENÇÃO DE METABOLITOS E INTERMEDIÁRIOS DE SÍNTESE 24

3.1 Síntese de compostos do tipo anfetamínico e seus metabolitos 24

3.2 Síntese de derivados do β-nitroestireno e do β-metil-β-nitroestireno 34

3.3 Síntese de aminocromos 37

3.4 Síntese de conjugados de glutationa com compostos do tipo fenólico 44

4. DESENVOLVIMENTO DE METODOLOGIAS ANALÍTICAS PARA APLICAÇÃO EM TOXICOLOGIA CLÍNICA E FORENSE 50

4.1 Separação e análise de aminocromos por cromatografia líquida de alta eficiência (HPLC) 50

4.2 Identificação de anfetaminas, metabolitos e seus intermediários de síntese por espectroscopia vibracional de Raman 53

5. DETERMINAÇÃO DE PROPRIEDADES FÍSICO-QUÍMICAS E PARÂMETROS ESTRUTURAIS DOS COMPOSTOS SINTETIZADOS 62

5.1 Análise conformacional através de cálculos de mecânica quântica 63

5.2 Determinação dos potenciais redox através de técnicas voltamétricas 66

5.3 Cálculo dos coeficientes de partilha 70

6. AVALIAÇÃO DA ACTIVIDADE BIOLÓGICA 73

6.1 Avaliação da actividade antibacteriana dos derivados do β-nitroestireno e do β-metil-β-nitroestireno 73

6.2 Análise da citotoxicidade e da condensação da cromatina induzidas pela 3,4-metilenodioximetanfetamina (MDMA) e seus metabolitos 77

7. CORRELAÇÃO ENTRE ESTRUTURA, PROPRIEDADES FÍSICO-QUÍMICAS E A ACTIVIDADE BIOLÓGICA DOS COMPOSTOS SINTETIZADOS 84

PARTE II – TRABALHO EXPERIMENTAL

8. TRABALHO EXPERIMENTAL 89

8.1 Estudo conformacional de derivados do β-nitroestireno por espectroscopia de Raman combinada com cálculos *ab initio*. 89

8.2 Identificação de precursores sintéticos de drogas do tipo anfetamínico usando espectroscopia de Raman e cálculos *ab initio*: derivados do β-metil-β-nitroestireno. 107

8.3 Derivados do β-nitroestireno como potenciais agentes antibacterianos: um estudo de relação estrutura – propriedade físico-química – actividade. 121

8.4 Síntese e análise de aminocromos por HPLC com detector de fotodíodos. Determinação de adrenocromo em sangue de rato. 135

8.5 Caracterização electroquímica e espectroscópica de drogas do tipo anfetamínico: aplicação à detecção da 3,4-metilenodioximetanfetamina (MDMA) e dos seus precursores sintéticos. 145

8.6 Síntese e perfil de citotoxicidade da 3,4-metilenodioximetanfetamina ("ecstasy") e seus metabolitos em células PC12 indiferenciadas: uma provável relação estrutura – toxicidade. 175

PARTE III – CONCLUSÕES, REFERÊNCIAS E ANEXOS

9. CONCLUSÕES 191

10. REFERÊNCIAS 195

11. ANEXOS 211

Resumo

Actualmente, a Química Farmacêutica, como ciência multidisciplinar que é, integra um conjunto de estudos que visam a avaliação da actividade, toxicidade e metabolismo dos compostos, em simultâneo com a determinação de parâmetros físico-químicos e estruturais relevantes para a expressão dos efeitos biológicos. À luz deste conceito, desenvolveu-se, no âmbito desta dissertação, um trabalho com o objectivo principal de contribuir para a definição de possíveis correlações entre a estrutura, as propriedades físico-químicas e a actividade de compostos biologicamente activos.

Inicialmente, uma série de metabolitos foram sintetizados, nomeadamente compostos resultantes do metabolismo oxidativo de catecolaminas – aminocromos, metabolitos da 3,4-metilenodioximetanfetamina (MDMA) e conjugados de compostos catecólicos com a glutationa. Também foram desenvolvidas metodologias analíticas adequadas à monitorização das reacções de oxidação das catecolaminas a aminocromos (metabolitos detectados *in vivo*) e de conjugação de compostos do tipo fenólico com a glutationa; estas poderão, no futuro, ser usadas para a separação, detecção e quantificação *in vivo* deste tipo de compostos.

Os estudos de relação estrutura – propriedade físico-química – actividade dos derivados do β-nitroestireno e dos metabolitos da MDMA sintetizados incidiram na avaliação da actividade antibacteriana dos primeiros e da citotoxicidade em células PC12 dos últimos. As propriedades estruturais (preferências conformacionais) e físico-químicas (coeficientes de partilha e potenciais redox) foram também determinadas para se avaliar a sua influência na referida actividade. Uma análise conformacional completa, por acoplamento de resultados de cálculos *ab initio* e espectroscopia de Raman, de anfetaminas e dos seus intermediários sintéticos (derivados do β-nitroestireno) foi também efectuada. Dos derivados do β-nitroestireno testados para a actividade antibacteriana, demonstrou-se que aqueles que possuem um grupo metilo no Cβ apresentam uma actividade significativa contra bactérias Gram-positivas. Uma evidente correlação entre a actividade e a capacidade de redução do grupo nitro terminal, evidenciada pelos potenciais redox dos compostos, foi também encontrada. Do mesmo modo se comprovou que as determinantes estruturais dos

compostos (nomeadamente a deslocalização electrónica e a planaridade das moléculas) influenciam a actividade antimicrobiana.

O perfil de citotoxicidade da MDMA e dos seus principais metabolitos foi estudado em células PC12, com análise concomitante da condensação da cromatina (característica da morte celular por apoptose), de modo a determinar a sua contribuição individual para a morte celular. Os resultados permitiram concluir que os metabolitos contendo o grupo catecol são mais citotóxicos do que a MDMA e os outros metabolitos de fase I. Pelo estudo dos potenciais redox dos compostos concluiu-se que um possível mecanismo oxidativo determina a toxicidade da MDMA e dos compostos relacionadas.

Finalmente, os resultados dos estudos de espectroscopia vibracional de drogas do tipo anfetamínico e dos seus intermediários e precursores sintéticos mostraram que os espectros possuem características específicas de cada um dos compostos, o que pode permitir a sua identificação fácil e rápida em amostras forenses ou clínicas.

Em suma, a informação compilada nesta dissertação pode contribuir, no futuro, para a compreensão dos mecanismos moleculares associados à actividade ou toxicidade de alguns compostos com interesse biológico.

Abstract

Medicinal Chemistry is a multidisciplinary field of research that combines a series of studies with the ultimate goal of correlate the bioactivity, toxicity and metabolism of the compounds with some relevant physico-chemical and structural parameters that may contribute to the activity. The present work represents a contribution to the definition of putative correlations between structure, physicochemical parameters and activity.

First, some metabolites were synthesised, namely compounds resulting from the oxidative metabolism of catecholamines – aminochromes, metabolites of 3,4-methylenedioxymethamphetamine (MDMA) and glutathione adducts of catecholic compounds. Synthetic and analytical methodologies were developed, with the ability of monitoring the oxidation of catecholamines to the respective aminochromes (metabolites detected *in vivo*) and the conjugation of the phenolic compounds with glutathione. The results may be useful, in the future, to the separation, identification and quantification, *in vivo*, of this type of compounds.

Structure – physicochemical properties – activity relationship studies on the synthesised β-nitrostyrene derivatives and MDMA and its phase I metabolites were performed through the evaluation of the antibacterial activity of the former and the cytotoxicity profile in PC12 cells of the latter. Structural (conformational preferences) and physicochemical parameters (partition coefficients and redox potentials) were also determined for a better understanding of their effect on bioactivity.

A complete conformational analysis, by *ab initio* MO calculations coupled with Raman spectroscopy, of amphetamines and their intermediates and precursors (β-nitrostyrene derivatives) was performed. β-Nitrostyrene derivatives were evaluated for their antibacterial activities and the results show that the compounds displaying a β-methyl group display significant activity towards Gram-positive bacteria. A clear correlation was detected between this activity and the ease of reduction of the nitro group of the side chain, highlighted by their redox potentials. It was demonstrated that structural preferences, namely the electron delocalisation and the planarity of the molecules, have also influence on the antimicrobial activity.

The cytotoxicity profile of MDMA and its major metabolites was studied in PC12 cells, together with the analysis of chromatin condensation (feature of cell death by apoptosis), in order to evaluate their contribution to cell death. The obtained data

show that the metabolites containing a catechol group are more cytotoxic than MDMA and other metabolites of phase I. Voltammetric studies allow to determine that an oxidative mechanism plays a major role in MDMA toxicity.

Vibrational spectroscopy studies on amphetamine-like metabolites and their synthetic precursors show that their spectra display individual features that allow their ready identification in clinical and forensic samples.

In summary, the data collected in this work may contribute to the understanding of molecular mechanisms associated with the activity or toxicity of a series of compounds with biological interest.

Résumé

Actuellement la Chimie Pharmaceutique, comme science multidisciplinaire qu'elle est, intègre dans un ensemble d'études qui veuillent envisager l'évaluation d'activité, toxicité et métabolisme de composés avec la détermination de paramètres physico-chimiques et structurels relevant pour l'expression de cet effet biologique. Par rapport ce concept, s'est développer, dans le travaille constant de cette dissertation, une étude avec l'objectif de contribuer pour la définition des possibles corrélations entre la structure, les propriétés physico-chimiques et l'activité d'une variété de composés.

Initialement, la synthèse d'une série de métabolites a été effectué, notamment composés résultant du métabolisme oxydative des catécholamines – aminochromes, métabolites de la 3,4-méthylènedioxymétamphétamine (MDMA) et conjugués de composés catécholiques avec la glutatione. Simultanément, ont été développé des méthodologies synthétiques et analytiques avec la capacité de monitorage l'oxydation des catécholamines en aminochromes (métabolites détectes *in vivo*) et la conjugaison avec la glutatione de composés phénoliques, celles-ci pourront dans le future, être utilisés dans la séparation, détection e quantification *in vivo* de ce type de composés.

Les études de relation structure – propriétés physico-chimiques – activité des dérives du β-nitrostyrène et des métabolites du MDMA synthétisent visé dans la détermination de l'activité antibactérienne des premiers et du cytotoxique en cellules PC12 des derniers. Les propriétés structurelles (préférences de conformation) et physico-chimiques (coefficient de partage et potentiels redox) ont été aussi déterminés pour étudier l'influence dans l'activité. Une analyse conformationnelle complète, par accouplement de résultats de calcules *ab initio* et spectrométrie de Raman, des amphétamines et de leurs intermédiaires synthétiques (dérives du β-nitrostyrène) ont été aussi réalise. Les β-nitrostyrènes ont été testé par l'activité antibactérienne et c'était démontré que les dérivés qui ont un groupe méthyle dans le Cβ ont une activité antibactérienne significative contre les bactéries Gram-positif. Une évidente corrélation entre l'activité et la capacité de réduction du groupe nitro terminal, prouvée par les potentiels redox de ces composés, a été trouvé. La conformation de ces composés a aussi influence dans l'activité antibactérienne.

Le profil cytotoxique de le MDMA et de ces principaux métabolites a été étudié dans des cellules PC12, avec l'analyse en parallèle de la condensation de la chromatine

(caractéristique de l'apoptose), a fin de déterminer sa contribution individuelle pour la mort cellulaire. Les résultats reflètent que les métabolites avec un groupe catéchol sont plus cytotoxiques que leurs du MDMA et les autres métabolites de phase I. L'étude des potentiels redox des composés détermine un possible mécanisme oxydative qu'influence la toxicité du MDMA e des drogues rapportées.

Finalement, les résultats des études de spectrométrie vibrationnel des drogues du type amphétamine et de ces intermédiaires et précurseurs synthétiques démontre que les spectres ont caractéristiques spécifiques un chacun des composés, ci que peut permettre son identification facile et rapide dans des échantillons forensique ou cliniques.

En rapport, l'information compile dans cette dissertation peuvent contribuer pour la compréhension de certains mécanismes moléculaires associés à l'activité ou toxicité d'une série de composée d'intérêt biologique.

Abreviaturas

ADN	Ácido Desoxirribonucleico
COMT	Catecol-*O*-metiltransferase
CV	*Cyclic Voltammetry* (Voltametria Cíclica)
DAD	*Diode Array Detector* (Detector de Fotodíodos)
DFT	*Density Functional Theory* (Teoria dos Funcionais de Densidade)
DPV	*Differential Pulse Voltammetry* (Voltametria de Impulso Diferencial)
EM	Espectrometria de Massa
*E*p	Potencial de Pico
FT-Raman	*Fourier Transformed Raman Spectroscopy* (Espectroscopia de Raman com Transformadas de Fourier)
GSH	Glutationa na sua forma reduzida
HF	Hartree-Fock
HPLC	Cromatografia Líquida de Alta Eficiência
5-HT	5-Hidroxitriptamina ou Serotonina
IC_{50}	*Inhibitory Concentration* (Concentração de Inibição da Viabilidade Celular a 50%)
IUPAC	*International Union of Pure and Applied Chemistry* (União Internacional de Química Pura e Aplicada)
IV	Infravermelho
log*P*	Coeficiente de Partilha
MAO	Monoamina Oxidase
MDA	3,4-Metilenodioxianfetamina
MDMA	3,4-Metilenodioximetanfetamina ou "Ecstasy"
α-MeDA	α-Metildopamina
MIC	*Minimum Inhibitory Concentration* (Concentração Inibitória Mínima)
MTT	Brometo de 3-(4,5-dimetiltiazol-2-il)-2,5-difeniltetrazólio
N-Me-α-MeDA	*N*-Metil-α-metildopamina
OM	Orbitais Moleculares
PC12	Células de Feocromocitoma de Ratinho

pK_a	Constante de Acidez
QSAR	*Quantitative Structure – Activity Relationship* (Relação(ões) Quantitativa(s) Estrutura – Actividade)
RMN	Ressonância Magnética Nuclear
ROS	*Reactive Oxygen Species* (Espécies Reactivas de Oxigénio)
SAR	*Structure – Activity Relationship* (Relação(ões) Estrutura – Actividade)
SMR	*Structure – Metabolism Relationship* (Relação(ões) Estrutura – Metabolismo)
SPR	*Structure – Property Relationship* (Relação(ões) Estrutura – Propriedades físico-químicas)
STR	*Structure – Toxicity Relationship* (Relação(ões) Estrutura – Toxicidade)
SWV	*Square Wave Voltammetry* (Voltametria de Onda Quadrada)
UV	Ultravioleta

PARTE I

INTRODUÇÃO

1. OBJECTIVOS E ESTRUTURA DA DISSERTAÇÃO

A presente dissertação foi organizada do modo a poder responder aos seguintes objectivos, traçados aquando da sua elaboração:

i) Planear e executar as vias sintéticas mais adequadas à obtenção de um conjunto de compostos com potencial interesse biológico: compostos que possuem o núcleo anfetamínico (nomeadamente MDMA e seus metabolitos), produtos da biotransformação oxidativa de catecolaminas e conjugados de compostos fenólicos com a glutationa.

ii) Desenvolver metodologias analíticas adequadas à detecção e monitorização de anfetaminas e catecolaminas, respectivos metabolitos e seus intermediários de síntese em diversos tipos de matrizes. Com este objectivo, estudou-se a aplicabilidade da espectroscopia de Raman na detecção inequívoca de anfetaminas e seus intermediários sintéticos e HPLC (em fase reversa e com detector de fotodíodos) para monitorização do processo de oxidação de catecolaminas.

iii) Caracterizar físico-quimicamente os compostos sintetizados por determinação (ou cálculo) de um conjunto de parâmetros físico-químicos (coeficientes de partilha e potenciais redox) e estruturais que permitam, após estudo das actividades biológicas, efectivar uma possível correlação entre elas.

iv) Avaliar a actividade antibacteriana dos derivados do β-nitroestireno, compostos intermediários de uma das vias sintéticas mais comuns das feniletilaminas. Determinar a citotoxicidade da MDMA e dos seus metabolitos em células PC12 (modelo para estudos de neurotoxicidade monoaminérgica), conjuntamente com a análise da condensação da cromatina, para detecção de características de apoptose ou necrose na morte celular induzida por estes compostos.

v) Estabelecer possíveis correlações entre a estrutura, a actividade biológica e as propriedades físico-químicas determinadas.

Assim, a dissertação foi estruturada da seguinte forma:

Parte I: num primeiro capítulo, denominado de Preâmbulo, apresenta-se uma breve panorâmica sobre o âmbito de estudo da Química Farmacêutica, nomeadamente os estudos de Relação Estrutura – Actividade (SAR) de compostos com interesse biológico. Neste capítulo enquadra-se o trabalho efectuado, especialmente no desenvolvimento e síntese de compostos bioactivos, estudos de metabolismo e determinação de actividade/toxicidade, bem como na determinação de propriedades físico-químicas relevantes para a expressão de determinada actividade biológica.

Nos capítulos seguintes listam-se mais exaustivamente os métodos usados para a consecução dos objectivos propostos inicialmente. Em particular abordam-se os estudos de:

i) síntese e obtenção de intermediários e metabolitos de compostos bioactivos (MDMA, catecolaminas e compostos polifenólicos);

ii) estabelecimento de metodologias analíticas que permitam uma análise fidedigna de amostras clínicas ou forenses de compostos com interesse em toxicologia (cromatografia líquida de alta eficiência para a análise de aminocromos e espectroscopia de Raman para análise de drogas e seus intermediários sintéticos);

iii) caracterização dos compostos sintetizados por determinação ou cálculo teórico de parâmetros físico-químicos e estruturais considerados relevantes, nomeadamente potenciais redox, coeficientes de partilha e análise conformacional;

iv) actividade biológica, mais concretamente por avaliação da actividade antibacteriana dos derivados do β-nitroestireno e de citotoxicidade da MDMA e dos seus metabolitos em células PC12;

v) relação estrutura – propriedade físico-química – actividade biológica dos compostos, de modo a poder estudar os requisitos necessários para o estabelecimento do farmacóforo ou toxicóforo.

Para cada um dos pontos anteriores é feita uma breve introdução, com a descrição da técnica, seus fundamentos teóricos e a justificação da sua aplicação nesta dissertação.

Ao longo destes capítulos introdutórios existem alusões aos resultados, com a respectiva discussão, que estão integradas num conjunto de artigos científicos, já publicados ou em fase de publicação.

Parte II: após a Introdução (Parte I), segue-se a Parte Experimental, onde se incluem um conjunto de publicações em revistas internacionais com arbitragem científica. Nestes artigos estão compilados os métodos usados, os resultados obtidos e também conclusões parcelares dos trabalhos incluídos nesta dissertação.

Partes III: na última parte os resultados são posteriormente resumidos em conclusões gerais, que foram estabelecidas em função dos objectivos inicialmente propostos.

2. PREÂMBULO

2.1 A Química Farmacêutica e os estudos de relação estrutura – actividade

A Química Farmacêutica, também frequentemente designada por Química Terapêutica ou Química Medicinal, é, segundo a IUPAC (*International Union of Pure and Applied Chemistry*), uma área de estudo interdisciplinar que abarca a descoberta, planeamento, desenvolvimento, obtenção, identificação e interpretação do mecanismo de acção ao nível molecular de compostos biologicamente activos (Wermuth *et al.*, 1998). Embora em Química Farmacêutica se dê especial ênfase ao estudo de fármacos, o seu âmbito não se restringe apenas a estes, incluindo também quaisquer outros compostos bioactivos no sentido mais lato do termo (como compostos endógenos e drogas de uso ilícito). Esta área disciplinar engloba também a síntese, identificação e estudo de metabolitos de xenobióticos e compostos biogénicos, bem como uma análise mais abrangente sobre o metabolismo e as vias de biotransformação mais relevantes destes compostos. A Química Farmacêutica é, assim, uma ciência que, além de envolver e de se basear em aspectos das diferentes áreas da química (química física, síntese orgânica, química analítica, química teórica, etc.), também integra conhecimentos de outras disciplinas biológicas e médicas (farmacologia, toxicologia, bioquímica, biologia molecular, etc.).

A obtenção de compostos com possível interesse biológico implica o planeamento racional e a síntese de novas substâncias químicas bioactivas (NCE, do inglês *new chemical entities*), ou, em alternativa, a síntese e modificação molecular ou isolamento, identificação e posterior elucidação estrutural de compostos naturais (normalmente com origem em plantas, animais ou microrganismos). O desenvolvimento de metodologias analíticas adequadas à identificação inequívoca e à quantificação dos compostos, inclusivamente em matrizes complexas como os meios biológicos, deve também mobilizar recursos, sob pena das actividades e propriedades inicialmente previstas não poderem ser comprovadas por falta de ensaios analíticos correctamente validados.

Todos estes factores convergem para a necessidade da descrição físico-química adequada dos compostos a estudar. O conhecimento da sua composição exacta e das suas características estruturais e conformacionais, isoladamente ou aquando da(s) sua(s) interação(ões) com os seus prováveis alvos biológicos, é fundamental para a compreensão dos processos bioquímicos, farmacológicos, toxicológicos e farmacocinéticos a nível molecular. Com base nestes conhecimentos podem estabelecer-se relações entre a estrutura química e a actividade (SAR, do inglês *structure – activity relationship*). Este tipo de análise também pode ser efectuada por via computacional, através da elaboração e validação de modelos matemáticos que quantificam as relações entre a estrutura química e a actividade farmacológica (QSAR, do inglês *quantitative structure – activity relationship*).

A construção de relações quantitativas entre a estrutura molecular dos compostos e a bioactividade correspondente é das vertentes mais recentes da Química Farmacêutica e aquela que tem concentrado actualmente um maior esforço. Desde a década de 1960, com os revolucionários e basilares trabalhos de Corwin Hansch, que se instituiram os alicerces dos estudos de QSAR, com o estabelecimento da relação entre a actividade biológica de alguns compostos e os seus coeficientes de partilha e as constantes de Hammett dos substituintes (Hansch *et al.*, 1963; Hansch e Fujita, 1964). Estes autores recorreram a modelos matemáticos que correlacionavam estrutura e actividade e, desde então, estes estudos desenvolveram-se exponencialmente no sentido de se proceder à planificação e desenho racional de novos compostos com possível aplicação terapêutica, conseguindo prever-se, deste modo, algumas características físico-químicas fundamentais para a expressão da actividade. Deve salientar-se que os trabalhos de correlação entre estrutura e actividade biológica podem, e devem, ser alicerçados em estudos prévios da relação entre a estrutura e as propriedades físico-químicas (lipofilia, acidez, etc.) dos compostos que se considerem importantes para a interpretação da actividade biológica.

Os estudos de SAR e QSAR abarcam obrigatoriamente quatro componentes distintos, (i) os compostos bioactivos, (ii) os alvos biológicos onde estes actuam, (iii) as respostas biológicas que produzem e que podem ser descritas por (iv) modelos matemáticos que relacionam as variações da actividade biológica com alterações na estrutura dos compostos (Testa, 1984) (Figura 1). A relação directa entre a velocidade relativa da adição nucleofílica não enzimática da glutationa a xenobióticos (conjugação) e a respectiva electrofilia é um exemplo típico deste tipo de análise (Testa *et al.*, 2005).

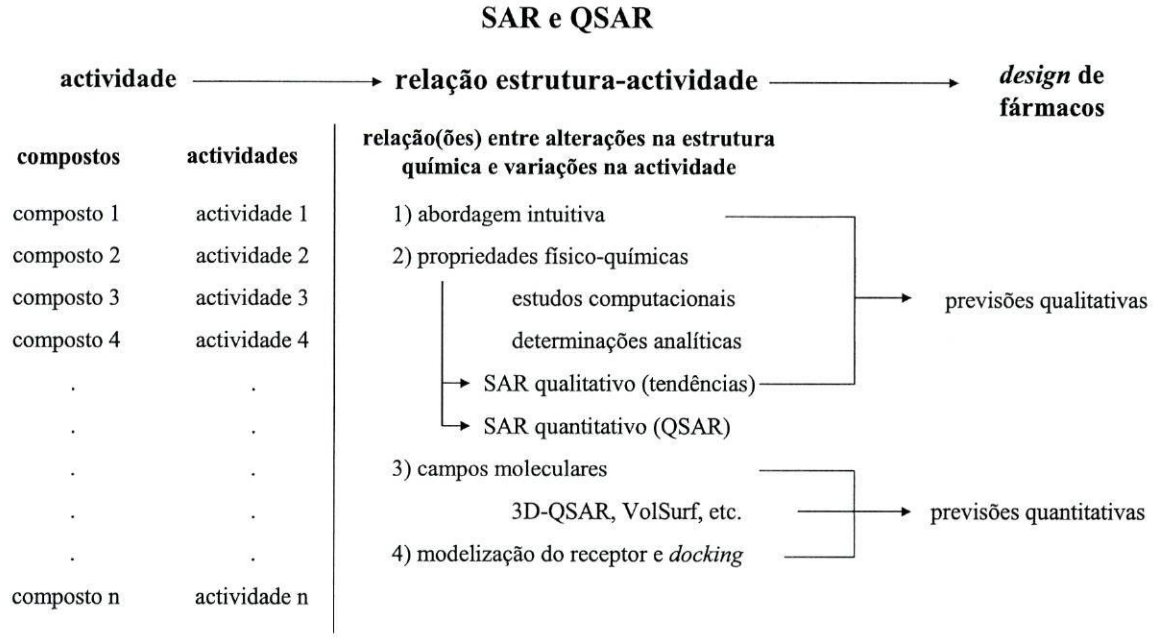

Figura 1. Representação esquemática da(s) relação(ões) estrutura – actividade qualitativa(s) (SAR) e quantitativa(s) (QSAR), com realce para as diversas abordagens no estudo das alterações na estrutura e como estas se podem repercutir na actividade de um composto (adaptado de Testa *et al.*, 2005).

2.2 O Metabolismo e os estudos de relação estrutura – toxicidade e estrutura – metabolismo

Por metabolismo considera-se o conjunto de alterações físicas e químicas que uma substância, endógena ou exógena, sofre no interior de um organismo. Os processos inerentes ao metabolismo de xenobióticos podem ser definidos, genericamente, como um mecanismo de destoxificação. Estes processos têm como objectivo facilitar a excreção do xenobiótico do organismo, convertendo compostos menos polares em compostos com características mais polares, os quais por serem mais hidrofílicos são mais facilmente excretados na bílis e na urina. Estas modificações estruturais dos xenobióticos são normalmente mediadas por enzimas e ocorrem maioritariamente no fígado, podendo, também, ser realizadas noutros órgãos, como intestino, rins ou cérebro (Testa *et al.*, 2004).

As reacções metabólicas processam-se, classicamente, em duas etapas fundamentais (Barreiro *et al.*, 1996):

i) reacções de fase I, que ocorrem principalmente por modificação, por via enzimática, de um composto por oxidação, redução ou hidrólise (ou a ocorrência simultânea de mais do que uma destas reacções). Estas reacções são catalisadas maioritariamente por enzimas do citosol e do retículo endoplasmático (enzimas microssomais). O sistema enzimático mais relevante, em termos quantitativos, é o citocromo P450, localizado nos microssomas hepáticos. Este sistema é responsável pelas reacções de fase I e é constituído por uma família de isoenzimas monoxigenases que estão associadas ao transporte de electrões e a processos redox e têm como característica comum a presença de um grupo heme.

ii) reacções de fase II, que correspondem a reacções relacionadas com a ligação de um xenobiótico, ou dos seus metabolitos de fase I, a moléculas endógenas (conjugação). As reacções de conjugação podem ocorrer com o ácido glucurónico, o grupo sulfato ou compostos contendo o grupo tiol (glutationa e proteínas contendo o grupo sulfidrilo), podendo também ser reacções de acilação ou metilação.

Apenas um número muito reduzido de compostos orgânicos, uma vez no interior dos organismos, escapa ileso ao arsenal de sistemas enzimáticos que vão modificar, mais ou menos pronunciadamente, a sua estrutura e consequentemente as suas propriedades físico-químicas. O estudo das alterações das propriedades físico-químicas dos compostos resultantes de reacções metabólicas constitui uma área de estudo ainda não convenientemente explorada. Como já foi referido, o(s) produto(s) resultante(s) das reacções de biotransformação de um composto são frequentemente inactivos, embora, não raras vezes, os metabolitos intermediários ou finais possam ter actividade (ou toxicidade) qualitativa ou quantitativamente diferente do composto inicial. Estas transformações podem, assim, contribuir positiva ou negativamente para uma alteração do perfil farmacológico ou toxicológico previsto para o composto inicial. A toxificação resultante da biotransformação revela a necessidade de um conhecimento conveniente das bases moleculares do metabolismo dos xenobióticos (Mayer e Testa, 1994). Muitos compostos, após biotransformação, originam intermediários metabólicos extremamente reactivos. Estes metabolitos são os mais relevantes em termos biológicos e podem ser

classificados, genericamente e do ponto de vista químico, como electrófilos ou radicais livres (Williams e Naisbitt, 2002). Os compostos electrofílicos (deficientes em electrões) podem interagir directamente com nucleófilos e macromoléculas endógenas (proteínas, bases do DNA, tióis, etc.) e daí advir toxicidade.

Consequentemente, num paralelismo com o farmacóforo (ou padrão farmacofórico, definido como o conjunto de características estéricas e electrónicas necessárias para assegurar as interacções moleculares óptimas com um alvo biológico específico) (Wermuth *et al.*, 1998) podemos reconhecer os termos toxicóforo e metabóforo. A definição de toxicóforo assenta, também, nas características estruturais do composto que manifesta toxicidade e descreve o arranjo estrutural específico que pode estar associado a um dado efeito tóxico a nível bioquímico. O toxicóforo corresponde, no fundo, à parte da molécula que apresenta a(s) propriedade(s) tóxica(s) atribuída(s) às substâncias, sendo que qualquer substância tóxica exerce o seu efeito por interacção do seu toxicóforo com biomoléculas endógenas. Estas interacções provocam alterações nos processos bioquímicos normais das células e podem traduzir-se na ruptura do seu equilíbrio fisiológico. Contudo, muitas vezes, não é o toxicóforo que interage directamente com a biomolécula, mas um metabolito resultante da sua bioactivação que, então, se liga e exerce o seu efeito (Williams e Naisbitt, 2002). De um modo geral, para substâncias que contêm o mesmo toxicóforo, a natureza dos seus efeitos tóxicos é idêntica, mas o órgão ou o local específico do corpo onde o efeito ocorre pode ser distinto. Todavia, em algumas situações, não se manifesta o mesmo efeito tóxico, devido principalmente a especificidades de cada composto em termos estruturais, físico-químicos ou farmacocinéticos. O metabóforo, por outro lado, pode ser definido como o conjunto de características estruturais dos substratos que influenciam e induzem as suas conversões metabólicas específicas (Erhardt, 1999; Erhardt, 2002). O objectivo de estabelecer os grupos toxicóforos ou metabóforos é uma forma de minimizar os custos envolvidos no desenvolvimento de novos fármacos, permitindo prever e diminuir os defeitos farmacocinéticos e toxicológicos que acompanham, uma grande parte das vezes, os compostos candidatos a fármacos (Kerns e Di, 2003).

A título de exemplo, funções químicas que possam originar quinonas reactivas representam um toxicóforo e, simultaneamente, um metabóforo, objecto de um número considerável de estudos (Williams e Naisbitt, 2002). Os compostos do tipo fenólico, bastante abundantes em produtos naturais e fármacos, ou compostos que possam ser biotransformados nestes (como a MDMA, por exemplo) são facilmente oxidados *in vivo*

a quinonas, as quais podem reagir com nucleófilos biológicos, como a glutationa (GSH), provocando stress químico e/ou oxidativo característicos deste tipo de compostos.

Vários aspectos relacionados com o estudo do metabolismo assumem especial relevância em Química Farmacêutica, nomeadamente (Testa e Soine, 2003):

i) a química e a bioquímica das reacções metabólicas e as respectivas consequências na toxificação ou destoxificação dos compostos;

ii) o papel da selectividade do substrato e do produto;

iii) os vários parâmetros da molécula que afectam a biotransformação;

iv) as alterações das propriedades físico-químicas (acidez, lipofilia, oxidabilidade, etc.) resultantes da biotransformação dos compostos;

v) os factores (genéticos, fisiológicos, externos, etc.) que possam influenciar o metabolismo;

vi) o planeamento racional de pró-fármacos e drogas macias (*soft drugs*);

vii) as previsões do metabolismo de xenobióticos baseadas em relações estrutura – metabolismo qualitativas e/ou quantitativas e

viii) a modelização molecular de receptores enzimáticos com estudos de *docking*.

O crescente interesse no estudo das reacções de biotransformação de um composto resulta principalmente da possibilidade de formação de (Testa *et al.*, 2004; Testa e Soine, 2003):

i) metabolitos tóxicos (toxificação), particularmente metabolitos reactivos com a capacidade de formar aductos covalentes com biomoléculas vitais;

ii) metabolitos que possuam propriedades físico-químicas significativamente diferentes dos compostos que lhes deram origem (como, por exemplo, um aumento da lipofilia, a qual pode facilitar os processos de bioacumulação);

iii) metabolitos activos a partir de compostos activos ou a partir de compostos inactivos (bioactivação) ou até

iv) metabolitos inactivos (bioinactivação).

De salientar que todas estas alterações podem implicar modificações nos perfis farmacocinético e farmacodinâmico dos compostos.

Frequentemente a designação SAR abrange também relações entre a estrutura e a toxicidade e entre a estrutura e o metabolismo. Todas as considerações enunciadas anteriormente para SAR e QSAR podem paralelamente ser postuladas em relação à toxicidade e ao metabolismo. Assim, substituindo o termo actividade por toxicidade (ou efeito tóxico) define-se a relação estrutura – toxicidade (STR, do inglês *structure – toxicity relationship*), a qual também podem ser de índole quantitativa (QSTR). No caso de estudos sobre a influência da estrutura molecular nas vias metabólicas preferenciais de um composto, pode estabelecer-se uma relação qualitativa estrutura – metabolismo (SMR, do inglês *structure – metabolism relationship*). As relações quantitativas estrutura – metabolismo (QSMR) representam as associações quantitativas entre as propriedades físico-químicas e/ou estruturais de uma substância e o seu comportamento metabólico. Todos estes estudos de toxicidade e parâmetros farmacocinéticos, por tradição, tinham um papel secundário no desenvolvimento de novos fármacos, assistindo-se, hoje em dia, a um aumento do número deste tipo de estudos, com o objectivo de obter, de modo mais racional, compostos mais eficazes e seguros (Kerns e Di, 2003).

Em resumo, a análise das relações qualitativas e quantitativas entre estrutura e actividade farmacológica desempenha um papel crucial na elucidação dos mecanismos de acção dos compostos e no *design* de fármacos com mais eficácia em termos farmacocinéticas e farmacodinâmicos (Fujita, 1997). Estes estudos devem ser sempre complementados com STR ou QSTR e SMR ou QSMR, os quais permitem minorar os efeitos secundários dos fármacos e podendo ser usados na previsão da sua toxicidade. Os modelos de STR baseados em mecanismos de toxicidade podem ser aplicados com muita vantagem a várias categorias de toxicidade bem definidas e também a vários conjuntos de compostos (Cronin e Schultz, 2001; Aptula *et al.*, 2005). Os desafios mais prementes nesta área situam-se no âmbito da toxicologia ambiental, alimentar e farmacêutica, sendo que, nesta última, o objectivo principal será a antecipação de um espectro de potenciais efeitos adversos dos compostos, baseando-se em resultados de ensaios *in vitro* ou em modelos animais realizados com outros compostos (Kazius *et al.*, 2005; Benigni, 2005). Regista-se actualmente o desenvolvimento de um ramo da toxicologia, designado por toxicologia preditiva, o qual usa modelos computacionais que relacionam a estrutura química com a actividade tóxica de um composto, tendo como finalidade a representação, a explicação e, mais importante, a previsão e a

caracterização da sua toxicidade (McKinney *et al.*, 2000). Estes estudos devem partir sempre da premissa que a toxicidade (propriedade, efeito ou actividade tóxica) de um composto é fundamentalmente governada pelas suas propriedades físico-químicas, que são, por sua vez, reflexo da sua estrutura química (propriedades electrónicas e geométricas).

3. OBTENÇÃO DE METABOLITOS E INTERMEDIÁRIOS DE SÍNTESE

As estratégias de SAR obrigam, em primeiro lugar, ao envolvimento da síntese química para, deste modo, se obterem os compostos pretendidos, para explorar os estudos conducentes à descoberta do farmacóforo, toxicóforo ou metabóforo. Como se depreende, a síntese orgânica constitui, assim, uma vertente primordial em Química Farmacêutica e sem a qual a obtenção dos compostos necessários para se efectuarem as correlações entre estrutura e actividade biológica seria impossível.

O planeamento e estruturação das vias sintéticas mais apropriadas à obtenção dos compostos desejados constituem a primeira parte desta dissertação. A selecção dos caminhos sintéticos recaiu sobre a análise do número de passos reaccionais, do rendimento, do controlo de reacções secundárias, do material disponível para a síntese e purificação, da pureza e do custo da síntese.

No presente trabalho sintetizaram-se compostos representativos das seguintes classes:

i) metabolitos de substâncias do tipo anfetamínico, nomeadamente da MDMA, e dos seus intermediários sintéticos mais relevantes (derivados do β-nitroestireno e do β-metil-β-nitroestireno),

ii) metabolitos resultantes de oxidação de catecolaminas – aminocromos e

iii) metabolitos resultantes da conjugação de compostos do tipo catecólico com tióis endógenos.

3.1 Síntese de compostos do tipo anfetamínico e seus metabolitos

A 3,4-metilenedioximetanfetamina, MDMA ou "ecstasy", é uma feniletilamina psicoactiva com uma estrutura química aparentada com a anfetamina (composto estimulante psicomotor) e com a mescalina (composto alucinogénico) (Figura 2), demonstrando, em simultâneo, estas propriedades estimulantes e alucinogénicas. As anfetaminas que contêm um anel metilenodioxi (–OCH_2O–) em C3 e C4, MDMA, MDA, MDE e MBDB (Figura 2) constituem uma classe de compostos com actividades farmacológicas distintas de outros grupos terapêuticos já definidos (Nichols, 1986).

Apesar de serem usadas exclusivamente com fins recreativos, alguns autores defendem que estes compostos podem ser usados em psicoterapia, aproveitando precisamente as suas propriedades farmacológicas, designadas como entactogénicas (Nichols, 1986; Greer e Tolbert, 1998).

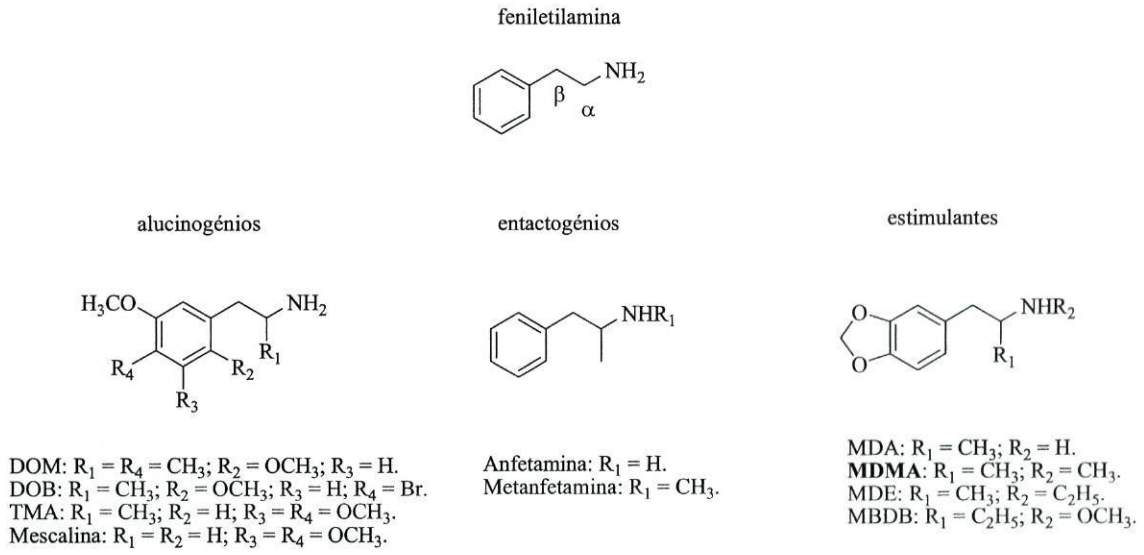

Figura 2. Estruturas químicas das β-feniletilaminas mais representativas, incluindo a 3,4-metilenodioximetanfetamina (MDMA).

Os entactogénios, como a MDMA, possuem apenas efeitos moderados como alucinogénio e estimulante central, provocando alguma euforia, aliada a sensação de felicidade e de elevada empatia ou proximidade emocional com as outras pessoas, coincidindo com uma maior necessidade de socialização (Downing, 1986; Greer e Tolbert, 1986; Nichols, 1986; Nichols *et al.*, 1986; Hermle *et al.*, 1993). Estes efeitos subjectivos tornaram a MDMA um composto bastante popular entre os adolescentes e jovens adultos. A MDMA é consumida principalmente em festas denominadas de *raves*, que ocorrem normalmente em clubes de dança ou em eventos especialmente organizados e onde a apologia deste tipo de cultura hedonista é valorizada.

Estes factos transformaram o (ab)uso desta droga num grave problema de saúde pública. Apesar da MDMA ser considerada pelos seus consumidores uma droga relativamente segura, ao seu consumo estão associados um conjunto de efeitos tóxicos e até mesmo alguma mortalidade (Schwartz e Miller, 1997; Christophersen, 2000; Strote *et al.*, 2002; Schifano *et al.*, 2003).

As características estruturais da MDMA e da MDA (3,4-metilenodioxianfetamina), sua precursora sintética e metabolito, que são

consideradas requisitos fundamentais para as suas propriedades psicoactivas são (Dal Cason, 1990):

i) o grupo metilo na amina: a modificação molecular por *N*-metilação da MDA, originando MDMA, diminui bastante, suprimindo até, os efeitos alucinogénicos, limitando também a sua duração de acção (Nichols *et al.*, 1986). Esta é uma característica geral das anfetaminas, pois compostos contendo uma amina primária têm propriedades alucinogénicas mais intensas do que aqueles que possuem uma amina substituída (secundária ou terciária). A substituição no grupo amina por uma cadeia alquílica aumenta a sua lipofilia e, consequentemente, estes compostos possuem uma actividade mais rápida, já que atravessam mais fácil e rapidamente as barreiras biológicas para atingirem o local de acção;

ii) o grupo metilo no Cα, originando uma cadeia lateral com três átomos de carbono, é fundamental para a expressão dos efeitos destes compostos. A sua ausência implica diminuição drástica da actividade, enquanto que a sua substituição por um grupo alquilo de dimensão superior, além de diminuir as actividades estimulantes e alucinogénicas, mantém as propriedades entactogénicas dos compostos. Estes dois grupos metilo da MDMA, um no Cα e outro na amina, aumentam os efeitos estimulantes centrais devido principalmente à sua maior lipofilia e resistência à inactivação pela MAO (monoamina oxidase);

iii) o padrão de substituição aromática, unicamente em C3 e C4, é característico destes compostos, divergindo dos alucinogénios mais potentes de núcleo feniletilamínico, como a mescalina, por exemplo, com substituição em C3, C4 e C5;

iv) a estereoquímica da MDMA é também importante para a sua actividade farmacológica. A MDMA é uma excepção à regra que refere que, no caso dos compostos com estrutura anfetamínica, o isómero com configuração absoluta R tem características alucinogénicas mais intensas. O isómero S-(+)-MDMA (dextrorrotatório) possui uma actividade superior sobre o sistema nervoso central quando comparado com o seu isómero R (Nichols *et al.*, 1986; Oberlender e Nichols, 1988). Além destas diferentes actividades farmacológicas, os dois enantiómeros possuem biodisponibilidade e metabolismo distintos. É

importante referir que, apesar destas diferenças, o "ecstasy" é consumido como mistura racémica;

v) outra característica estrutural importante e com implicações na sua farmacocinética é o facto destes compostos serem aminas, podendo existir na forma de sal ou de base livre. As bases livres são muito voláteis e insolúveis em água, enquanto que os sais são facilmente solúveis em água, podendo assim a MDMA ser administrada por via intravenosa ou oral. A administração oral é de longe a mais usada no caso desta droga, dado que a MDMA é normalmente vendida em comprimidos (Moore *et al.*, 1996).

Metabolismo da 3,4-metilenedioximetanfetamina (MDMA)

As principais vias metabólicas da MDMA estão descritas pormenorizadamente (Ensslin *et al.*, 1996; Kreth *et al.*, 2000; Maurer *et al.*, 2000) e as mais relevantes, em termos quantitativos, estão apresentadas na Figura 3. As principais vias envolvidas no metabolismo da MDMA em mamíferos são a *O*-desmetilenação, a *N*-desmetilação, a desaminação (com posterior oxidação ao derivado do ácido benzóico respectivo) e a conjugação. A conjugação pode decorrer por: (i) *O*-metilação dos metabolitos *O*-desmetilenados por acção da COMT (catecol-*O*-metiltransferase), (ii) conjugação com o ácido glucurónico (O-glucuronidação), (iii) conjugação com moléculas endógenas contendo o grupo tiol – glutationa, cisteína, *N*-acetilcisteína, (iv) e conjugação com a glicina ou (v) com o grupo sulfato (O-sulfatação), podendo estas reacções ocorrer simultaneamente (Lim e Foltz, 1988) (Figura 3). O isómero S-(+)-MDMA é metabolizado mais rápida e extensivamente do que o isómero R-(–)-MDMA (Cho *et al.*, 1990).

A maior parte da MDMA absorvida sofre *O*-desmetilenação a 3,4-diidroximetanfetamina (N-metil-α-metildopamina, N-Me-α-MeDA) pela isoenzima do citocromo P450 CYP2D6 (Tucker *et al.*, 1994; Lin *et al.*, 1997; Wu *et al.*, 1997), considerando-se também importante, neste passo metabólico, a contribuição de outras isoenzimas (CYP1A2, 2B6 e 3A4) (Kreth *et al.*, 2000; Maurer *et al.*, 2000). Algumas das enzimas referidas saturam com concentrações relativamente baixas de MDMA. Assim, pode acontecer que, para doses mais elevadas, estas enzimas fiquem saturadas e, deste modo, quantidades desproporcionadamente elevadas de MDMA são detectadas noutros tecidos, como sangue ou cérebro (de la Torre *et al.*, 2000). A *O*-desmetilenação

prefigura-se como um passo de toxificação, visto que origina compostos com o grupo catecol, os quais se podem oxidar a *o*-quinona e produzir os efeitos tóxicos reconhecidos para este tipo de compostos (Monks *et al.*, 2004). Uma parte significativa da MDMA é também *N*-desmetilada, principalmente via CYP2B6 e, em menor extensão, CYP1A2 e 2D6, dando origem, em humanos, à formação da 3,4-metilenodioxianfetamina (MDA) (Maurer *et al.*, 2000), a qual pode também sofrer *O*-desmetilenação a 3,4-diidroxianfetamina (α-metildopamina, α-MeDA). Tanto a α-MeDA como a N-Me-α-MeDA (metabolitos com o grupo catecol livre) podem posteriormente ser monometiladas, por mediação da COMT, preferencialmente no grupo fenol da posição 3 do anel aromático, com formação da 4-hidroxi-3-metoxianfetamina (3-*O*-Me-α-MeDA) e da 4-hidroxi-3-metoximetanfetamina (3-*O*-Me-N-Me-α-MeDA). Esta metilação pode também ocorrer no fenol em C4, mas de uma forma menos espressiva do que a anterior. Como a velocidade da *O*-desmetilenação é superior à da *N*-desmetilação, os principais metabolitos da MDMA no plasma e na urina são precisamente a N-Me-α-MeDA, a qual pode atingir concentrações semelhantes à da MDMA, e a 3-*O*-Me-N-Me-α-MeDA (Segura *et al.*, 2001). Todos os metabolitos referidos podem ser identificados na urina, principalmente nas suas formas conjugadas com o sulfato e com o ácido glucurónico (Maurer, 1996; De la Torre *et al.*, 2000; Kraemer e Maurer, 2002). Os metabolitos não conjugados da MDMA estão presentes no sangue, cérebro, fígado, fezes e urina por um período de 24 horas após a administração da droga (Lim e Foltz, 1988). A subsequente degradação da cadeia lateral aminada dá origem a metabolitos oxodesaminados (metilcetonas) que podem ser posteriormente metabolizados aos respectivos ácidos benzóicos 3,4-dissubstituídos por conjugação com a glicina (NH_2CH_2COOH) (Maurer, 1996). Finalmente, a MDMA e a MDA também podem sofrer hidroxilação aromática, com formação de 6-OH-MDMA e 6-OH-MDA, que via desmetilenação originam respectivamente 2,4,5-triidroximetanfetamina (6-OH-N-Me-α-MeDA) e 2,4,5-triidroximetanfetamina (6-OH-α-MeDA) (Lim e Foltz, 1991), compostos aparentados à neurotoxina 6-hidroxidopamina. A conjugação posterior com o ácido glucurónico, sulfato, glicina e GSH são, aparentemente, passos metabólicos fundamentais na destoxificação da MDMA. Nos últimos anos tem-se assistido a um estudo mais aprofundado do papel destes metabolitos, principalmente os conjugados com a GSH, na toxicidade induzida por esta droga (Bai *et al.*, 1999; Monks *et al.*, 2004).

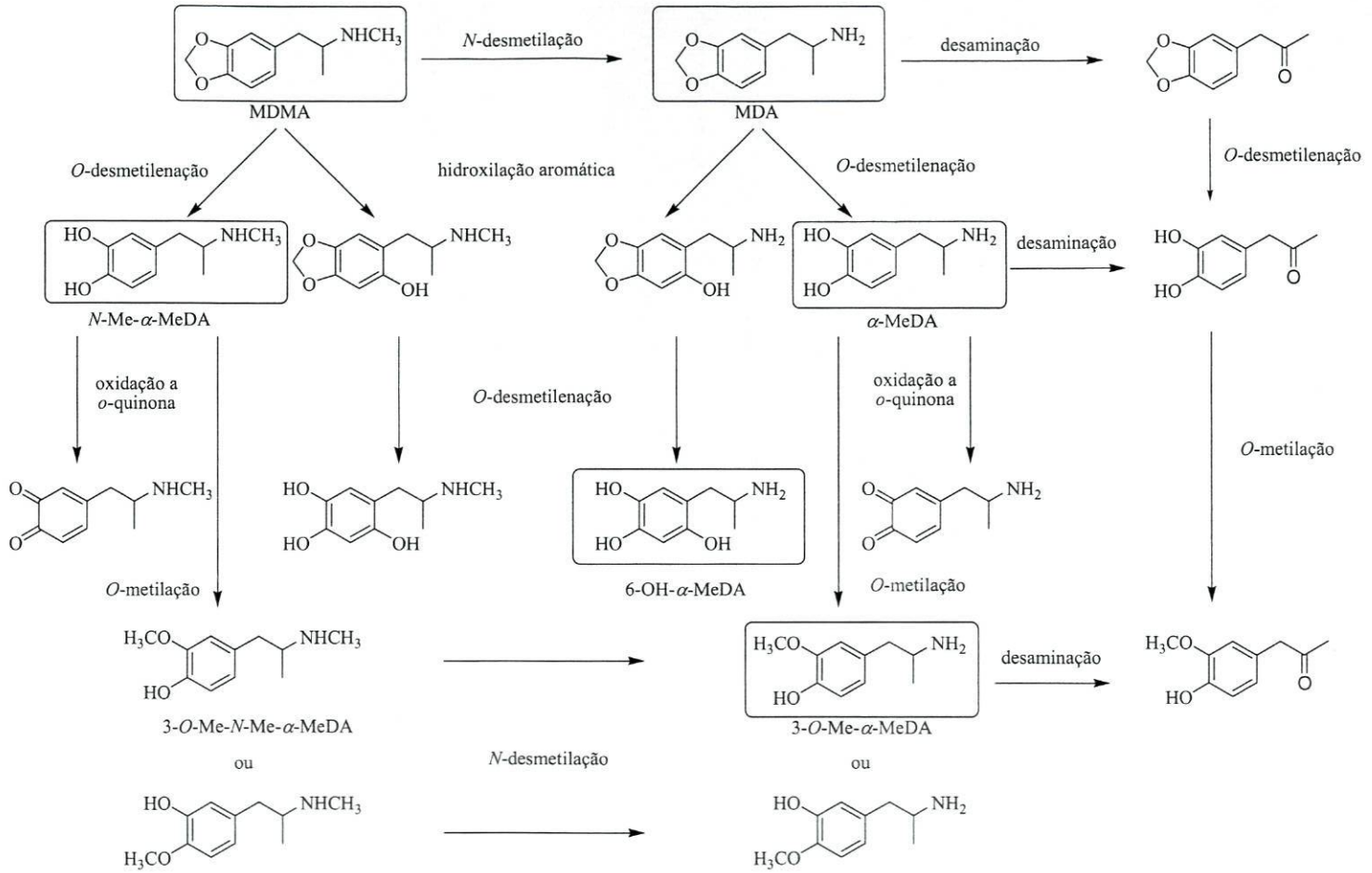

Figura 3. Principais vias metabólicas propostas para MDMA (esquema adaptado de Lim e Foltz, 1988 e de De la Torre *et al.*, 2004). Os compostos com possibilidade de se transformarem em *o*-quinonas podem sofrer conjugação posterior com o sulfato, ácido glucurónico ou compostos endógenos contendo o grupo tiol (glutationa, cisteína e *N*-acetilcisteína), enquanto as fenilacetonas sofrem conjugação posterior com a glicina.

Síntese da MDMA e dos seus principais metabolitos

A síntese de compostos contendo o núcleo geral das anfetaminas [$(C_6H_5CH_2CH(CH_3)NH_2)$] pode ser efectuada por um conjunto diversificado de caminhos reaccionais (Dal Cason, 1990; Błachut *et al.*, 2002; Freeman e Alder, 2002; Palhol *et al.*, 2002; Świst *et al.*, 2005a) (Figura 4). As principais vias usadas na síntese clandestina da MDMA são a síntese de Leuckart (a via mais usada na Europa, e que consiste na transformação do grupo carbonilo da 3,4-metilenodioxifenilpropan-2-ona num grupo *N*-formil e posterior hidrólise ou redução) (Verweij, 1989; Dal Cason, 1990), vários métodos de aminação redutiva, a via do nitropropeno (ou β-nitroestireno) e a via do bromopropano (Dal Cason, 1990).

Muitas vezes, a obtenção ilegal de drogas do tipo anfetamínico em geral, contendo o núcleo ($C_6H_5CH_2CH(CH_3)NH_2$), e da MDMA em particular, processa-se pela via do nitropropeno, através da preparação de um intermediário específico, o derivado β-metil-β-nitroestireno respectivo (Poortman e Lock, 1999). Este composto é obtido por uma reacção de condensação nitroaldólica, usando como materiais de partida o benzaldeído, com o padrão de substituição aromática adequada, e o nitroetano (Figura 5).

Apesar de a cada uma destas vias sintéticas estarem associadas vantagens e desvantagens (Dal Cason, 1990), os laboratórios de produção de "ecstasy" e outras drogas do tipo anfetamínico seleccionam os métodos sintéticos pela sua simplicidade de execução. Por norma, métodos que requerem menos passos intermediários e o mínimo de conhecimentos de síntese química e purificação de compostos orgânicos são os mais usados.

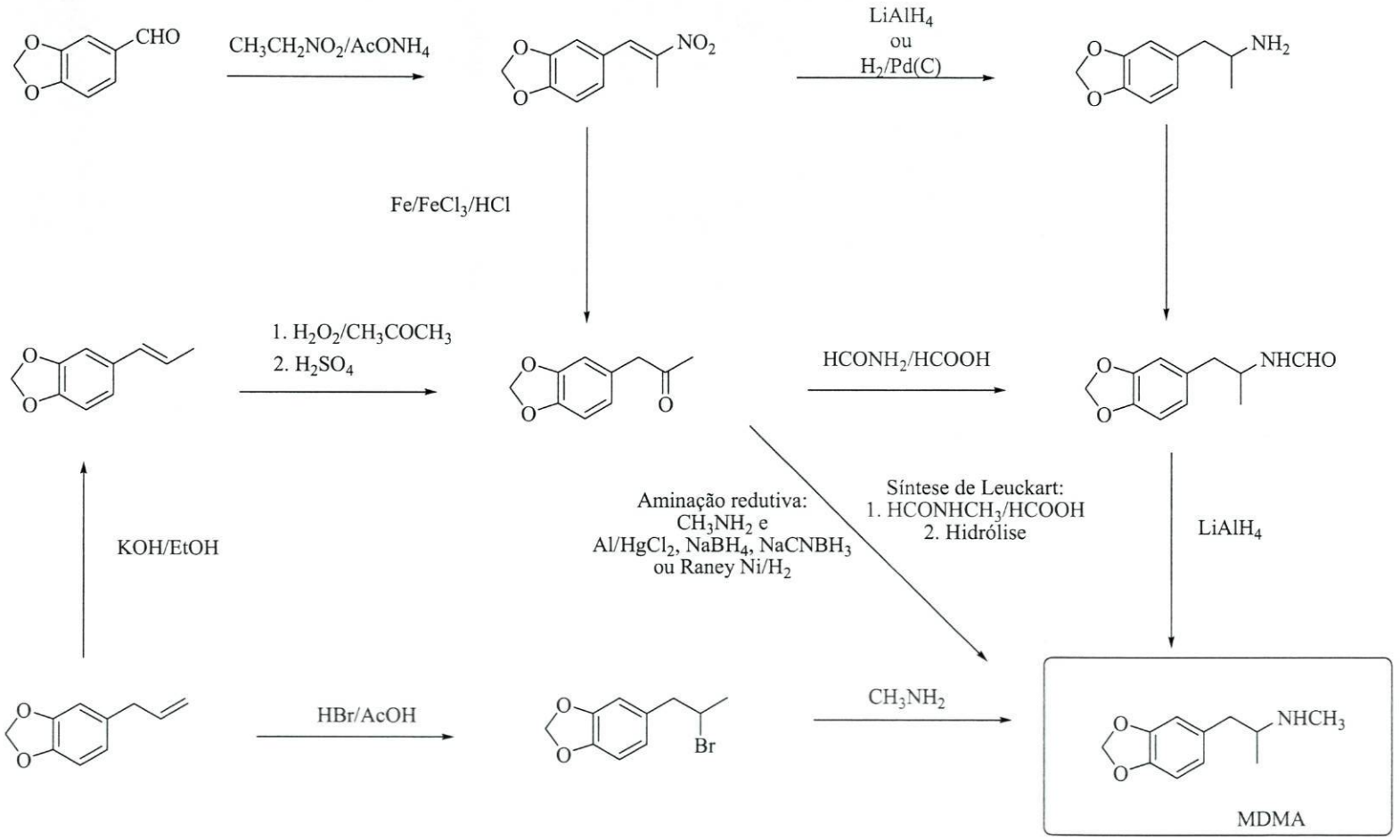

Figura 4. Principais vias sintéticas descritas para a obtenção da 3,4-metilenedioximetanfetamina (MDMA ou "ecstasy").

No trabalho constante desta dissertação, a escolha da via sintética recaiu sobre a via do nitropropeno, conforme esquematizado na Figura 5.

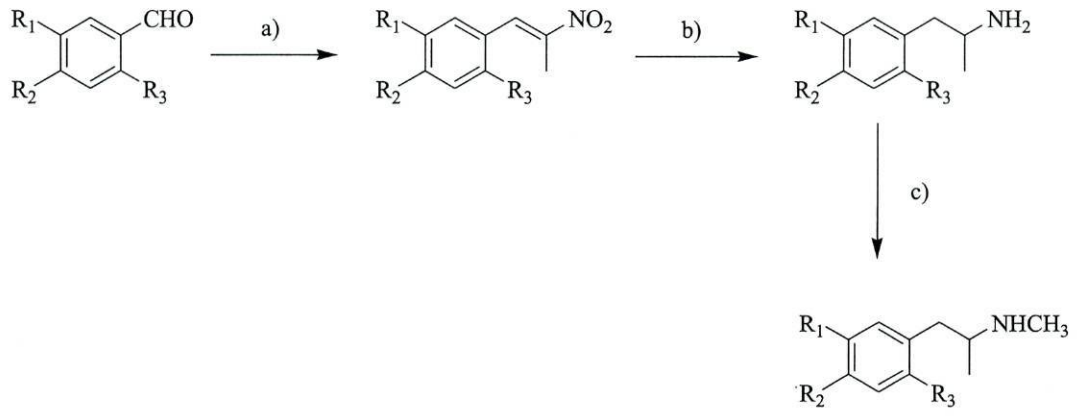

Figura 5. Esquema reaccional geral correspondente à síntese da MDMA e dos seus metabolitos. Condições reaccionais: a) $EtNO_2$, NH_4CH_3COO, refluxo; b) $LiAlH_4$, THF, refluxo; c) 1. $ClCOOC_2H_5$, H_2O, NaOH, 0 °C; 2. $LiAlH_4$, THF, refluxo. As condições pormenorizadas estão descritas no artigo apresentado em 8.6. Neste esquema não estão discriminados os passos de protecção e desprotecção dos grupos funcionais das moléculas.

Após a condensação nitroaldólica, os derivados do β-nitroestireno obtidos foram submetidos a uma reacção de redução simultânea da ligação dupla e do grupo nitro, com $LiAlH_4$ ou por hidrogenação catalítica. De salientar que a síntese de diferentes anfetaminas de uso mais generalizado, como a MDMA, a MDA, a 4-metoxianfetamina (PMA) e a 4-tiometilanfetamina (MTA) pode ser realizada através do esquema sintético proposto na Figura 5.

Como referido anteriormente, a simples substituição de um ou mais hidrogénios da amina terminal da MDA por grupos alquílicos (apenas um grupo CH_3 no caso da MDMA) transforma o composto noutros com maior potencial de abuso. Neste trabalho foram testadas várias vias sintéticas para a *N*-metilação da MDA (Figura 6), visto que este passo reaccional foi considerado limitante (quebra brusca de rendimento) na síntese esquematizada na Figura 5.

Os metabolitos da MDMA sintetizados estão assinalados na Figura 3 e estes estudos de síntese estão descritos mais pormenorizadamente na parte experimental, em artigos já publicados ou em publicação (ver em 8.5 e 8.6).

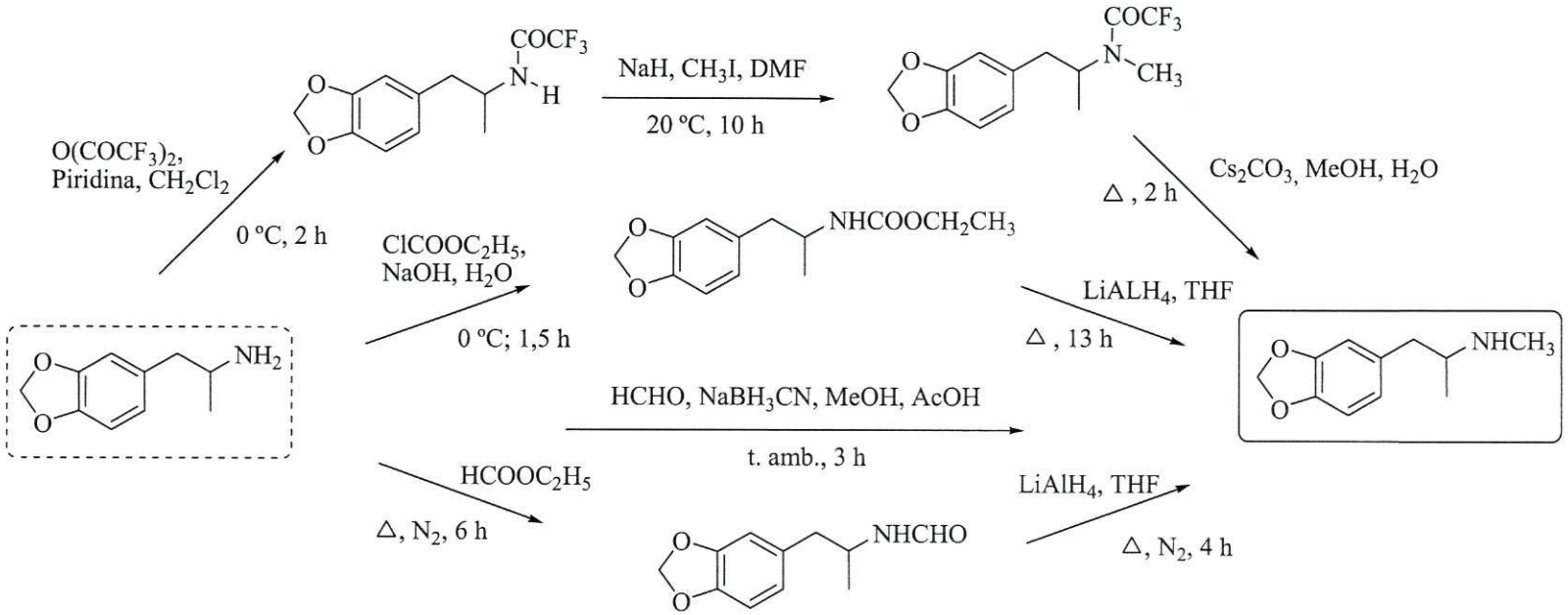

Figura 6. Vias sintéticas conducentes à *N*-metilação da 3,4-metilenodioxianfetamina (MDA).

3.2 Síntese de derivados do β-nitroestireno e do β-metil-β-nitroestireno

Compostos que possuem um grupo nitro (NO_2) conjugado com uma dupla ligação, nitroalcenos, e em particular compostos que têm por base o núcleo do β-nitroestireno ($C_6H_5CH=CHNO_2$), são matérias-primas extremamente versáteis em síntese orgânica. Estas nitrolefinas conjugadas funcionam como alcenos activados que podem ser facilmente usados na obtenção de uma enorme variedade de blocos construtores, sendo produtos de partida para a obtenção de nitroalcanos, aminas, cetoximas, hidroxilaminas ou aldoximas, por exemplo (Barret e Graboski, 1986).

Os β-nitroestirenos podem ser considerados como análogos nitrogenados de compostos carbonílicos α,β-insaturados e, por isso, são especialmente reactivos como aceitadores em adições de Michael ou como dienófilos fortes em reacções de Diels-Alder. Através deste tipo de mecanismos, os β-nitroestirenos, devido às suas propriedades electrofílicas, podem sofrer reacções de adição com vários nucleófilos (Varma *et al.*, 1997) e assim formar aductos com vários compostos, como, por exemplo, a vitamina C (Schmidt e Eger, 1996) e compostos organometálicos (Yao *et al.*, 1996; Yao *et al.*, 1998).

A obtenção de derivados do β-nitroestireno pode ser realizada por nitração directa do estireno (Varma *et al.*, 1998). No entanto, a via mais comum corresponde a uma reacção de condensação nitroaldólica entre o benzaldeído, com o padrão de substituição aromática pretendido, e o nitroalcano considerado adequado. Esta via sintética envolve, em primeiro lugar, uma reacção de Henry entre o composto carbonílico e o nitroalcano, ocorrendo por um ataque do carbanião do nitroalcano, estabilizado pela presença do grupo retirador de electrões, ao grupo carbonilo. Este passo dá origem a um β-nitroálcool, o qual sofre desidratação posterior, formando o β-nitroestireno pretendido (Figura 7). O composto intermediário nem sempre se consegue isolar facilmente, principalmente quando se usam aldeídos aromáticos (Ballini e Bosica, 1997).

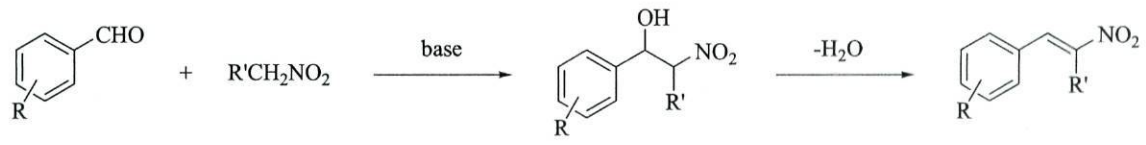

Figura 7. Esquema geral da síntese dos derivados do β-nitroestireno (R' = H) e do β-metil-β-nitroestireno (R' = CH_3).

A condensação nitroaldólica é uma reacção clássica de síntese que implica a formação de uma ligação carbono-carbono. Esta reacção dá-se, preferencialmente, na presença de um catalisador básico, de natureza orgânica ou inorgânica, incluindo aminas primárias e terciárias, hidróxidos de metais alcalinos, carbonatos e alcóxidos (Ballini e Bosica, 1997; Wang e Wang, 2002). O acetato de amónio é uma das bases mais vulgarmente usadas na catálise desta reacção, ou, em alternativa, podem usar-se soluções tampão de acetato de amónio em ácido acético (Gairaud e Lappin, 1953). Alguns estudos efectuados também descrevem a aplicação de catálise heterogénea, como, por exemplo, propilamina ancorada em suportes de sílica; este processo origina bons resultados em termos de rendimento e de pureza do produto final (Demicheli *et al.*, 2001; Sartori *et al.*, 2004). De modo a minimizar o aquecimento da reacção a temperaturas elevadas (necessário para que a reacção ocorra num período de tempo útil) tem sido também proposto o uso de microondas (Varma *et al.*, 1997). Paralelamente a esta reacção de condensação podem ocorrer outras reacções indesejadas, como a reacção de Cannizzaro (devido ao uso do aldeído e do catalisador básico) ou até mesmo polimerização aquando da formação dos nitroalcenos (Sartori *et al.*, 2004). Estas reacções podem ser minimizadas, ou mesmo completamente evitadas, através de um controlo cuidadoso do carácter básico do catalisador usado (Barret e Graboski, 1986).

Os nitroestirenos são altamente insolúveis em água e, por isso, a reacção normalmente decorre em meio não aquoso. Devido à existência de uma deslocalização electrónica pronunciada ao longo da dupla ligação e do anel aromático (sistema altamente conjugado), estes compostos são normalmente muito corados, com colorações que vão do amarelo ao cor-de-laranja intenso. Os derivados do β-nitroestireno apresentam uma predominância do isómero *E* (trans). Como nestes sistemas o grupo nitro está relativamente distante do anel aromático e conjugado com uma ligação dupla etilénica, estes compostos permitem o estudo das consequências da transmissão dos efeitos electrónicos dos substituintes a uma longa distância (Clavijo *et. al.*, 1994).

Na presente dissertação duas séries de nitroestirenos (derivados do β-nitroestireno e do β-metil-β-nitroestireno) foram sintetizadas, partindo dos benzaldeídos com a substituição no grupo aromático correspondente ao produto final desejado. A via sintética usada foi a reacção de Henry, por condensação com nitrometano, para os derivados do β-nitroestireno, ou com nitroetano, para os derivados do β-metil-β-nitroestireno. Os próprios nitroalcanos foram usados como solventes da reacção e foram aquecidos a refluxo, usando acetato de amónio como catalisador. Estas condições reaccionais foram adaptadas de um procedimento descrito anteriormente (Parker *et al.*, 1998), traduzindo-se em rendimentos elevados, sempre acima de 70%.

Tabela 1. Derivados do β-nitroestireno e do β-metil-β-nitroestireno sintetizados.

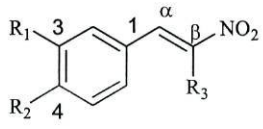

Composto	R_1	R_2	R_3
β-nitroestireno	H	H	H
β-metil-β-nitroestireno	H	H	CH_3
3,4-diidroxi-β-nitroestireno	OH	OH	H
3,4-diidroxi-β-metil-β-nitroestireno	OH	OH	CH_3
3,4-dimetoxi-β-nitroestireno	OCH_3	OCH_3	H
3,4-dimetoxi-β-metil-β-nitroestireno	OCH_3	OCH_3	CH_3
3-hidroxi-4-metoxi-β-nitroestireno	OH	OCH_3	H
3-hidroxi-4-metoxi-β-metil-β-nitroestireno	OH	OCH_3	CH_3
4-hidroxi-3-metoxi-β-nitroestireno	OCH_3	OH	H
4-hidroxi-3-metoxi-β-metil-β-nitroestireno	OCH_3	OH	CH_3
3,4-metilenodioxi-β-nitroestireno	$-OCH_2O-$		H
3,4-metilenodioxi-β-metil-β-nitroestireno	$-OCH_2O-$		CH_3

Os derivados do β-nitroestireno e do β-metil-β-nitroestireno sintetizados foram usados numa série de estudos de caracterização físico-química e estrutural e na avaliação da actividade antibacteriana, conforme descrito em 8.1, 8.2 e 8.3.

3.3 Síntese de aminocromos

As catecolaminas, como o próprio nome indica, são compostos que possuem na sua constituição química um grupo catecol – dois grupos hidroxilo fenólicos em C3 e C4 – e uma cadeia lateral em C1 com um grupo amina terminal (Figura 8).

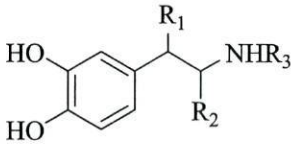

	R_1	R_2	R_3
adrenalina	OH	H	CH_3
noradrenalina	OH	H	H
dopamina	H	H	H
dopa	H	COOH	H
isoprenalina	OH	H	$CH(CH_3)_2$

Figura 8. Estrutura geral das catecolaminas estudadas nesta dissertação.

As catecolaminas endógenas (como, por exemplo, a adrenalina, a noradrenalina e a dopamina) são compostos simpaticomiméticos com uma acção primordial na condução dos estímulos nervosos (neurotransmissores), sendo que a adrenalina (ou epinefrina) e a noradrenalina são catecolaminas fundamentais na transmissão nervosa no sistema nervoso autónomo simpático. À acção da adrenalina estão associados estados de excitação, alerta, nervosismo ou medo e também o aumento da pressão sanguínea e dos batimentos cardíacos (Eisenhofer *et al.*, 2004). Assiste-se actualmente a um incremento do estudo deste tipo de compostos, nomeadamente a dopamina, devido essencialmente ao crescente interesse na investigação dos fenómenos moleculares associados à doença de Parkinson. Estes parecem estar relacionados, através do metabolismo oxidativo da dopamina, com uma perturbação da função dopaminérgica. As catecolaminas exógenas incluem alguns fármacos como a isoprenalina (ou isoproterenol) e também vários metabolitos, nomeadamente de anfetaminas, como a MDMA. A isoprenalina é uma catecolamina sintética que, apesar de actualmente não ser usada em terapêutica, é utilizada como modelo em estudos de metabolismo, bioactividade e toxicidade das catecolaminas.

Metabolismo das catecolaminas

A biotransformação das catecolaminas em humanos decorre, fundamentalmente, através de duas vias metabólicas principais, catalisadas pelas seguintes enzimas (Eisenhofer *et al.*, 1996) (Figura 9):

i) MAO (monoamina oxidase), que medeia a conversão das catecolaminas em compostos sem o grupo amina (desaminação oxidativa) e implicando a sua transformação em grupo aldeído e a

ii) COMT (catecol-*O*-metiltransferase), que catalisa a metilação do grupo fenol em C3 com a formação de um análogo metoxilado.

A MAO e a COMT distribuem-se de modo mais ou menos uniforme em todo o organismo, embora a quantidade de COMT em neurónios adrenérgicos seja relativamente inferior, quando comparada com a MAO. Todos os passos metabólicos descritos na Figura 9 concorrem entre si e ocorrem simultaneamente. As catecolaminas são normalmente excretadas na urina, sob a forma de derivados do ácido vanílico (Eisenhofer *et al.*, 1996). Outras reacções de fase II (conjugação com o sulfato, com o ácido glucurónico ou com moléculas endógenas contendo o grupo tiol) também representam um papel importante na biotransformação destes compostos.

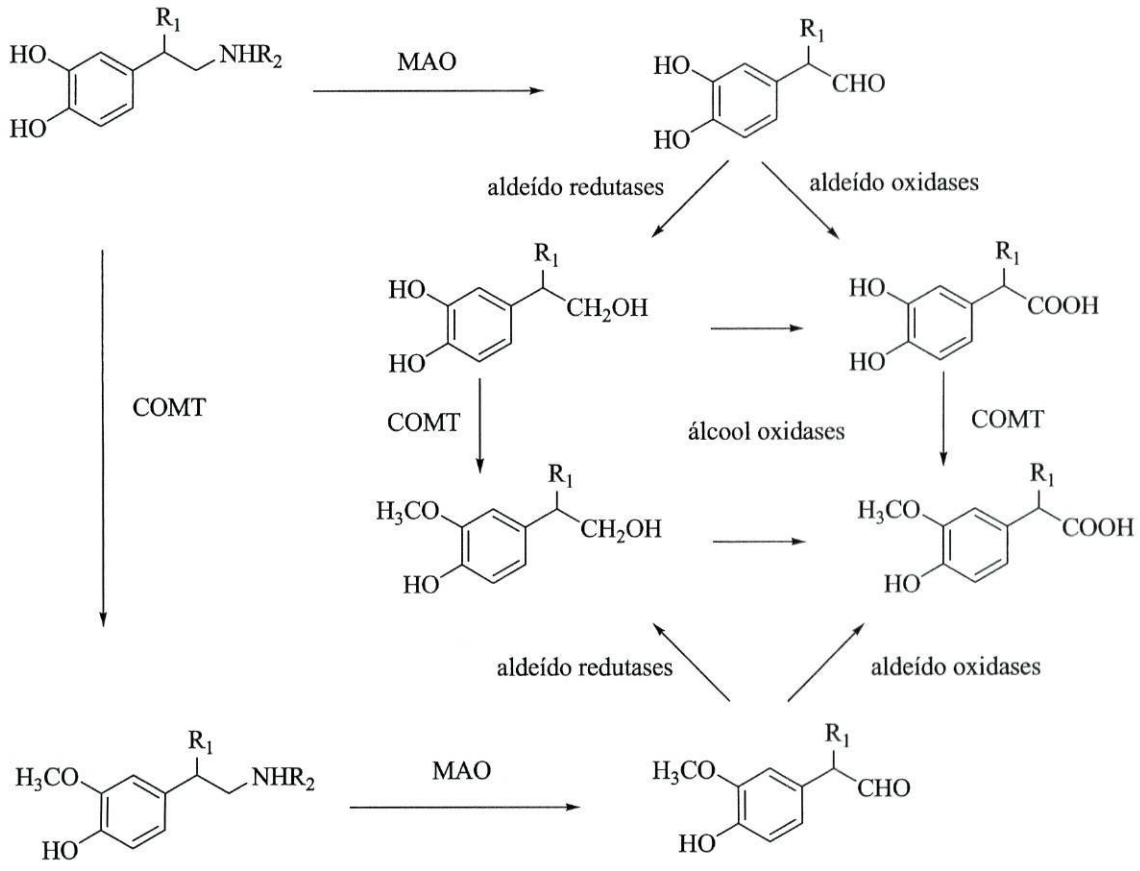

Figura 9. Principais passos metabólicos associados ao metabolismo das catecolaminas.

Apesar destas vias metabólicas serem as mais significativas *in vivo*, outras vias poderão ocorrer aquando da biotransformação das catecolaminas, nomeadamente o surgimento de metabolitos designados de aminocromos, provenientes da sua oxidação (Figura 10).

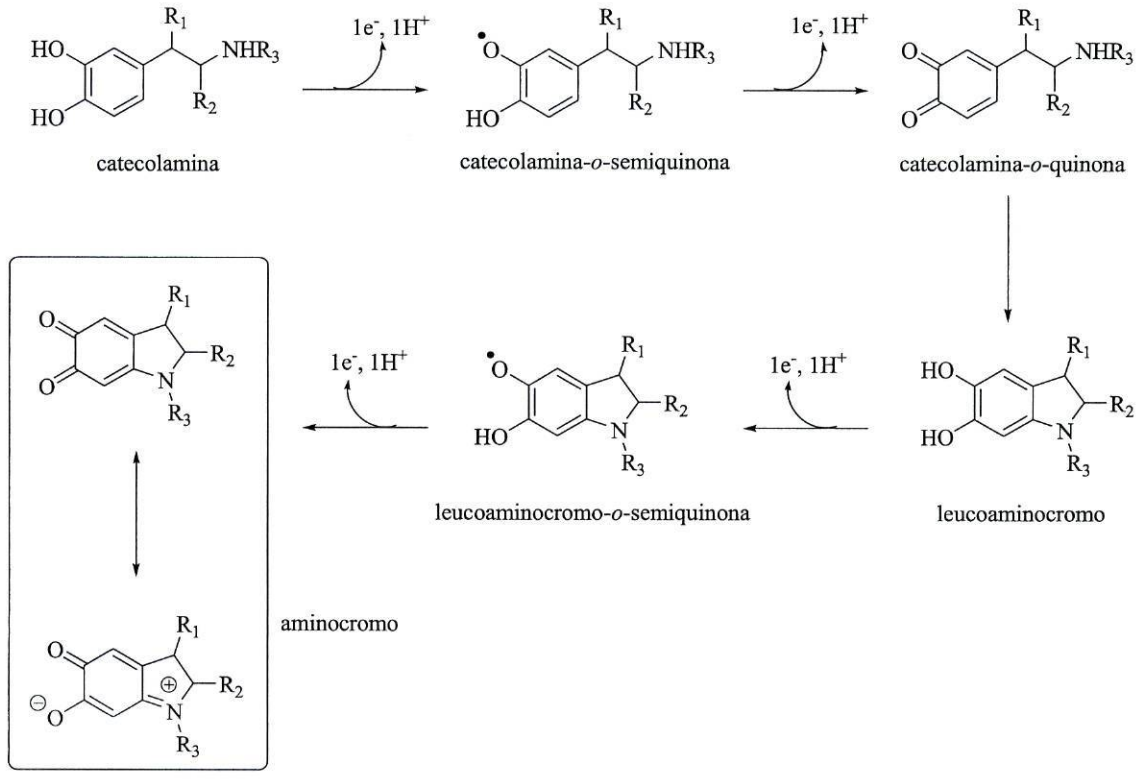

Figura 10. Mecanismo proposto para a oxidação *in vivo* das catecolaminas, com formação dos respectivos aminocromos (adaptado de Bindoli *et al.*, 1989 e Bindoli *et al.*, 1992).

Apesar do fenómeno de oxidação e autoxidação das catecolaminas em solução (originando pigmentos corados que polimerizam e formam melaninas insolúveis de cor negra) ser conhecido há muito tempo, a demonstração de que este fenómeno ocorre efectivamente *in vivo* é relativamente recente (Costa *et al.*, 1992). Estas evidências foram verificadas por identificação de dopaminocromo, da *o*-semiquinona da dopamina e também da sua *o*-hidroquinona no cérebro (Costa *et al.*, 1992).

Os metabolitos provenientes da oxidação das catecolaminas, como as suas *o*-quinonas, podem induzir stress oxidativo, sendo possíveis mediadores bioquímicos de uma série de manifestações tóxicas atribuídas a este tipo de aminas (Michel e Hefti, 1990). Os aminocromos também podem surgir como metabolitos inerentes à presença de espécies reactivas de oxigénio (ROS, do inglês *reactive oxygen species*) (Misra e Fridovich, 1972; Bindoli *et al.*, 1989; Bindoli *et al.*, 1992). Contudo, o papel exacto que os aminocromos podem assumir *in vivo* é ainda tema de amplo estudo, pensando-se que poderão participar na manifestação dos efeitos neurotóxicos e cardiotóxicos (Rona, 1985) induzidos pelas catecolaminas. A neurotoxicidade pode estar relacionada com o

facto dos aminocromos serem os precursores biossintéticos da neuromelanina, uma substância citotóxica *in vivo* (Graham, 1978). Por outro lado, a estes compostos estão também associadas manifestações bioquímicas de cardiotoxicidade (Dhalla *et al.*, 1978; Behonick *et al.*, 2001), demonstradas através de ensaios *in vivo* (Rupp *et al.*, 1994) e *in vitro* (Remião *et al.*, 2001).

A oxidação *in vivo* das catecolaminas pode ocorrer por uma reacção de autoxidação catalisada pelo próprio composto, a qual pode ocorrer espontaneamente em ambiente aeróbio (Bindoli *et al.*, 1992; Remião *et al.*, 2001). Na autoxidação das catecolaminas as características do meio são fundamentais, nomeadamente o pH, a catálise por enzimas [xantina oxidase (Foppoli *et al.*, 1997), a peroxidase (Bindoli *et al.*, 1992), a tirosinase (Heacock, 1959), a lipoxigenase (Núñez-Delicado *et al.*, 1996), várias catecol oxidases (Bindoli *et al.*, 1992), a mieloperoxidase e a citocromo c oxidase] e metais de transição (Remião *et al.*, 2001; Remião *et al.*, 2002) ou espécies reactivas radicalares (Bindoli *et al.*, 1992). De facto, alguns catiões como o Cu^{2+}, Mn^{2+}, Co^{2+}, Fe^{3+} e vários quelatos contendo cobre e ferro (Bindoli *et al.*, 1992), a ceruloplasmina (contém cobre) (Bindoli *et al.*, 1992) e a ferrilmioglobina (Giulivi e Cadenas, 1998) são exemplos de agentes que também podem promover a formação *in vivo* de aminocromos.

A oxidação das catecolaminas é um processo que se desenrola em duas etapas fundamentais, nas quais ocorre a formação de um conjunto de intermediários bastante reactivos e em que o balanço final corresponde à remoção de um total de quatro electrões. As catecolaminas são inicialmente oxidadas às respectivas *o*-semiquinonas, que posteriormente, por dismutação e espontaneamente, originam as *o*-quinonas (compostos extremamente instáveis e reactivos). As *o*-quinonas das catecolaminas, dependendo das condições do meio reaccional, podem, então, sofrer uma ciclização 1,4-intramolecular irreversível, com formação de um composto de natureza indólica. Esta reacção envolve um ataque nucleofílico do átomo de azoto (não protonado) da cadeia lateral ao carbono da posição 6 do anel quinonóide activado, que nestas condições funciona como electrófilo, havendo formação de um intermediário instável designado de leucoaminocromo. Os leucoaminocromos são subsequentemente oxidados a aminocromos (2,3-diidroindol-5,6-dionas), através da formação de leucoaminocromo-*o*-semiquinonas (Harley-Mason, 1948; Bindoli *et al.*, 1989) (Figura 10).

Síntese

Os aminocromos foram estudados pela primeira vez na década de 1930 (Green e Richter, 1937) tendo por base a oxidação da adrenalina a um aminocromo de cor vermelha intensa, designado então por adrenocromo. Nos anos subsequentes, a reactividade e as propriedades físico-químicas dos aminocromos foram sendo progressivamente estudadas, principalmente através da caracterização sistemática do adrenocromo (Harley-Mason, 1948; Heacock, 1959; Heacock, 1965; Hawley *et al.*, 1967).

A conversão das catecolaminas em aminocromos depende da sua reactividade, a qual está intimamente relacionada com o número e tipo de substituintes presentes na molécula e que influenciam a velocidade e a extensão da ciclização (Hawley *et al.*, 1967; Chavdarian *et al.*, 1978). A presença de grupos dadores de electrões, como grupos alquílicos, na cadeia lateral carbonada aumenta a velocidade de ciclização, enquanto que a presença deste tipo de substituintes no átomo de azoto do grupo amina terminal também aumenta, mas muito mais significativamente, a velocidade desta reacção (Hawley *et al.*, 1967; Chavdarian *et al.*, 1978). Os efeitos estéricos também influenciam a ciclização, principalmente quando o substituinte é muito volumoso, enquanto que o pK_a da amina parece não se correlacionar com a velocidade de ciclização das catecolaminas (Chavdarian *et al.*, 1978).

A formação dos aminocromos pode ocorrer de forma independente do pH, embora, em meio alcalino, a tendência para a sua formação seja mais evidente. Os aminocomos apresentam-se, em solução aquosa, predominantemente na forma de quinoniminas de estrutura zwitteriónica (Harley-Mason, 1948), sendo moderadamente estáveis a temperaturas baixas e facilmente solúveis em água e álcoois. Em solução aquosa estes compostos sofrem um rearranjo espontâneo a pigmentos do tipo da aminolutina.

Os aminocromos, devido à sua elevada instabilidade, podem sofrer, em solução ou *in vivo*, vários tipos de rearranjos, resultantes de reacções de oxidação e redução (Heacock, 1959, Bindoli *et al.*, 1992). Todos estes compostos, aminocromos e os seus rearranjos, podem originar, com relativa facilidade, dímeros ou mesmo polímeros de cor escura e insolúveis (designados de melaninas) (Bindoli *et al.*, 1992). A redução dos

aminocromos a leucoaminocromos (compostos incolores) também parece ocorrer, em solução ou em meio biológico, como, por exemplo, na presença de determinados agentes antioxidantes (ácido ascórbico, glutationa ou redutases). Os aminocromos, como compostos electrofílicos que são, podem interagir com vários nucleófilos, como a GSH, por reacções de adição ou substituição, ou com aminas (presentes em proteínas, por exemplo), que embora nucleófilos mais fracos que os tióis, podem levar à formação de bases de Shiff e conjugados.

No presente trabalho, foram estudados vários processos conducentes à reacção de oxidação das catecolaminas (adrenalina, noradrenalina, dopa, dopamina e isoprenalina) e formação dos aminocromos correspondentes (respectivamente adrenocromo, noradrenocromo, dopacromo, dopaminocromo e isoprenocromo) (Figuras 8 e 10). Como foi referido anteriormente, a autoxidação das catecolaminas é um processo muito lento, tendo sido estudada a influência de um conjunto de agentes catalíticos, quer do tipo enzimático (catalisadores que actuam por um mecanismo oxidativo, como a peroxidase e a tirosinase), quer não enzimático (agentes oxidantes inorgânicos, como o hexacianoferrato (III) de potássio, o óxido de prata (I), o sulfato de cobre (II) e o periodato de sódio). O controlo das reacções foi efectuado por HPLC, que permitiu, através da comparação dos rendimentos, seleccionar o melhor agente oxidante. Após separação cromatográfica dos produtos da reacção, recolheram-se as fracções contendo os compostos resultantes da oxidação e estas foram analisadas por espectrometria de massa, de modo a detectar a presença dos aminocromos.

O desenvolvimento de uma metodologia de HPLC para monitorização da oxidação das catecolaminas e da formação dos respectivos aminocromos *in vivo* (ver em 4.1) está descrito mais detalhadamente na parte experimental (ver em 8.4).

3.4 Síntese de conjugados de glutationa com compostos do tipo fenólico

Como já foi referido anteriormente, no desenvolvimento de novos compostos com possível aplicabilidade terapêutica é fundamental o estudo dos seus metabolitos quimicamente reactivos, visto que, muitas vezes, estes são responsáveis pela toxicidade induzida pelo composto original. As empresas farmacêuticas têm vindo a implementar procedimentos para identificar as características estruturais que podem ser sujeitas a activação metabólica. Assim, é possível que através de modificações moleculares apropriadas, se minimize o potencial para bioactivação a electrófilos reactivos (Evans *et al.*, 2004; Kalgutkar e Soglia, 2005). Normalmente este tipo de aproximações envolve uma combinação de estudos *in vivo* e *in vitro* nos quais os metabolitos reactivos são identificados indirectamente através da caracterização estrutural dos produtos finais mais estáveis que se formam. Estes estudos foram incrementados nos últimos anos devido à melhoria significativa das metodologias analíticas, como a cromatografia líquida com detecção de massa (LC-MS/MS) e RMN.

Os catecóis (*orto*-hidroxibenzenos) representam um grupo funcional comum a um grande número de compostos. Muitas substâncias de origem natural, como, por exemplo, antioxidantes do tipo polifenólico (ácido cafeico, flavonóides, etc.) ou catecolaminas possuem um núcleo catecólico na sua constituição. Os catecóis também se podem formar *in vivo* durante os processos metabólicos de alguns xenobióticos. A título de exemplo, referem-se os hidrocarbonetos aromáticos que podem originar catecóis por hidroxilação aromática catalisada pelo citocromo P450 ou compostos que possuem grupos funcionais como éteres ou ésteres aromáticos, os quais também podem gerar catecóis *in vivo* (*e.g.* MDMA) (Brunmark e Cadenas, 1989; O'Brien, 1991).

Devido à presença de dois átomos de hidrogénio permutáveis estas moléculas são bastante reactivas em termos biológicos, tendo capacidade de manifestarem simultaneamente comportamento pró- e antioxidante. Normalmente a actividade pró-oxidante dos catecóis é evidenciada após a sua autoxidação com formação de *o*-quinonas reactivas, consideradas, na maior parte dos casos, como agentes citotóxicos (Brunmark e Cadenas, 1989; Monks *et al.*, 1992). As quinonas são simultaneamente

oxidantes (induzindo ciclos redox e stress oxidativo) e electrofílicas (formando aductos covalentes com macromoléculas endógenas).

In vivo, existem dois tipos principais de mecanismos de toxicidade associados à formação das quinonas:

(i) o primeiro, e mais estudado, manifesta-se pela ocorrência de uma reacção de adição de Michael que ocorre entre um nucleófilo celular e a quinona, e especificamente na posição mais electronicamente disponível (electrofílica) no anel aromático (Brunmark e Cadenas, 1989; O'Brien, 1991). Se o nucleófilo celular for a GSH (glutationa), este mecanismo pode levar à sua deplecção no meio intracelular. Proteínas possuindo o grupo tiol (especialmente contendo resíduos de cisteína) podem também actuar como nucleófilos, levando a um comprometimento da sua função. Finalmente outro tipo de aductos podem ser formados com as bases de DNA, devido aos átomos de azoto também poderem actuar como nucleófilos.

(ii) outro mecanismo de citotoxicidade relacionado com a formação de quinonas é o aumento do stress oxidativo causado por activação de ciclos redox intracelulares, os quais geram espécies reactivas de oxigénio e de azoto. Uma etapa possível de iniciação ocorre entre estas espécies reactivas e o catecol inicial (QH_2) levando à formação do radical semiquinona ($QH^{\bullet}$), ou da sua base conjugada ($Q^{\bullet-}$), visto que o pK_a da semiquinona é tendencialmente baixo (Brunmark e Cadenas, 1989). Um ciclo redox pode então estabelecer-se ocorrendo um primeiro passo de propagação ($Q^{\bullet-} + O_2 \rightarrow Q + O_2^{\bullet-}$), seguido de outro de redução envolvendo um electrão (mediada por enzimas como a citocromo P450 redutase), o qual converte Q novamente $Q^{\bullet-}$. *In vivo* o anião superóxido pode posteriormente ser transformado em peróxido de hidrogénio, numa reacção catalisada pela superóxido dismutase (SOD).

Contudo não se devem descartar outros mecanismos, que podem ocorrer no meio extracelular, nomeadamente a autoxidação do catecol e posterior formação de peróxido de hidrogénio. Este processo ocorre independente de sistemas enzimáticos (Watanabe e Forman, 2003), não exigindo um ciclo redox. Em qualquer dos casos, o mecanismo de acção *in vivo* requer a biorredução da quinona como primeiro passo na activação (Monks *et al.*, 1992).

A GSH (γ-glutamil-L-cisteinilglicina) é um tripeptídeo que faz parte do sistema antioxidante endógeno e que é encontrado em quase todas as células vivas das bactérias, plantas e animais, sendo particularmente abundante no fígado (Boyland e Chasseaud, 1969). A GSH possui propriedades nucleofílicas, inerentes ao grupo sulfidrilo do resíduo de cisteína, podendo através do átomo de enxofre efectuar um ataque nucleofílico ao sistema quinonóide, altamente deficiente de electrões, e levar à formação de compostos de adição ou conjugação chamados de aductos ou conjugados. A adição nucleofílica a uma quinona representa uma reacção de redução envolvendo dois electrões (Monks *et al.*, 1992) e corresponde à adição do grupo tiol à dupla ligação do sistema carbonílico α,β-insaturado.

Um grande número de compostos electrofílicos podem formar conjugados com a glutationa, como, por exemplo, compostos fenólicos (Figura 11). Este processo pode decorrer não enzimaticamente ou, de modo mais eficiente, por catálise de S-transferases.

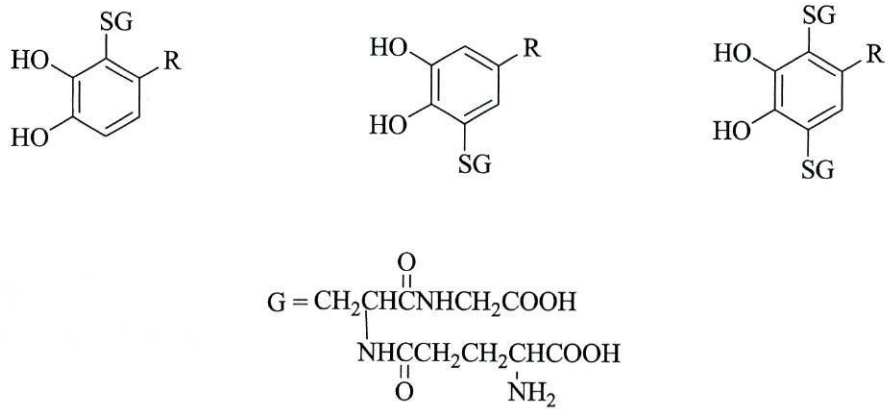

Figura 11. Estrutura química dos conjugados da glutationa com compostos catecólicos estudados. Os conjugados com o ácido cafeico: ácido 2-S-glutationilcafeico, ácido 5-S-glutationilcafeico e ácido 2,5-S-diglutationilcafeico correspondem aos compostos possuindo R = CH=CHCOOH. Os conjugados com a α-metildopamina: 2-S-glutationil-α-metildopamina, 5-S-glutationil-α-metildopamina e 2,5-S-diglutationil-α-metildopamina correspondem aos compostos possuindo R = $CH_2CH(CH_3)NH_2$.

O papel destes compostos está ainda a ser estudado pela comunidade científica (Monks e Lau, 1997). Sabe-se, no entanto, que a conjugação com a glutationa é um dos processos de biotransformação no qual se formam compostos mais hidrofílicos, por

obtenção dos derivados do ácido mercaptúrico, por hidrólise da glutationa a cisteína e posterior acetilação do resíduo de cisteína a N-acetilcisteína.

No entanto, devido à ubiquidade da glutationa no organismo (já foi detectada no fígado, cérebro, rim, etc.), estes conjugados podem formar-se no interior das células e induzir efeitos tóxicos. A precipitação destes conjugados e falência das funções celulares é apontada como a razão principal para a falência renal causada por alguns polifenóis, por exemplo (Monks e Lau, 1997).

Síntese de metabolitos de fase II da MDMA

No contexto desta dissertação, efectuou-se a síntese de metabolitos de fase II da MDMA, correspondentes à conjugação do seu metabolito de fase I α-MeDA com a glutationa (GSH).

A síntese de conjugados da α-MeDA com a glutationa foi adaptada de um procedimento experimental descrito anteriormente (Hiramatsu *et al.*, 1990; Miller *et al.*, 1995). Sucintamente, a uma solução de composto fenólico numa concentração de 2mM, em tampão de fosfato de sódio (50 mM; pH 7,4), foi adicionada tirosinase (200 U/ml). Após 1 min com agitação, juntou-se GSH numa concentração final de 10 mM. A mistura reaccional foi deixada a agitar durante mais 15 min e o decurso da reaccção foi monitorizado por HPLC (mesmas condições usadas no trabalho preparativo). No final da reacção a enzima foi precipitada por adição de 1% de HCOOH. Após filtração por um filtro de 0,2 μm de diâmetro, a solução foi purificada por HPLC preparativo – fase estacionária: RP18, 5 μm, 250 × 10 mm; volume de injecção: 175 μl; fase móvel: 1% HCOOH em H_2O/metanol (95:5) a um fluxo de 3 ml/min, usando um detector espectrofotométrico a cerca de 300 nm. As fracções contendo preferencialmente o monoconjugado com a glutationa e o biconjugado (detectados por espectrometria de massa) foram reunidas e liofilizadas e os produtos finais controlados por RMN e EM.

Esta parte do trabalho foi realizada no Centro de Toxicologia Molecular e Celular da Universidade do Texas em Austin e os compostos sintetizados e isolados (5-S-glutationil-α-MeDA e 2,5-S-diglutationil-α-MeDA) foram usados no trabalho experimental apresentado em anexo nesta dissertação (ver em 11.1) e num outro trabalho em que foi estudada a nefrotoxicidade destes conjugados (Carvalho *et al.*, 2002).

Síntese de metabolitos de fase II do ácido cafeico

A autoxidação e a oxidação enzimática dos derivados do ácido cafeico (antioxidante natural existente, por exemplo, nas uvas e no vinho) são consideradas reacções indesejáveis em produtos alimentares de origem vegetal, visto que podem conduzir, por exemplo, a perda nutricional e toxicidade (Cillier e Singleton, 1991). A extensão da oxidação deste tipo de compostos está muito dependente de vários factores, como o pH, a concentração de oxigénio e a presença de enzimas como polifenol oxidases (Cillier e Singleton, 1989; Cheynier e Moutounet, 1992), e que podem levar à formação de compostos altamente reactivos do tipo *o*-quinona. Estas *o*-quinonas do ácido cafeico podem ser reduzidas ou reagir com nucleófilos (Cillier e Singleton, 1990), verificando-se, na presença de glutationa, a formação simultânea de GSH oxidada e do(s) conjugado(s) do ácido cafeico com a GSH. A importância relativa destas reacções depende das concentrações de GSH e de ácido cafeico (Cheynier e Van Hulst, 1988; Cillier e Singleton, 1990). Embora se tivessem já identificado estes aductos no vinho ainda não se sabe qual o seu perfil de toxicidade. Os trabalhos até agora realizados permitiram verificar que o ácido cafeico e o seu conjugado ácido 2-S-glutationilcafeico são respectivamente inibidores irreversíveis e reversíveis das enzimas glutationa S-transferases (GST) (Ploemen *et al.*, 1993).

Assim, a partir do conhecimento da reactividade química das *o*-quinonas de compostos fenólicos (evidenciada pelos estudos de síntese dos conjugados da α-MeDA), efectuou-se um estudo preliminar de síntese de conjugados entre o ácido cafeico e a GSH. A metodologia sintética anteriormente descrita foi aplicada à obtenção destes aductos, procedendo-se a ligeiras alterações. Deste modo, efectuaram-se apenas ajustes nas condições cromatográficas: a fase móvel usada foi 1% HCOOH em H_2O/metanol (80:20). Nestas condições obtiveram-se vários compostos, sendo que as fracções contendo o composto maioritário foram reunidas, liofilizadas e o produto obtido foi identificado, por RMN (Figura 12) e EM, como o monoaducto do ácido cafeico (correspondente à posição 2 no anel aromático, mais electrofílica) com a GSH.

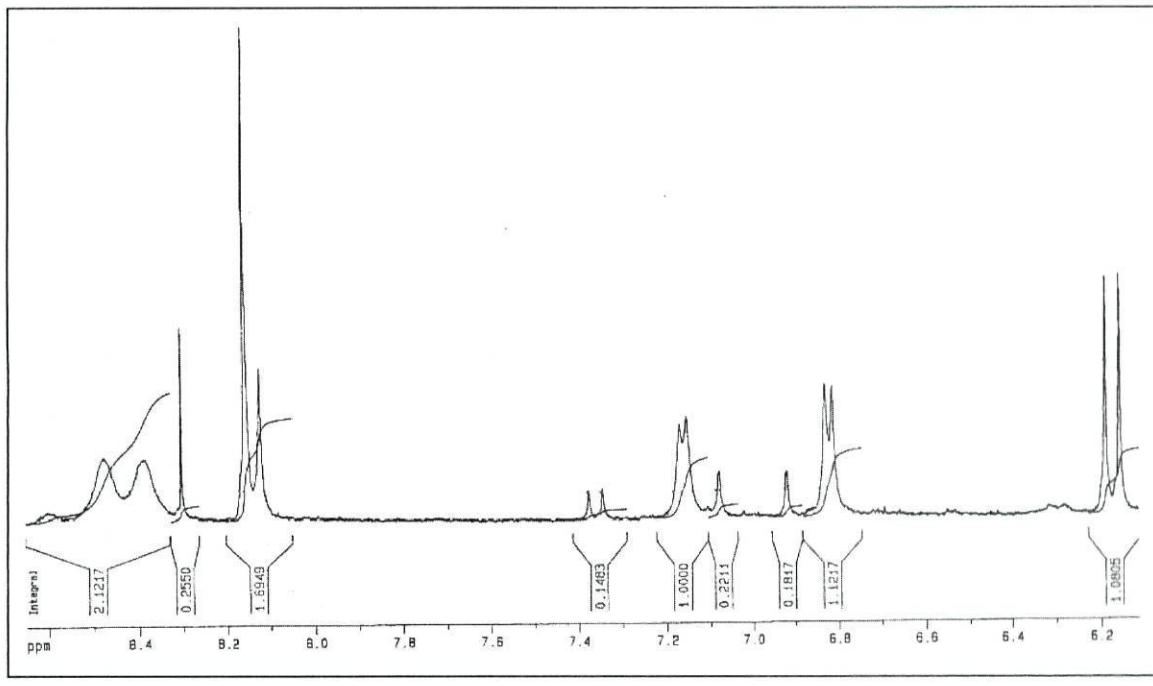

Figura 12. Parte do espectro de RMN de ^{1}H da mistura de diastereoisómeros obtida da reacção de síntese de conjugados do ácido cafeico com a glutationa e onde estão representados os protões aromáticos e vinílicos. O produto maioritário desta reacção foi o ácido 2-S-glutationilcafeico que nesta zona do espectro apresenta os seguintes sinais: 6,18 (1H; *d*; *J*=15,9; Hα), 6,82 (1H; *d*; *J*=8,3; H(5)), 7,16 (1H; *d*; *J*=8,3, H(6)), 8,14 (1H; *d*; *J*=15,9; Hβ), 8.39 e 8.47 (2H; br*s*; OH).

Por análise do espectro de RMN de ^{1}H e de massa do produto de reacção entre o ácido cafeico e a glutationa (registado em dimetilsulfóxido-*d*6 num espectrómetro que opera a 500,13 e 125,67 MHz) concluiu-se que as fracções recolhidas se tratavam de uma mistura de dois diastereoisómeros com a configuração *trans*, os ácidos 2-S-glutationilcafeico e 5-S-glutationilcafeico (numa razão de 83:17).

4. DESENVOLVIMENTO DE METODOLOGIAS ANALÍTICAS PARA APLICAÇÃO EM TOXICOLOGIA CLÍNICA E FORENSE

A procura de metodologias robustas que permitam, em Toxicologia Analítica e Forense, uma análise rápida e eficiente de um número crescente de amostras tem sido objecto de muitos estudos recentes. Nestas áreas de estudo, regista-se uma procura constante de metodologias sensíveis e não destrutivas, que possibilitem a análise *in situ* e que não exijam um tratamento complexo das amostras (amostras apreendidas pelas autoridades competentes ou amostras biológicas – sangue, urina, tecidos, entre outros).

Com o objectivo de contribuir para o estabelecimento de métodos com possível aplicação em laboratórios de análises clínicas e forenses, nesta dissertação efectuaram-se os seguintes trabalhos:

i) separação, identificação e quantificação de metabolitos de catecolaminas provenientes de reacções de oxidação, por HPLC e com detector de fotodíodos;

ii) caracterização espectroscópica, por espectroscopia de Raman, de anfetaminas, seus metabolitos principais e intermediários sintéticos e aplicação desta técnica na detecção e identificação inequívoca destes compostos.

4.1 Separação e análise de aminocromos por cromatografia líquida de alta eficiência (HPLC)

Poucas metodologias analíticas foram implementadas para a adequada detecção, separação e quantificação de aminocromos, quer *in vivo*, quer *in vitro* (Dhalla *et al.*, 1989; Ochs *et al.*, 2005). Apesar de alguns trabalhos descritos na literatura permitirem efectuar a análise de aminocromos, ainda não existe, tanto quanto foi possível apurar, um método que seja simultaneamente sensível e universal para detectar os aminocromos de todas as catecolaminas endógenas. Com este objectivo, foi desenvolvido, neste trabalho, uma metodologia para a separação e análise (qualitativa e quantitativa) de

aminocromos por cromatografia líquida de alta eficiência (HPLC, do inglês *high performance liquid chromatography*) com detecção por detector de fotodíodos (DAD, do inglês *photodiode array detector*) (Figura 13). Este método permitiu ainda separar e quantificar, em simultâneo, cada par catecolamina-aminocromo.

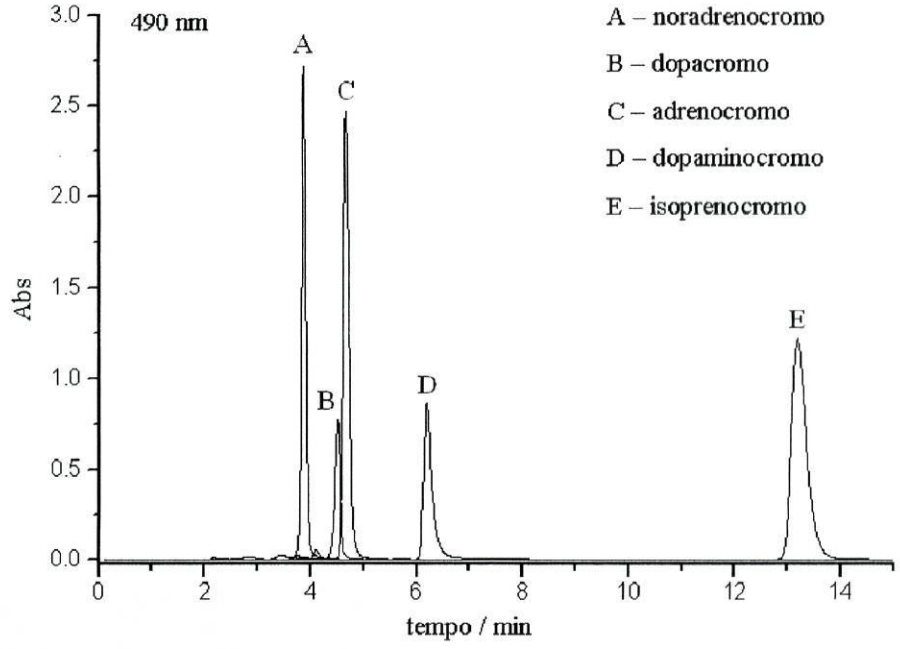

Figura 13. Cromatograma (490 nm) que representa a separação dos vários aminocromos, após a sua síntese a partir das catecolaminas respectivas, nas condições descritas na parte experimental (ver em 8.4).

A primeira parte do trabalho versou sobre o estudo do perfil e da velocidade de oxidação das catecolaminas na presença de vários agentes oxidantes não enzimáticos (hexacianoferrato (III) de potássio, óxido de prata (I), sulfato de cobre (II), periodato de sódio) ou enzimáticos (tirosinase). Deste estudo concluiu-se que o periodato de sódio permite um maior rendimento da reacção, enquanto que a tirosinase, por exemplo, possibilita uma oxidação gradual, embora em menor extensão, das catecolaminas estudadas. Após esta análise preliminar da oxidação das catecolaminas, sintetizaram-se os respectivos aminocromos, usando periodato de sódio, nas condições experimentais descritas (ver em 3.3 e 8.4). A reacção de oxidação das catecolaminas foi monitorizada

FACULDADE DE FARMÁCIA DO PORTO BIBLIOTECA

por HPLC-DAD e os cromatogramas foram analisados a 279 nm (comprimento de onda correspondente ao ponto do espectro onde se observa a absorvência máxima das catecolaminas) e a 490 nm (absorvência máxima dos aminocromos). A percentagem de oxidação das catecolaminas foi calculada como a percentagem de decréscimo da área do pico durante um intervalo de tempo especificado.

Devido à instabilidade dos aminocromos sintetizados, foram efectuados estudos prévios com o adrenocromo adquirido comercialmente e o produto de oxidação da adrenalina em solução. Assim, ambos os produtos foram caracterizados por espectrofotometria no UV/Vísivel e EM, tendo-se confirmado a identidade do produto sintetizado e o seu grau de pureza. A elevada pureza do adrenocromo obtido por este procedimento foi demonstrada por comparação da absorção a 490 nm numa dada concentração e uma solução da mesma concentração de adrenocromo comercial. Após estes estudos, efectuou-se a purificação por HPLC dos produtos brutos das reacções de oxidação das diferentes catecolaminas seguida da recolha das fracções contendo presumivelmente os aminocromos pretendidos, para posterior análise por espectrometria de massa. Esta técnica permitiu identificar todos os aminocromos obtidos e estabelecer os seus padrões de fragmentação (Lemos-Amado *et al.*, 2001), caracterizando-se assim, de forma inequívoca, a presença destes compostos nos produtos de oxidação das catecolaminas. O sistema analítico desenvolvido neste trabalho foi posteriormente aplicado à quantificação de adrenocromo em sangue de rato, após administração de adrenalina, permitindo prever, num futuro próximo, a sua aplicação como biomarcador de stress oxidativo induzido pelas catecolaminas.

Os resultados correspondentes à síntese de aminocromos, ao desenvolvimento do método analítico e a sua aplicação na detecção *in vivo* de aminocromos estão publicados e o artigo é apresentado na parte experimental (ver em 8.4).

4.2 Identificação de anfetaminas, metabolitos e seus intermediários de síntese por espectroscopia vibracional de Raman

Nos últimos anos tem havido um aumento do consumo, e consequentemente da produção ilegal, de uma enorme variedade de drogas ilícitas, com especial relevo para a MDMA e compostos relacionados. Este incremento deve-se, em grande parte, à facilidade de consulta de literatura adequada (que com a vulgarização da internet tem sido mais notória), ao acesso mais livre a matérias-primas e equipamento básico, e aos avanços químicos e tecnológicos que tornam os processos de síntese mais simples. Embora na União Europeia o comércio dos principais precursores directamente relacionados com a síntese da MDMA seja controlado, verifica-se que são apreendidas, todos os anos, quantidades significativas de comprimidos de MDMA.

Nas amostras de drogas ilícitas, a presença de impurezas, em quantidades mais ou menos elevadas, pode dever-se a uma série de factores (Gimeno *et al.*, 2002; Daéid e Waddell, 2005): (i) podem ser produtos intermediários da síntese ou subprodutos do processo de fabrico (reacções laterais); (ii) podem já estar presentes nos reagentes iniciais usados na síntese ou nos solventes, mantendo-se inalteradas até ao produto final ou sofrendo alterações durante os vários passos sintéticos; ou, finalmente, (iii) podem ser devidas às próprias condições de armazenamento (luz, humidade, temperatura, tipo de recipiente) ou à (iv) adição de substâncias com uma finalidade específica (diluentes, compostos que aumentem o efeito desejado, adulterantes, etc.) e que, por sua vez, ainda podem reagir com o composto original (Gimeno *et al.*, 2002). A quantidade destes produtos secundários e intermediários pode estar aumentada, em última instância, por erros nos procedimentos técnicos da síntese ou a uma purificação pouco cuidadosa, etapa sempre descurada na produção ilícita, orientada para o lucro mais rápido.

Os efeitos provocados pelo abuso de drogas psicoactivas têm sido amplamente estudados nos últimos anos; no entanto, as pesquisas efectuadas sobre os efeitos dos precursores sintéticos das drogas de abuso, os quais podem aparecer em quantidades relativamente elevadas nos produtos consumidos (Sondermann e Kovar, 1999; Gimeno *et al.*, 2002), têm sido insatisfatórias. A toxicidade muitas vezes atribuída às drogas ilícitas pode ser causada pela presença de produtos secundários na amostra, o que torna premente o desenvolvimento de metodologias que permitam a caracterização e identificação inequívoca destes compostos. Como exemplo, refere-se que a ingestão de

drogas de abuso contaminadas com nitroestirenos, intermediários da síntese de anfetaminas, pode levar à manifestação de efeitos indesejados nos seus consumidores, como alteração da resposta imune (Carter *et al.*, 2002).

Em anos mais recentes, tem sido efectuada uma análise exaustiva de amostras ilícitas de comprimidos de "ecstasy", tendo-se registado uma grande variabilidade na sua composição, quer qualitativa quer quantitativa (Sherlock *et al.*, 1999; Sondermann e Kovar, 1999). Uma enorme variedade de impurezas foi detectada em amostras de MDMA apreendidas (Verweij, 1992; Gimeno *et al.*, 2002; Palhol *et al.*, 2002; Świst *et al.*, 2005a; Świst *et al.*, 2005b; Świst *et al.*, 2005c), nomeadamente os principais precursores e intermediários sintéticos das vias mais comuns (síntese de Leuckart, aminação redutiva, vias do nitropropeno e do bromopropano): o isosafrol, o safrol, o piperonal (matéria-prima da via do nitropropeno) e a 3,4-metilenodioxifenilpropan-2-ona (3,4-MDP-2P) (Verweij, 1989; Gimeno *et al.*, 2002; Świst *et al.*, 2005a) (Figura 4). Alguns autores estabelecem ainda como uma das impurezas comuns da síntese da MDMA, os β-metil-β-nitroestirenos, obtidos pela via com o mesmo nome (Verweij, 1992). A preparação de compostos relacionados com a MDMA (*e.g.* MDA, MTA – 4-metiltioanfetamina, PMA – 4-metoxianfetamina ou DOM – 2,5-dimetoxi-4-metilanfetamina) ocorre, muitas vezes, também através da obtenção prévia do respectivo precursor β-metil-β-nitroestireno (Poortman e Lock, 1999). As impurezas específicas de cada uma das vias sintéticas anteriores podem ser usadas para a determinação do processo usado na produção ilícita das drogas do tipo anfetamínico, podendo funcionar como marcadores de síntese.

Nos últimos anos assiste-se a um crescente investimento no desenvolvimento de sistemas robustos, quer analíticos quer estatísticos, que possibilitem, através do conhecimento do perfil de impurezas da amostra, uma ligação das drogas apreendidas com a sua origem geográfica, permitindo a identificação do laboratório responsável pela produção da droga e concluindo se duas apreensões distintas correspondem ao mesmo produtor ou ao mesmo lote de produção (Verweij, 1989; Lurie *et al.*, 2000; Gimeno *et al.*, 2002).

Muitos processos são usados no estudo do perfil químico de amostras de MDMA e compostos relacionados (Daéid e Waddell, 2005), nomeadamente técnicas cromatográficas, como por exemplo a cromatografia gasosa acoplada a um espectrómetro de massa como detector (GC-MS) (Gimeno *et al.*, 2002; Gimeno *et al.*,

2003; Świst *et al.*, 2005a; Świst *et al.*, 2005b; Świst *et al.*, 2005c). Outra técnica cromatográfica igualmente muito utilizada é a cromatografia líquida de alta eficiência (HPLC), associada aos mais diversos tipos de detectores (Lurie *et al.*, 2000; Herráez-Hernández *et al.*, 2001). No entanto, estes métodos são destrutivos, implicando a perda da amostra, factor que é bastante relevante em análises forenses. No sentido de obviar este problema, assiste-se actualmente a um incremento do uso de técnicas espectroscópicas, as quais permitem também o estudo do perfil de impurezas em amostras apreendidas, nomeadamente espectroscopia de Raman (Bell *et al.*, 2000a; Bell *et al.*, 2000b).

Espectroscopia vibracional de Raman

Como qualquer técnica espectroscópica, a espectroscopia de Raman tem por base a interacção de uma radiação incidente com a matéria. Quando o campo eléctrico de uma onda electromagnética interage com uma amostra, a luz pode ser absorvida, transmitida ou difundida, sendo que os fenómenos de difusão podem dividir-se em três tipos:

i) difusão de Rayleigh (com carácter elástico), que possui a mesma frequência da radiação incidente, originando uma banda muito intensa mas com informação vibracional pouco relevante.

ii) difusão de anti-Stokes (com carácter inelástico), de frequência maior do que a radiação incidente, apresentado menor intensidade de bandas (região do espectro com desvio negativos relativamente à banda de Rayleigh).

iii) difusão de Stokes (com carácter inelástico), com menor frequência do que a radiação incidente, apresentando maior intensidade de bandas (região do espectro com desvio negativos relativamente à banda de Rayleigh). Esta é a zona normalmente observada experimentalmente.

Estes dois tipos de difusão inelástica de uma radiação monocromática correspondem ao denominado efeito de Raman, descrito pela primeira vez em 1928 por Chandrasekhar Venkata Raman (1888-1970) (Raman, 1928; Raman e Krishnan, 1928). Neste efeito a radiação incidente numa determinada amostra é difundida com frequência diferente, implicando por isso perdas ou ganhos energéticos. A maior parte da radiação

é absorvida ou transmitida, sendo que apenas uma fracção muito reduzida da radiação incidente (cerca de 1 ppm) é difundida por efeito de Raman (a maior parte da radiação difundida sofre colisão elástica) e, por isso, as bandas resultantes possuem uma intensidade extremamente baixa. Com o intuito de obviar este problema (baixa sensibilidade), recorre-se à excitação da amostra com uma fonte de radiação monocromática muito intensa (radiação laser), e ao uso de detectores muito sensíveis (como por exemplo, CCD, *charge coupled devices*).

Para uma molécula poder ser visualizada em termos de espectroscopia de Raman, a luz incidente e a perturbação induzida pelo campo eléctrico deve implicar alteração da polarizabilidade da molécula, uma propriedade que determina a extensão da difusão de fotões em Raman. A absorção no infravermelho, por seu lado, exige uma mudança no momento dipolar permanente durante a vibração e, consequentemente, as intensidades relativas das bandas produzidas por todas os complexos movimentos vibracionais da amostra serão muito diferentes nas duas técnicas, que se complementam. De facto, como algumas vibrações activas em Raman podem ser proibidas em infravermelho, estes dois métodos devem ser realizados em conjunto para um estudo vibracional completo da molécula (Ellis *et al.*, 1989).

Desde que foi descoberto o fenómeno de difusão inelástica da luz (Raman, 1928; Raman e Krishnan, 1928), a espectroscopia de Raman tem sido usada com bastante acuidade como instrumento analítico para a identificação de vários tipos de compostos (moleculares, iónicos, complexos, etc.), visto que produz um espectro que contém uma impressão digital de cada substância (especificidade), factor aliás comum a qualquer espectroscopia vibracional. Uma análise cuidada de um espectro de Raman fornece informação sobre algumas características das moléculas, como é o caso das propriedades conformacionais e os modos e tipos de vibração presentes, podendo extrair-se informação sobre os parâmetros geométricos dos compostos.

A Espectroscopia de Raman apresenta um conjunto de vantagens que devem ser analisadas e ponderadas de modo crítico quando se pretende a sua utilização em análise química aplicada a vários campos científicos (Hendra *et al.*, 1995; Vankeirsbilck *et al.*, 2002; Schmitt e Popp, 2006), tornando-a uma técnica analítica de rotina (quer em termos qualitativos quer quantitativos):

i) as bandas de Raman são geralmente mais estreitas do que as de infravermelho (IV), principalmente quando se estudam macromoléculas biológicas;

ii) os estudos podem ser conduzidos com compostos orgânicos ou inorgânicos, sólidos, líquidos e soluções (facto muito importante para estudos efectuados em condições fisiológicas ou em soluções aquosas), já que as bandas de água são muito pouco intensas em Raman ao contrário do que acontece em infravermelho;

iii) método não destrutivo da amostra;

iv) pode ser usada no estudo de substâncias corrosivas, tóxicas ou higroscópicas, sem comprometer a instrumentação ou o operador;

v) não exige tratamento prévio das amostras o que se traduz em completa recuperação desta e maior facilidade na amostragem;

vi) elevada especificidade (permite distinguir compostos muito similares entre si em termos químicos) e versatilidade;

vii) proporciona análises muito rápidas (por vezes menos de um minuto para a aquisição do espectro);

viii) quando se faz o estudo do preço por análise a espectroscopia de Raman acaba por se revelar um método económico, tendo, por isso, um custo por análise bastante competitivo;

ix) as análises por espectroscopia de Raman podem ser facilmente efectuadas por pessoal relativamente pouco treinado, devido à simplificação que os aparelhos têm sofrido ultimamente.

Apesar das vantagens enunciadas, algumas desvantagens estão inerentes ao uso desta técnica:

i) possui uma baixa sensibilidade; visto que apenas um pequeno número dos fotões incidentes é difundido inelasticamente; por isso, a detecção de compostos em baixas concentrações é limitada.

ii) o estudo de moléculas com elevada fluorescência é mais complicado.

Aliás, a fluorescência apresentada por algumas amostras (intrínseca ou devida a impurezas) é um problema que é necessário ultrapassar, de modo a obter um bom espectro de Raman. De facto, este efeito é, muitas vezes, mais intenso do que o efeito Raman, podendo o espectro estar totalmente encoberto pelas bandas de fluorescência. A intensidade da radiação de excitação, por seu lado, deve ser cuidadosamente ajustada (de acordo com a natureza do composto analisado), já que uma radiação incidente demasiado energética pode levar à degradação da amostra. Na técnica de Raman

convencional uma radiação laser monocromática é focada numa amostra e a luz dispersada é detectada, processada e monitorizada por um sistema espectrofotométrico. Os problemas inerentes à fluorescência da amostra podem ser eliminados se se recorrer a uma excitação com um laser no infravermelho próximo e a um interferómetro de IV modificado com transformadas de Fourier (Chase, 1986).

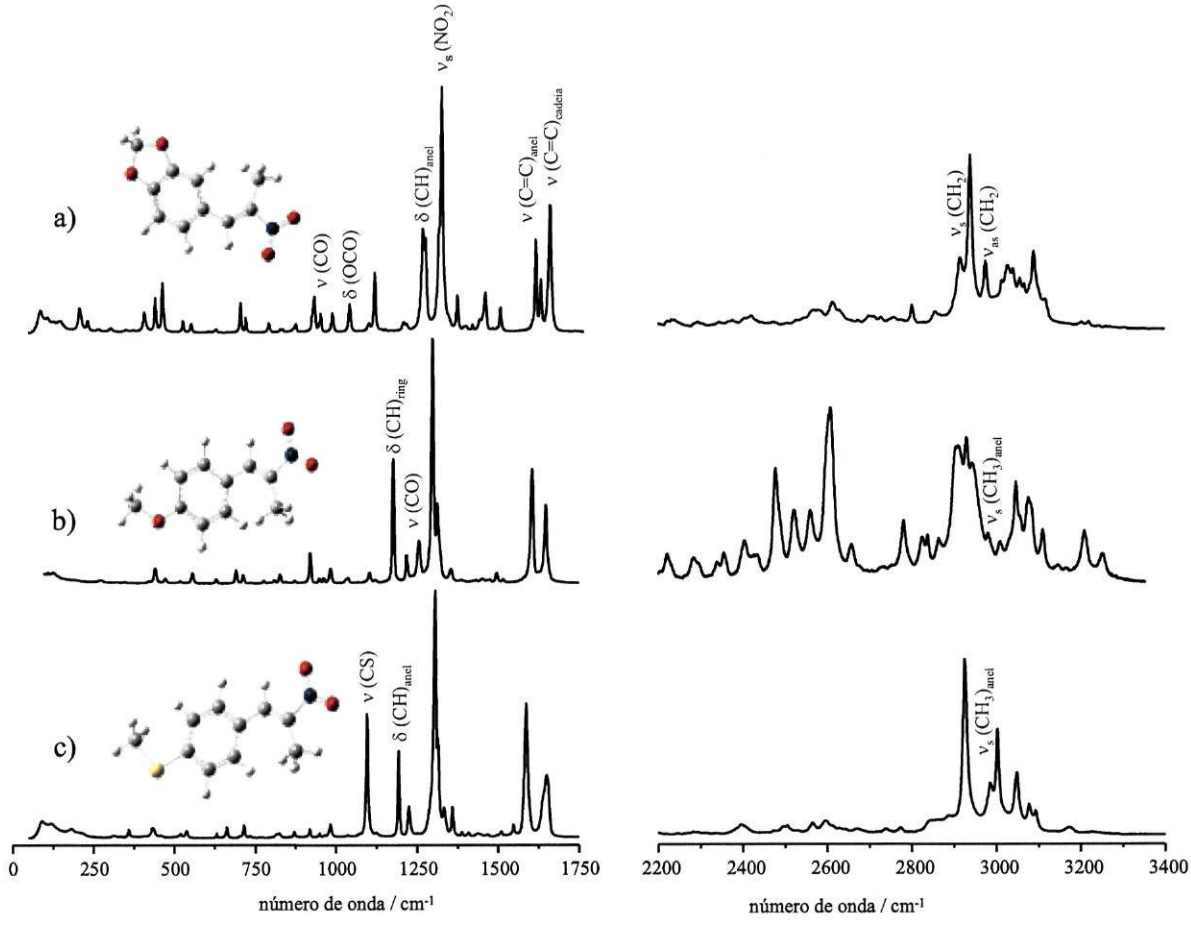

Figura 14. Espectros de Raman (FT-Raman) experimentais (75-1750 cm^{-1} e 2200-3400 cm^{-1}) dos seguintes β-metil-β-nitroestirenos precursores de drogas do tipo anfetamínico, no estado sólido a 25 °C: 3,4-metilenodioxi-β-metil-β-nitroestireno (**a**), 4-metoxi-β-metil-β-nitroestireno (**b**) e 4-metiltio-β-metil-β-nitroestireno (**c**) (δ – deformação angular no plano; ν – elongação; ν_s – elongação simétrica; ν_{as} – elongação anti-simétrica).

A interpretação de um espectro de Raman pode tornar-se uma tarefa difícil quando esta se baseia apenas em dados puramente experimentais, visto que a atribuição das bandas obtidas experimentalmente a vibrações específicas pode ser bastante ambígua. Uma atribuição que se pretenda fiável das bandas de Raman observadas exige, por isso, um conhecimento detalhado da estrutura geométrica e electrónica do composto e pode ser realizada por uma comparação com um espectro calculado teoricamente. Assim, cálculos de mecânica quântica (em particular ao nível do DFT) são actualmente complementos indispensáveis a uma análise do espectro de Raman. Existem presentemente programas computacionais específicos (como o Gaussian) para efectuar os cálculos das frequências vibracionais harmónicas e intensidades dos sinais nos espectros de Raman (ver em 5.1). Por comparação entre os cálculos e o espectro obtido experimentalmente, podem assim atribuir-se com segurança os vários modos de vibração do composto. Esta análise comparativa deve ser cuidadosa, principalmente porque os cálculos das frequências vibracionais são geralmente realizados considerando as moléculas isoladas ou em solução. No entanto, em amostras sólidas podem ocorrer interacções inter- e intramoleculares (*ex.* formação de dímeros por ligações de hidrogénio), que não são consideradas nos cálculos teóricos referidos.

A espectroscopia de Raman pode ser, deste modo, uma técnica analítica muito útil, em Química Farmacêutica, na identificação de matérias-primas (permitindo criar bibliotecas de espectros para posterior utilização), em determinações quantitativas ou semiquantitativas, em estudos de interacções fármaco-fármaco ou fármaco-excipiente (Carvalho *et al.*, 2006), ou em estudos de fenómenos de polimorfismo (Cutmore e Skett, 1993; Vankeirsbilck *et al.*, 2002). A técnica de espectroscopia de Raman provou, durante os últimos anos, ser também um método simples para análises clínicas ou forenses, especificamente no estudo da composição de comprimidos de "ecstasy" (Bell *et al.*, 2000a; Bell *et al.*, 2000b), ou de β-feniletilaminas relacionadas como a MDA, a anfetamina e a metanfetamina (Figura 2), mesmo na presença de adulterantes e/ou diluentes (Bell *et al.*, 2000b).

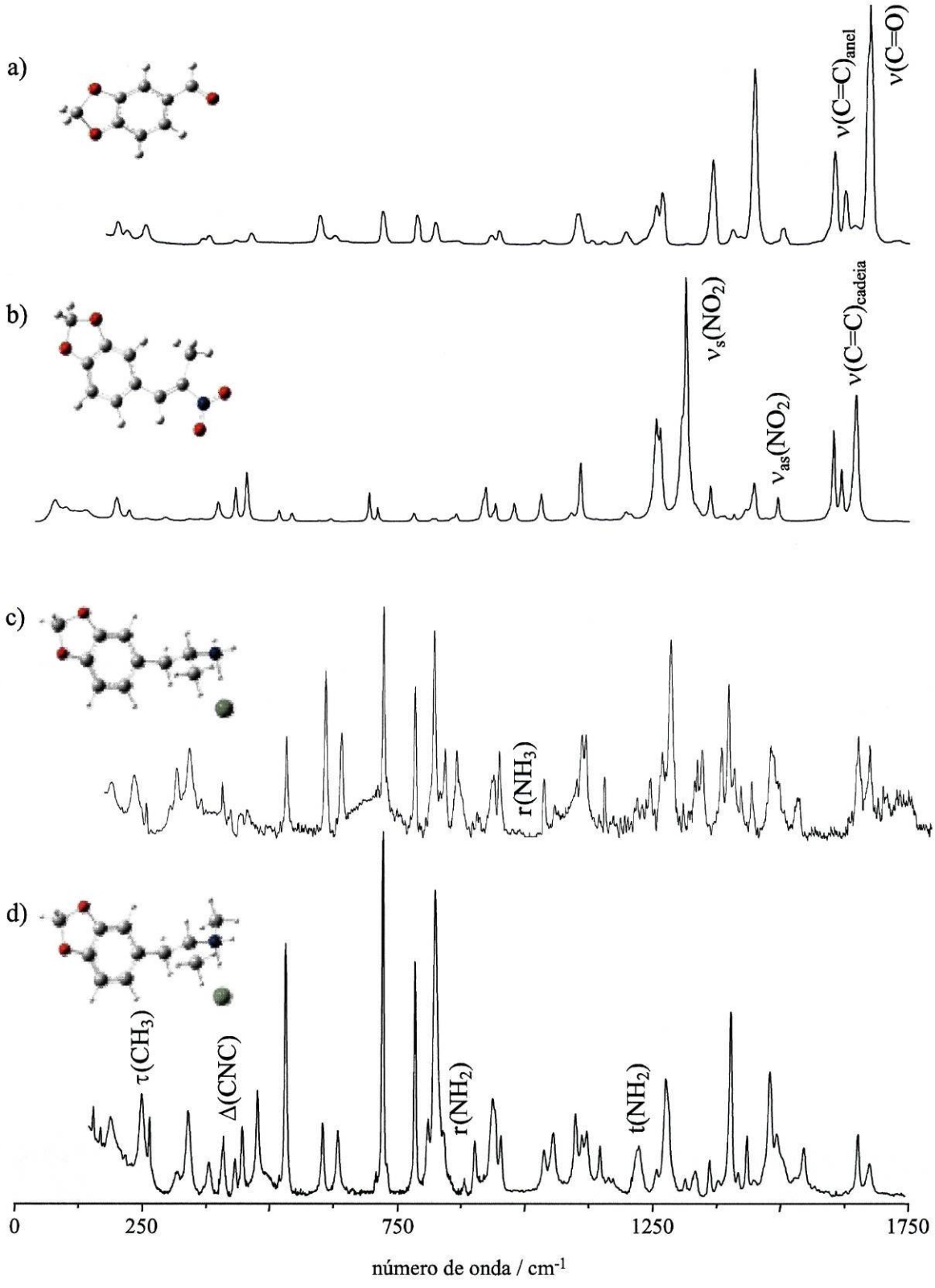

Figura 15. Espectros de Raman experimentais (100-1750 cm^{-1}) dos seguintes compostos, no estado sólido a 25 °C: piperonal (**a**), 3,4-metilenodioxi-β-metil-β-nitroestireno (**b**), MDA (**c**) e MDMA (**d**) – estes dois últimos na forma de cloridrato (Δ – deformação angular no plano dos átomos de esqueleto; ν – elongação; ν_s – elongação simétrica; ν_{as} – elongação anti-simétrica; r – *rocking*; t – *twisting* e τ – torção).

Com a finalidade de alargar a aplicabilidade desta técnica em análises forenses, foi desenvolvido no presente trabalho um conjunto de estudos que visam a identificação inequívoca de drogas – MDMA e MDA – e dos seus precursores e intermediários sintéticos do tipo β-nitroestireno (Figuras 14 e 15). Estes resultados estão apresentados na parte esperimental (ver em 8.1, 8.2 e 8.5). Num futuro próximo os resultados obtidos irão permitir engrossar o conjunto de informação existente para a identificação espectroscópica rápida e inequívoca de metabolitos, precursores e intermediários de síntese de drogas (By *et al.*, 1992), bem como das próprias drogas.

5. DETERMINAÇÃO DE PROPRIEDADES FÍSICO-QUÍMICAS E PARÂMETROS ESTRUTURAIS DOS COMPOSTOS SINTETIZADOS

Como referido anteriormente nesta dissertação, as características estruturais (conjunto de efeitos electrostáticos, hidrofóbicos e estéricos) de um determinado composto são responsáveis pelas suas propriedades físico-químicas, actividade biológica e também pelas suas propriedades farmacocinéticas (incluindo metabolismo).

Um elevado número de propriedades físico-químicas e estruturais têm sido descritas como tendo uma influência marcante no comportamento farmacocinético e farmacodinâmico de xenobióticos, permitindo até, em determinadas condições, prever estes comportamentos (Testa *et al.*, 2000a; Tavares, 2004). Esta previsão pode ser efectuada por SAR e/ou SPR, os quais estudam as modificações na estrutura de modo a melhorar a entrega e a ligação ao alvo. Algumas modificações estruturais efectuadas em SAR e SPR englobam parâmetros diversos como o tamanho molecular, a capacidade de estabelecimento de pontes de hidrogénio, a polaridade, a ionizabilidade e o bloqueio de posições consideradas instáveis. Estes estudos devem ser sempre complementados com a análise das propriedades físico-químicas, de modo a melhorar a ADME (absorção, distribuição, metabolismo e eliminação), como, por exemplo, a solubilidade, a lipofilia relativa das formas neutra e ionizada, a estabilidade físico-química, o pK_a (grau de ionização).

Com o objectivo de caracterizar estrutural e físico-quimicamente os compostos sintetizados para posterior estabelecimento de relações estrutura – propriedade físico-química – actividade biológica, realizaram-se os seguintes estudos:

i) cálculos de mecânica quântica para análise das preferências conformacionais dos compostos sintetizados;

ii) determinações dos potenciais redox por técnicas voltamétricas e

iii) cálculos dos coeficientes de partilha para avaliação do carácter lipofílico das substâncias em análise.

Um dos métodos *ab initio* mais comuns consiste no formalismo de Hartree-Fock de Campo Auto-Consistente (HF-SCF, do inglês *Self-Consistent Field*). Este método possui uma grande limitação, visto não considerar o tratamento dos possíveis efeitos de correlação electrónica (particularmente importantes em sistemas insaturados). Assim, recorreu-se à Teoria dos Funcionais de Densidade (DFT, do inglês *Density Functional Theory*), que considera os efeitos de correlação electrónica, segundo a seguinte expressão:

$$E = E^T + E^V + E^J + E^{XC}$$

Deste modo, a energia electrónica total (E) está dividida em quatro parcelas calculadas individualmente: a energia cinética proveniente do movimento dos electrões (E^T); a energia potencial associada à atracção núcleo-electrão e à repulsão núcleo-núcleo (E^V); o termo de repulsão electrão-electrão (E^J); e finalmente a energia de correlação electrónica, que representa todos os outros tipos de interacção electrão-electrão (E^{XC}) não incluídos nos termos anteriores. O método DFT representa assim a correlação electrónica através de funções de densidade, constituídas por uma junção de funções de troca e de correlação (*ex.* funcional B3LYP) (Russo *et al.*, 1995; Ignaczak e Gomes, 1996; Cotton e Feng, 1997; Cotton e Feng, 1998).

A análise conformacional de um sistema molecular consiste na determinação das geometrias ou conformações energeticamente mais favoráveis (confórmeros), e estas podem ser obtidas através de métodos de mecânica molecular, de mecânica quântica, ou por análise experimental (por cristalografia de raios X ou técnicas espectroscópicas, por exemplo) (Sant'Anna, 2002). Ao levar a cabo a análise conformacional de uma dada molécula são geradas várias conformações por variação dos respectivos ângulos diedros, de modo a considerar todas as geometrias possíveis para o sistema. Estas são depois optimizadas, verificando-se se são mínimos na respectiva curva de energia potencial (confórmeros). Os valores das energias conformacionais relativas assim determinados para os diferentes confórmeros permitem o cálculo das respectivas populações a uma dada temperatura, obtendo-se, deste modo, informação precisa sobre as preferencias conformacionais do sistema em estudo. Este tipo de tratamento possibilita ainda a simulação teórica dos espectros (*ex.* vibracionais e de ressonância magnética nuclear) da molécula, e consequentemente a sua atribuição exacta.

No presente trabalho, efectuou-se uma análise conformacional completa da MDMA, dos seus precursores sintéticos e dos seus metabolitos (Figura 16), assim como dos derivados do β-nitroestireno e do β-metil-β-nitroestireno (Figura 17), mediante o acoplamento da espectroscopia de Raman a cálculos *ab initio* de OM (ao nível do DFT). O objectivo final destes estudos foi a determinação do efeito das preferências estruturais destes compostos na sua actividade biológica, para estabelecimento de relações estrutura – actividade, como descrito em estudos análogos levados a cabo para outros compostos semelhantes (Rastogi *et al.*, 2000; Fiuza *et al.*, 2004).

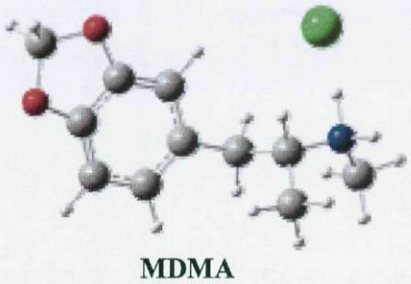

MDMA

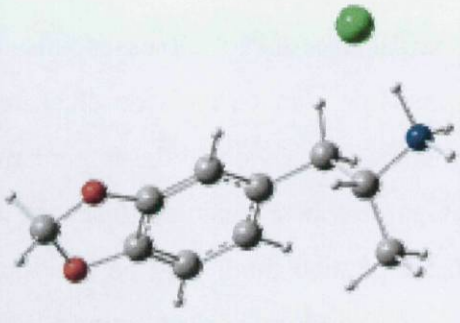

MDA

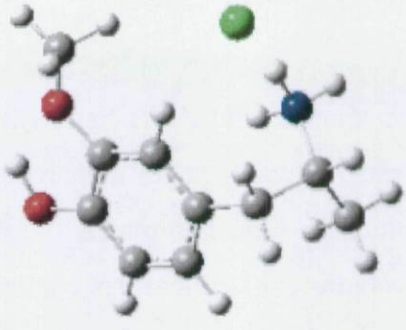

3-*O*-Me-α-MeDA

Figura 16. Representação esquemática dos confórmeros mais estáveis calculados (B3LYP/6-31G*) para o cloridrato de 3,4-metilenodioximetanfetamina (MDMA) e para os seus metabolitos cloridratos de 3,4-metilenodioxianfetamina (MDA) e de 4-hidroxi-3-metoxianfetamina (3-*O*-Me-α-MeDA).

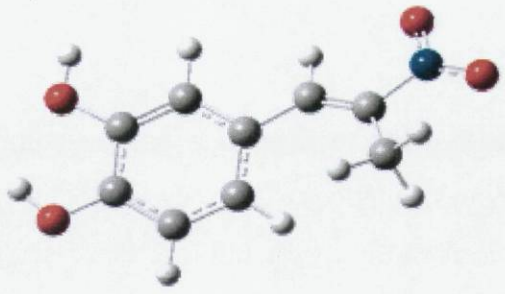

Figura 17. Representação esquemática do confórmero mais estável calculado (B3LYP/6-31G*) para o 3,4-diidroxi-β-metil-β-nitroestireno.

Os estudos da optimização das geometrias moleculares foram reunidos e os resultados integrados na parte experimental desta dissertação, na forma de artigo (ver em 8.1, 8.2, 8.3 e 8.5).

5.2 Determinação dos potenciais redox através de técnicas voltamétricas

Os processos redox, envolvendo reacções de oxidação-redução, são essenciais ao funcionamento dos sistemas biológicos. Estes processos de transferência de electrões estão envolvidos em numerosos fenómenos bioquímicos e fisiológicos e desempenham também uma importante função em muitos estados patológicos, postulando-se que o estado redox global das células poderá ser um alvo terapêutico de eleição para alguns tipos de doenças (Hrbac e Kohen, 2000). O potencial redox é, deste modo, um parâmetro valioso, podendo a sua determinação ser um auxiliar no diagnóstico e tratamento de algumas doenças.

Qualquer composto que possua um ou mais grupos funcionais com capacidade de serem oxidados ou reduzidos podem ser estudados por técnicas electroquímicas, para avaliação do seu potencial redox. Os potenciais redox dos compostos bioactivos fornecem uma informação relevante sobre a possibilidade de ocorrência de transferência de electrões *in vivo*. Em estudos de SPR usa-se, frequentemente, este parâmetro na tentativa de estabelecer uma correlação entre a sua estrutura, as propriedades

físico-químicas intrínsecas e a actividade biológica (Koyama *et al.*, 2001). A correlação entre a facilidade de redução/oxidação (representada por E_p – potencial de pico ou $E_{1/2}$ – potencial de meia onda) e a(s) actividade(s) biológica(s) é considerada como relevante para a compreensão do mecanismo de acção de algumas classes de compostos em vários processos patológicos, assim como para a previsão das actividades biológicas e para o *design* de compostos potencialmente activos (Kovacic e Becvar, 2000). Trabalhos efectuados sobre a relação entre os potenciais redox e a actividade biológica para quinonas, por exemplo, permitiram verificar que o potencial de redução de primeira onda é um parâmetro que determina a sua actividade biológica (Lima *et al.*, 2002). Outros trabalhos realizados estudaram os potenciais redox de compostos que possuem grupos nitro ou grupos isósteros, como o grupo azoxi (NNO), e concluíram também que estes estão intimamente relacionados com a sua actividade (Squella *et al.*, 1999; Abreu *et al.*, 2002; Paula *et al.*, 2003; Squella *et al.*, 2005).

Técnicas voltamétricas

As técnicas voltamétricas são métodos electroquímicos que permitem estudar o potencial redox e que consistem em aplicar sobre um eléctrodo de trabalho um potencial contínuo, o qual varia com o tempo. Na solução em contacto com o eléctrodo ocorrem, nestas condições, reacções de oxidação e redução das espécies electroactivas. Estas técnicas possuem algumas vantagens relativamente a outras metodologias: (i) a possibilidade das medidas serem efectuadas directamente na amostra, sem necessidade de etapas de purificação ou separação prévias; (ii) a rapidez de análise aliada ao baixo custo da instrumentação e dos materiais utilizados e (iii) a baixa sensibilidade em relação à presença de interferentes. As técnicas de análise electroquímica podem também ser usadas em estudos mecanísticos associados a oxidações ou reduções de fármacos e compostos relacionados e na sua identificação e determinação quantitativa (Wring e Hart, 1992; Lawrence *et al.*, 2002; Özkan *et al.*, 2003; Garrido *et al.*, 2004a; Garrido *et al.*, 2004b; Garrido *et al.*, 2004c).

As técnicas voltamétricas usadas no presente trabalho foram: (i) voltametria de impulso diferencial (DPV, do inglês *differential pulse voltammetry*), (ii) voltametria de onda quadrada (SWV, do inglês *square wave voltammetry*) e (iii) voltametria cíclica (CV, do inglês *cyclic voltammetry*).

i) Voltametria de Impulso Diferencial (DPV)

Esta técnica baseia-se na sobreposição de pequenos impulsos de amplitude constante (de 10 a 100 mV) a uma rampa linear de potencial, sendo a intensidade de corrente registada, o resultado da diferença entre a corrente obtida antes da aplicação do impulso e depois deste. A representação gráfica da diferença de corrente (ΔI) em função do potencial aplicado dá origem a um pico cuja altura é directamente proporcional à concentração de analito (voltamograma). O potencial de pico, E_p, pode ser usado para identificar a espécie, visto ser aproximadamente igual ao potencial de meia onda, $E_{1/2}$.

ii) Voltametria de Onda Quadrada (SWV)

Esta técnica electroquímica baseia-se na sobreposição de uma onda quadrada simétrica a uma rampa de potencial. A intensidade de corrente é medida no final do impulso directo e no final do impulso inverso; a representação gráfica da diferença entre estas duas correntes, corrente total, em função do potencial aplicado origina um voltamograma, em que a corrente de pico também é proporcional à concentração da espécie. Esta técnica voltamétrica é muito sensível e os limites de detecção são comparáveis aos das técnicas cromatográficas e espectroscópicas (Souza *et al.*, 2003). Nesta técnica as velocidades de varrimento efectivas podem chegar a 1 Vs^{-1}, permitindo uma maior rapidez na análise e menor consumo de espécies electroactivas, bem como diminuição dos problemas associados ao bloqueio da superfície do eléctrodo (O'Dea *et al.*, 1985).

iii) Voltametria cíclica (CV)

A técnica de voltametria cíclica baseia-se no varrimento do potencial directo e inverso em vários ciclos sucessivos (variação linear do potencial com inversões periódicas), conseguindo-se observar os picos catódicos e anódicos da espécie electroactiva sob análise. Esta técnica é bastante aplicada para fins qualitativos e pode ser aplicada para a detecção de intermediários e de reacções acopladas a processos electroquímicos.

Na presente dissertação, as técnicas electroquímicas descritas foram aplicadas ao estudo de correlação entre características físico-químicas dos compostos sintetizados e a sua actividade biológica, com o objectivo de estabelecer o papel do potencial redox no mecanismo de acção subjacente à actividade. Assim, por um lado determinaram-se os potenciais redox dos derivados do β-nitroestireno (Figura 18) e da MDMA e seus metabolitos principais e, por outro lado, avaliaram-se as suas actividades biológicas (actividade antimicrobiana para os β-nitroestirenos e citotoxicidade em células PC12 para os metabolitos da MDMA). Os resultados obtidos recorrendo a estas técnicas electroquímicas, juntamente com a sua correlação com a actividade, estão apresentados em forma de artigo na parte experimental (ver em 8.3, 8.5 e 8.6).

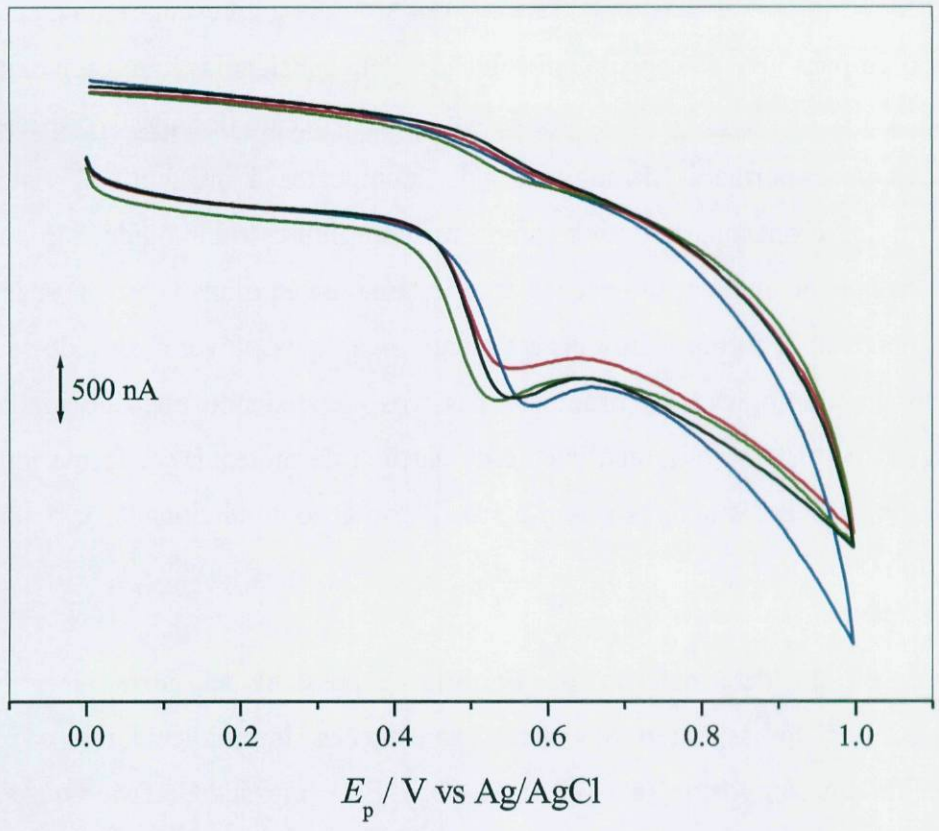

Figura 18. Voltamogramas cíclicos dos seguintes β-metil-β-nitroestirenos: (——) 3,4-dimetoxi-β-metil-β-nitroestireno, (——) 3-hidroxi-4-metoxi-β-metil-β-nitroestireno, (——) 4-hidroxi-3-metoxi-β-metil-β-nitroestireno, e (——) 3,4-diidroxi-β-metil-β-nitroestireno. Velocidade de varrimento: 75 mVs^{-1}.

5.3 Cálculo dos coeficientes de partilha

O carácter lipofílico de uma molécula, de um fragmento ou de um substituinte representa a sua afinidade para um ambiente lipofílico. A lipofilia é considerada um dos descritores moleculares mais importantes para efectuar a correlação de propriedades físico-químicas com a actividade biológica, sendo usualmente avaliada pela determinação do valor de log*P*. O log*P* é definido como o logaritmo do coeficiente de partilha entre o *n*-octanol e a água e reflecte o equilíbrio de partilha do composto entre um solvente polar e outro apolar (Tavares, 2004; Ran *et al.*, 2002). Em estudos de QSAR o sistema de solventes preferencial para a determinação do log*P* é o sistema *n*-octanol/água (ou tampão fosfato 7,4), embora possam ser usados outros sistemas (diferente fase orgânica e/ou fase aquosa) (Lien *et al.*, 1968; Cronin *et al.*, 2002).

O termo log*P* é apenas usado no caso dos solutos se apresentarem no seu estado neutro (válido para uma só espécie em solução). Para substâncias total ou parcialmente ionizadas a pH fisiológico deve utilizar-se a designação de log*D*, coeficiente de distribuição. A importância da ionização dos compostos é indiscutível, visto que a maior parte dos fármacos, ou outros compostos com interesse biológico, são ácidos ou bases fracas que, quando em solução, se apresentam num equilíbrio entre as suas formas neutra e ionizada. A forma neutra é geralmente mais lipossolúvel e difunde-se através das membranas biológicas por processos passivos, dependendo estes do gradiente de concentração do sistema e do coeficiente de partilha da molécula. A forma ionizada é absorvida por processos activos e tem a sua distribuição condicionada pelo seu pK_a e pelo pH do meio.

Através da determinação da lipofilia é possível ter uma ideia bastante aproximada das forças intermoleculares, interacções intramoleculares e estrutura molecular de um composto (Testa *et al.*, 2000b). Esta propriedade físico-química tem uma enorme influência no comportamento farmacocinético dos compostos, nomeadamente em relação à extensão e velocidade de absorção e distribuição, à ligação ao receptor, à biotransformação e à excreção. Por exemplo, de uma forma geral, um aumento da lipofilia implica um aumento da permeabilidade e diminuição da excreção renal (van de Waterbeemd *et al.*, 2001).

O valor de log*P* de um composto pode ser determinado experimentalmente recorrendo a uma grande diversidade de técnicas que avaliam o comportamento da sua distribuição num sistema bifásico (Avdeef e Testa, 2002). Esta distribuição pode ser avaliada num sistema líquido-líquido, através da técnica de "shake flask" com o sistema *n*-octanol/água (Edelbach e Lodge, 2000) ou num sistema sólido-líquido, através de métodos cromatográficos – HPLC em fase reversa ou TLC (do inglês *thin-layer chromatography*, cromatografia em camada fina) (Eadsforth e Moser, 1983; Pagliari *et al.*, 1995; Edelbach e Lodge, 2000; Lombardo *et al.*, 2000). Outros métodos, como o pHmétrico, estão também descritos na literatura (Avdeef e Testa, 2002). De uma maneira geral, estes métodos clássicos de determinação experimental do log*P* só permitem a determinação de coeficientes de partilha aparentes e devem ser usados em estudos de QSAR com alguma parcimónia, visto que estes valores são altamente dependentes das condições experimentais (Bouchard *et al.*, 2002). A determinação dos coeficientes de partilha de substâncias ionizadas pode também ser efectuada pelo método "shake-flask" ou pHmétrico; contudo, a natureza dos contra-iões influencia o resultado experimental, daí que se tenham vindo a usar outras técnicas para aplicar nestes estudos, como a voltametria cíclica, por exemplo (Bouchard *et al.*, 2001).

Apesar das suas vantagens, as determinações experimentais dos coeficientes de partilha implicam um grande consumo de tempo, recursos e material e, acima de tudo, somente podem ser realizadas quando o composto está disponível para as experiências. Além destas desvantagens, a determinação experimental dos valores de log*P* está restrita apenas a alguns compostos, sendo, muitas vezes, difícil considerar os possíveis efeitos da ionização das moléculas. Por isso, em muitas situações em que apenas uma estimativa da lipofilia dos compostos é necessária, é normalmente efectuada a previsão do valor de log*P*, recorrendo apenas às características estruturais dos compostos. Com este objectivo foram desenvolvidas uma série de aproximações teóricas para efectuar a previsão deste parâmetro para fármacos e metabolitos (Buchwald e Bodor, 1998). Como regra, todas as reacções metabólicas dos xenobióticos deveriam dar origem a metabolitos mais polares e mais hidrossolúveis do que o composto original. Contudo, um número razoavelmente elevado de xenobióticos e seus metabolitos, que se assemelham a compostos endógenos, tornam-se substratos do metabolismo de endobióticos, dando origem a produtos de lipofilia mais pronunciada (Fears, 1986). Alguns exemplos destas reacções podem ser a mono-*O*-metilação de compostos com o

grupo catecol, esterificações de álcoois com ácidos gordos ou esterificações de ácidos carboxílicos com colesterol.

Neste trabalho efectuou-se uma estimativa dos valores de coeficiente de partilha recorrendo a um método preconizado anteriormente (Parham *et al.*, 2000). Este método é baseado na análise de uma rede neuronal artificial de vários descritores de propriedades, obtidos de uma base de dados com mais de 2000 compostos. Os descritores das propriedades usados abrangem os descritores de estrutura do estado electrotopológico ("E-state") que codificam a acessibilidade dos electrões para cada átomo (*i.e.* o potencial para interacção intermolecular não covalente), índices de conectividade molecular que codificam informação sobre variações de esqueleto e índices "K shape" que descrevem a forma integral da molécula.

Os log*P* foram, assim, calculados para os intermediários de síntese com estrutura química baseada no β-nitroestireno (ver em 8.3) com potencial actividade antibacteriana, de modo a permitir o estudo da correlação do carácter lipofílico com a actividade. Do mesmo modo, calcularam-se os valores de log*P* da MDMA e dos seus metabolitos (Tabela 2), cujos resultados foram correlacionados com a citotoxicidade demonstrada em células PC12 (ver em 8.6).

Tabela 2. Valores de log*P* calculados, pelo método descrito em 8.3, para a MDMA e para os seus principais metabolitos.

Composto	log*P*
MDMA	2,28
MDA	1,71
N-Me-α-MeDa	0,62
α-MeDa	0,48
3-O-Me-N-Me-α-MeDa	1,07
3-O-Me-α-MeDa	0,92
4-O-Me-N-Me-α-MeDA	1,07
4-*O*-Me-α-MeDA	0,92
6-OH-MDMA	1,11
6-OH-MDA	1,11
6-OH-N-Me-α-MeDA	-0,09
6-OH-α-MeDA	-0,24

6. AVALIAÇÃO DA ACTIVIDADE BIOLÓGICA

Nesta dissertação estudaram-se as seguintes actividades biológicas, para possível aplicação em estudos de SAR e STR, após integração destes resultados com os estudos de caracterização físico-química e estrutural dos compostos:

i) avaliação da actividade antibacteriana dos derivados do β-nitroestireno e do β-metil-β-nitroestireno;
ii) análise da citotoxicidade e da condensação da cromatina induzidas pela MDMA e pelos seus principais metabolitos (6.2).

A actividade biológica foi avaliada por quantificação da dose e do efeito desencadeado pelos compostos em análise, por determinação de alguns parâmetros como IC_{50} (concentração de inibição da viabilidade celular a 50%) ou MIC (concentração inibitória mínima).

6.1 Avaliação da actividade antibacteriana dos derivados do β-nitroestireno e do β-metil-β-nitroestireno

Os derivados do β-nitroestireno e do β-metil-β-nitroestireno, e compostos análogos, apresentam um variadíssimo leque de actividades biológicas, as quais têm vindo a ser estudadas ao longo dos últimos cinquenta anos.

Desde a década de 1970 que se demonstrou que os derivados do β-nitroestireno são citotóxicos e inibem o carcinoma ascítico de Krebs II (Doré e Viel, 1975). A citotoxicidade determinada foi correlacionada com a electrofilia e o índice de Hückel da ligação nitrovinílica, permitindo concluir que o farmacóforo para este tipo de actividade antitumoral corresponde ao anel aromático, à dupla ligação etilénica e ao grupo nitro (Doré e Viel, 1975). Estudos mais recentes permitiram confirmar as conclusões anteriores, tendo-se verificado que, por exemplo, os aductos de vários derivados do β-nitroestireno com o ácido ascórbico são citotóxicos e indutores da apoptose em linhas

celulares. Estes actuam como inibidores de fosfatases de proteínas (são relativamente selectivos para as fosfatases da serina/treonina 2A) (Fathi *et al.*, 2000), mostrando ser potenciais agentes anticancerígenos. Também nestes estudos o nitroestireno foi considerado como o farmacóforo, essencial para o efeito pró-apoptótico manifestado por estes aductos (Kaap *et al.*, 2003). Outros compostos baseados no núcleo do β-nitroestireno demonstraram ser inibidores *in vitro* das fosfatases da tirosina (PTP, do inglês *protein tyrosine phosphatases*), enzimas que possuem uma função importante nos processos de transdução de sinal celular (Park e Pei, 2004), e da telomerase (Kim *et al.*, 2003). Esta última enzima é expressa na maior parte das células tumorais, mas não em células somáticas normais, sendo actualmente considerada como um possível alvo em quimioterapia. Estes derivados demonstraram ainda possuir actividade antiproliferativa em linhas celulares de queratinócitos de ratinho (Traxler *et al.*, 1991) e de cancro do estômago (Carter *et al.*, 2002).

Outras actividades relacionadas com a resposta imune têm sido descritas para os derivados do β-nitroestireno, como uma diminuição da produção de interleucina 12 (IL12), interleucina 6 (IL6) e óxido nítrico por parte dos macrófagos (Carter *et al.*, 2002). Os derivados do β-nitroestireno são conhecidos também por apresentarem toxicidade para um vasto conjunto de organismos, nomeadamente fazendo parte das defesas químicas naturais de alguns artrópodes (Kuwahara *et al.*, 2002). A sua toxicidade em insectos foi também estudada (Garbow e Gaede, 1990).

Outros resultados evidenciaram que os β-nitroestirenos possuem actividade promissora como agentes antibacterianos, antifúngicos e antiparasitários (Brian *et al.*, 1946; Cavier *et al.*, 1978; Mikami *et al.*, 1991), propondo-se a sua aplicabilidade terapêutica em humanos, ou em veterinária, devido à sua relativa selectividade. Mais recentemente foi descrito que aductos do β-nitroestireno e do β-metil-β-nitroestireno com compostos contendo o grupo tiol apresentam actividade antibacteriana significativa contra bactérias Gram-positivas (Gökçe *et al.*, 2005).

Actividade antibacteriana

Apesar de, nos últimos anos, se ter vindo a coligir um grande manancial de informação e investigação na tentativa de descobrir novos antibióticos, ironicamente poucas classes de antibióticos foram introduzidas na terapêutica nos últimos quarenta

anos. Na sua grande maioria, os antibióticos introduzidos foram modificações moleculares de antibióticos já existentes. Como consequência, as bactérias mais comuns desenvolveram resistências para os compostos usados, tornando premente a procura de novos antibióticos, ou em alternativa a modificação e melhoria das características daqueles já existentes.

Quase todas as grandes classes de antibióticos de uso corrente possuem limitações em relação ao seu uso clínico devido ao aparecimento de resistências bacterianas e à cada vez mais rápida difusão de bactérias patogénicas multi-resistentes (Russel, 2003; Fadda *et al.*, 2004; Hamilton-Miller, 2004). O aparecimento de resistências aos antibióticos β-lactâmicos, macrólidos, quinolonas ou vancomicina é, nos dias de hoje, um grave ameaça à saúde pública a nível mundial (Russel, 2003; Hanaki *et al.*, 2004). A maior parte das bactérias que aparecem em ambientes hospitalares são resistentes a pelo menos um dos principais antibióticos mais usados para estas infecções (Coates *et al.*, 2002). Em particular, o rápido desenvolvimento de resistência entre as bactérias Gram-positivas clinicamente mais relevantes está a tornar-se um sério problema (Butaye *et al.*, 2003; Yee, 2003). Assim, é urgente e emergente a procura de novos compostos que não se encaixem nas classes estruturais dos antibióticos existentes no mercado (Coates *et al.*, 2002; Woodford, 2003).

A procura de novas moléculas com actividade antibacteriana assenta, hoje em dia, no estudo da relação da actividade com as propriedades e a estrutura química, através de estudos de SAR. Alguns estudos apontam o papel importante de estudos de SAR e QSAR no desenvolvimento de agentes antimicrobianos (Vicini *et al.*, 2002; Narasimhan *et al.*, 2004) e, em particular, indiciam como extremamente importantes estudos de alguns parâmetros físico-químicos, como a lipofilia e parâmetros estéricos e electrónicos (Narasimhan *et al.*, 2004).

O objectivo primordial deste trabalho foi a tentativa de demonstrar a importância do núcleo central da estrutura do β-nitroestireno e o seu estabelecimento como provável farmacóforo para a actividade antibacteriana. Os resultados obtidos demonstraram uma maior actividade contra bactérias Gram-positivas, os quais estão de acordo com conclusões obtidas em trabalhos anteriores (Schales e Graefe, 1952; Worthen e Bond, 1970). A actividade antibacteriana foi avaliada pelo método da microdiluição e foi expressa como concentração inibitória mínima (MIC, do inglês *minimum inhibitory*

concentation). Esta actividade foi determinada em várias estirpes e isolados clínicos de diferentes espécies de bactérias patogénicas para o Homem (ver em 8.3).

O conceito de bioactivação de um fármaco, através da sua biorredução, como mecanismo de acção e estratégia para actuar nos alvos celulares tem sido objecto de estudo, nomeadamente dos antibióticos (*e.g.* nitroimidazois e nitrofuramos) e de agentes anticancerígenos (Rauth *et al.*, 1998).

No presente trabalho foi também efectuado o estudo da correlação das propriedades redox dos compostos com a actividade observada. Estes estudos foram alicerçados em trabalhos anteriores, que demonstraram, por voltametria cíclica, haver uma correlação entre parâmetros electroquímicos, espectroscópicos e estruturais (nomeadamente a electrofilia) de compostos que possuem um grupo nitro aromático ou conjugado com uma ligação dupla e a sua actividade biológica (Squella *et al.*, 1999; Abreu *et al.*, 2002; Paula *et al.*, 2003; Squella *et al.*, 2005).

Apesar da actividade antibacteriana destes compostos pode estar relacionada com a adição de um nucleófilo celular à dupla ligação activada, a redução do grupo nitro por parte das bactérias (as nitrorredutases bacterianas têm a capacidade de promover esta alteração) já foi estudada, principalmente para compostos com grupo nitro aromático; mas mesmo os grupos nitro alifáticos podem ser reduzidos ao seu análogo com a amina alifática por parte de bactérias anaeróbias intestinais, por exemplo (Mori *et al.*, 1990).

O primeiro passo na redução do grupo nitro é a formação do radical ião nitro. A onda principal é devida a uma redução ao derivado hidroxilamina, envolvendo quatro electrões e quatro protões (Squella *et al.*, 1999). De notar, que este processo é idêntico àquele que está associado à redução aos compostos que possuem grupo nitro aromático, de acordo com a seguinte equação:

$$R\text{-}C_6H_5CH{=}C(R')NO_2 + 4\,e^- + 4\,H^+ \longrightarrow R\text{-}C_6H_5CH{=}C(R')NHOH + H_2O$$

Em que R' = H, no caso dos β-nitroestirenos e R' = CH_3, no caso dos β-metil-β-nitroestirenos. É importante realçar que esta reacção ocorre a valores de pH próximos do fisiológico e que posteriormente, o grupo hidroxilamina insaturado pode sofrer rearranjo a fenilacetaldoxima (Squella *et al.*, 1999).

6.2 Análise da citotoxicidade e da condensação da cromatina induzidas pela 3,4-metilenodioximetanfetamina (MDMA) e seus metabolitos

A semelhança estrutural existente entre a MDMA e os neurotransmissores dopamina, adrenalina e serotonina (5-hidroxitriptamina ou 5-HT) levou a que se colocasse a hipótese de que a sua actividade biológica poderia mimetizar, em maior ou menor grau, a actividade destes neurotransmissores.

O efeito bioquímico agudo mais marcado da MDMA corresponde a um aumento da neurotransmissão serotoninérgica provocado por uma libertação, independente do cálcio, de serotonina nos terminais nervosos (Johnson *et al.*, 1986). Existem ainda evidências clínicas e experimentais que relacionam a MDMA, e outras feniletilaminas, com o aumento da quantidade de outros neurotransmissores nos terminais respectivos (Huether *et al.*, 1997). A MDMA está descrita como um potente inibidor da recaptação pré-sináptica da serotonina, facilitando também a sua libertação (Steele *et al.*, 1987; Lyles e Cadet, 2003). Segundo vários autores, a MDMA não actua directamente, mas a sua acção ocorre preferencialmente por ligação, e posterior bloqueio, dos transportadores membranares envolvidos na recaptação da serotonina e nos transportadores dos sistemas vesiculares de armazenamento (Rudnick e Wall, 1992; Liechti *et al.*, 2000; De la Torre *et al.*, 2004). Um efeito similar, mas em menor extensão, é também registado em relação à dopamina e noradrenalina (Lyles e Cadet, 2003). A MDMA reverte o sentido do transporte membranar, facilitando o efluxo destes neurotransmissores para a fenda sináptica, ocorrendo uma activação aumentada dos receptores pós-sinápticos (Cole e Sumnall, 2003; Green *et al.*, 2003). A MDMA é um inibidor moderado da monoamina oxidase (MAO), possuindo alguma, mas comparativamente menor, acção directa, sobre alguns receptores pós-sinápticos. A sua acção pode decorrer, assim, da ligação a vários tipos de receptores: serotoninérgicos do tipo 2 (5-HT_2) (Titeler *et al.*, 1988), muscarínicos M_1, os receptores H1 da histamina e adrenérgicos α_2 (Battaglia *et al.*, 1988; Pierce e Peroutka, 1988; Cole e Sumnall, 2003; Green *et al.*, 2003). No entanto, maioritariamente, a actividade neuroquímica é de índole indirecta. É contudo aceite que os aumentos dos níveis de serotonina e de

dopamina correspondem ao principal mecanismo subjacente aos efeitos centrais característicos da MDMA e feniletilaminas análogas.

O consumo de MDMA traduz-se nos sinais típicos de uma estimulação simpaticomimética central moderada (devido a uma semelhança estrutural com a anfetamina) e de alguma actividade alucinogénica (devido a uma semelhança com a mescalina) (Figura 2). Os efeitos farmacológicos da MDMA variam de acordo com a dose, a frequência e a duração do uso. Assim, os efeitos mais frequentemente associados à MDMA, pouco tempo após ingestão, são: euforia, sensação de bem-estar e felicidade, extroversão, aumento da sociabilidade e da empatia com os outros, alguns distúrbios de percepção moderados (de cores e sons, por exemplo), mas sem alucinações, e alguns sintomas somáticos relacionados com os seus efeitos cardiovasculares e autónomos (aumento da pressão arterial e do ritmo cardíaco, midríase, etc.) (Downing, 1986; Vollenweider *et al.*, 1998; De la Torre *et al.*, 2004).

Os efeitos secundários agudos da MDMA estão também relacionados com as propriedades simpaticomiméticas e serotoninérgicas da MDMA e incluem: náusea, tonturas, dificuldade de concentração, confusão, ansiedade, vómitos, hipertensão, palpitações, dores de cabeça, diaforese, falta de apetite, sede, dores e tensão muscular, visão turva, insónia e boca seca com acessos de calor ou de frio (Greer e Tolbert, 1986; Vollenweider *et al.*, 1998; De la Torre *et al.*, 2004).

Vários efeitos tóxicos estão descritos para a MDMA e para os seus principais metabolitos, nomeadamente hepatotoxicidade, cardiotoxicidade e nefrotoxicidade, entre outros (Green *et al.*, 2003). Os mecanismos moleculares inerentes à toxicidade da MDMA estão ainda por determinar, embora estudos indiquem que o metabolismo é um factor fundamental para as manifestações tóxicas. Os efeitos tóxicos agudos prendem-se com a sua actividade farmacológica, dado que o efeito mais significativo é, precisamente, a síndrome serotoninérgica (rigidez muscular aumentada e hipertermia). A MDMA, tal como o seu metabolito MDA, é considerada uma neurotoxina serotoninérgica numa grande variedade de espécies animais (Ricaurte *et al.*, 1985; Stone *et al.*, 1987; Ricaurte *et al.*, 1988). Esta toxicidade é atribuída à neurodegeneração do sistema serotoninérgico, cujo impacto, a longo termo, ainda não está completamente estudado. Em termos puramente clínicos, este tipo de neurotoxicidade tem sido relacionado com a perda gradual de funções cognitivas, como a memória, aumento da

agressividade e uma maior incidência de distúrbios psicopatológicos (depressão, entre outros) (Cole e Sumnall, 2003; Green *et al.*, 2003). No entanto, o mecanismo que está subjacente à neurotoxicidade observada ainda não foi completamente estabelecido, não obstante terem sido propostas várias teorias, como o aumento da temperatura corporal ou a formação de radicais livres (McCann *et al.*, 2000; Morgan, 2000). De salientar que após injecção directa de MDMA e MDA no cérebro não se observam os efeitos da toxicidade descritos após administração periférica dos compostos; estes apenas provocam uma indução da libertação de neurotransmissores (Esteban *et al.*, 2001). Estes resultados reforçam a hipótese da necessidade de uma activação metabólica prévia da MDMA e da MDA, para justificar a neurotoxicidade. Alguns trabalhos sugerem que a toxicidade da MDMA em geral, e a neurotoxicidade em particular, possa estar associada à formação *in vivo* de um ou mais metabolitos (Hiramatsu *et al.*, 1990). No entanto, é importante referir que, após administração intracerebroventricular dos principais metabolitos do "ecstasy" – α-MeDA, N-Me-α-MeDA e 3-*O*-Me-α-MeDA – se verificou que estes também não reproduziam a toxicidade da MDMA (McCann *et al.*, 1991; Chu *et al.*, 1996).

A procura de metabolitos neurotóxicos da MDMA tem, hoje em dia, recaído num conjunto quantitativamente menos representativo de metabolitos, os aductos do tipo tioéter da α-MeDA e da N-Me-α-MeDA com a glutationa e com a cisteína (Bai *et al.*, 1999). Os resultados obtidos com os metabolitos 5-S-glutationil-α-MeDA e o 2,5-S-diglutationil-α-MeDA permitiram verificar a existência de efeitos comportamentais e bioquímicos idênticos aos observados para a MDMA (aumento da concentração de serotonina e de dopamina), sendo também observados efeitos neurodegenerativos após a sua administração directa no cérebro.

No entanto, outras hipóteses quanto à formação de metabolitos neurotóxicos necessitam ser correctamente averiguadas, nomeadamente a possibilidade da 6-OH-α-MeDA, metabolito da MDMA estruturalmente semelhante à neurotoxina 6-hidroxidopamina, poder participar nestas manifestações (Johnson *et al.*, 1992; Elayan *et al.*, 1992). Os metabolitos catecólicos da MDMA (α-MeDA e N-Me-α-MeDA) também podem levar à formação dos aminocromos respectivos, os quais podem também induzir neurotoxicidade, através de mecanismos envolvendo stress oxidativo.

Citotoxicidade para células PC12

Os estudos *in vitro* que recorrem à análise dos efeitos de determinado composto em linhas celulares são extremamente importantes, quer nas etapas preliminares de desenvolvimento de novos fármacos, quer no estudo do potencial tóxico de xenobióticos e seus metabolitos. Embora nem sempre seja possível estabelecer um paralelismo absoluto entre os resultados obtidos em culturas celulares e aqueles obtidos em experiências *in vivo*, este tipo de ensaios permite delinear estratégias mais racionais e económicas, possibilitando testar uma maior variedade e número de compostos num menor período de tempo.

No trabalho apresentado nesta dissertação, o perfil de citotoxicidade da MDMA e dos seus principais metabolitos foi estudado através da análise de viabilidade celular em células PC12. A linha celular PC12 deriva de um tumor das células cromafins da glândula suprarrenal de ratinho, designado de feocromocitoma. Estas células, após isolamento e na presença de factor de crescimento, podem diferenciar-se em células que mimetizam o comportamento dos neurónios dopaminérgicos. Na ausência deste factor, elas permanecem indiferenciadas, possuindo mais dopamina e menos acetilcolina do que as diferenciadas. A semelhança das células PC12 indiferenciadas com neurónios simpaticomiméticos (nomeadamente dopaminérgicos) (Shafer e Atchinson, 1991; Lein *et al.*, 2005) permitiu efectuar um *screening* de toxicidade da MDMA e dos seus metabolitos.

Nestes estudos avaliou-se a citotoxicidade da MDMA e dos seus metabolitos através da medida de parâmetros relativos à proliferação e viabilidade celulares. A quantificação dos resultados obtidos foi efectuada pelo método do MTT (brometo de 3-(4,5-dimetiltiazol-2-il)-2,5-difeniltetrazólio), um sal que pode ser incorporado pelas células viáveis. Estas possuem intacta a capacidade de reduzirem o MTT a um derivado do tipo formazano de cor azul e insolúvel em água, sendo a redução catalisada por desidrogenases celulares citoplasmáticas activas. A viabilidade celular foi, de seguida, determinada por espectrofotometria, sendo a quantidade de formazano formada directamente proporcional ao número de células metabolicamente activas.

Análise da condensação da cromatina

A elucidação dos mecanismos moleculares associados à toxicidade dos xenobióticos é uma das áreas em franco desenvolvimento em toxicologia, nomeadamente os estudos dos processos associados à morte celular (Orrenius e Zhivotovsky, 2006). Os mecanismos fisiológicos de morte celular são fundamentais como estratégia de defesa do organismo, na remoção de células alteradas, na resposta a fenómenos de citotoxicidade e no desenvolvimento embrionário normal. A remoção de células indesejáveis ocorre principalmente por um de dois processos, necrose ou apoptose, ou mesmo por características de ambos, em simultâneo, na mesma célula.

Um composto tóxico povoca normalmente morte celular por bloqueio dos processos metabólicos vitais. Dependendo da sua concentração e da susceptibilidade específica das células, podem ser activadas diferentes vias que poderão implicar morte celular. Dos processos de morte celular, a necrose e a apoptose são, sem dúvida, os mais estudados e caracterizados. Anteriormente às primeiras descrições do fenómeno da apoptose (Kerr, 1971; Kerr *et al.*, 1972), a necrose ou "morte celular acidental" era considerada como o processo universal de morte celular. Actualmente encontram-se já descritos vários parâmetros bioquímicos e morfológicos que diferenciam a apoptose (ou morte celular programada) da necrose (Kroemer *et al.*, 2005).

A morte celular por apoptose traduz-se em alterações morfológicas, sem perda da integridade membranar. Nomeadamente, ocorre agregação da cromatina com marginalização subsequente contra o invólucro nuclear, diminuição do volume do citoplasma, fragmentação nuclear e desenvolvimento de protuberâncias na superfície celular. Estes fenómenos são seguidos por formação de corpos apoptóticos com membrana plasmática integral, que são fagocitados por macrófagos ou células adjacentes. A apoptose é considerada como uma forma activa ou programada de morte celular, altamente regulada por enzimas e que requer energia metabólica (dependente de ATP). Por outro lado, a necrose caracteriza-se por acumulação da cromatina, intumescimento e desintegração de organitos celulares, aparecimento de floculações na matriz da mitocôndria, lise ou ruptura da membrana plasmática, terminando em desintegração celular com libertação dos seus componentes para o exterior. Este processo não requer energia, sendo uma forma não controlada ou patológica de morte

celular (Orrenius e Zhivotovsky, 2006). No entanto, a morte celular necrótica pode também ocorrer como um evento programado, contribuindo para o desenvolvimento dos órgãos e para a manutenção da homeostase dos tecidos (Zong e Thompson, 2006). Alguns estudos mais recentes sugerem uma possível sobreposição destes dois tipos de morte celular, podendo, assim, coexistir na mesma célula características de apoptose e de necrose. De referir que a inibição da apoptose após o seu início, pode resultar em morte celular com características necróticas. Apesar da existência destas características diferenciadoras, a distinção entre estes dois tipos de morte celular é, por vezes, ambígua.

Alguns factores podem favorecer um dos mecanismos de morte celular em detrimento do outro, nomeadamente: (i) a expressão genética – na apoptose os níveis da expressão de proteína p53 estão aumentados (Green e Kroemer, 2004), (ii) a transdução de sinal, (iii) as proteases – a activação da cascata de caspases é um processo associado à apoptose, (iv) as espécies reactivas de oxigénio e (v) o metabolismo celular/geração de ATP.

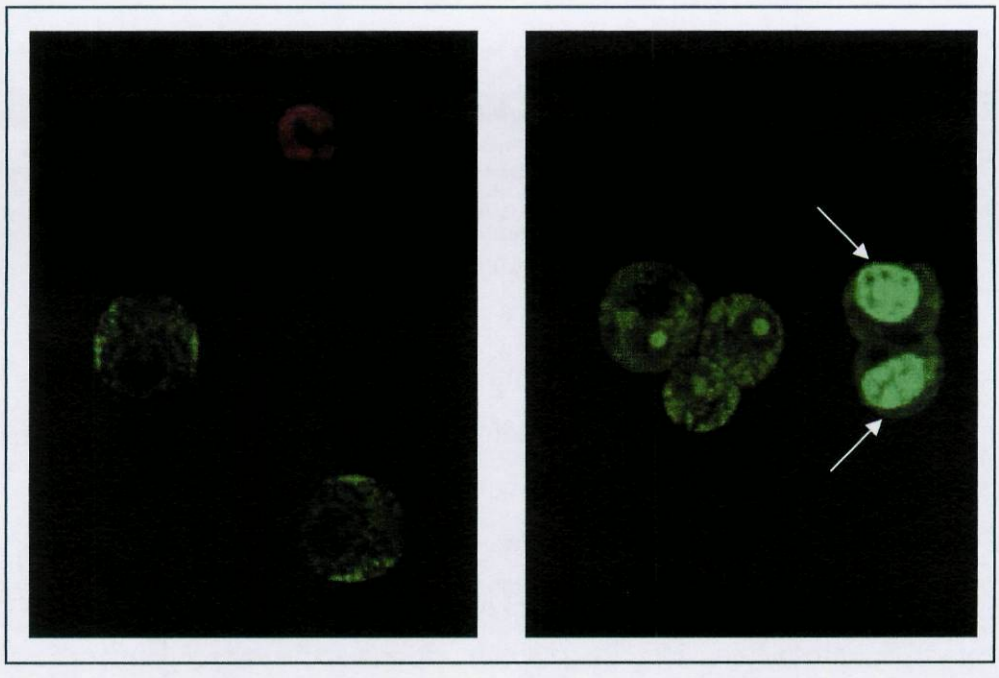

Figura 19. Representação fotográfica da análise da condensação da cromatina em células PC12 expostas à MDMA. As células marcadas com SYTO-13 apresentam fluorescência verde (células viáveis e células que apresentam características de apoptose primária). As células marcadas com iodeto de propídeo apresentam fluorescência vermelha (células necróticas). As setas indicam a condensação de cromatina.

As alterações bioquímicas, morfológicas ou fisiológicas verificadas durante o processo de morte celular podem ser observadas, e determinadas, de modo a distinguir, num conjunto de células, as viáveis, as que apresentam características de apoptose e as que apresentam características de necrose (mesmo em simultâneo na mesma célula).

Assim, neste trabalho procedeu-se à observação de evidências morfológicas de apoptose e/ou necrose, após incubação das células PC12 com a MDMA e os seus metabolitos (Figura 19). Com este objectivo usaram-se as sondas fluorescentes SYTO-13 e iodeto de propídeo conforme descrito no artigo apresentado na parte experimental (ver em 8.6). Os resultados obtidos permitem reforçar a hipótese que apoptose pode ser um dos mecanismos associados à neurodegeneração provocada pelo consumo de MDMA (Jiménez *et al.*, 2004).

7. CORRELAÇÃO ENTRE ESTRUTURA, PROPRIEDADES FÍSICO-QUÍMICAS E A ACTIVIDADE BIOLÓGICA DOS COMPOSTOS SINTETIZADOS

Nos estudos clássicos de relação estrutura-actividade (SAR) exigia-se a síntese de diversos análogos de estrutura relacionada com um composto protótipo, e a subsequente realização de testes de actividade biológica. No entanto, com os avanços registados nesta área, foi possível estabelecer um conjunto de generalizações sobre a influência de mudanças estruturais específicas (como, por exemplo, o tamanho da cadeia carbonada, a natureza e o grau de substituição e a estereoquímica de um determinado composto), nos parâmetros físico-químicos e nos efeitos biológicos (actividade farmacológica, metabolismo ou toxicidade).

No trabalho apresentado nesta dissertação, foi possível inferir, após avaliação da actividade antibacteriana de uma série de derivados do β-nitroestireno e do β-metil-β-nitroestireno e estudo das suas características físico-químicas e determinantes estruturais, um conjunto de correlações evidenciadas na Figura 20. Estas estão descritas em pormenor no artigo apresentado em 8.3.

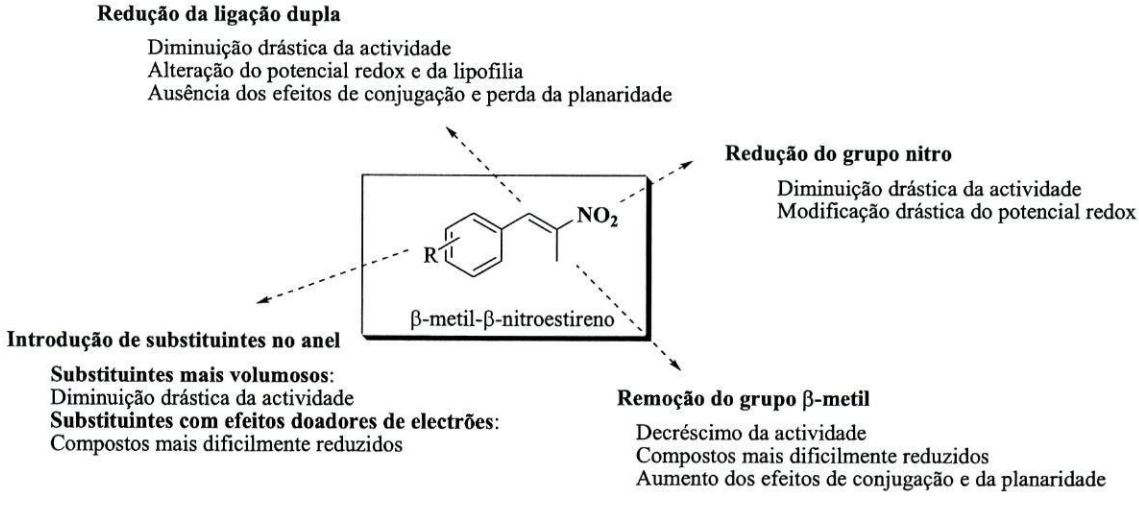

Figura 20. Efeitos das alterações estruturais dos derivados do β-nitroestireno nas características físico-químicas dos compostos e na actividade antibacteriana.

Os estudos de relação estrutura – propriedade – actividade citotóxica, para células PC12, efectuados com a MDMA e os seus metabolitos permitiram retirar algumas conclusões, expressas na Figura 21.

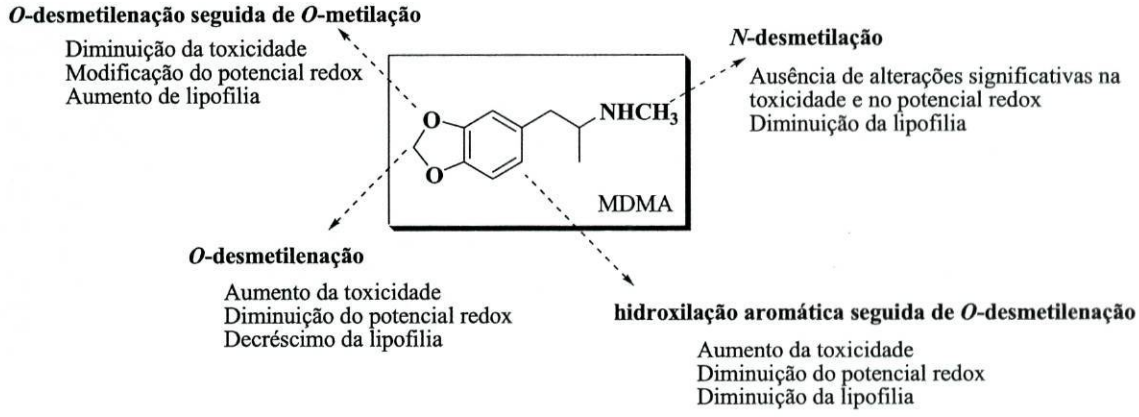

Figura 21. Efeitos das alterações estruturais, relacionadas com o metabolismo da MDMA, nas características físico-químicas destes compostos e na sua citotoxicidade em células PC12.

De salientar que os metabolitos mais facilmente oxidáveis e que apresentam maior hidrossolubilidade são aqueles que possuem o grupo catecol, estando estes resultados de acordo com estudos anteriores com catecóis em células PC12, os quais também revelaram que quanto mais lipofílico o composto menos citotóxico este é (Chichirau *et al.*, 2005).

PARTE II

TRABALHO EXPERIMENTAL

8. TRABALHO EXPERIMENTAL

8.1 Estudo conformacional de derivados do β-nitroestireno por espectroscopia de Raman combinada com cálculos *ab initio*.

Artigo reproduzido da revista *Journal of Molecular Structure* (2004) 692: 91-106, com permissão da Elsevier, Ltd.

Available online at www.sciencedirect.com
SCIENCE DIRECT®
Journal of Molecular Structure 692 (2004) 91–106
Journal of MOLECULAR STRUCTURE
www.elsevier.com/locate/molstruc

β-Nitrostyrene derivatives—a conformational study by combined Raman spectroscopy and ab initio MO calculations

R. Calheiros[a,b], N. Milhazes[c,d], F. Borges[c], M.P.M. Marques[a,b,*]

[a]*Research Unit 'Molecular Physical-Chemistry', University of Coimbra, 3001-401 Coimbra, Portugal*
[b]*Department of Biochemistry, Faculty of Sciences and Technology, University Coimbra, Ap. 3126, 3001-401 Coimbra, Portugal*
[c]*Department of CEQUP/Chemistry, Faculty of Sciences and Technology, University of Porto, 4169-007 Porto, Portugal*
[d]*Superior Institute of Health Sciences-North, 4580 Paredes, Portugal*

Received 11 November 2003; revised 9 January 2004; accepted 12 January 2004

Abstract

A complete conformational analysis of β-nitrostyrene and β-methyl-β-nitrostyrene derivatives was carried out by Raman spectroscopy coupled to ab initio MO calculations. Apart from the optimised geometrical parameters of the most stable conformers of the molecules under study, the corresponding harmonic vibrational frequencies were calculated, as well as potential-energy profiles for several internal rotations within the molecules. At the light of these results, a complete assignment of the Raman spectra of the solid samples was performed. The conformational behaviour of this kind of systems was found to be mainly determined by the stabilising effect of π-electron delocalisation.
© 2004 Elsevier B.V. All rights reserved.

Keywords: β-nitrostyrene; β-methyl-β-nitrostyrene; Raman spectroscopy; Ab initio calculations; Conformational analysis

1. Introduction

β-Nitrostyrenes and their derivatives are important starting materials for the synthesis of a variety of useful building blocks, such as nitroalkanes, amines, ketoximes, hydroxylamines and aldoximes [1,2]. Moreover, conjugated nitroalkenes are exceptionally good Michael acceptors, namely towards organometallic reagents [3] and vitamin C [4]. Nitrostyrenes are activated alkenes displaying an electron-withdrawing NO_2 group, which have been shown to predominate in the ground state *E* (*trans*) configuration of the nitro and phenyl groups relative to the carbon chain double bond [5].

Apart from their well recognised antimicrobial and antifungal activities [6], nitrostyrene derivatives have lately been shown to constitute a novel class of chemical compounds with good potential for further development as promising anticancer drugs [7,8]. In fact, some reported studies [8] propose a nitrovinyl side chain attached to an aromatic ring as the pharmacophore structure of a new group of pro-apoptotic agents.

Once the biological activity of this type of compounds is thought to be strongly dependent on their structural characteristics—similarly to what has been found for phenolic acids and phenolic ester analogues [9]—a series of ring-substituted nitrostyrenes was synthesised in our lab, and screened for their in vitro and in vivo antiproliferative and cytotoxic properties (both in human cancer cells and in live mice).

The present work reports the conformational analysis of β-nitrostyrene derivatives, as well as of some of their analogues and synthetic precursors, by Raman spectroscopy coupled to ab initio MO methods (at the DFT level). The compounds studied were: 1,2-dihydroxybenzene (catechol, CAT), 3,4-dihydroxybenzaldehyde (3,4-OH-BA), styrene (S), β-methyl-styrene (MeS), β-nitrostyrene (NS), β-methyl-β-nitrostyrene (MeNS), 3,4-dihydroxy-β-nitrostyrene (3,4-OH-NS) and 3,4-dihydroxy-β-methyl-β-nitrostyrene (3,4-OH-MeNS) (Fig. 1).

* Corresponding author. Address: Department of Biochemistry, Faculty of Sciences and Technology, University Coimbra, Ap. 3126, 3001-401 Coimbra, Portugal. Tel.: +351-239854462; fax: +351-239826541.
E-mail address: pmc@ci.uc.pt (M.P.M. Marques).

0022-2860/$ - see front matter © 2004 Elsevier B.V. All rights reserved.
doi:10.1016/j.molstruc.2004.01.012

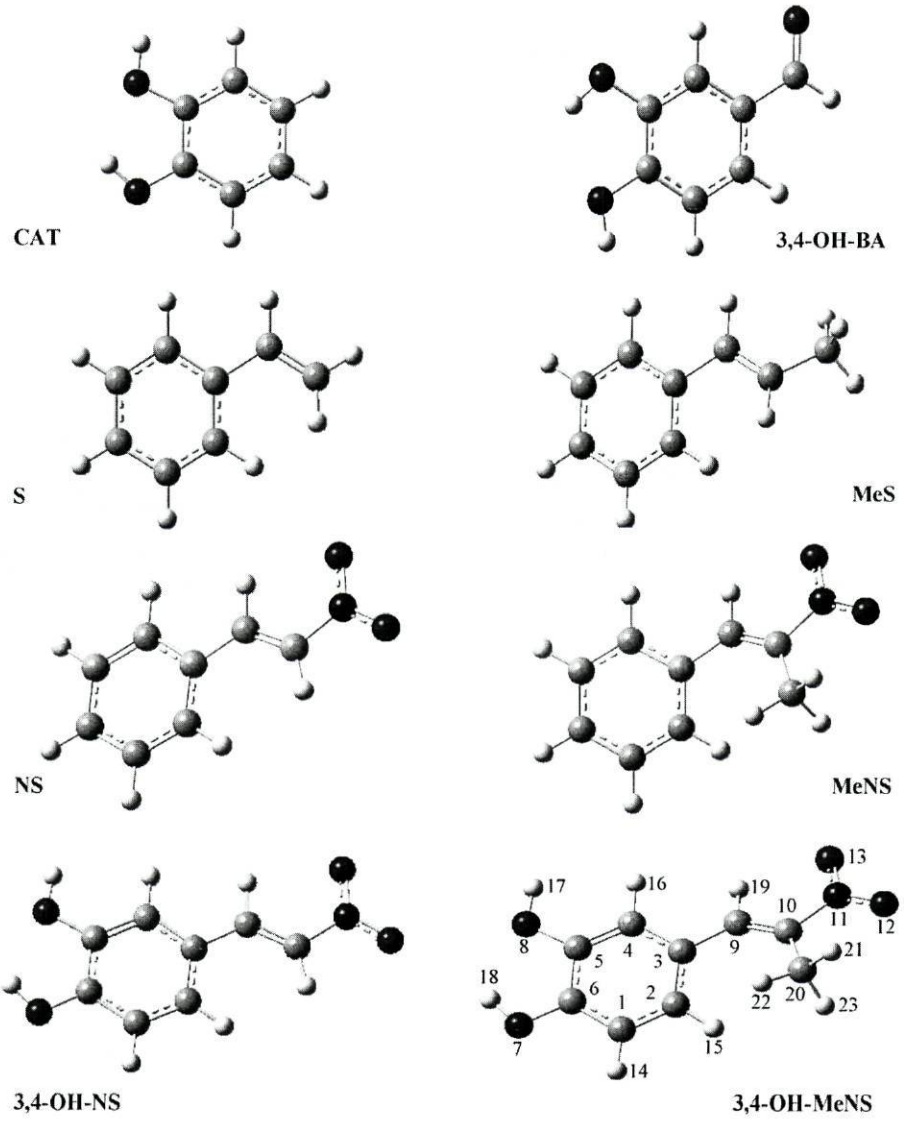

Fig. 1. Schematic representation of the β-nitrostyrene derivatives, and their analogues, studied in the present work. For NS, MeNS, 3,4-OH-NS and 3,4-OH-MeNS, the calculated (B3LYP/6-31G**) lowest energy conformers are displayed (the atom numbering is included, and is applicable to all the compounds studied, irrespective of the type of atom).

2. Experimental

2.1. Synthesis

The synthetic procedure was adapted from Parker et al. [10] with slight modifications. A mixture of the benzaldehyde (5.0 g), with the corresponding substitution pattern, and ammonium acetate (0.5 g) was dissolved in nitroethane (50 ml)—for the β-methyl-β-nitrostyrene derivatives—or in nitromethane (50 ml)—for the β-nitrostyrene derivatives—and refluxed for 5 h. After cooling to room temperature the reaction mixtures were partially evaporated in a rotary evaporator, diluted with diethyl ether and washed twice with water. The organic layer was dried over anhydrous magnesium sulphate, filtered and concentrated. The remaining residues were recrystallised from diethylether/petroleum ether. The synthesised compounds were identified by both NMR and electron impact mass spectra (EI-MS).

β-Methyl-β-nitrostyrene (MeNS). Yield 6.38 g, 83%; ^{1}H NMR δ: 2.38 (3H, s, C*H*$_3$), 7.47–7.51 (3H, m, Ar*H*), 7.56–7.59 (2H, m, Ar*H*), 8.08 (1H, s, H(α)); ^{13}C NMR δ: *13.9* CH_3, *129.0* (2 × *C*HAr), 129.2 C(β), *130.3* (2 × *C*HAr), *133.2* *C*HAr, *147.7* C(1); EI-MS *m/z* (%): 163 ($M^{+\cdot}$, 16), 146 (15), 115 (100), 105 (99), 91 (56), 77 (51), 65 (15); m.p. 58–61 °C.

3,4-Dihydroxy-β-nitrostyrene (3,4-OH-NS). Yield 2.26 g, 34%; ^{1}H NMR δ: 6.81 (1H, d, J = 8.7, H(5)), 7.19 (1H, d, J = 2.2, H(2)), 7.20 (1H, dd, J = 8.0; 2.2, H(6)), 7.93 (1H, d, J = 13.5, H(α)), 7.98 (1H, d, J = 13.5, H(β)),

9.70 (2H, *brs*, *OH*); ^{13}C NMR δ: *116.0 C*HAr, *116.4 C*HAr, 121.5 C(1), *123.8 C*HAr, *134.6* C(α), *140.4* C(β), 145.8 C(3), 150.5 C(4); EI-MS *m/z* (%): 181 ($M^{+\cdot}$, 100), 134 (85), 89 (47), 77 (31), 63 (24); m.p. 148–151 °C.

3,4-Dihydroxy-β-methyl-β-nitrostyrene (3,4-OH-MeNS). Yield 2.55 g, 35%; ^{1}H NMR δ: 2.40 (3H, s, CH_3) 6.85 (1H, d, $J = 8.2$, H(5)), 6.97 (1H, dd, $J = 8.3$; 2.0, H(6)), 7.05 (1H, d, $J = 2.0$, H(2)), 7.96 (1H, s, H(α)), 9.58 (2H, *brs*, *OH*); ^{13}C NMR δ: 14.0 CH_3, *116.0 C*HAr, *117.5 C*HAr, 123.1 C(1), *124.0 C*HAr, *134.2* C(α), *144.3*C(β), 145.6 C(3), 148.4 C(4); EI-MS *m/z* (%): 195 ($M^{+\cdot}$, 99), 148 (69), 138 (24), 119 (16), 110 (17), 103 (100), 91 (40), 83 (23), 77 (53), 65 (23), 55 (17); m.p. 140–141 °C.

2.2. Apparatus

^{1}H and ^{13}C NMR data were acquired, at room temperature, on a Brüker AMX 300 spectrometer operating at 300.13 and 75.47 MHz, respectively. Dimethylsulfoxide-d_6 was used as a solvent; chemical shifts are expressed in δ (ppm) values relative to tetramethylsilane (TMS) as internal reference; coupling constants (J) are given in Hertz. Assignments were also made from distortionless enhancement by polarization transfer (DEPT) (see italicised values). EI-MS were carried out on a VG AutoSpec instrument; the data are reported as *m/z* (% of relative intensity of the most important fragments). Melting points were obtained on a Köfler microscope (Reichert Thermovar) and are uncorrected.

2.3. Ab initio MO calculations

The ab initio calculations—full geometry optimisation and calculation of the harmonic vibrational frequencies—were performed using the GAUSSIAN 98W program [11], within the Density Functional Theory (DFT) approach, in order to properly account for the electron correlation effects (particularly important in this kind of systems). The widely employed hybrid method denoted by B3LYP [12–17], which includes a mixture of HF and DFT exchange terms and the gradient-corrected correlation functional of Lee et al. [18,19], as proposed and parameterised by Becke [20,21], was used, along with the double-zeta split valence basis sets 6-31G* and 6-31G** [22,23].

Molecular geometries were fully optimised by the Berny algorithm, using redundant internal coordinates [24]: the bond lengths to within ca. 0.1 pm and the bond angles to within ca. 0.1°. The final root-mean-square (rms) gradients were always less than 3×10^{-4} hartree bohr^{-1} or hartree rad^{-1}. No geometrical constraints were imposed on the molecules under study. The 6-31G** basis set was used for all geometry optimisations, while for most of the rotational energy barrier calculations the smaller basis set 6-31G* was found to yield good results. All frequency calculations were run at the B3LYP/6-31G** level and wavenumbers above 400 cm^{-1} were scaled [25] before comparing them with reported experimental data.

Quantitative potential-energy profiles for rotation around different bonds within the molecule were obtained, by scanning the corresponding dihedrals and using least-squares fitted Fourier-type functions of a dihedral angle, τ [26,27]:

$$P = \sum_{n=1}^{3} \frac{1}{2} P_n [1 - \cos(n\tau)] + \sum_{m=1}^{2} \frac{1}{2} P'_m \sin(m\tau) \quad (1)$$

The parameters P_n and P'_m correspond to potential-energy (V_n and V_m terms), bond-distance or bond-angle differences relative to a reference value. According to the symmetry of the nitrostyrene molecules presently studied, namely the methyl substituted ones, both cosine and sine terms were considered in the fitting of the experimental data.

2.4. Spectroscopic methods

The Raman spectra were obtained, at room temperature, on a triple monochromator Jobin-Yvon T64000 Raman system (0.640 m, *f*/7.5) with holographic gratings of 1800 grooves mm^{-1}. The detection system was a non-intensified Charge Coupled Device (CCD). The entrance slit was set to 100 μm and the slit between the premonochromator and the spectrograph was opened to 14.0 mm. The 514.5 nm line of an Ar^+ laser (Coherent, model Innova 300) was used as excitation radiation, providing 5–100 mW at the sample position. Samples (pure solids) were sealed in Kimax glass capillary tubes of 0.8 mm inner diameter. Under the above mentioned conditions, the error in wavenumbers was estimated to be within 1 cm^{-1}.

In some cases, the Ar^+ laser 514.5 nm excitation line led to quite strong fluorescence backgrounds, which were avoided by lowering the laser power or, when this was not enough, by using a 1064 nm line provided by a Nd:YAG laser (FT-Raman experiments).

Fourier transform Raman spectra were recorded on a RFS 100/S Bruker spectrometer, with a 180° geometry, equipped with an InGaAs detector. Near-infrared excitation was provided by the 1064 nm line of a Nd:YAG laser (Coherent, model Compass-1064/500N). A laser power of 200 mW at the sample position was used in all cases, and resolution was set to 2 cm^{-1}.

FT-IR data was collected (in KBr pellets) on a MATSON 7000 spectrometer, operating in the 400–4000 cm^{-1} range, using a 2 cm^{-1} resolution.

2.5. Chemicals

trans-β-Nitrostyrene, 1,2-dihydroxybenzene, 3,4-dihydroxybenzaldehyde, styrene, *trans*-β-methylstyrene, ammonium acetate, nitroethane and nitromethane were purchased from Sigma-Aldrich Química S.A. (Sintra, Portugal). All other reagents and solvents were *pro-analysis* grade, purchased from Merck (Lisbon, Portugal).

3. Results and discussion

3.1. Ab initio MO calculations

A complete geometry optimisation was carried out for some of the nitrostyrenes under study, namely: β-nitrostyrene (NS), β-methyl-β-nitrostyrene (MeNS), 3,4-dihydroxy-β-nitrostyrene (3,4-OH-NS) and 3,4-dihydroxy-β-methyl-β-nitrostyrene (3,4-OH-MeNS). The effect of several structural parameters on the overall stability of these molecules was investigated: (i) orientation of the phenolic hydroxyls, relative to the ring—dihedrals ($H_{17}O_8C_5C_4$) and ($H_{18}O_7C_6C_5$) equal to 0 or 180° (Fig. 1); (ii) relative orientation of the aromatic ring and the NO_2 group relative to the $C_9{=}C_{10}$ bond—($C_3C_9C_{10}N_{11}$) dihedral equal to 0 or 180°, defining a *Z* or *E* configuration, respectively; (iii) position of the methyl

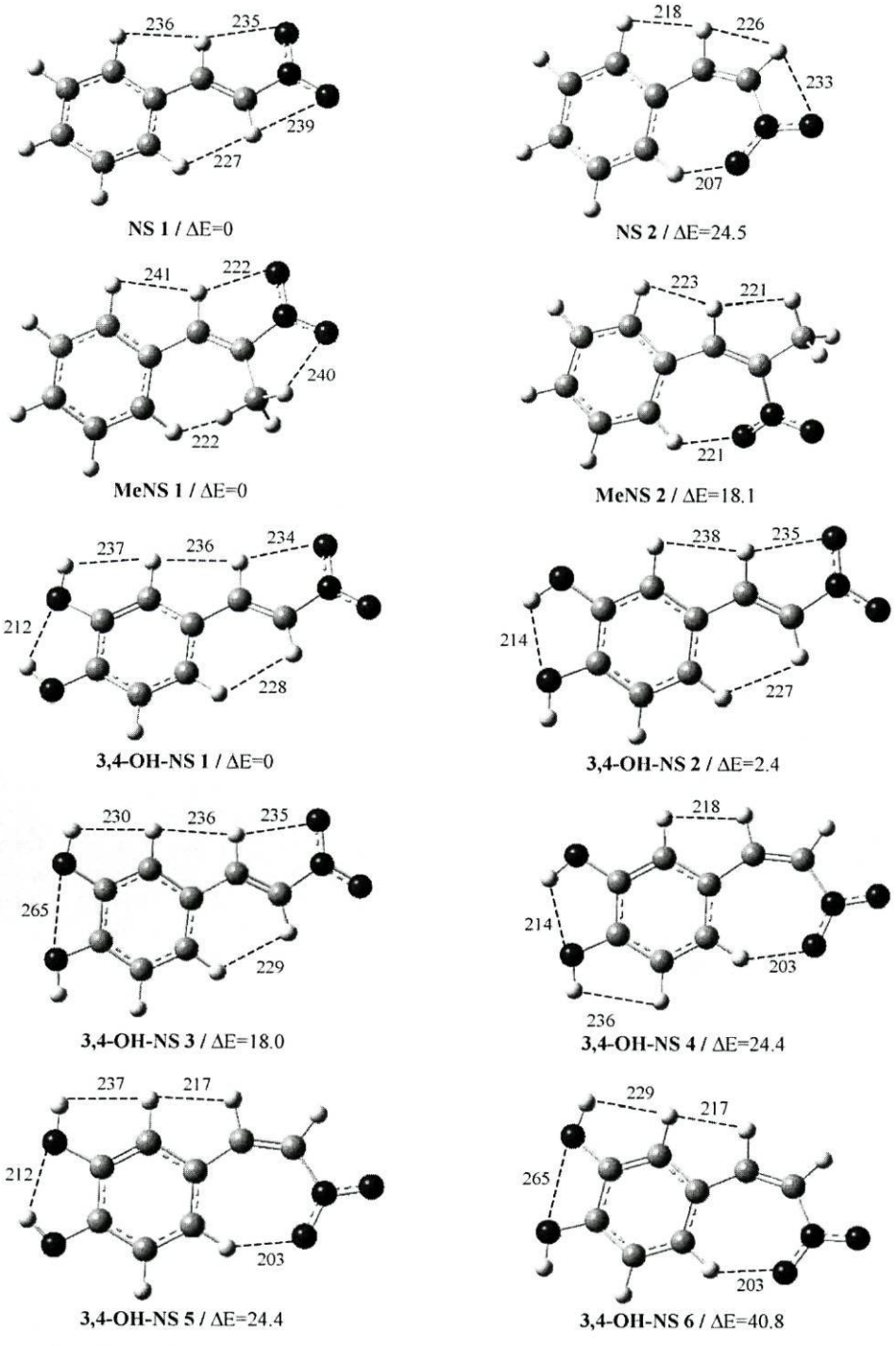

Fig. 2. Schematic representation of the calculated (B3LYP/6-31G**) conformers for β-nitrostyrene (NS), β-methyl-β-nitrostyrene (MeNS) and 3,4-dihydroxy-β-nitrostyrene (3,4-OH-NS) (displaying intramolecular hydrogen bonds—distances in pm. Relative energies are in kJ mol^{-1}).

Table 1
Optimised geometries for the most stable conformers of NS, MeNS and 3,4-OH-NS (B3LYP/6-31G** level of calculation)

μ (D)[a]	NS 1 5.8	MeNS **1** 5.2	3,4-OH-NS 1 6.2
Bond lengths (pm)			
C_1-C_2[b]	139.0	139.3	138.9
C_2-C_3	140.9	140.8	140.8
C_3-C_4	140.7	140.9	141.2
C_4-C_5	139.3	139.1	138.4
C_5-C_6	139.5	139.6	140.8
C_6-C_1	139.9	139.6	139.6
C_3-C_9	146.0	146.4	145.3
C_9-C_{10}	134.0	134.6	134.3
$C_{10}-C_{20}$		149.6	
C_5-O_8			137.4
C_6-O_7			135.4
$C_{10}-N_{11}$	145.1	148.4	144.7
$N_{11}-O_{12}$	123.5	123.3	123.5
$N_{11}-O_{13}$	123.3	123.2	123.5
O_8-H_{17}			0.96
O_7-H_{18}			0.97
C_1-H_{14}	108.6	108.6	108.4
C_2-H_{15}	108.5	108.4	108.4
C_4-H_{16}	108.6	108.6	108.8
C_5-H_8	108.5	108.6	
C_6-H_7	108.6	108.6	
C_9-H_{19}	108.7	108.6	108.7
$C_{10}-H_{20}$	108.0		108.0
$C_{20}-H_{21}$		109.1	
$C_{20}-H_{22}$		109.1	
$C_{20}-H_{23}$		109.6	
Bond angles (°)			
$C_2-C_3-C_4$	118.5	118.2	118.3
$C_2-C_3-C_9$	123.2	124.1	123.5
$C_3-C_9-C_{10}$	127.1	129.1	127.4
$C_9-C_{10}-C_{20}$		130.1	
$C_6-C_5-O_8$			114.6
$C_9-C_{10}-N_{11}$	120.5	115.7	120.3
$C_{10}-N_{11}-O_{12}$	115.7	116.4	115.8
$O_{12}-N_{11}-O_{13}$	124.8	124.0	124.6
$C_5-O_8-H_{17}$			110.3
$C_{10}-C_9-H_{19}$	115.9	115.0	115.5
$C_9-C_{10}-H_{20}$	127.8		127.7
$C_{10}-C_{20}-H_{21}$		110.1	
$C_{10}-C_{20}-H_{22}$		110.1	
$H_{21}-C_{20}-H_{22}$		109.2	
$H_{21}-C_{20}-H_{23}$		106.7	
Dihedral angles (°)			
$C_3-C_4-C_5-C_6$	0.0	−1.3	0.0
$C_5-C_4-C_3-C_9$	0.0	−179.7	180.0
$C_4-C_3-C_9-C_{10}$	180.0	152.3	−180.0
$C_3-C_9-C_{10}-C_{20}$		−3.9	
$C_3-C_9-C_{10}-N_{11}$	180.0	177.8	180.0
$C_9-C_{10}-N_{11}-O_{12}$	180.0	−177.5	−180.0
$C_9-C_{10}-N_{11}-O_{13}$	0.0	2.0	0.0
$C_4-C_5-O_8-H_{17}$			0.0
$C_5-C_6-O_7-H_{18}$			0.0
$C_3-C_4-C_5-H_8$	−180.0	179.2	
$C_4-C_5-C_6-H_7$	180.0	−179.4	
$C_5-C_6-C_1-H_{14}$	180.0	−178.4	180.0
$C_6-C_1-C_2-H_{15}$	180.0	−177.6	180.0
$C_2-C_3-C_4-H_{16}$	180.0	−178.5	180.0
$C_2-C_3-C_9-H_{19}$	−180.0	151.8	−180.0
$C_3-C_9-C_{10}-H_{20}$	0.0		0.0
$C_9-C_{10}-C_{20}-H_{21}$		−137.4	
$C_9-C_{10}-C_{20}-H_{22}$		−16.9	

[a] $1D = 1/3 \times 10^{-2}$ cm.
[b] Atoms are numbered according to Fig. 1; the same atom numbering is applicable to all the compounds studied, irrespective of the type of atom.

group relative to the ring OH's—dihedral ($C_{10}C_9C_3C_4$) either 0 or 180°. The conformational behaviour of this kind of compounds is mainly determined by electronic effects, as well as by the possibility of occurrence of (C)H···O intramolecular hydrogen bonds, which are medium strength, directional interactions (with a preference for linearity), long known to be relevant for the overall stability of numerous systems [28].

Two stable conformations were calculated for both NS and MeNS, while six were obtained for the dihydroxylated analogue 3,4-OH-NS, only one of these, in each case, being significantly populated at room temperature (Fig. 2). All the conformers were found to display a planar or quasi-planar geometry, differing in the configuration of the phenyl and NO_2 groups relative to the linear chain double bond—either *E* or *Z*—and in the orientation of the ring hydroxyls. The *E* conformers with identical orientations of the ring OH's were determined to be the lowest energy ones (Table 1).

For 3,4-OH-MeNS, in turn, ten different conformers were calculated (Figs. 3 and 4), the most stable ones also having an *E* orientation of the aromatic ring and the terminal nitro group relative to the $C_9{=}C_{10}$ bond ($(C_3C_9C_{10}N_{11}) = 180°/(C_{20}C_{10}C_9C_3) = 0°$), along with an identical orientation of both OH ring substituents—conformers **1** ($\Delta E = 0$), **2** ($\Delta E = 0.6$ kJ mol^{-1}) and **3** ($\Delta E = 1.5$ kJ mol^{-1})—with populations at room temperature of 43, 34 and 23%, respectively (Table 2). Actually, the large energy difference between conformations **2** and **4** ($\Delta E = 13.6$ kJ mol^{-1}) is due solely to the change in the ($C_3C_9C_{10}N_{11}$) dihedral angle from 180 to 0° (Fig. 3). In fact, despite the small $O_{13}\cdots H_{16}(C)$ interatomic distance (201 pm, Fig. 3) in 3,4-OH-MeNS **4**, leading to the formation of a 7-membered intramolecular ring, the $H_{15}\cdots H_{19}$ and $H_{23}\cdots H_{19}$ steric hindrance (H···H distances of 216 and 214 pm, respectively) overrules that stabilising factor. As expected, no stable geometry was obtained when both ring hydroxyl groups are directed towards each other. However, three conformers were found for opposite orientations of the phenolic OH's—3,4-OH-MeNS **5** ($\Delta E = 18.1$ kJ mol^{-1}), **9** ($\Delta E = 33.9$ kJ mol^{-1}) and **10** ($\Delta E = 38.7$ kJ mol^{-1})—these being the less stable ones (e.g. 3,4-OH-MeNS **5** vs. 3,4-OH-MeNS **1** and **2**, Fig. 3). For such an arrangement of the OH groups, a ($C_3C_9C_{10}C_{20}$)

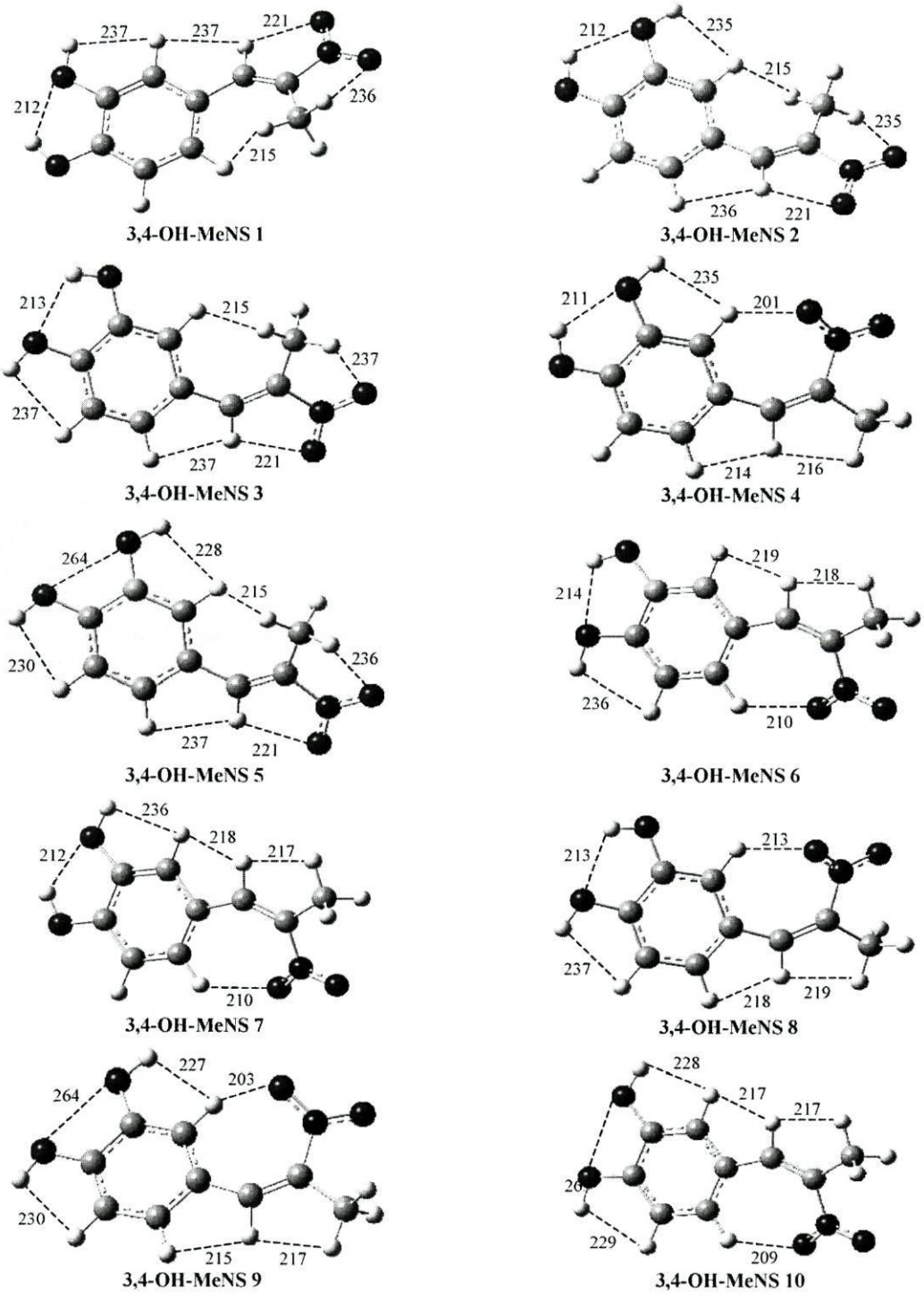

Fig. 3. Schematic representation of the calculated (B3LYP/6-31G**) lowest energy conformers for 3,4-OH-MeNS (displaying intramolecular hydrogen bonds—distances in pm).

dihedral equal to 0° yielded more stable geometries than ($C_3C_9C_{10}C_{20}$) = 180°—3,4-OH-MeNS **5** vs. **9** (Figs. 3 and 4)—on account of the steric repulsion between H_{15} and H_{19} ($H_{15}\cdots H_{19}$ of 215 pm), and H_{19} and H_{22} ($H_{15}\cdots H_{19}$ of 217 pm), which is present in conformer **9**. In contrast, whenever the two ring hydroxyls display the same orientation an energetically favoured geometry results, probably due to the formation of intramolecular hydrogen interactions between O_8 and H_{18}, or O_7 and H_{17} ($O\cdots H$ distances between 211 and 214 pm, Fig. 3).

Moreover, for a ($C_3C_9C_{10}N_{11}$) dihedral equal to 180°, a *syn* orientation of the NO_2 group relative to the OH ring

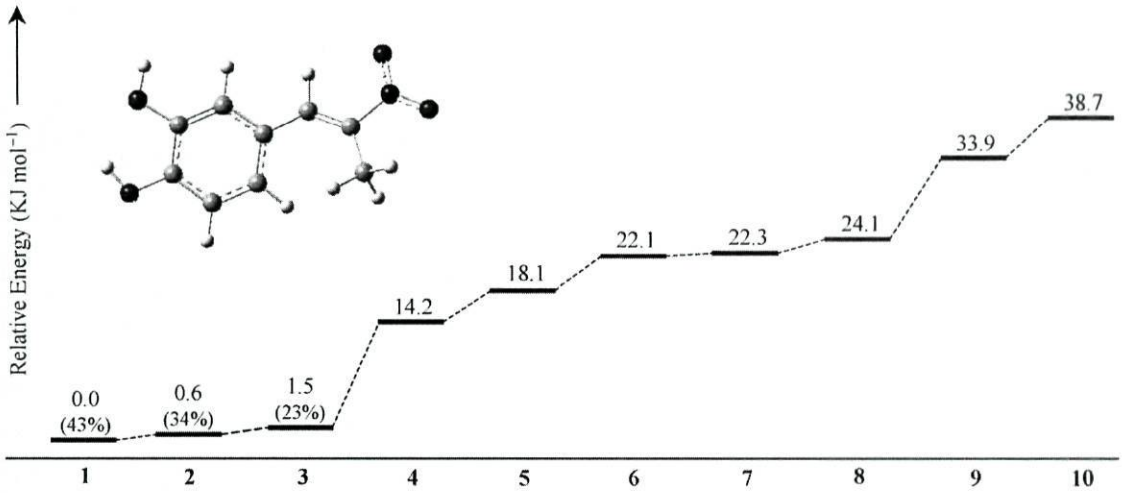

Fig. 4. Schematic representation of the relative conformational energies (and populations, at 25 °C) of the calculated (B3LYP/6-31G**) conformers for 3,4-OH-MeNS.

substituents is energetically favoured, as it allows a more effective electron delocalisation—3,4-OH-MeNS **1** ($\Delta E = 0$) vs. **2** ($\Delta E = 0.6$ kJ mol^{-1}). Also, the zero ($C_4C_3C_9C_{10}$) dihedral in conformation **2** leads to a serious steric hindrance between atoms H_{22} and H_{16}, and H_{19} and H_{15} ($H_{22}\cdots H_{16}$ and $H_{19}\cdots H_{15}$ distances equal to 215 and 236 pm, respectively, Fig. 3). As to the position of the methyl group, it was verified that the geometries displaying a ($C_4C_3C_9C_{10}$) dihedral angle of 0°, a *syn* orientation relative to the ring hydroxyls is favoured (3,4-OH-MeNS **2** ($\Delta E = 0.6$ kJ mol^{-1}) vs. **3** ($\Delta E = 1.5$ kJ mol^{-1}), Fig. 3).

Conformer 3,4-OH-MeNS **10** (($C_4C_3C_9C_{10}$) = 180°) was found to be highly unfavoured relative to 3,4-OH-MeNS **5** (($C_4C_3C_9C_{10}$) = 0°), due to the formation of a medium strength intramolecular H-bond between O_{12} and H_{23} in the latter ($O\cdots H$ distance of 236 pm, Fig. 3), which can not occur in the former ($O\cdots H$ distance of 257 pm).

Although both hydroxyl groups were found to be coplanar with the aromatic ring in all conformers calculated for 3,4-OH-MeNS, the remaining part of the molecule deviates from planarity—($C_2C_3C_9C_{10}$) ca. 23°, ($C_{20}C_{10}C_9C_3$) ca. 4° and ($O_{12}N_{11}C_{10}C_9$) ca. 2°—the most stable geometries displaying one of the methyl hydrogens approaching an oxygen from the NO_2 group, which allows a medium strength H-bond to be formed ($O\cdots H$ distances between 235 and 237 pm, Fig. 3), as well as a minimisation of the H–H steric repulsions.

Rotational isomerism was also investigated for the methyl-nitrostyrene 3,4-OH- -MeNS, by scanning particular dihedral angles—($O_{12}N_{11}C_{10}C_9$), ($H_{22}C_{20}C_{10}N_{11}$) and ($C_{10}C_9C_3C_4$)—which define, respectively, the internal rotation of the nitro and methyl groups, and the orientation of the pendant carbon chain relative to the aromatic ring.

The value of the ($O_{12}N_{11}C_{10}C_9$) dihedral determines the rotation around the C_{10}–N_{11} bond, i.e. the orientation of the NO_2 terminal relative to both the aromatic ring and the double bond in the carbon side chain of the 3,4-OH-MeNS molecule. The analysis of the Fourier components of the corresponding potential-energy variation (Fig. 5) manifests the preference for a planar geometry of the nitro group, once the cosine term in 90° is clearly destabilising—$V_2^{90°} = 30.2$ kJ mol^{-1}—as compared to the 60 and 180° contributions—$V_1^{180°}$ and $V_3^{60°}$ equal to -1.2 kJ mol^{-1}—e.g. geometries 3,4-OH-MeNS **1**, ($O_{12}N_{11}C_{10}C_9$) = $-177.1°/\Delta E = 0$ and 3,4-OH-MeNS **8**, ($O_{12}N_{11}C_{10}C_9$) = $17.5°/\Delta E = 24.1$ kJ mol^{-1}. The negative value of $V_3^{60°}$ is also explained by the stabilising intramolecular H-bond type interactions, which may occur between NO_2 and one of the methyl hydrogen atoms (e.g. conformers 1, 2 or 3, $O_{12}\cdots H(C_{20})$ ca. 236 pm, Fig. 3). The energy barrier for this internal rotation process—from ($O_{12}C_{11}C_{10}C_9$) = 90 to 180°—was calculated to be 31.8 kJ mol^{-1}.

The internal rotation of the 3,4-OH-MeNS methyl group, in turn, is associated to a variation of dihedral ($H_{22}C_{20}C_{10}C_9$), which was studied for the most stable geometry of the molecule (*E* configuration, with ($H_{17}O_8C_5C_4$)/($H_{18}O_7C_6C_5$) = 0°). The best fitting of the experimental data was obtaining by using a combination of both cosine and sine terms—$V_6^{30°} = -0.7$ kJ mol^{-1}, $V_3'^{60°} = 0.8$ kJ mol^{-1} and $V_6'^{30°} = 1.1$ kJ mol^{-1} (Fig. 6)—a maximum being obtained for ($H_{22}C_{20}C_{10}C_9$) = 15°, and three minima occurring for ($H_{22}C_{20}C_{10}C_9$) = 105 (the most favoured geometry), 30 and 90°. This conformational behaviour is a consequence of the balance between the stabilising (C_{20})H$\cdots$O(N_{11}) intramolecular hydrogen-type interactions and the energetically unfavoured (C_{20})H$\cdots H_{15}$ steric hindrances (Table 3).

The orientation of the carbon side chain relative to the aromatic ring is defined by the dihedral angle ($C_{10}C_9C_3C_4$). Once more, the values of the Fourier components of the corresponding potential-energy variation reflect a clear preference for planarity—a minimum occurs for ($C_{10}C_9C_3$

Table 2
Relative energies and optimised geometries for the most stable conformers of 3,4-dihydroxy-β-methyl-β-nitrostyrene (3,4-OH-MeNS) (B3LYP/6-31G** level of calculation)

ΔE (kJ mol^{-1})/μ(D)[a]	3,4-OH-MeNS **1** 0.0/5.1	3,4-OH-MeNS **2** 0.6/5.7	3,4-OH-MeNS **3** 1.5/7.3
Bond lengths (pm)			
C_1-C_2[b]	139.2	139.3	139.1
C_2-C_3	140.8	140.7	140.8
C_3-C_4	141.4	141.1	141.3
C_4-C_5	138.3	138.8	138.5
C_5-C_6	140.9	140.8	140.9
C_6-C_1	139.3	139.3	139.3
C_3-C_9	145.8	146.0	145.7
C_9-C_{10}	134.9	134.8	134.9
$C_{10}-C_{20}$	149.6	149.6	149.6
C_5-O_8	137.4	136.0	137.4
C_6-O_7	135.5	137.1	135.5
$C_{10}-N_{11}$	148.0	148.1	147.8
$N_{11}-O_{12}$	123.4	123.4	123.4
$N_{11}-O_{13}$	123.4	123.4	123.5
O_8-H_{17}	96.5	96.9	96.5
O_7-H_{18}	97.0	96.6	97.0
C_1-H_{14}	108.5	108.7	108.4
C_2-H_{15}	108.2	108.5	108.5
C_4-H_{16}	108.8	108.2	108.5
C_9-H_{19}	108.6	108.6	108.6
$C_{20}-H_{21}$	109.1	109.6	109.1
$C_{20}-H_{22}$	109.6	109.1	109.8
$C_{20}-H_{23}$	109.1	109.1	109.1
Bond angles (°)			
$C_2-C_3-C_4$	117.9	117.9	118.4
$C_2-C_3-C_9$	124.8	117.7	117.4
$C_3-C_9-C_{10}$	129.8	130.0	129.7
$C_9-C_{10}-C_{20}$	129.9	129.9	130.1
$C_6-C_5-O_8$	114.6	114.4	120.4
$C_9-C_{10}-N_{11}$	115.6	115.7	115.6
$C_{10}-N_{11}-O_{12}$	119.6	119.6	119.6
$O_{12}-N_{11}-O_{13}$	123.8	123.8	123.8
$C_5-O_8-H_{17}$	110.2	110.3	107.9
$C_{10}-C_9-H_{19}$	114.5	114.6	114.7
$C_{10}-C_{20}-H_{21}$	110.0	110.1	112.0
$C_{10}-C_{20}-H_{22}$	112.1	112.2	110.1
$H_{21}-C_{20}-H_{22}$	109.2	109.0	106.8
$H_{21}-C_{20}-H_{23}$	108.5	108.7	108.6
Dihedral angles (°)			
$C_3-C_4-C_5-C_6$	−1.3	−1.3	0.0
$C_5-C_4-C_3-C_9$	−179.9	−179.7	179.9
$C_4-C_3-C_9-C_{10}$	157.5	−23.4	23.6
$C_3-C_9-C_{10}-C_{20}$	−4.1	−4.6	4.0
$C_3-C_9-C_{10}-N_{11}$	177.4	177.1	−177.5
$C_9-C_{10}-N_{11}-O_{12}$	−177.2	−177.4	177.3
$C_9-C_{10}-N_{11}-O_{13}$	2.3	2.0	−2.2
$C_4-C_5-O_8-H_{17}$	0.4	−0.1	179.6
$C_5-C_6-O_7-H_{18}$	−0.1	0.0	178.5
$C_5-C_6-C_1-H_{14}$	−178.4	179.1	−179.2
$C_6-C_1-C_2-H_{15}$	−177.5	179.6	−179.7
$C_2-C_3-C_4-H_{16}$	−178.8	175.9	−175.9
$C_2-C_3-C_9-H_{19}$	156.7	−20.4	21.5
$C_9-C_{10}-C_{20}-H_{21}$	−21.5	−21.9	−100.3
$C_9-C_{10}-C_{20}-H_{22}$	99.3	99.3	20.6

[a] Total value of energy for the most stable conformer of 3,4-OH-MeNS is −703,925705439 Hartree (1 Hartree = 2625.5001 kJ mol^{-1}); 1D = 1/3 × 10^{-2} cm.

[b] Atoms are numbered according to Fig. 1; the same atom numbering is applicable to all the compounds studied, irrespective of the type of atom.

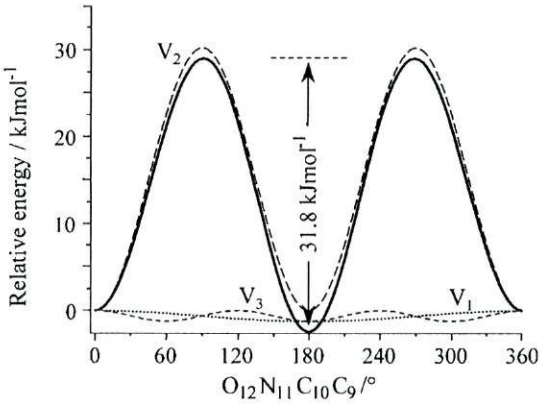

Fig. 5. Optimised conformational energy profile, and its Fourier deconvolution, for the internal rotation around the $N_{11}-C_{10}$ bond of 3,4-OH-MeNS. $V_1 = -1.2$ kJ mol^{-1}, $V_2 = 30.2$ kJ mol^{-1}, $V_3 = -1.2$ kJ mol^{-1} (B3LYP/6-31G* level of calculation).

$C_4) = 150°$ and the cosine term in 90° is by far the primary positive contribution to this profile, $V_2^{90°} = 12.5$ kJ mol^{-1}, as compared to the one in 180°, $V_1^{180°} = -3.1$ kJ mol^{-1} (Fig. 7). This may be attributed to the significant stabilisation due to π-electron delocalisation, which is considerably more effective for a linear *zig-zag* like unsaturated chain, coplanar with the aromatic ring. The fact that the lowest energy conformation was not found to occur for a ($C_{10}C_9C_3C_4$) dihedral equal to 180° is explained by the presence of the methyl group, responsible for $(C_{20})H\cdots H_{15}$ destabilising interactions, which are minimised in the slightly tilted geometry ($(C_{10}C_9C_3C_4) = 150°$, $(C_{20})H\cdots H_{15}$ distances of 222 and 275 pm) as compared to the completely planar one ($(C_{10}C_9C_3C_4) = 180°$, $(C_{20})H\cdots H_{15}$ distances of 222 pm). A value of 16.5 kJ mol^{-1} was determined for the energy barrier corresponding to this internal rotational process—from ($C_{10}C_9C_3C_4$) equal to 150–90°.

The results presently obtained are in perfect accordance with previously reported data on catechol [29], styrene [30] and β-methylstyrene [31], which were, however, determined by either semi-empirical methods (e.g. AM1), or by

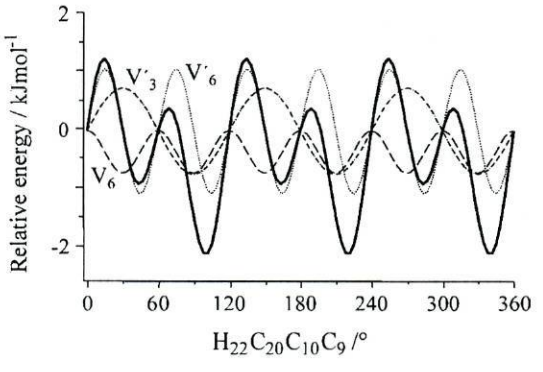

Fig. 6. Optimised conformational energy profile, and its Fourier deconvolution, for the internal rotation around the $C_{20}-C_{10}$ bond of 3,4-OH-MeNS. $V_6 = -0.7$ kJ mol^{-1}, $V'_3 = 0.8$ kJ mol^{-1}, $V'_6 = 1.1$ kJ mol^{-1} (B3LYP/6-31G* level of calculation).

Table 3
Intramolecular $(C_{20})H\cdots H_{15}$ and $(C_{20})H\cdots O(N)$ distances for the distinct geometries yielded by variation of the $(H_{22}C_{20}C_{10}C_9)$ dihedral angle within the 3,4-OH-MeNS molecule (internal rotation of the CH_3 group) (B3LYP/6-31G** level of calculation)

$(H_{22}C_{20}C_{10}C_9)$ (°)	ΔE[a] (kJ mol^{-1})	$d_{(C_{20})H\cdots H_{15}}$[b] (pm)	$d_{(C_{20})H\cdots O(N)}$ (pm)
15	4.38	205	253
30	0.14	218/251	231
45	1.08	220/231	222
60	1.66	221/221	219
75	1.11	219/229	223
90	0.18	218/249	231
99[c]	–	216/266	236
105	0	215/275	240/286
120	1.17	212	250/269

[a] Conformational energies relative to the geometry with $(H_{22}C_{20}C_{10}C_9) = 105°$.
[b] Atoms are numbered according to Fig. 1.
[c] Lowest energy conformer obtained for 3,4-OH-MeNS.

ab initio MO calculations with smaller basis sets than the ones used along this work.

3.2. Raman spectroscopy

Fig. 8 comprises the Raman spectra of the phenolic derivatives studied (in the solid state), in the 75–1750 and 2200–3600 cm^{-1} regions. Harmonic vibrational frequencies were calculated for all conformers of NS, MeNS, 3,4-OH-NS and 3,4-OH-MeNS. A complete assignment of the experimental vibrational features was carried out (Tables 4–6), based on these theoretical calculations, as well as on results previously reported for similar systems [34,35].

Common to all the compounds investigated are the features due to: (i) the NO_2 group—symmetric and asymmetric stretching, at 1250–1336 cm^{-1} and ca. 1550 cm^{-1}, respectively, strong and somewhat weaker

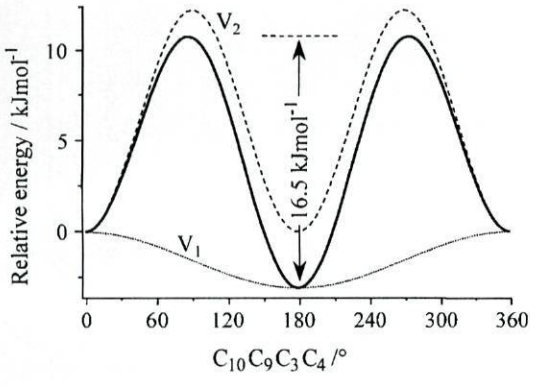

Fig. 7. Optimised conformational energy profile, and its Fourier deconvolution, for the internal rotation around the C_9–C_3 bond of 3,4-OH-MeNS. $V_1 = -3.1$ kJ mol^{-1}, $V_2 = 12.5$ kJ mol^{-1} (B3LYP/6-31G* level of calculation).

absorptions, the latter being often overlapped with the ring C=C stretching; rocking, wagging and scissoring modes, at ca. 500, 700 and 750–800 cm^{-1}, respectively; (ii) the linear chain C=C double bond—stretching vibrations at ca. 1635 cm^{-1}; (iii) the aromatic ring—C=C stretching vibrations, at ca. 1470–1600 cm^{-1}; out-of-plane ring wagging modes—between ca. 870 and 1000 cm^{-1}, for this type of tri-substituted benzenes; (iv) the CH deformations—both wagging, at ca. 1300 cm^{-1}, and rocking modes, at 700–900 cm^{-1}; (v) and the CH typical stretching vibrations, both symmetric and assymmetric, respectively, around 3000–3250 cm^{-1}. While the bands due to the nitro group—around 1300 and 1600 cm^{-1}—are the most intense ones in the spectra of the nitrostyrenes, for the NO_2-free compounds the strongest features are the ones due to the ring wagging modes, at ca. 1000 cm^{-1}.

Either in the pure liquid or the solid states, phenols usually occur as hydrogen-bonded dimers (and oligomers). Thus, the Raman spectra (in the solid phase) of the hydroxyl-substituted nitrostyrenes—3,4-OH-NS and 3,4-OH-MeNS—comprise the high frequency pattern characteristic of the ring hydroxyl stretching modes: a sharp, moderately intense band at 3520–3400 cm^{-1}—free OH stretch—and a very broad strong absorption near 3300 cm^{-1}—O–H···O stretch (Tables 5 and 6). Also detected are the features at 1315–1400 cm^{-1}, corresponding to the in-plane and out-of-plane C–OH deformations (respectively), and at ca. 1280 cm^{-1}, due to the stretching of the phenol C–O bonds (Tables 5 and 6). In turn, the β-methyl-β-nitrostyrenes—MeNS and 3,4-OH-MeNS—yield the typical CH_3 vibrational bands (Tables 5 and 6): symmetric and antisymmetric stretching modes, between 2800 and 3090 cm^{-1}; symmetric and antisymmetric deformations, at ca. 1320 and 1510 cm^{-1}; rocking modes, around 1000 cm^{-1}; and torsions, at 180–250 cm^{-1}.

It was verified that the presence of the methyl group, responsible for significant inductive effects, as a substituent of the unsaturated carbon chain, led to clear changes in the Raman pattern (Fig. 8, Tables 4–6), namely a clear shift (ca. 20–30 cm^{-1}) of the ν $(C{=}C)_{chain}$ to higher wavenumbers—S (1634 cm^{-1}) vs. MeS (1663 cm^{-1}), NS (1633 cm^{-1}) vs. MeNS (1654 cm^{-1}), and 3,4-OH-NS (1612 cm^{-1}) vs. 3,4-OH-MeNS (1637 cm^{-1}). Furthermore, in the absence of CH_3 substitution, a large deviation (100–120 cm^{-1}) of the NO_2 scissoring mode to low frequency values is detected—NS (737 cm^{-1}) vs. MeNS (850 cm^{-1}), and 3,4-OH-NS (725 cm^{-1}) vs. 3,4-OH-MeNS (857/867 cm^{-1}). Also, OH substitution of the aromatic ring was found to give rise to low frequency shifts (62–65 cm^{-1}) of the ν_s (NO_2) band, which may be explained by electron delocalisation effects, favoured in the hydroxylated nitrostyrenes—NS (1336 cm^{-1}) vs. 3,4-OH-NS (1279 cm^{-1}), MeNS (1316 cm^{-1}) vs. 3,4-OH-MeNS (1251 cm^{-1}).

The only phenolic aldehyde studied—3,4-OH-BA—exhibits the characteristic $\nu_{C=O}$ band at 1653 cm^{-1} (Table 4). The aldehyde CH is responsible for the feature

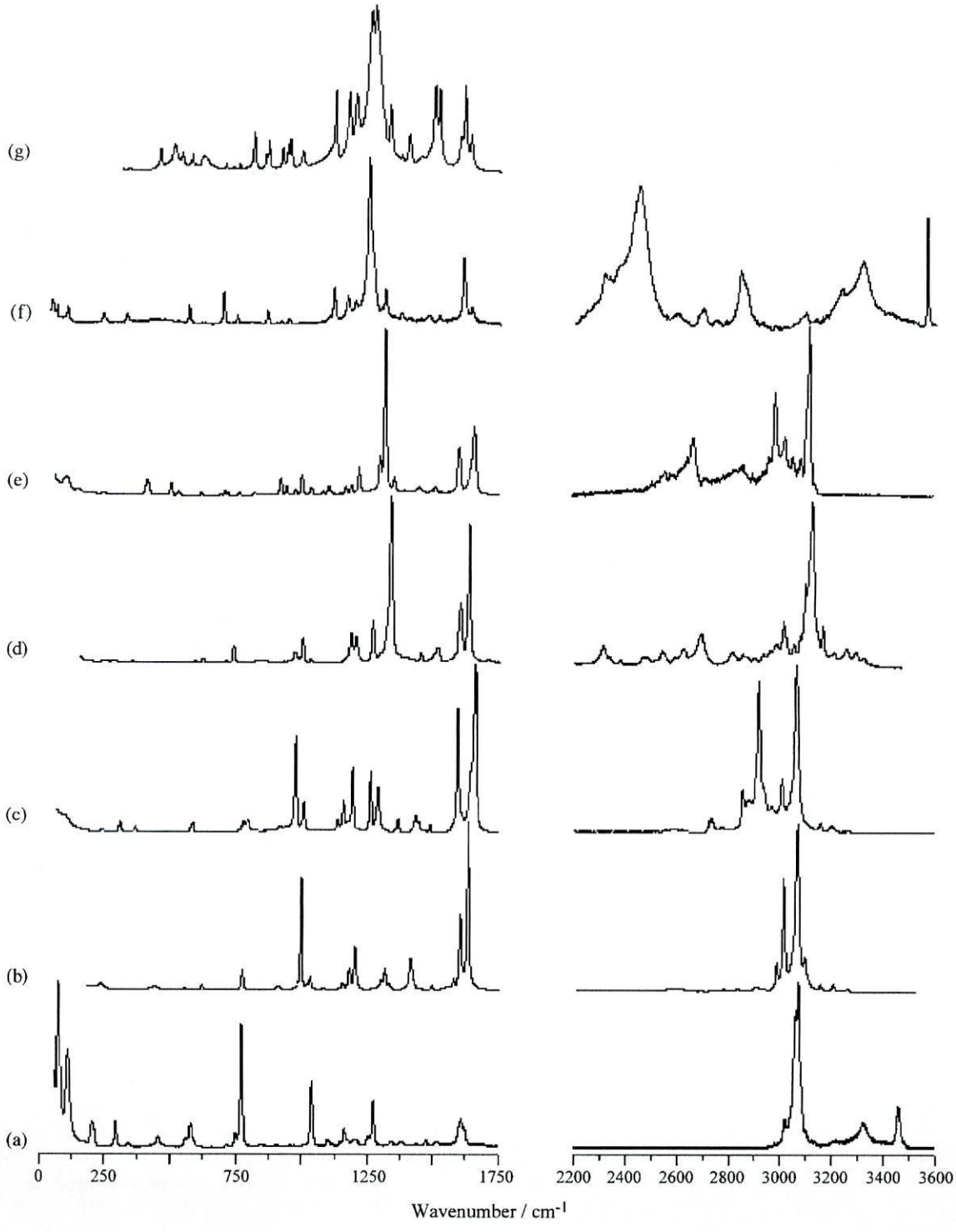

Fig. 8. Experimental Raman spectra (75–1750, 2200–3600 cm^{-1}) of some of the β-nitrostyrene derivatives and their analogues studied in the present work (solid state, at 25 °C): (a) CAT; (b) S; (c) MeS; (d) NS; (e) MeNS; (f) 3,4-OH-MeNS. (g) FTIR spectra (400–1750 cm^{-1}, in KBr pellet) of 3,4-OH-MeNS.

at 1388 cm^{-1}—rocking vibration—as for the characteristic doublet at ca. 2740 and 2890 cm^{-1}, due to a Fermi resonance process between the overtone of that bending mode and the CH stretching fundamental.

The FT-IR spectrum of the β-methyl-β-nitrostyrene of 3,4-OH-MeNS, in the 400–1750 cm^{-1} range, is represented in Fig. 8. The bands due to the stretching modes of the NO_2 group (asymmetric), and the ring and chain double bonds are easily detected, at 1594, 1612 and 1635 cm^{-1}, respectively. Moreover, the bands at ca. 1500 cm^{-1}—CH_3 antisymmetric deformation modes—hardly observed in Raman, appear as well defined, moderately strong features in the FT-IR

Table 4
Raman experimental wavenumbers (cm^{-1}) for CAT, 3,4-OH-BA, S and MeS, in the solid state

Experimental Raman				Approximate description[a]
CAT	3,4-OH-BA	S	MeS	
3459				$\nu\ (O_8H_{17})$
3324	3326			$\nu\ (O_7H_{18})$
		3258		$\nu\ (CH)_{ring}$
3211	3181	3203	3195	$\nu\ (CH)_{ring}$
		3154	3155	$\nu\ (CH)_{chain}$
3102	3114	3094 (3080[b])	3101	$\nu\ (CH)_{ring}$
3071				$\nu\ (CH)_{ring}$
3069	3081	3065 (3068[b])	3062	$\nu\ (CH)_{ring}$
3058 (3032[c])	3053	3059	3057	$\nu\ (CH)_{ring}$
		3050 (3050[b])	3046	$\nu\ (CH)_{chain}$
3019		3012 (3030[b])	3004	$\nu\ (CH)_{ring}$
	2980			FR ($\delta\ (CH) + \nu\ (CH)$)
		2984		$\nu\ (CH_2)$
	2964		2964	$\nu\ (CH)_{ring}$
			2935	$\nu\ (CH)$
			2916	$\nu\ (CH)_{chain}$
		2909		$\nu\ (CH_2)$
	2890		2874 (2881[d])	$\nu_{as}\ (CH_3)$
			2852	$\nu_{s}\ (CH_3)$
	1653			$\nu\ (C = O)$
		1634 (1639[b])	1663 (1668[d])	$\nu\ (C = C)_{chain}$
1621	1645		1647	$\nu\ (CC)_{ring}$
1609 (1625[c])	1592	1604	1599	$\nu\ (CC)_{ring}$
	1582	1578	1579	$\nu\ (CC)_{ring}$
1516	1532	1498 (1499[b])	1495	$\nu\ (CC)_{ring}$
1476	1474			$\delta\ (CH)_{ring}$
	1450	1452 (1432[b])		$\delta\ (CH)_{ring} + \delta\ (CH_2)$ (sciss.)
			1444	$\delta\ (CH)_{ring} + \delta_{as}\ (CH_3)$
1442	1440			$\delta\ (CH)_{ring}$
	1420	1415		$\delta\ (CH)_{ring}$
1381	1388			$\delta\ (CH) + \nu\ (CC)$
			1377 (1390[d])	$\delta_{s}\ (CH_3)$
1348				$\delta\ (CH)_{ring}$
		1337		$\omega\ (CH_2)$
		1320		$\delta_{as}\ (CH_3)$
		1306	1305	$\delta\ (CH)_{chain}\ \nu\ (CC)_{ring}$
	1292			$\delta\ (OH)$
1275 (1251[c])	1271			$\nu\ CO)$
1254			1277	$\nu\ (CC)_{ring}$
		1206	1210	$\delta\ (CH)_{chain}$
1204				$\nu\ (CC)_{ring}$
1177	1188	1184		$\nu\ (CC)_{ring}$
			1177	$\delta\ (CH) + \delta\ (OH)$
1164	1163			$\nu\ (CC)_{ring}$
1151		1158	1156	$\nu\ (CC)$
1104	1116			$\delta\ (CH)_{ring} + \delta\ (OH)$
1041 (1014[c])		1035 (1022[b])	1031	$\delta\ (CH)_{ring} + \nu\ (CC)_{ring}$
		1001 (1003[b])		$\gamma\ (CH)_{ring} + t\ (CH_2)$
	973		1002	$\gamma\ (CH)_{ring}$
			944	$\gamma\ (CH)_{ring}$
907		912 (932[b])		$\omega\ (CH_2)$
846			824	$\gamma\ (CH)_{ring}$
	812		809	$\gamma\ (CH)_{ring}$
774 (756[c])		777 (771[b])		$\gamma\ (CH)_{ring}$
751	755			$\delta\ (CC)_{ring}$
719				$\delta\ (CC)_{ring}$
	628	622	618	$\delta\ (CC)_{ring}$
581	589			$\delta\ (CC)_{ring}$
	502	557 (548[b])		$\delta\ (CC)_{ring}$

(continued on next page)

Table 4 (*continued*)

Experimental Raman				Approximate description[a]
CAT	3,4-OH-BA	S	MeS	
457	448	445 (426[b])		δ $(CC)_{ring}$
	426			γ (OH)
			408 (407[d])	γ (CCC)
	406			γ (OH)
	388			γ (OH)
344	362		351	γ (CCC)
296				γ (CCC)
			284	τ (CH_3)
	239	239		δ (CCC)
	222			δ (CCC)
211	214	214		Skeletal modes
206	212			γ (OH)
112	122		132	τ (CH_3)
	104			Skeletal modes
	80			Skeletal modes
77	72			Skeletal modes
	54			Skeletal modes

[a] Atoms are numbered according to Fig. 1; the same atom numbering is applicable to all the compounds studied, irrespective of the type of atom. d and g stand for in-plane and out-of-plane deformations, respectively.
[b] Calculated values [30].
[c] Refs. [29,32,33].
[d] Ref. [31].

Table 5
Raman experimental and calculated wavenumbers (cm^{-1}) for the most stable conformers of NS, MeNS and 3,4-OH-NS, in the solid state

NS		MeNS		3,4-OH-NS		Approximate description[a]
Exp	Calc[b]	Exp	Calc	Exp[c]	Calc	
				3410	3694 (74;123)	ν (O_8H_{17})
				3306	3626 (151;234)	ν (O_7H_{18}) + ν (OH···O)
3231	3144 (7;34)			3117	3144 (8;38)	ν $(CH)_{chain}$
3195	3091 (14;293)		3099 (6;96)	3063	3098 (4;125)	ν_s $(CH)_{ring}$
3153	3083 (23;39)	3070	3086 (24;230)	3040	3082 (4;34)	ν_{as} $(CH)_{ring}$
3111	3076 (7;106)	3057	3076 (15;86)			ν (CH)
3070	3070 (0;65)	3035	3072 (2;60)	2968	3067 (0;38)	ν $(CH)_{chain}$
3046	3067 (0;58)		3067 (0;98)			ν (CH)
3004	3063 (3;10)	2971	3061 (2;18)	2906	3050 (9;45)	ν_{as} $(CH)_{ring}$
2968						
		2936	3041 (4;49)			ν_{as} (CH_3)
		2912	3005 (7;82)			ν_{as} (CH_3)
		2805	2938 (8;160)			ν_s (CH_3)
2666		2619				$2 \times \nu_s$ (NO_2)
2602						
2524						$2 \times \delta$ (CH)
2453		2510				
2305						(1000 + 1336) cm^{-1} comb. mode
1633	1639 (130;666)	1654	1652 (53;646)	1612	1636 (108;493)	ν C=C
1600	1593 (15;569)	1596	1593 (4;486)		1600 (104;768)	ν $(CC)_{ring}$
1580	1568 (25;5)		1566 (1;22)	1597	1581 (181;314)	ν $(CC)_{ring}$
1514	1555 (150;151)	1505	1561 (171;49)	1486	1549 (175;263)	ν_{as} (NO_2)
1500	1480 (5;12)	1484	1479 (5;26)	1476	1515 (161;3)	δ $(CH)_{ring}$
			1440 (10;31)			δ_{as} (CH_3)
					1429 (43;5)	ν $(CC)_{ring}$ + δ (OH)
			1433 (14;5)			δ_{as} (CH_3) + δ (CH)
		1443	1427 (7;22)			δ_{as} (CH_3) + δ $(CH)_{ring}$
1450	1433 (15;20)					δ $(CH)_{ring}$ + ν $(CC)_{ring}$

Table 5 (*continued*)

NS		MeNS		3,4-OH-NS		Approximate description[a]
Exp	Calc[b]	Exp	Calc	Exp[c]	Calc	
		1385	1383 (29;16)			δ_s (CH_3) + δ $(CH)_{chain}$
				1328	1373 (27;37)	δ (O_7H_{18})
1395		1349	1335 (18;67)	1313		δ $(CH)_{chain}$ + δ_s (CH_3)
1336	1338 (517;641)	1316	1319 (395;474)	1274	1337 (416;979)	ν_s (NO_2) + δ_s (CH_3)
	1318 (6;18)		1313 (4;11)			δ $(CH)_{ring}$
					1314 (2;31)	δ (CH) + δ (OH)
		1296	1290 (24;109)	1295	1290 (692;530)	δ $(CH)_{ring}$ + ν $(CC)_{ring}$
	1307 (8;9)	1216	1200 (18;145)		1275 (87;3)	δ (CH) + ν $(CC)_{ring}$
	1274 (0;15)			1243	1265 (10;83)	δ $(CH)_{chain}$
1266	1238 (27;224)			1212	1213 (28;79)	δ $(CH)_{chain}$
1203	1182 (14;42)			1199	1176 (209;177)	δ (CH) + δ (O_7H_{18})
1184	1163 (21;91)	1185	1166 (5;39)	1176	1155 (1;4)	δ $(CH)_{ring}$
				1159	1133 (165;59)	δ (O_8H_{17})
	1145 (0;13)	1164	1145 (0;11)			δ $(CH)_{ring}$
1162	1070 (5;1)	1102	1085 (11;19)	1121	1089 (85;2)	δ (CH)
1031	1015 (1;19)	1080	1066 (6;10)			δ $(CH)_{ring}$
		1034	1027 (0;18)			r (CH_3)
	982 (23;5)					
1000	976 (0;42)	999	1017 (0;20)	993	1133 (165;59)	δ $(CH)_{ring}$
				972	975 (26;4)	γ $(CH)_{chain}$
970	965 (3;0)					γ (CH)
	957 (70;37)				963 (104;46)	ν (CN)
			976 (4;52)	931	937 (3;5)	δ $(CC)_{ring}$
	939 (0;0)		967 (1;2)			γ $(CH)_{ring}$
		975	962 (64;8)	922		r (CH_3)
	899 (0;2)	942	942 (3;12)	863	910 (1;1)	γ $(CH)_{ring}$ (as wag)
	838 (1;5)					δ (CC)
		918	932 (15;58)		826 (4;4)	γ $(CH)_{chain}$ + γ $(CH)_{ring}$ (as wag)
	827 (7;8)	870	897 (2;10)	840	806 (50;8)	γ $(CH)_{chain}$ + γ $(CH)_{ring}$ (as wag)
		855	850 (48;4)	828		δ (NO_2) (scis.)
	817 (6;8)	821	826 (0;9)	820	798 (8;5)	γ $(CH)_{ring}$ (as wag)
				812	792 (15;17)	δ $(CC)_{ring}$
		763	804 (8;9)			δ $(CCC)_{chain}$
				779	772 (5;14)	δ $(CC)_{ring}$
	753 (39;2)	720	750 (33;8)			γ $(CH)_{ring}$ (s wag) + γ $(CC)_{ring}$
		707	704 (6;10)		707 (0;0)	ω (NO_2) + γ (CH)
737	720 (12;23)			725	704 (13;35)	δ (NO_2) (sciss.)
		690	689 (12;4)			γ $(CH)_{ring}$ (s wag)
710	693 (10;1)					γ $(CH)_{ring}$ (s wag) + ω (NO_2)
618	667 (14;0)	617	678 (16;4)		667 (0;0)	γ $(CC)_{ring}$
594	609 (0;7)	593	608 (0;7)		580 (23;3)	δ $(CC)_{ring}$
574	585 (20;1)		583 (8;1)	576	566 (8;2)	δ $(CC)_{ring}$
534	481 (7;0)	531	498 (9;18)		575 (6;0)	γ (CC)
515	523 (2;2)	503	521 (7;6)	524	527 (1;5)	r (NO_2) + δ $(CC)_{chain}$
					459 (71;3)	γ (O_7H_{18})
					437 (14;0)	γ (O_7H_{18}) + γ $(CC)_{ring}$
		413	413 (4;16)			γ $(CC)_{chain}$
	396 (0;0)					γ $(CC)_{ring}$
352						
285						
253	346 (0;2)				431 (22;2)	δ (CCC)
			404 (2;6)		384 (3;2)	γ $(CC)_{ring}$
			381 (1;1)			γ (CCC)
					318 (4;1)	δ (COH)
					291 (1;6)	δ (CCC)
185	290 (1;3)	281	331 (1;1)		277 (2;0)	γ (CCC)
132	257 (0;2)	245	284 (1;3)	229	242 (0;1)	δ (CCN)
					226 (154;2)	γ (O_8H_{17})
			246 (2;1)	158	182 (6;4)	Skeletal modes
		149	190 (0;3)			τ (CH_3)

(*continued on next page*)

Table 5 (*continued*)

NS		MeNS		3,4-OH-NS		Approximate description[a]
Exp	Calc[b]	Exp	Calc	Exp[c]	Calc	
		105	118 (1;1)			τ (CH_3)
110	130 (2;1)				136 (3;1)	Skeletal modes
90	109 (2;0)	95	89 (0;5)		93 (3;0)	Skeletal modes
71	90 (1;3)		65 (1;3)		70 (2; 1)	Skeletal modes
	37 (0;0)		40 (0;5)		37 (0;0)	Skeletal modes

[a] Atoms are numbered according to Fig. 1; the same atom numbering is applicable to all the compounds studied, irrespective of the type of atom. d and g stand for in-plane and out-of-plane deformations, respectively.
[b] B3LYP/6-31G** level; wavenumbers above 400 cm^{-1} are scaled by 0.9614 [25] (IR intensities in km mol^{-1}; Raman scattering activities in Å amu^{-1}).
[c] FT-Raman.

Table 6
Raman and IR experimental and calculated wavenumbers (cm^{-1}) for the most stable conformers of 3,4-OH-MeNS, in the solid state

Experimental		Calculated[a]		Approximate description[b]
Raman	IR	3,4-OHMeNS **1**	3,4-OHMeNS **2**	
3521	3518	3693 (72;123)	3690 (117;277)	ν (O_8H_{17})
		3628 (145;222)	3639 (101;95)	ν (O_7H_{18})
3297				ν (OH···O)
3219				ν (OH···O)
		3115 (3;54)	3117 (1;33)	ν $(CH)_{ring}$
3092		3090 (4;106)	3081 (4;107)	ν $(CH)_{ring}$
2939		2934 (10;175)	2935 (9;169)	ν_{as} (CH_3)
2878		3070 (0;39)	3073 (2;15)	ν_s (CH)
2861		3049 (9;46)	3053 (17;118)	ν_{as} (CH)
2729		3041 (3;56)	3042 (3;54)	ν_{as} $(CH_3)^1$ / ν_s $(CH_3)^2$
2636		3004 (8;75)	3006 (7;76)	ν_s $(CH_3)^1$/ν_{as} $(CH_3)^2$
2498				$2 \times \nu_s$ (NO_2)
2429				
2377				$2 \times \delta$ (CH)
1635	1635	1646 (61;620)	1647 (65;747)	ν $(C{=}C)_{chain}$
	1612	1602 (120;303)	1604 (84;865)	ν $(CC)_{ring}$
1606	1594	1580 (165;105)	1581 (46;2)	ν $(CC)_{ring}$
1512	1514	1554 (140;8)	1556 (153;89)	ν_{as} (NO_2) + ν $(CC)_{ring}$
		1514 (1;40)	1499 (188;0)	ν $(CC)_{ring}$
1473	1497	1443 (37;19)	1455 (3;88)	δ_{as} (CH_3)
	1444	1436 (52;5)	1441 (5;41)	δ_{as} (CH_3)
		1425 (41;15)	1432 (15;25)	δ_{as} (CH_3) + ν $(CC)_{ring}$
1398	1400	1382 (15;76)	1385 (25;15)	δ_s (CH_3) + δ $(CH)_{chain}$ + δ (O_7H_{18})
1370	1371	1374 (4;81)	1349 (20;66)	δ (O_8H_{17}) + δ_s $(CH_3)^2$ + ν $(CC)_{ring}$
1343				
1328	1329	1340 (263;739)	1328 (8;67)	δ $(CH)_{chain}$ + δ_s (CH_3) + δ (O_7H_{18})
1315				
1311	1303			
1295				
1266				
1250	1273	1314 (342;482)	1317 (209;514)	ν_s (NO_2) + δ_s (CH_3) + δ $(CH)^1$ + δ $(O_7H_{18})^2$
	1258	1294 (394;118)	1303 (323;308)	δ (OH) + δ $(CH)^1_{ring}$ + ν_s $(NO_2)^2$
		1280 (52;26)	1283 (534;371)	δ $(CH)_{ring}$ + ν $(CO)^1$ + ν $(CC)^1_{ring}$
1172		1261 (198;210)	1240 (26;26)	δ (CH)
		1183 (4;3)	1180 (55;4)	δ (O_7H_{18}) + δ (CH)
1120	1121	1156 (130;32)	1161 (26;137)	δ (CH) + δ (OH)
1102	1102	1135 (100;3)	1135 (41;4)	δ (O_8H_{17}) + δ $(CH)_{ring}$
1037		1093 (22;66)	1097 (214;77)	δ $(CH)_{ring}$ + δ (O_8H_{17})
1001		1082 (1;20)	1078 (2;23)	δ (CH_3) + δ $(CH)_{chain}$
999	998	1026 (38;12)	1026 (0;22)	r (CH_3) + γ $(CH)^1_{chain}$
950	950	977 (58;131)	978 (40;10)	δ (CH) + r (CH_3)
940	940	934 (23;0)	932 (17;82)	γ $(CH)_{chain}$
920	920	919 (29;10)	932 (65;32)	δ (CH) + r (CH_3) + γ $(CH)^1_{chain}$ + δ $(CH)^1_{ring}$ (as wag)

Table 6 (*continued*)

Experimental		Calculated[a]		Approximate description[b]
Raman	IR	3,4-OHMeNS **1**	3,4-OHMeNS **2**	
866	867	914 (51;6)	883 (2;1)	δ $(CH)_{ring}$ (as. wag)
	858	838 (34;2)	853 (25;7)	δ (CCN) + δ (NO_2) (sciss) + r (CH_3) + δ $(CH)^1_{ring}$ (s wag)
	813	821 (10;10)	841 (49;4)	δ $(CH)_{ring}$ (s wag)
		803 (5;15)	784 (22;11)	δ $(CH)_{ring}$ (as wag)
755	758	776 (11;13)	774 (28;9)	δ $(CH)_{ring}$ (s wag) + ν (CO) + ν (CC)
	736	767 (8;1)	740 (4;20)	γ (CC) + δ $(CH)_{ring}$ (s wag) + ν (CO)
723	723	712 (1;31)	712 (6;1)	δ $(NO_2)_{wag}$
706	706	686 (2;1)	690 (3;25)	δ (CH_3) + δ_{as} (CCN) + γ (CC)
	621	668 (12;1)	668 (1;3)	γ (ring) + δ (CH_3)
590	591	594 (19; 4)	596 (10;6)	γ (ring)
576	578	575 (5;8)	572 (1;9)	δ_s (ring)
573	575	561 (3;20)	555 (23;6)	δ (CC)
	542			
532	535	523 (59;2)	512 (11;12)	r (NO_2) + ν (CN)
	512			
	478			
	459	458 (3;20)	464 (9;10)	γ (O_7H_{18}) + δ (CCC)
		448 (59;2)	449 (4;14)	γ (O_7H_{18}) + γ $(CCC)_{chain}$
		435 (34;14)	425 (18;23)	γ (O_7H_{18}) + γ (CCC)
		427 (19;3)	414 (55;2)	γ (CCC)
353		376 (1;15)	376 (1;0)	δ (CH_3)
338		348 (1;0)	346 (2;1)	γ $(CCC)_{ring}$ + δ (CCN)
		304 (4;0)	301 (5;0)	δ (OH) + δ (COH)
252		279 (0;2)	291 (3;1)	δ (CCC) + δ (CH_3) + δ (O_8H_{17})
		244 (10; 4)	269 (71;2)	γ (OH) + τ $(CH_3)^1$
		239 (1;4)	245 (97;4)	τ $(CH_3)^1$ + γ $(O_8H_{17})^2$
		225 (139;2)	222 (7;2)	δ (CH_3) + γ $(O_8H_{17})^1$
		189 (11;2)	175 (0;6)	τ (CH_3)
117		163 (2;3)	167 (0;0)	τ (CH_3)
111		99 (3;1)	97 (1;0)	τ (CH_3)
77		69 (0;3)	68 (0;3)	Skeletal modes
73		59 (3;1)	59 (1;1)	Skeletal modes
58		34 (1;3)	35 (1;3)	Skeletal modes

[a] B3LYP/6-31G** level; wavenumbers above 400 cm^{-1} are scaled by 0.9614 [25] (IR intensities in km mol^{-1}; Raman scattering activities in Å amu^{-1}).
[b] Atoms are numbered according to Fig. 1; the same atom numbering is applicable to all the compounds studied, irrespective of the type of atom. The indices 1 and 2 refer to conformers 3,4-OHMeNS **1** and 3,4-OHMeNS **2**; δ and γ stand for in-plane and out-of-plane deformations, respectively.

spectrum. Also, the signal at 1273 cm^{-1}, assigned to the NO_2 symmetric stretching, is far more intense than in Raman (at 1266 cm^{-1}), as well as the features due to the NO_2 scissoring modes, between 850 and 900 cm^{-1}, which is in complete accordance with the theoretical results (Table 6).

The spectra did not reveal any changes upon aging of the compounds, which were stored in the dark in order to avoid decomposition due to oxidation and/or dimerisation processes. This is contrary to previous observations in analogous phenols containing a carboxylic function instead of a nitro group, which were found to yield different Raman and FTIR patterns upon aging (even in the solid state) [36–38]. In turn, it was evident that similar molecules give rise to rather distinct Raman patterns—according to their small structural differences—which allows them to be easily distinguished by this spectroscopic technique.

A good overall agreement was obtained between the experimental and calculated frequency values (after scaling according to Scott and Radom [25]), as well as between these and data previously obtained by the authors for the carboxylic compounds caffeic acid [34] and THPPE [35]. Moreover, the present results are in conformity with those reported for similar molecules, namely some of the synthetic precursors of the nitrostyrenes under study [29–33,39] and carboxylated phenols [36–38].

4. Conclusions

A complete conformational analysis was carried out for differently substituted β-nitrostyrenes, through Raman spectroscopy coupled to ab initio methods. Several conformers were calculated for β-nitrostyrene (NS), β-methyl-β-nitrostyrene (MeNS), 3,4-dihydroxy-β-nitrostyrene (3,4-OH-NS) and 3,4-dihydroxy-β-methyl-β-nitrostyrene (3,4-OH-MeNS), varying in the orientation of both

the pendant arm ring substituent and the phenolic hydroxyl groups. The conformational preferences of these compounds were found to be mainly determined by electrostatic factors, as well as by the formation of (C)H···O and (O)H···O intramolecular interactions. Consequently, the calculated relative energies indicate a clear preference for a planar geometry, i.e. for the presence of a completely conjugated system, strongly stabilised through π-electron delocalisation. The few deviations from planarity were explained by the occurrence of strong steric hindrance effects in the planar conformations. A quantitative potential-energy analysis of several internal rotation processes within the molecules under study was carried out.

The results gathered along this work are in very good accordance with the ones obtained in a previous study on the analogous compounds 3-(3,4-dihydroxyphenyl)-2- -propenoic acid (caffeic acid) [34] and 3-(3,4,5-trihydroxyphenyl)-2-propenoic acid (THPPE) [35].

This kind of conformational analysis based on both spectroscopic and theoretical methods, yielding information at the molecular level, is becoming more and more important for the elucidation of the structure-activity relationships ruling the properties of compounds of biological interest, mainly when coupled to biochemical activity assessment experiments. Evaluation assays on the anticancer activity of phenolic derivatives—namely the β-nitrostyrenes described in this work—are presently in course in our laboratory [40], the knowledge of the conformational characteristics of such systems being essential for the interpretation of the biological results. In fact, this type of structure-activity studies may help to decide which structural features of a molecule give rise to its activity, thus contributing for the design of compounds with enhanced cytotoxic properties (e.g. new anticancer drugs).

Acknowledgements

RC and MPM thank the Chemistry Department of the University of Aveiro (in the person of Dr Helena Nogueira), where the FT-Raman and FT-IR experiments were carried out. FB and NM acknowledge FCT—Unit I and D n° 226/94, and Project POCTI/QCA III (co-financed by the european community fund FEDER)—for financial support. NM is grateful to FCT for a PhD fellowship (PRAXIS XXI/BD/18520/98).

References

[1] A.G.M. Barret, G.G. Graboski, Chem. Rev. 86 (1986) 751.
[2] R.S. Varma, K.P. Naicker, P.J. Liesen, Tetrahedron Lett. 39 (1998) 3977.
[3] C.-F. Yao, W.C. Chen, Y.M. Lin, Tetrahedron Lett. 37 (1996) 6339.
[4] M. Schmidt, K. Eger, Pharmazie 51 (1996) 11.
[5] K. Bailey, D. Legault, Org. Magn. Res. 16 (1981) 47.
[6] L.R. Worthen, H.W. Bond, J. Pharm. Sci. 59 (1970) 1185.
[7] J.H. Kim, J.H. Kim, G.E. Lee, J.E. Lee, I.K. Chung, Mol. Pharmacol. 63 (2003) 1117.
[8] S. Kaap, I. Quentin, D. Tamiru, M. Shaheen, K. Eger, H.J. Steinfelder, Biochem. Pharmacol. 65 (2003) 603.
[9] P. Groupy, A. Fleuriet, M.J. Amiota, J.J. Macheix, J. Agric. Food Chem. 92 (1991) 39.
[10] M.A. Parker, D. Marona-Lewicka, D. Kurrasch, A.T. Shulgin, D.E. Nichols, J. Med. Chem. 41 (1998) 1001.
[11] M.J. Frisch, et al., GAUSSIAN 98, Revision A.9, Gaussian Inc, Pittsburgh PA, 1998.
[12] T.V. Russo, R.L. Martin, P.J. Hay, J. Phys. Chem. 99 (1995) 17085.
[13] A. Ignaczak, J.A.N.F. Gomes, Chem. Phys. Lett. 257 (1996) 609.
[14] F.A. Cotton, X. Feng, J. Am. Chem. Soc. 119 (1997) 7514.
[15] A. Ignaczak, J.A.N.F. Gomes, J. Electroanal. Chem. 420 (1997) 209.
[16] T. Wagener, G. Frenking, Inorg. Chem. 37 (1998) 1805.
[17] F.A. Cotton, X. Feng, J. Am. Chem. Soc. 120 (1998) 3387.
[18] C. Lee, W. Yang, R.G. Parr, Phys. Rev. B37 (1988) 785.
[19] B. Miehlich, A. Savin, H. Stoll, H. Preuss, Chem. Phys. Lett. 157 (1989) 200.
[20] A. Becke, Phys. Rev. A38 (1988) 3098.
[21] A. Becke, J. Chem. Phys. 98 (1993) 5648.
[22] P.C. Hariharan, J.A. Pople, Theor. Chim. Acta 28 (1973) 213.
[23] M.M. Francl, W.J. Pietro, W.J. Hehre, J.S. Binkley, M.S. Gordon, D.J. DeFrees, J.A. Pople, J. Chem. Phys. 77 (1982) 3654.
[24] C. Peng, P.Y. Ayala, H.B. Schlegel, M.J. Frisch, Comp. Chem. 17 (1996) 49.
[25] A.P. Scott, L. Radom, J. Phys. Chem. 100 (1996) 16502.
[26] L. Radom, W.J. Hehre, J.A. Pople, J. Am. Chem. Soc. 94 (1972) 2371.
[27] L.A.E. Batista de Carvalho, A.M. Amorim da Costa, J.J.C. Teixeira-Dias, J. Mol. Struct. (THEOCHEM) 205 (1990) 327.
[28] G.R. Desiraju, T. Steiner, The weak hydrogen bond in structural chemistry and biology, IUCr Monographs on Chystallography-9, Oxford University Press, UK, 1999, and references therein.
[29] F.J. Ramírez, J.T. López Navarrete, Vib. Spec. 4 (1993) 321.
[30] R. Hargitai, P.G. Szalay, G. Pongor, G. Fogarasi, J. Mol. Struct. (THEOCHEM) 306 (1994) 293.
[31] Y. Haas, S. Kendler, E. Zingher, H. Zuckermann, S. Zilberg, J. Chem. Phys. 103 (1995) 37.
[32] S.J. Greaves, W.W. Griffith, Spectrochim. Acta 47A (1991) 133.
[33] M. Gerhards, W. Perl, S. Schumm, U. Henrichs, C. Jacoby, K. Kleinermanns, J. Chem. Phys. 104 (1996) 9362.
[34] E. Besien, M.P.M. Marques, J. Mol. Struct. (THEOCHEM) 625 (2003) 265.
[35] Fiuza, S.M., Gomes, C.A., Milhazes, N., Borges, F., Marques, M.P.M., J. Molec. Struct., in press.
[36] S. Sánchez-Cortés, J.V. García-Ramos, Spectrochim. Acta A55 (1999) 2935.
[37] S. Sánchez-Cortés, J.V. García-Ramos, Appl. Spectrosc. 54 (2000) 230.
[38] S. Sánchez-Cortés, J.V. García-Ramos, J. Colloid Interf. Sci. 231 (2000) 98.
[39] R.E. Clavijo, R. Araya-Maturana, B.K. Cassels, B. Weiss-López, Spectrochim. Acta 50A (1994) 2105.
[40] C.A. Gomes, M.T. Girão da Cruz, J.L. Andrade, N. Milhazes, F. Borges, M.P.M. Marques, J. Med. Chem. 46 (2003) 5395.

8.2 Identificação de precursores sintéticos de drogas do tipo anfetamínico usando espectroscopia de Raman e cálculos *ab initio*: derivados do β-metil-β-nitroestireno.

Artigo reproduzido da revista *The Analyst* (2004) 129: 1106-1117, com permissão da Royal Society of Chemistry.

ARTICLE

THE ANALYST
www.rsc.org/analyst

Identification of synthetic precursors of amphetamine-like drugs using Raman spectroscopy and *ab initio* calculations: β-Methyl-β-nitrostyrene derivatives

Nuno Milhazes,[a,b] Fernanda Borges,[a,c] Rita Calheiros[c] and M. Paula M. Marques*[c,d]

[a] *Departamento de Química Orgânica, Faculdade de Farmácia, Universidade do Porto, 4050-47 Porto, Portugal*

[b] *ISCS-Norte, Rua Central da Gandra, 1317, 4585-116 Gandra, PRD, Portugal*

[c] *Unidade I&D "Química-Física Molecular", Faculdade de Ciências e Tecnologia, Universidade de Coimbra, Ap. 3126, 3001-401 Coimbra, Portugal*

[d] *Departamento de Bioquímica, Faculdade de Ciências e Tecnologia, Universidade de Coimbra, Ap. 3126, 3001-401 Coimbra, Portugal. E-mail: pmc@ci.uc.pt*

Received 8th April 2004, Accepted 27th July 2004
First published as an Advance Article on the web 6th September 2004

The present work reports a vibrational spectroscopic study of several β-methyl-β-nitrostyrene derivatives, which are important intermediates in the synthesis of illicit amphetamine-like drugs, such as 3,4-methylenedioxymethamphetamine (MDMA), 3,4-methylenedioxyamphetamine (MDA), *p*-methoxyamphetamine (PMA) and 4-methylthioamphetamine (4-MTA). A complete conformational analysis of 3,4-methylenedioxy-β-methyl-β-nitrostyrene (3,4-MD-MeNS), 4-methoxy-β-methyl-β-nitrostyrene (4-MeO-MeNS), 4-methylthio-β-methyl-β-nitrostyrene (4-MeS-MeNS), was carried out by Raman spectroscopy coupled to *ab initio* MO calculations—both complete geometry optimisation and harmonic frequency calculation. The Raman spectra show characteristic features of these precursors, which allow their ready differentiation and identification. It was verified that the conformational behaviour of these systems is mainly determined by the stabilising effect of π-electron delocalisation.

1 Introduction

Nitroalkenes in general, and β-nitrostyrene derivatives in particular, are very versatile compounds in synthetic organic chemistry, namely as starting materials for the synthesis of a variety of useful building blocks such as nitroalkanes, amines, ketoximes, hydroxylamines and aldoximes.[1–3] Conjugated nitroalkenes are especially reactive, since they are excellent Michael acceptors both to organometallic reagents[4] and ascorbic acid.[5]

The illegal manufacture of amphetamine-like drugs of abuse relies upon the preparation of the appropriate β-methyl-β-nitrostyrene precursors, *via* Knoevenagel-type condensation. This route is one of the synthetic pathways used in the preparation of the following recreational drugs: 3,4-methylenedioxymethamphetamine ("ecstasy" or MDMA), 3,4-methylenedioxyamphetamine (MDA), 4-methylthioamphetamine (MTA) and 4-methoxyamphetamine (PMA).[6] The abuse of psychoactive drugs such as the above mentioned ones is known to produce serious health problems in users, which can even result in death. While there has been much research on the effect of these drugs in humans, little has been investigated on the effect of the side products and synthetic reaction by-products. β-Nitrostyrene, an intermediate of amphetamine synthesis, has been shown to affect both cell viability and macrophage function.[7] Thus, ingestion of nitrostyrene-contaminated drugs of abuse (*e.g.* "ecstasy") is likely to have a considerable adverse effect on the user (namely on their immune response).[7]

Since different synthetic precursors and intermediates are usually found in illegally produced drugs of abuse,[8] the determination of their presence in these products, as well as their thorough characterisation, is of considerable forensic interest as a means of tracking the clandestine laboratories engaged in the production of such drugs. In addition it could be an important tool for the knowledge of the toxicity profile of the drugs.

Raman spectroscopy has proved, in the last few years, to be a simple and reliable method for the determination of the composition profile of solid samples (*e.g.* seized "ecstasy" tablets).[9–13] Actually, due to its non-invasiveness, high sensitivity and good reproducibility, apart from the fact that it needs virtually no sample preparation, this technique is presently becoming an important tool for the screening of illicit drugs in forensic laboratories, once it yields unique fingerprint spectra, specific for each compound. Moreover the method can be applied either for pure compounds or mixtures.

Reports dealing with the identification of specific synthetic markers of amphetamine-like drugs are scarce. Although several synthetic routes are usually followed (Fig. 1), namely the Leuckart method, the nitrostyrene route used in the present study is also a routine strategy, yielding intermediates with a high cytoxicity (unpublished data). The present work reports the spectral characterisation, through Raman spectroscopy, of the following synthetic precursors of amphetamine-like drugs: 3,4-methylenedioxy-β-methyl-β-nitrostyrene (3,4-MD-MeNS), 4-methoxy-β-methyl-β-nitrostyrene (4-MeO-MeNS) and 4-methylthio-β-methyl-β-nitrostyrene (4-MeS-MeNS). A complete conformational analysis of these compounds was also performed by *ab initio* MO methods—both complete geometry optimisation and harmonic frequency calculation—thus allowing a thorough assignment of the experimental spectral features. The results thus obtained will, in the future, allow a rapid and unequivocal spectroscopic identification of these synthetic precursors of illegally produced drugs of abuse.

2 Materials and methods

2.1 Synthesis

The synthesis of each β-methyl-β-nitrostyrene was performed as described in a recent paper,[14] using nitroethane and the

DOI: 10.1039/b405290k

This journal is © The Royal Society of Chemistry 2004

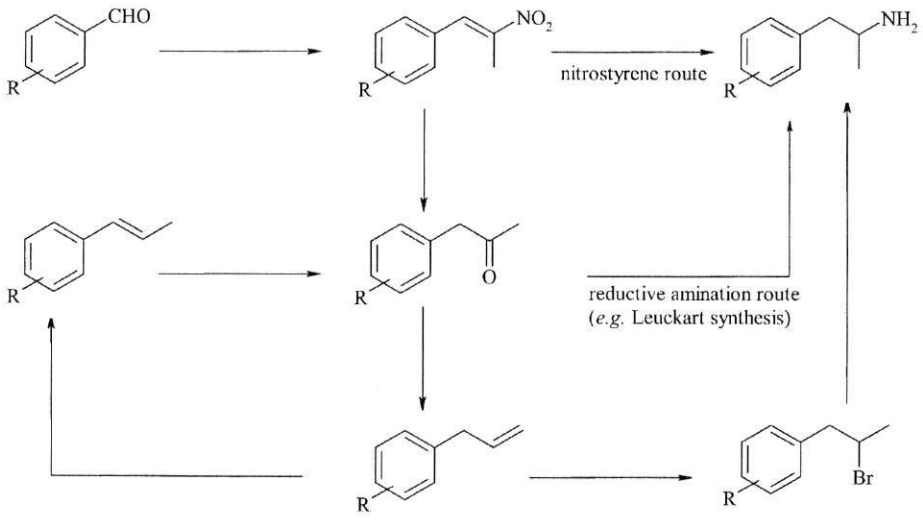

Fig. 1 Schematic representation of the general synthetic routes for amphetamine-like drugs.

benzaldehyde with the corresponding aromatic substitution pattern (Fig. 1). The synthesised compounds were identified by both NMR and electron impact mass spectroscopy (EI-MS).

3,4-Methylenedioxy-β-methyl-β-nitrostyrene (3,4-MD-MeNS). Yield 91%; ^{1}H NMR δ: 2.40 (3H, s, CH_3), 6.12 (2H, s, CH_2), 7.06 (1H, d, J = 8.1, H(5)), 7.18 (1H, dd, J = 8.2; 1.6, H(6)), 7.22 (1H, d, J = 1.6, H(2)), 8.04 (1H, s, H(α)); ^{13}C NMR δ: 14.0 CH_3, 101.9 CH_3, 108.8 *C*HAr, 109.8 *C*HAr, 125.9 C(1), 126.4 *C*HAr, 133.4 C(α), 146.0 C(β), 147.8 C(3), 149.1 C(4); EI-MS *m/z* (%): 207 ($M^{+\cdot}$, 100), 160 (82), 131 (18), 77 (49); mp 91–92 °C.

4-Methoxy-β-methyl-β-nitrostyrene (4-MeO-MeNS). Yield 84%; ^{1}H NMR δ: 2.42 (3H, s, CH_3), 3.83 (3H, s, OCH_3), 7.07 (2H, d, J = 8.8, H(3) and (5)), 7.60 (2H, d, J = 8.4, H(2) and H(6)), 8.08 (1H, s, H(α)); ^{13}C NMR δ: 13.9 CH_3, 55.4 OCH_3, 114.5 (2C, C(3) and C (5)), 124.3 C(1), 132.5 (2C, C(2) and C (6)), 133.3 C(α), 145.4 C(β), 160.9 C(4); EI-MS *m/z* (%): 193 ($M^{+\cdot}$, 85), 146 (100), 131 (44), 115 (49), 103 (57), 91 (44), 77 (43), 63 (23); mp 40–43 °C.

4-Methylthio-β-methyl-β-nitrostyrene (4-MeS-MeNS). Yield 67%; ^{1}H NMR δ: 2.42 (3H, s, CH_3), 2.53 (3H, *s*, SCH_3), 7.36 (2H, d, J = 8.4, H(3) and (5)), 7.55 (2H, d, J = 8.4, H(2) and H(6)), 8.07 (1H, s, H(α)); ^{13}C NMR δ: 14.1 CH_3, 14.1 SCH_3, 125.5 (2C, C(3) and C (5)), 128.2 C(1), 131.0 (2C, C(2) and C (6)), 133.0 C(α), 142.0 C(β), 146.8 C(4); EI-MS *m/z* (%): 209 ($M^{+\cdot}$, 100), 162 (78), 147 (41), 132 (24), 115 (95), 103 (18), 89 (19), 77 (19), 63 (21); mp 69–70 °C.

2.2 Apparatus

^{1}H and ^{13}C NMR data were acquired at room temperature, on a Brüker AMX 300 spectrometer operating at 300.13 and 75.47 MHz, respectively. Dimethylsulfoxide-d_6 was used as a solvent. Chemical shifts are expressed in δ (ppm) values relative to tetramethylsilane (TMS) as an internal reference; coupling constants (J) are given in Hz. Assignments were also made from DEPT (distortionless enhancement by polarization transfer) (underlined values). EI-MS was carried out on a VG AutoSpec instrument; the data are reported as *m/z* (% of relative intensity of the most important fragments). Melting points were obtained on a Köfler microscope (Reichert Thermovar) and are uncorrected.

2.3 *Ab initio* MO calculations

The *ab initio* molecular orbital calculations—full geometry optimisation and calculation of the harmonic vibrational frequencies—were performed using the GAUSSIAN 98W program,[15] within the Density Functional Theory (DFT) approach in order to properly account for the electron correlation effects (particularly important in this kind of conjugated system). The widely employed hybrid method denoted by B3LYP,[16–21] which includes a mixture of HF and DFT exchange terms and the gradient-corrected correlation functional of Lee, Yang and Parr,[22,23] as proposed and parameterised by Becke,[24,25] was used, along with the double-zeta split valence basis set 6–31G**.[26,27] All frequency calculations were run at the B3LYP/6-31G** level, and wavenumbers above 400 cm^{-1} were scaled[28] before comparing them with the experimental data.

Molecular geometries were fully optimised by the Berny algorithm, using redundant internal coordinates:[29] The bond lengths to within *ca.* 0.1 pm and the bond angles to within *ca.* 0.1°. The final root-mean-square (rms) gradients were always less than 3×10^{-4} E_h a_0^{-1} or E_h rad^{-1}. No geometrical constraints were imposed on the molecules under study.

2.4 Spectroscopic methods

The Raman spectra were obtained at room temperature, on a triple monochromator Jobin-Yvon T64000 Raman system (0.640 m, *f*/7.5), with holographic gratings of 1800 grooves mm^{-1}. The detection system was a non-intensified CCD (Charge Coupled Device). The entrance slit was set to 200 μm and the slit between the premonochromator and the spectrograph was opened to 14.0 mm. The 514.5 nm line of an Ar^+ laser (Coherent, model Innova 300) was used as the excitation radiation, providing between 10 to 90 mW at the sample position. Under the above mentioned conditions, the error in wavenumbers was estimated to be within 1 cm^{-1}.

Room-temperature FT-Raman spectra were recorded on an RFS-100 Bruker FT-spectrometer, using an Nd:YAG laser with an excitation wavelength of 1064 nm. Each spectrum is the average of two repeated measurements of 150 scans each, at a 2 cm^{-1} resolution. In all experiments, the samples were sealed in Kimax glass tubes of 0.8 mm inner diameter.

2.5 Chemicals

4-Methoxybenzaldehyde, 4-methylthiobenzaldehyde, 3,4-methylenedioxybenzaldehyde, ammonium acetate and nitroethane were obtained from Sigma-Aldrich Química S.A. (Sintra, Portugal). All other reagents and solvents were *pro analysis* grade, purchased from Merck (Lisbon, Portugal).

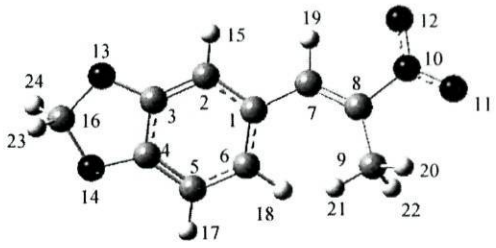

3,4-MD-MeNS

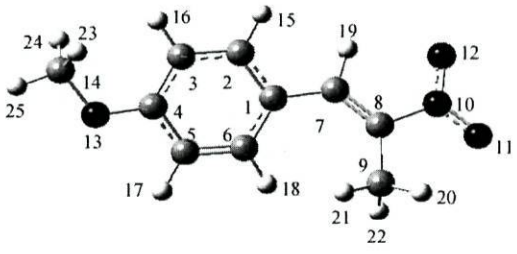

4-MeO-MeNS

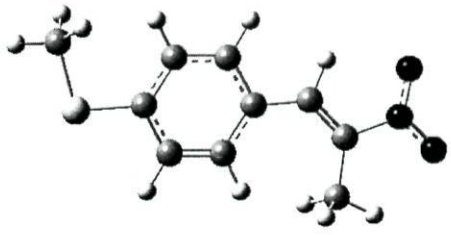

4-MeS-MeNS

Fig. 2 Most stable conformers for the precursors of amphetamine-like drugs studied in the present work (at the B3LYP/6-31G** level of calculation. The atom numbering is included).

3 Results and discussion

3.1 *Ab initio* MO calculations

A complete geometry optimisation was carried out for the three β-methyl-β-nitrostyrene derivatives studied: 3,4-methylenedioxy-β-methyl-β-nitrostyrene (3,4-MD-MeNS), 4-methoxy-β-methyl-β-nitrostyrene (4-MeO-MeNS) and 4-methylthio-β-methyl-β-nitrostyrene (4-MeS-MeNS) (Fig. 2). The effect of several structural parameters on the overall stability of these compounds was investigated, namely: (i) orientation of both the aromatic ring and the NO_2 group relative to the C_7=C_8 bond—($C_1C_7C_8N_{10}$) dihedral equal to 0° or 180°, defining either a *Z* or an *E* configuration, respectively; (ii) position of the CH_3 and NO_2 groups relative to the ring—($C_2C_1C_7C_8$) dihedral either 0° or 180°.

3,4-Methylenedioxy-β-methyl-β-nitrostyrene. Four different conformers were calculated for 3,4-MD-MeNS, the most stable ones displaying an *E* orientation of both the aromatic ring and the terminal nitro group relative to the C_7=C_8 bond—conformers 1 (ΔE = 0) and 2 (ΔE = 0.6 kJ mol^{-1}) (Fig. 3), with populations at room temperature of 59% and 41%, respectively. In fact, the geometries with a dihedral ($C_1C_7C_8N_{10}$) ≈ 180° were found to be highly favoured relative to the ones displaying a *Z* conformation (($C_1C_7C_8N_{10}$) = 0°)—3,4-MD-MeNS 3 (ΔE = 19.4 kJ mol^{-1}) and 4 (ΔE = 22.0 kJ mol^{-1}) (Fig. 3)—most probably due to a more effective π-electron delocalisation, as well as to a minimisation of steric repulsions. Moreover, the large energy difference between conformations 1 and 3 (ΔE = 19.4 kJ mol^{-1}), or 2 and 4 (ΔE = 21.4 kJ mol^{-1}), is solely due to the change in the ($C_1C_7C_8N_{10}$) dihedral angle

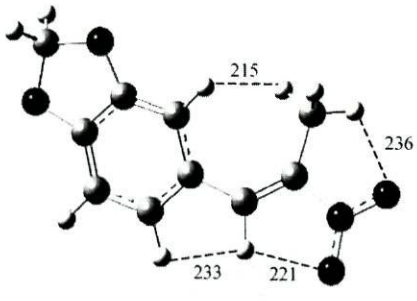

3,4-MD-MeNS1 / ΔE=0

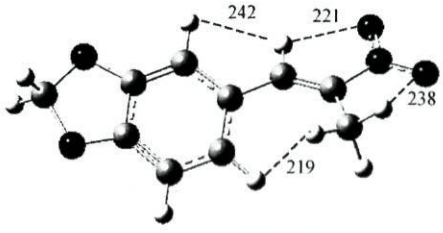

3,4-MD-MeNS2 / ΔE=0.6

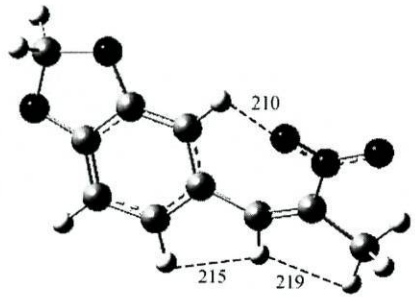

3,4-MD-MeNS3 / ΔE=19.4

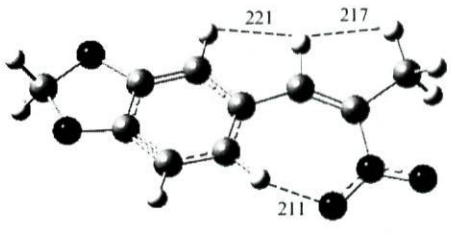

3,4-MD-MeNS4 / ΔE=22.0

Fig. 3 Schematic representation of the calculated (B3LYP/6-31G**) conformers for 3,4-MD-MeNS. (Intramolecular hydrogen bonds are shown. Distances in pm; relative energies in kJ mol^{-1}).

from 180° to 0°, which leads to stronger steric repulsions between H_{18} and H_{19} in conformer 3 ($H_{18}\cdots H_{19}$ of 215 pm), or H_{15} and H_{19} in conformer 4 ($H_{15}\cdots H_{19}$ of 221 pm), relative to the *E* conformers. In addition, the greater stability of 3,4-MD-NeNS 1 and 2 can be explained by the formation of a medium strength intramolecular H-bond between H_{20} (methyl group) and O_{11} (NO_2 group), (C)H···O(N) distance being equal to 236 and 238 pm, respectively (Fig. 3), which does not occur in the *Z* conformations.

A higher deviation of the side carbon chain relative to the aromatic ring was detected for those geometries displaying an *E* conformation—3,4-MD-MeNS 1 ($(C_2C_1C_7C_8) = -23.5°$) and 3,4-MD-MeNS 2 ($(C_2C_1O_7C_8) = 154.4°$)—relative to the *Z* conformers—3,4-MD-MeNS 3 ($(C_2C_1O_7C_8) = 12.5°$) and 3,4-MD-MeNS 4 ($(C_2C_1O_7C_8) = -165.7°$). This is due to steric hindrance effects between H atoms from the CH_3 group and the aromatic ring (H···H intramolecular distances between 215 and 219 pm), which can only occur in the *E* isomers. The NO_2 group displays a clear preference for planarity (dihedrals ($C_1C_7C_8N_{10}$) and ($C_7C_8N_{10}O_{11}$) around 177° in conformers 1 and 2, Table 1), once it allows a more effective electron delocalisation between the aromatic ring, the C=C double bond and the terminal NO_2.

As expected for this kind of compound, the most stable conformers were found to display a slight deviation from planarity relative to the aromatic ring of both the methylene-dioxy group ($(C_2C_3O_{13}C_{16}) = 176.9°$; $(C_3O_{13}C_{16}O_{14}) = 7.0°$, Table 1) and the carbon side chain ($(C_2C_1C_7C_8) = -23.5°$; $(C_1C_7C_8C_9) = -4.4°$, Table 1), on account of the steric hindrance occurring between hydrogen atoms within the molecule (*e.g.* $H_{15}\cdots H_{21}$ and $H_{15}\cdots H_{21}$, H···H distances equal to 215 and 233 pm, respectively).

4-Methoxy-β-methyl-β-nitrostyrene and 4-methylthio-β-methyl-β-nitrostyrene. Four stable geometries were calculated for both 4-MeO-MeNS and 4-MeS-MeNS, but only the *E* conformers, 1 ($\Delta E = 0$) and 2 ($\Delta E = 0.3$ kJ mol^{-1}), were found to be significantly populated at room temperature—53% and 47%, respectively, for both compounds (Fig. 4). As previously discussed for 3,4-MD-MeNS, the higher stability of the *E* conformations is easily explained by an effective π-electron delocalisation (which is favoured for this geometry), along with the formation of a stabilising intramolecular H-bond between H_{20} (CH_3 group) and O_{11} (NO_2 group), with a (C)$H_{20}\cdots O_{11}$(N) distance between 236 and 238 pm (Fig. 4).

For these two *para* substituted nitrostyrenes, the *Z* conformations—4-MeO-MeNS 3 ($\Delta E = 19.2$ kJ mol^{-1}) and 4 ($\Delta E = 20.0$ kJ mol^{-1}), 4-MeS-MeNS 3 ($\Delta E = 19.3$ kJ mol^{-1}) and 4 ($\Delta E = 20.0$ kJ mol^{-1})—were found to be highly unfavourable relative to the *E* ones, probably due to repulsive effects coupled to a less effective π-electron delocalisation. In fact, the *Z* conformers display strong intramolecular repulsions between atoms H_{15} and H_{19} ($H_{15}\cdots H_{19}$ distance between 217 and 218 pm), or H_{18} and H_{19} ($H_{18}\cdots H_{19}$ distance between 217 and 219 pm), which leads to a lower stabilisation. Moreover, in these *Z* isomers there is a slightly larger deviation of the nitro group relative to the carbon chain, resulting in a less effective π-electron delocalisation within the molecule and consequently to higher relative conformational energies—*e.g.* 4-MeO-MeNS 1 ($(C_1C_7C_8N_{10}) = 177.3°$, $(C_7C_8N_{10}O_{11}) = -177.2°$)) *vs.* 4-MeO-MeNS 3 ($(C_1C_7C_8N_{10}) = 5.1°$, $(C_7C_8N_{10}O_{11}) = -169.8°$)), and 4-MeS-MeNS 1 ($(C_1C_7C_8N_{10}) = 175.5°$, $(C_7C_8N_{10}O_{11}) = -177.2°$)) *vs.* 4-MeS-MeNS 3 ($(C_1C_7C_8N_{10}) = -5.4°$, $(C_7C_8N_{10}O_{11}) = 166.4°$)) (Fig. 4).

For all energy minima, the OMe and SMe groups were found to be planar or *quasi*-planar relative to the aromatic ring ($(C_3C_4O_{13}C_{14}) = -0.2°$, $(C_3C_4S_{13}C_{14}) = 0.3°$, Tables 2 and 3). The atoms H_{23} and H_{24} from the CH_3 group are thus equidistant to H_{16}, leading to a minimisation of H···H steric repulsions.

Table 1 Calculated geometrical parameters (B3LYP/6-31G**) for the most stable conformers of 3,4-MD-MeNS

[a](ΔE/kJ mol^{-1})/([b] μ/D)	3,4-MD-MeNS 1 0.0/6.3	3,4-MD-MeNS 2 0.9/6.2
Bond lengths/pm		
[c]C_1–C_2	142.1	142.2
C_2–C_3	137.6	137.5
C_3–C_4	139.6	139.5
C_4–C_5	138.2	138.2
C_5–C_6	140.1	140.3
C_6–C_1	140.9	140.7
C_1–C_7	145.9	146.1
C_7–C_8	134.9	134.8
C_8–C_9	149.6	149.6
C_3–O_{13}	137.3	137.2
C_4–O_{14}	136.7	136.7
C_{16}–O_{13}	143.2	143.3
C_{16}–O_{14}	143.6	143.7
C_8–N_{10}	148.0	148.1
N_{10}–O_{11}	123.4	123.4
N_{10}–O_{12}	123.3	123.3
C_2–H_{15}	108.1	108.4
C_5–H_{17}	108.3	108.4
C_6–H_{18}	108.5	108.2
C_{16}–H_{23}	109.4	109.6
C_{16}–H_{24}	109.8	109.6
C_7–H_{19}	108.6	108.6
C_9–H_{20}	109.1	109.1
C_9–H_{21}	109.1	109.1
C_9–H_{22}	109.6	109.6
Bond angles/degrees		
C_6–C_1–C_2	119.3	119.4
C_6–C_1–C_7	117.0	123.7
C_1–C_7–C_8	129.9	129.5
C_7–C_8–C_9	130.2	130.0
C_4–C_3–O_{13}	109.5	109.6
C_3–O_{13}–C_{16}	106.1	106.2
C_7–C_8–N_{10}	115.6	115.7
C_8–N_{10}–O_{11}	116.6	116.6
O_{11}–N_{10}–O_{12}	123.8	123.8
C_8–C_7–H_{19}	114.6	114.8
C_8–C_9–H_{20}	110.0	110.1
C_8–C_9–H_{21}	110.2	110.0
H_{20}–C_9–H_{21}	109.0	109.3
H_{20}–C_9–H_{22}	106.7	106.7
H_{23}–C_{16}–H_{24}	111.0	110.9
Dihedral angles/degrees		
C_1–C_2–C_3–C_4	0.3	−1.3
C_3–C_2–C_1–C_7	179.9	179.9
C_2–C_1–C_7–C_8	−23.5	154.4
C_1–C_7–C_8–C_9	−4.4	−4.4
C_1–C_7–C_8–N_{10}	177.3	177.5
C_7–C_8–N_{10}–O_{11}	−177.4	−177.7
C_2–C_3–O_{13}–C_{16}	176.9	−179.7
C_3–O_{13}–C_{16}–O_{14}	7.1	−1.7
C_3–O_{13}–C_{16}–H_{23}	126.0	117.4
C_3–O_{13}–C_{16}–H_{24}	−111.9	−120.7
C_6–C_1–C_2–H_{15}	175.5	−178.7
C_3–C_4–C_5–H_{17}	178.9	−178.3
C_4–C_5–C_6–H_{18}	179.8	−177.4
C_6–C_1–C_7–H_{19}	−20.7	153.5
C_7–C_8–C_9–H_{20}	−141.3	−139.8
C_7–C_8–C_9–H_{21}	−21.1	−19.3

[a] Total value of energy for the most stable conformer of 3,4-MD-MeNS is −703.925705439 E_h (1 E_h = 2625.5001 kJ mol^{-1}). [b] D = 1/3 × 10^{-2} C m. [c] Atoms are numbered according to Fig. 2.

3.2 Raman spectroscopy

The Raman spectra of the drug precursors investigated in this work (solid state) are represented in Fig. 5, for both the 75–1750 cm^{-1} and 2200–3400 cm^{-1} regions. Experimental Raman wavenumbers for 3,4-MD-MeNS, 4-MeO-MeNS and

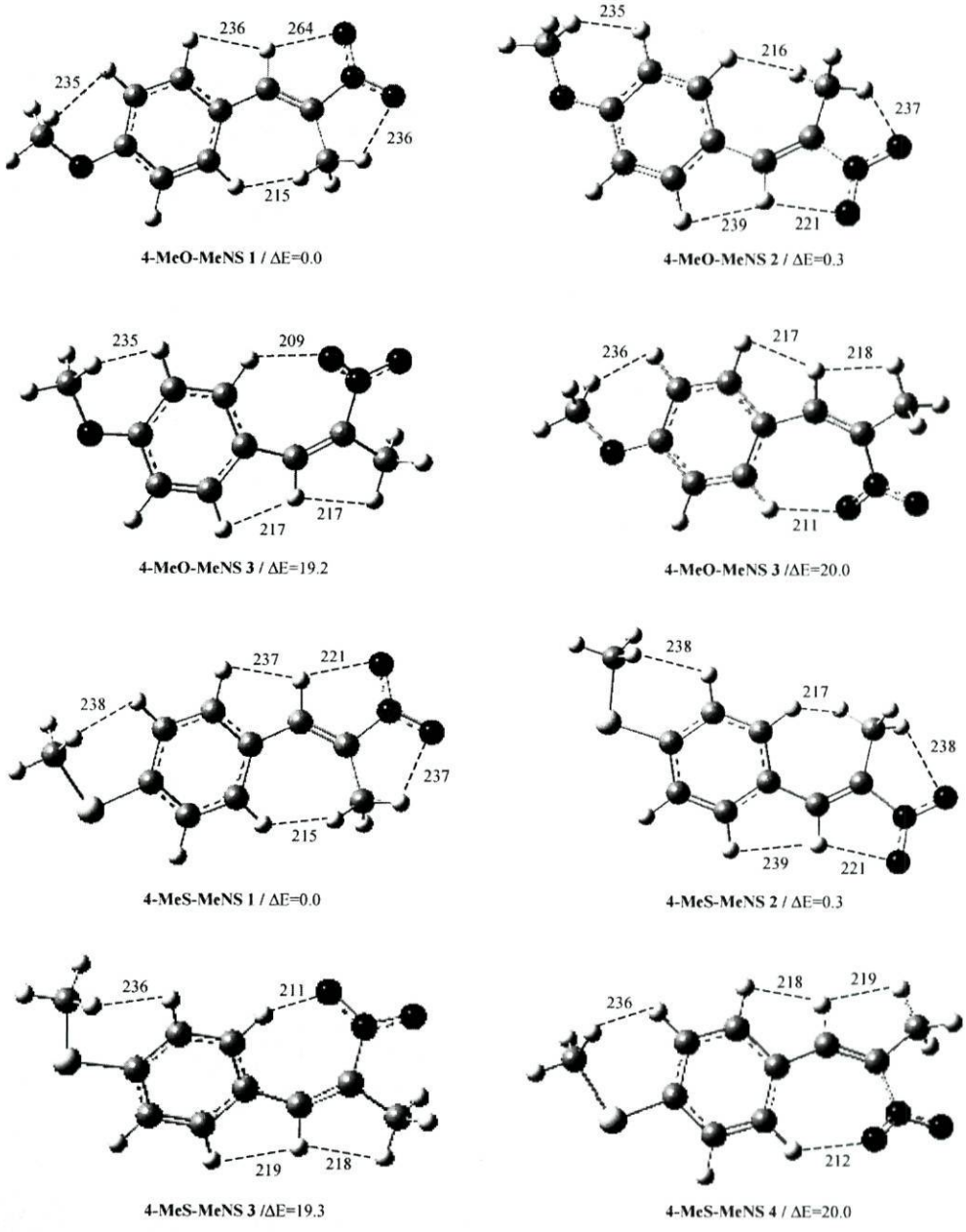

Fig. 4 Schematic representation of the calculated (B3LYP/6-31G**) conformers for 4-MeO-MeNS and 4-MeS-MeNS. (Intramolecular hydrogen bonds are shown. Distances in pm; relative energies in kJ mol^{-1}.)

4-MeS-MeNS are listed in Tables 4, 5 and 6, respectively, along with the calculated values for the two most stable conformers found for each compound.

A complete assignment of the experimental vibrational features was carried out (Tables 4 to 6), in the light of both the theoretical results presently performed and the spectroscopic data previously reported for β-methyl-β-nitrostyrene derivatives[14,30,31] and similar systems.[32–38]

The main Raman spectral features common to all compounds studied were (Fig. 5): (i) the C=C ring stretching vibrations, at *ca.* 1515–1645 cm^{-1} and 1220–1390 cm^{-1}; the in-plane and out-of-plane C=C ring deformations, respectively around 630–1100 cm^{-1} and 425–717 cm^{-1}; the out-of-plane C=C ring deformation, at *ca.* 717 cm^{-1}, which was often found to be overlapped with the NO_2 wagging mode; (ii) the linear chain C=C stretching vibrations, at *ca.* 1646–1650 cm^{-1}; (iii) the NO_2 symmetric and antisymmetric stretching modes, at *ca.* 1300 cm^{-1} and *ca.* 1550 cm^{-1}, respectively; the NO_2 scissoring modes at *ca.* 830–880 cm^{-1}; (iv) The CH_3 symmetric and antisymmetric stretching modes, respectively around 2907–2987 cm^{-1} and 2976–3045 cm^{-1}, along with the other CH stretching vibrations between 3000 cm^{-1} and 3250 cm^{-1}.

The Raman band due to the symmetric stretching of the nitro group, detected at *ca.* 1300 cm^{-1}, is the most intense one in all the spectra presently recorded (Fig. 5). In turn, relatively intense bands at *ca.* 1310 cm^{-1} and 1605 to 1641 cm^{-1}—assigned to ν $(C{=}C)_{ring}$—are often overlapped with both ν_s (NO_2) (at *ca.* 1298 to 1316 cm^{-1}) and ν $(C{=}C)_{chain}$ (at *ca.* 1650 cm^{-1}), respectively (Tables 4 to 6). Moreover, the moderately intense bands detected between 1170 and 1260 cm^{-1}, associated to the C–H in-plane ring deformations, were easily detected for all three nitrostyrenes studied. The Raman spectra of these compounds also yield typical features of the methyl group, namely δ_s $(CH_3)_{chain}$ (1355 to 1365 cm^{-1}), δ_{as} $(CH_3)_{chain}$ (1434 to 1452 cm^{-1}) and τ $(CH_3)_{chain}$ (218 to 303 cm^{-1}), the latter with very low intensity (Tables 4 to 6).

Despite the common vibrational features, the β-methyl-β-nitrostyrene derivatives under study were found to give rise to distinctive Raman patterns, which allow them to be easily

Table 2 Calculated geometrical parameters (B3LYP/6-31G**) for the most stable conformers of 4-MeO-MeNS

[a](ΔE/kJ mol^{-1})/[b](μ/D)	4-MeO-MeNS 1 0.0/6.7	4-MeO-MeNS 2 0.3/6.8
Bond lengths/pm		
[c]C_1–C_2	140.7	140.6
C_2–C_3	139.1	139.3
C_3–C_4	140.2	140.2
C_4–C_5	140.5	140.5
C_5–C_6	138.4	138.3
C_6–C_1	141.3	141.3
C_1–C_7	145.8	145.9
C_7–C_8	134.9	134.9
C_8–C_9	149.6	149.6
C_4–O_{13}	135.8	135.8
O_{13}–C_{14}	142.2	142.2
C_8–N_{10}	147.9	147.9
N_{10}–O_{11}	123.4	123.4
N_{10}–O_{12}	123.3	123.3
C_2–H_{15}	108.5	108.3
C_3–H_{16}	108.3	108.3
C_5–H_{17}	108.5	108.5
C_6–H_{18}	108.3	108.6
C_7–H_{19}	108.6	108.6
C_9–H_{20}	109.1	109.1
C_9–H_{21}	109.1	109.1
C_9–H_{22}	109.6	109.6
C_{14}–H_{23}	109.8	109.7
C_{14}–H_{24}	109.7	109.7
C_{14}–H_{25}	109.0	109.0
Bond angles/degrees		
C_6–C_1–C_2	117.3	117.3
C_6–C_1–C_7	124.9	117.9
C_1–C_7–C_8	129.8	129.6
C_7–C_8–C_9	129.9	129.9
C_4–O_{13}–C_{14}	118.5	118.6
C_7–C_8–N_{10}	115.7	115.8
C_8–N_{10}–O_{11}	116.6	116.6
O_{11}–N_{10}–O_{12}	123.7	123.8
O_{13}–C_{14}–H_{23}	111.5	111.5
O_{13}–C_{14}–H_{24}	111.5	111.5
C_1–C_2–H_{15}	118.9	120.0
C_2–C_3–H_{16}	119.5	119.2
C_8–C_7–H_{19}	114.6	114.7
C_8–C_9–H_{20}	110.1	110.1
C_8–C_9–H_{21}	110.1	110.0
H_{20}–C_9–H_{21}	109.1	109.2
H_{20}–C_9–H_{22}	106.8	106.8
H_{23}–C_{14}–H_{24}	109.3	109.3
H_{23}–C_{14}–H_{25}	109.3	109.3
Dihedral angles/degrees		
C_1–C_2–C_3–C_4	−1.3	−0.1
C_3–C_2–C_1–C_7	−179.6	−179.5
C_2–C_1–C_7–C_8	158.3	−25.7
C_1–C_7–C_8–C_9	−4.3	−4.4
C_1–C_7–C_8–N_{10}	177.3	177.3
C_7–C_8–N_{10}–O_{11}	−177.2	−177.7
C_2–C_3–C_4–O_{13}	−179.6	179.6
C_3–C_4–O_{13}–C_{14}	−0.2	0.7
C_6–C_1–C_2–H_{15}	−178.5	175.8
C_1–C_2–C_3–H_{16}	179.2	179.2
C_3–C_4–C_5–H_{17}	−178.2	179.0
C_4–C_5–C_6–H_{18}	−177.7	179.5
C_6–C_1–C_7–H_{19}	157.4	−22.2
C_7–C_8–C_9–H_{20}	−141.8	−140.5
C_7–C_8–C_9–H_{21}	−21.5	−20.1
C_4–O_{13}–C_{14}–H_{23}	−61.2	−62.0
C_4–O_{13}–C_{14}–H_{24}	61.2	60.4

[a] Total value of energy for the most stable conformer of 4-MeO-MeNS is −668.009740128 E_h (1 E_h = 2625.5001 kJ mol^{-1}). [b] D = 1/3 × 10^{-2} C m. [c] Atoms are numbered according to Fig. 2.

Table 3 Calculated geometrical parameters (B3LYP/6-31G**) for the most stable conformers of 4-MeS-MeNS

[a](ΔE/kJ mol^{-1})/[b](μ/D)	4-MeS-MeNS 1 0.0/6.1	4-MeS-MeNS 2 0.3/7.3
Bond lengths/pm		
[c]C_1–C_2	140.7	140.7
C_2–C_3	139.0	139.2
C_3–C_4	140.2	140.2
C_4–C_5	140.6	140.7
C_5–C_6	138.6	138.5
C_6–C_1	141.3	141.1
C_1–C_7	145.9	146.9
C_7–C_8	134.8	134.8
C_8–C_9	149.6	149.6
C_4–S_{13}	177.5	177.5
S_{13}–C_{14}	182.2	182.2
C_8–N_{10}	148.1	148.0
N_{10}–O_{11}	123.4	123.4
N_{10}–O_{12}	123.3	123.3
C_2–H_{15}	108.6	108.3
C_3–H_{16}	108.3	108.4
C_5–H_{17}	108.6	108.6
C_6–H_{18}	108.3	108.6
C_7–H_{19}	108.6	108.6
C_9–H_{20}	109.1	109.1
C_9–H_{21}	109.1	109.1
C_9–H_{22}	109.6	109.6
C_{14}–H_{23}	109.2	109.2
C_{14}–H_{24}	109.2	109.2
C_{14}–H_{25}	109.2	109.2
Bond angles/degrees		
C_6–C_1–C_2	117.3	117.3
C_6–C_1–C_7	124.9	117.9
C_1–C_7–C_8	129.7	129.4
C_7–C_8–C_9	130.0	129.9
C_4–S_{13}–C_{14}	103.8	103.8
C_7–C_8–N_{10}	115.7	115.9
C_8–N_{10}–O_{11}	116.6	116.6
O_{11}–N_{10}–O_{12}	123.8	123.9
S_{13}–C_{14}–H_{23}	111.5	111.5
S_{13}–C_{14}–H_{24}	111.6	111.5
C_2–C_3–H_{15}	118.9	120.0
C_2–C_3–H_{16}	119.0	118.7
C_8–C_7–H_{19}	114.7	114.8
C_8–C_9–H_{20}	110.1	110.0
C_8–C_9–H_{21}	110.1	110.1
H_{20}–C_9–H_{21}	109.1	109.2
H_{20}–C_9–H_{22}	106.8	106.8
H_{23}–C_{14}–H_{24}	110.4	110.4
H_{23}–C_{14}–H_{25}	108.9	108.9
Dihedral angles/degrees		
C_1–C_2–C_3–C_4	−1.3	−0.1
C_3–C_2–C_1–C_7	−179.5	−179.5
C_2–C_1–C_7–C_8	157.2	−26.4
C_1–C_7–C_8–C_9	−4.1	−4.3
C_1–C_7–C_8–N_{10}	177.5	177.4
C_7–C_8–N_{10}–O_{11}	−177.2	−177.6
C_2–C_3–C_4–S_{13}	−179.8	−179.5
C_3–C_4–S_{13}–C_{14}	0.3	0.5
C_6–C_1–C_2–H_{15}	−178.5	175.8
C_1–C_2–C_3–H_{16}	179.1	179.2
C_3–C_4–C_5–H_{17}	−178.2	179.0
C_4–C_5–C_6–H_{18}	−177.7	179.5
C_6–C_1–C_7–H_{19}	156.5	−22.9
C_7–C_8–C_9–H_{20}	−141.0	−139.8
C_7–C_8–C_9–H_{21}	−20.7	−19.4
C_4–S_{13}–C_{14}–H_{23}	111.5	111.5
C_4–S_{13}–C_{14}–H_{24}	−61.9	−62.3

[a] Total value of energy for the most stable conformer of 4-MeS-MeNS is −990.987429241 E_h (1 E_h = 2625.5001 kJ mol^{-1}). [b] D = 1/3 × 10^{-2} C m. [c] Atoms are numbered according to Fig. 2, irrespective of the type of atom (O or S).

identified through this spectroscopic technique. 3,4-MD-MeNS is characterised by the frequencies at 1201 cm^{-1} (t (CH_2), 1034 cm^{-1}, (δ (OCO) and δ $(CH)_{ring}$) and 945 cm^{-1} (ν ($C_{16}O$)). MeO-MeNS and 4-MeS-MeNS, in turn, are readily identified by the medium intensity bands due to the ϕ-O and ϕ-S stretching modes detected at 1256 and 1095 cm^{-1}, respectively, as well as by the low intensity features observed at 1037 and

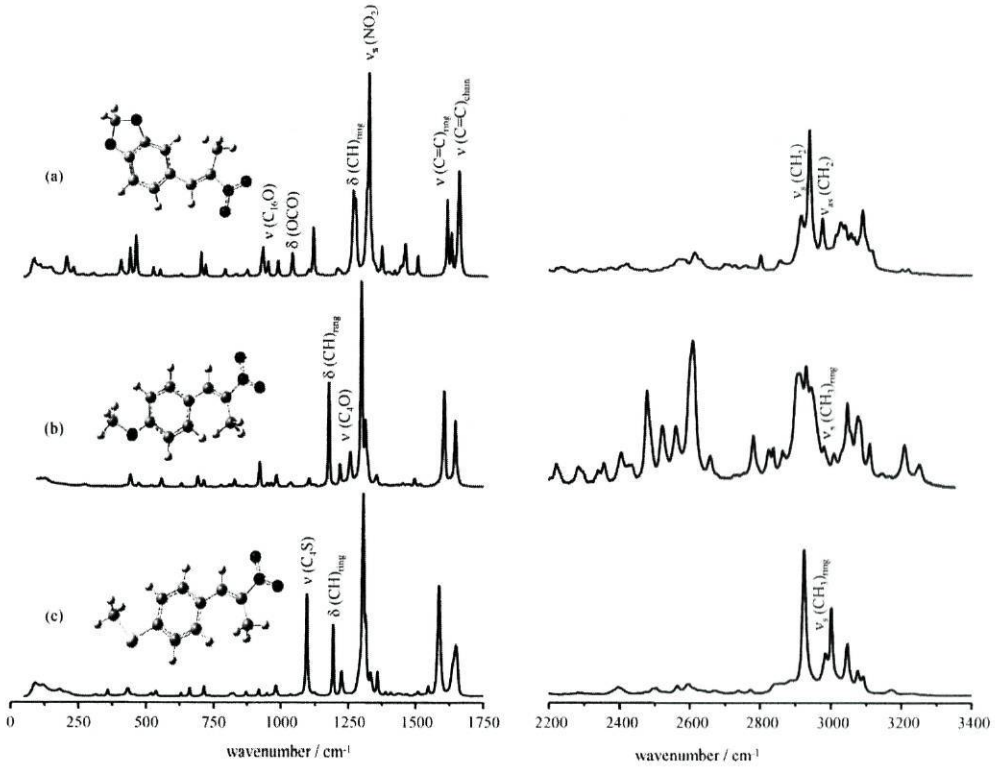

Fig. 5 Experimental Raman spectra (75–1750 cm^{-1} and 2200–3400 cm^{-1}) in the solid state (at 25 °C) for some of the precursors of amphetamine-like drugs studied in the present work: (a) 3,4-MD-MeNS (FT-Raman); (b) 4-MeO-MeNS; (c) 4-MeS-MeNS (FT-Raman).

662 cm^{-1}, ascribed to ν (C_4O) and ν (C_4S), respectively (Fig. 5, Tables 5 and 6).

When comparing the results reported for β-methyl-β-nitrostyrene (MeNS)[14] with the ones now obtained for compounds 4-MeO-MeNS and 4-MeS-MeNS, it is evident that the presence of a *para* substituent in the aromatic ring (either O–CH_3 or S–CH_3) has a strong effect on both the CH_3 and NO_2 vibrational modes: $\delta_s(CH_3)_{chain}$ is shifted to lower frequency values relative to the ones measured for MeNS (1385 cm^{-1})—$\Delta\nu \approx 30$ cm^{-1} for 4-MeO-MeNS and $\Delta\nu \approx 26$ cm^{-1} for 4-MeS-MeNS, while ν_s (NO_2) displays a shift from 1316 cm^{-1} to 1298 or 1306 cm^{-1}, respectively for OCH_3 and SCH_3 substitutions.

Indeed, for these *para* substituted compounds it was found that an O → S substitution leads to a quite large downward shift of the C–O and C–S stretching modes: a deviation of 161 cm^{-1} was obtained for ν ($C_{14}O$) and ν ($C_{14}S$), while a 375 cm^{-1} shift was determined for ν (C_4O) and ν (C_4S) (Fig. 5, Tables 5 and 6). This is easily explained by the decrease of the force constant of the C–S oscillator relative to the C–O one, due to the lower electronegativity of the S atom and the higher C–S bond length—135.8 (C_4–O_{13}) *vs.* 177.5 pm (C_4–S_{13}) and 142.2 (C_{14}–O_{13}) *vs.* 182.2 pm (C_{14}–S_{13}) (Tables 2 and 3). Furthermore, the vibrational modes assigned to the methyl group, particularly the symmetric deformations, are rather sensitive to the electronegativity of the attached atom (either O or S). Therefore, by replacing oxygen by sulfur the corresponding band at 1432 cm^{-1} is shifted to 1332 cm^{-1} (Tables 5 and 6). Also, the O → S substitution is responsible for the deviation of δ_{as} (CH_3) from 1469 to 1409 cm^{-1}. Moreover, it was verified that replacing O by S substitution causes an upward shift of ν_{as} (NO_2) (1298 to 1313 cm^{-1}) and a downward shift of δ_{as} $(CH_3)_{chain}$ (1469 to 1438 cm^{-1}).

These results suggest that π-electron delocalisation is more pronounced in 4-MeO-MeNS than in 4-MeS-MeNS, due to the electronegativity difference between the oxygen and sulfur atoms, this effect being very clearly reflected in the corresponding vibrational spectra, as discussed above.

A good overall agreement was obtained between the experimental and calculated frequency values, as well as between these results and data obtained by the authors for other nitrostyrenes derivatives,[14] namely β-methyl-β-nitrostyrene, the synthetic precursor of methamphetamine. Furthermore, the present results are in conformity with those previously reported for 2,5-dimethoxy-4-methyl-β-methyl-β-nitrostyrene (the precursor of 2,5-dimethoxy-4-methylamphetamine)[30] and similar systems.[31–38]

The present study allowed the assignment of specific vibrational features, characteristic of each of the β-methyl-β-nitrostyrenes investigated. Therefore, these results will be very useful for the identification of compounds present in illegally manufactured drugs of abuse, as well as for determining the corresponding synthetic routes and, hopefully, for tracking the clandestine laboratories where production takes place.

4 Conclusions

A complete conformational analysis was carried out for the synthetic precursors of amphetamine-like drugs 3,4-methylenedioxy-β-methyl-β-nitrostyrene (3,4-MD-MeNS), 4-methoxy-β-methyl-β-nitrostyrene (4-MeO-MeNS) and 4-methylthio-β-methyl-β-nitrostyrene (4-MeS-MeNS), by Raman spectroscopy combined to *ab initio* MO calculations.

Several distinct conformers were obtained for these compounds, varying in the orientation of the CH_3 and NO_2 groups relative to both the aromatic ring and the C_7=C_8 bond. A clear preference for a planar geometry was found in all cases, except when strong steric hindrance effects occurred in the planar conformations. In fact, the most stable geometries were found to be the ones allowing a more effective balance between the following parameters: π-electron delocalisation, minimisation of repulsive effects and formation of stabilising (C)H···O intramolecular close contacts. The results presently described are in very good accordance with the ones obtained in previous studies on similar β-nitrostyrene derivatives.

Despite their undisputable interest, the number of reported

Table 4 Raman experimental (solid state) and calculated (B3LYP/6-31G**) wavenumbers (cm^{-1}) for the most stable conformers of 3,4-MD-MeNS

	[a]Calculated		
Experimental	3,4-MD-MeNS 1	3,4-MD-MeNS 2	[b]Approximate description
3116	3128 (1;33)	3114 (2;76)	ν $(CH)_{ring}$
3097	3105 (4;161)	3099 (4;95)	ν $(CH)_{ring}$
3088	3079 (1;76)	3096 (1;47)	ν (CH)
3065	3073 (3;10)	3071 (1;30)	ν (CH)
3040	3041 (3;56)	3040 (3;55)	ν_{as} (CH_3)
3027	3005 (8;75)	3004 (8;81)	ν_{as} (CH_3)
2975	2980 (46;200)	2972 (43;202)	ν_{as} (CH_2)
2938	2934 (10;174)	2935 (9;186)	ν_s (CH_3)
2915	2917 (140;275)	2922 (150;299)	ν_s (CH_2)
2860			(1256 + 1604 cm^{-1})
2803			(1308 + 1495 cm^{-1})
2759			(1112 + 1647 cm^{-1})
2632			2 × ν_s (NO_2)
2616			2 × ν $(CC)_{ring}$
2582			(1266 + 1316 cm^{-1})
2578			(1256 + 1316 cm^{-1})
2368			(1112 + 1256 cm^{-1})
1647	1644 (86;898)	1649 (61;621)	ν $(C{=}C)_{chain}$
1619	1604 (39;553)	1602 (63;989)	ν $(CC)_{ring}$
1604	1587 (21;188)	1591 (3;6)	ν $(CC)_{ring}$
1495	1555 (146;113)	1556 (168;116)	ν_{as} (NO_2)
	1503 (8;54)	1504 (8;59)	δ (CH_2) (sciss.)
	1479 (273;8)	1480 (312;5)	δ $(CH)_{ring}$ + δ (CH_2) (sciss.)
	1442 (4;49)	1443 (1;73)	δ_{as} (CH_3)
1450	1438 (92;147)	1436 (45;58)	ν $(CC)_{ring}$ + δ_{as} (CH_3)
1434	1431 (48;126)	1425 (46;58)	δ_{as} (CH_3)
	1389 (1;37)	1389 (2;33)	ω (CH_2)
	1385 (20;15)	1380 (35;55)	δ_s (CH_3) + δ $(CH)_{chain}$
1365	1350 (19;108)	1353 (10;25)	δ_s (CH_3) + δ $(CH)_{chain}$
	1319 (88;194)	1323 (12;4)	δ (CH)
1316	1313 (386;936)	1311 (648;1515)	ν_s (NO_2) + δ_s (CH_3)
1308	1262 (645;299)	1263 (18;74)	ν $(CC)_{ring}$
1266	1245 (2;4)	1248 (434;41)	δ (CH)
1256	1190 (12;127)	1181 (1;57)	δ (CH)
1201	1156 (1;13)	1154 (0;10)	t (CH_2)
1142	1121 (9;4)	1127 (2;4)	δ $(CH)_{ring}$
	1100 (10;1)	1099 (10;1)	r (CH_2)
1112	1092 (68;174)	1086 (10;10)	δ (CC)
1094	1077 (3;11)	1079 (63;131)	δ (CC)
1034	1030 (126;1)	1030 (3;1)	δ (OCO) + δ $(CH)_{ring}$ + r (CH_3)
	1025 (7;25)	1026 (1;25)	r (CH_3)
982	967 (72;30)	970 (64;21)	r (CH_3)
945	937 (35;2)	938 (37;13)	ν $(C_{16}O)$
926	934 (17;100)	929 (42;160)	γ $(CH)_{chain}$
	912 (39;19)	907 (19;1)	δ $(CC)_{ring}$
869	898 (3;6)	902 (21;7)	γ $(CH)_{ring}$
	845 (33;6)	844 (29;2)	γ $(CH)_{ring}$
830	840 (45;4)	837 (50;7)	δ (NO_2) (sciss.) + γ $(CH)_{ring}$
	806 (8;16)	801 (17;7)	δ $(CC)_{ring}$ + δ $(CO_{14}C)$
787	795 (25;5)	796 (17;21)	γ $(CH)_{ring}$
	768 (4;15)	768 (8;7)	γ $(CH)_{ring}$ + δ (CO_8C)
717	713 (6;2)	719 (2;0)	ω (NO_2) + γ (CCC)
700	707 (1;23)	712 (8;1)	δ (COC)
	689 (6;23)	695 (1;58)	γ (CCC) + ν (CN)
625	678 (2;12)	679 (1;2)	γ $(CCC)_{ring}$
604	610 (5;4)	605 (1;8)	δ (CCC)
550	590 (10;3)	593 (11;1)	γ $(CCC)_{ring}$
524	535 (9;9)	543 (8;1)	δ $(CCC)_{ring}$
	516 (6;17)	518 (3;22)	δ (CNO)
461	451 (8;34)	442 (10;21)	Δ $(CCC)_{chain}$
439	429 (6;9)	411 (9;4)	$\Delta(CCC)_{ring}$
405	401 (3;10)	406 (2;13)	Δ (CCN)
	386 (1;0)	389 (1;1)	Γ(CCC)
	351 (1;2)	353 (2;4)	Γ (CCC)
303	300 (5;3)	290 (2;1)	τ (CH_3)
230	259 (0;2)	249 (1;3)	Γ $(CCC)_{ring}$
207	229 (1;3)	242 (0;7)	Γ (CCC)
147	200 (0;4)	206 (1;1)	Skeletal mode
115	179 (0;2)	183 (0;3)	τ (CH_3)
	100 (1;0)	103 (1;3)	τ (CH_3)
77	75 (4;1)	71 (1;2)	Skeletal mode
58	63 (5;3)	61 (2;1)	Skeletal mode

Table 4 Raman experimental (solid state) and calculated (B3LYP/6-31G**) wavenumbers (cm^{-1}) for the most stable conformers of 3,4-MD-MeNS (*Continued*)

	[a]Calculated		
Experimental	3,4-MD-MeNS 1	3,4-MD-MeNS 2	[b]Approximate description
	48 (3;2)	36 (0;3)	Skeletal mode
	37 (0;3)	15 (7;1)	Skeletal mode

[a] B3LYP/6-31G** level; wavenumbers above 400 cm^{-1} are scaled by 0.9614 [28] (IR intensities in km mol^{-1}; Raman scattering activities in Å amu^{-1}). [b] Atoms are numbered according to Fig. 2.; δ and γ stand for in-plane and out-of-plane deformations, respectively; Δ and Γ stand for in-plane and out-of-plane skeletal deformations, respectively.

Table 5 Raman experimental (solid state) and calculated (B3LYP/6-31G**) wavenumbers (cm^{-1}) for the most stable conformers of 4-MeO-MeNS

	[a]Calculated		
Experimental	4-MeO-MeNS 1	4-MeO-MeNS 2	[b]Approximate description
3107	3107 (3;92)	3108 (7;87)	$\nu\ (CH)_{ring}$
	3103 (12; 86)	3094 (2;73)	$\nu\ (CH)_{ring}$
3083	3087 (4;90)	3093 (10;113)	$\nu\ (CH)_{ring}$
3076	3072 (0;52)	3072 (0;59)	$\nu\ (CH)_{chain}$
3055	3065 (7;30)	3066 (6;30)	$\nu\ (CH)$
3045	3040 (3;60)	3039 (3;59)	$\nu_{as}\ (CH_3)_{chain}$
3033	3036 (22;156)	3036 (23;159)	$\nu_{as}\ (CH_3)_{ring}$
3007	3003 (8;76)	3002 (8;75)	$\nu_{as}\ (CH_3)_{chain}$
2976	2971 (36;64)	2970 (36;56)	$\nu_{as}\ (CH_3)_{ring}$
2944			$(1298 + 1646\ cm^{-1})$
2928	2933 (10;182)	2933 (10;170)	$\nu_{s}\ (CH_3)_{chain}$
2907	2907 (65;137)	2906 (59;125)	$\nu_{s}\ (CH_3)_{ring}$
2782			$(1177 + 1605\ cm^{-1})$
2610			$(1298 + 1312\ cm^{-1})$
2596			$2 \times \nu_{s}\ (NO_2)$
2554			$(1256 + 1298\ cm^{-1})$
2526			$(921 + 1605\ cm^{-1})$
2474			$(1218 + 1256\ cm^{-1})$
1646	1644 (63;837)	1645 (57;723)	$\nu\ (C{=}C)_{chain}$
1605	1600 (262;1062)	1599 (270;1145)	$\nu\ (CC)_{ring}$
1516	1550 (28;53)	1551 (16;4)	$\nu\ (CC)_{ring}$
1495	1554 (155;125)	1555 (147;123)	$\nu_{as}\ (NO_2)$
1476	1500 (97;47)	1499 (98;45)	$\nu\ (CC)_{ring}$
	1458 (40;13)	1458 (49;16)	$\delta_{as}\ (CH_3)_{ring}$
1469	1448 (6;31)	1447 (6;30)	$\delta_{as}\ (CH_3)_{ring}$
1452	1441 (9;38)	1442 (5;37)	$\delta_{as}\ (CH_3)_{chain}$
	1433 (18;18)	1432 (15;17)	$\delta_{as}\ (CH_3)_{chain} + \delta_{s}\ (CH_3)_{ring}$
1432	1431 (13;5)	1432 (15;9)	$\delta_{s}\ (CH_3)_{ring}$
	1411 (13;39)	1409 (2;1)	$\delta\ (CH) + \delta_{s}\ (CH_3)_{chain}$
1387	1382 (28;17)	1382 (31;20)	$\delta_{s}\ (CH_3)_{chain}$
1355	1340 (27;99)	1340 (4;59)	$\delta_{s}\ (CH_3)_{chain} + \delta\ (CH)_{chain}$
1298	1313 (401;974)	1316 (213;479)	$\nu_{s}\ (NO_2) + \delta\ (CH)$
1312	1303 (62;16)	1302 (466;834)	$\nu\ (CC)_{ring}$
	1289 (30;107)	1292 (2;40)	$\delta\ (CH)_{ring}$
1256	1258 (583;217)	1258 (386;45)	$\nu\ (C_4O + \delta_{s}\ (CH_3)_{chain} + \delta\ (CH)$
1218	1208 (15;216)	1205 (25;148)	$\delta\ (CH)_{ring}$
	1164 (7;6)	1164 (21;19)	$r\ (CH_3)_{ring}$
1177	1161 (137;193)	1159 (115;179)	$\delta\ (CH)_{ring}$
1123	1132 (1;5)	1132 (1;5)	$r\ (CH_3)_{ring}$
1105	1106 (6;3)	1106 (16;11)	$\delta\ (CH)_{ring}$
	1079 (30;68)	1080 (25;62)	$r\ (CH_3)_{chain} + \delta\ (CH)_{chain}$
1037	1030 (60;1)	1030 (59;1)	$\nu\ (C_{14}O)$
	1026 (1;23)	1026 (1; 25)	$r\ (CH_3)_{chain}$
984	986 (5;3)	987 (4;2)	$\delta\ (CC)_{ring}$
964	963 (91;26)	963 (89;23)	$r\ (CH_3)_{chain}$
951	939 (16;76)	942 (17;76)	$\omega_{as}\ (CH)_{ring} + \gamma\ (CH)_{chain}$
922	934 (8;23)	926 (6;26)	$\omega_{as}\ (CH)_{ring}$
875	912 (6;20)	919 (10;30)	$\omega_{as}\ (CH)_{ring} + \gamma\ (CH)_{chain}$
846	853 (47;17)	853 (45;18)	$\delta\ (NO_2)\ (sciss.) + \delta\ (CC)_{ring}$
829	824 (42;9)	825 (37;11)	$\omega_{s}\ (CH)_{ring}$
812	811 (25;40)	810 (28;29)	$\omega_{s}\ (CH)_{ring}$
780	794 (7;4)	794 (8;15)	$\omega_{as}\ (CH)_{ring}$
	752 (5;13)	759 (1;13)	$\delta\ (CC)$
716	718 (5;0)	718 (4;0)	$\omega\ (NO_2) + \gamma\ (CC)_{ring}$
694	698 (8;20)	696 (10;14)	$\gamma\ (CC)_{ring} + \omega\ (NO_2)$
	682 (3;11)	677 (3;12)	$\gamma\ (CC)_{ring} + \delta\ (CC)_{chain}$
633	621 (0;6)	622 (1;7)	$\delta\ (CC)_{ring}$

Table 5 Raman experimental (solid state) and calculated (B3LYP/6-31G**) wavenumbers (cm^{-1}) for the most stable conformers of 4-MeO-MeNS (*Continued*)

Experimental	[a]Calculated		[b]Approximate description
	4-MeO-MeNS 1	4-MeO-MeNS 2	
560	547 (22;2)	545 (26;10)	δ (COC)
528	529 (13;2)	527 (17;1)	$\gamma\ (CC)_{ring}$
	520 (5;16)	513 (7;12)	$\gamma\ (CC)_{ring}$
476	449 (2;1)	464 (2;17)	δ (COC) + $\delta\ (CC)_{chain}$
445	438 (13;54)	436 (8;30)	$\gamma\ (CC)_{chain}$
425	413 (0;1)	414 (2;5)	$\gamma\ (CC)_{ring}$
	389 (1;1)	387 (1;0)	Δ (CCN) + Γ (CCC)
351	355 (3;1)	358 (3;2)	Γ (CCC)
	340 (5;1)	325 (0;3)	$\Delta\ (CCC)_{chain}$ + Δ (COC)
277	253 (0;1)	271 (3;1)	$\tau\ (CH_3)$
	239 (0;1)	251(0;1)	$\tau\ (CH_3)_{ring}$
	236 (0;1)	219 (2;4)	$\tau\ (CH_3)_{chain}$
	196 (0;1)	194 (0;1)	$\tau\ (CH_3)$
130	173 (0;5)	184 (0;4)	$\tau\ (CH_3)_{chain}$
114	110 (4;3)	111 (5;2)	Skeletal mode
	101 (3;1)	101 (1;1)	Skeletal mode
75	65 (1;2)	66 (1;3)	Skeletal mode
	56 (1;1)	51 (0;0)	Skeletal mode
	37 (0;3)	41 (0;4)	Skeletal mode

[a] B3LYP/6-31G** level; wavenumbers above 400 cm^{-1} are scaled by 0.9614 [28] (IR intensities in km mol^{-1}; Raman scattering activities in Å amu^{-1}). [b] Atoms are numbered according to Fig. 2.; δ and γ stand for in-plane and out-of-plane deformations, respectively; Δ and Γ stand for in-plane and out-of-plane skeletal deformations, respectively.

Table 6 Raman experimental (solid state) and calculated (B3LYP/6-31G**) wavenumbers (cm^{-1}) for the most stable conformers of 4-MeS-MeNS

Experimental	[a]Calculated		[b]Approximate description
	4-MeS-MeNS 1	4-MeS-MeNS 2	
3174	3104 (4;65)	3151 (5;39)	$\nu\ (CH)_{ring}$
3093	3098 (10;74)	3099 (9;82)	$\nu\ (CH)_{ring}$
3079	3072 (0;55)	3093 (7;157)	$\nu\ (CH)_{chain}$
	3067 (2;85)	3059 (12;68)	ν (CH)
	3063 (8;21)	3036 (23;164)	ν (CH)
3047	3041 (3;62)	3031 (17;78)	$\nu_{as}\ (CH_3)_{chain}$
	3039 (3;145)	3021 (4;38)	$\nu_{as}\ (CH_3)_{ring}$
	3029 (7;58)	2998 (10;129)	$\nu_{as}\ (CH_3)_{ring}$
3003	3004 (8;82)	2974 (34;55)	$\nu_{as}\ (CH_3)_{chain}$
2987	2944 (18;169)	2940 (20;310)	$\nu_{s}\ (CH_3)_{ring}$
2926	2934 (9;202)	2909 (60;131)	$\nu_{s}\ (CH_3)_{chain}$
2745			(1195 + 1650 cm^{-1})
2612			2 × $\nu_s\ (NO_2)$
2502			(1196 + 1306 cm^{-1})
2401			(1095 + 1306 cm^{-1})
2393			2 × $\delta\ (CH)_{ring}$
1650	1645 (87;1317)	1630 (62;425)	$\nu\ (C = C)_{chain}$
1641	1586 (177;1848)	1596 (448;1089)	$\nu\ (CC)_{ring}$
1587	1556 (155;170)	1554 (11;9)	$\nu_{as}\ (NO_2)$
1547	1532 (8;66)	1535 (98;126)	$\nu\ (CC)_{ring}$
1509	1479 (38;22)	1497 (97;51)	$\nu\ (CC)_{ring} + \delta\ (CH)_{ring}$
1468	1441 (26;10)	1458 (51;15)	$\delta_{as}\ (CH_3)_{ring}$
1438	1440 (12;43)	1449 (14;12)	$\delta_{as}\ (CH_3)_{chain}$
	1432 (16;19)	1447 (6;31)	$\delta_{as}\ (CH_3)\ _{chain}$
1409	1426 (10;30)	1432 (13;9)	$\delta_{as}\ (CH_3)_{ring}$
1389	1398 (21;30)	1425 (6;19)	$\nu\ (CC)_{ring} + \delta_s\ (CH_3)_{ring}$
	1382 (21;17)	1412 (9;28)	$\delta_s\ (CH_3)_{chain} + \delta\ (CH)$
1360	1338 (23;164)	1382 (25;219)	$\delta_s\ (CH_3)_{chain} + \delta\ (CH)_{chain}$
1334	1322 (1;21)	1366 (51;76)	$\delta_s\ (CH_3)_{ring}$
1313	1292 (63;283)	1299 (163;265)	$\nu\ (CC)_{ring}$
1306	1313 (599;1515)	1319 (249;477)	$\nu_s\ (NO_2) + \delta_s\ (CH_3)_{chain} + \delta\ (CH)$
	1280 (9;17)	1289 (11;22)	$\nu\ (CC)_{ring}$
1225	1210 (20;222)	1261 (374;74)	$\nu\ (CC)_{ring} + \delta\ (CH)_{ring}$
1196	1177 (29;315)	1203 (59;209)	$\delta\ (CH)_{ring}$
	1115 (4;2)	1165 (41;31)	$\delta\ (CH)_{ring}$
1124	1080 (10;45)	1164 (191;171)	$\delta\ (CC)_{chain} + \delta\ (CH)$
1095	1070 (144;408)	1131 (1;4)	$\nu\ (C_4S)$
1037	1026 (0;33)	1126 (30;22)	$r\ (CH_3)_{chain}$
982	991 (2;3)	1100 (14;13)	$\delta\ (CC)_{ring}$
964	963 (83;67)	1032 (7;5)	$r\ (CH_3) + \delta\ (CH)\ _{chain}$
	957 (20;12)	1031 (52;1)	$r\ (CH_3)_{ring}$
	945 (1;15)	999 (41;7)	$r\ (CH_3)_{ring} + \gamma\ (CH)_{chain} + \omega_{as}\ (CH)_{ring}$

Table 6 Raman experimental (solid state) and calculated (B3LYP/6-31G**) wavenumbers (cm^{-1}) for the most stable conformers of 4-MeS-MeNS (*Continued*)

Experimental	[a]Calculated		[b]Approximate description
	4-MeS-MeNS 1	4-MeS-MeNS 2	
948	941 (16;78)	985 (3;1)	r $(CH_3)_{ring}$ + γ $(CH)_{chain}$ + ω_{as} $(CH)_{ring}$
	936 (8;36)	945 (2;6)	γ $(CH)_{chain}$ + ω_{as} $(CH)_{ring}$
920	918 (9;61)	932 (2;9)	γ $(CH)_{chain}$ + ω_{as} $(CH)_{ring}$
875	851 (48;14)	897 (15;27)	δ (NO_2) (sciss.) + δ $(CC)_{ring}$
820	813 (36;6)	863 (28;7)	ω_s $(CH)_{ring}$
	808 (0;17)	824 (24;38)	ω_{as} $(CH)_{ring}$
735	793 (25;14)	812 (29;23)	ω_s $(CH)_{ring}$
716	719 (0;4)	793 (0;5)	ω (NO_2) + γ $(CC)_{ring}$
	710 (6;13)	757 (4;2)	ω (NO_2) + δ $(CC)_{chain}$
662	694 (6;24)	736 (15;9)	ν $(C_{14}S)$ + γ $(CC)_{ring}$
	683 (4;7)	698 (1;2)	γ $(CC)_{ring}$
632	643 (1;17)	646 (1;12)	γ $(CC)_{ring}$
	620 (0;7)	608 (4;6)	δ $(CC)_{ring}$
537	524 (6;16)	579 (11;3)	δ (CCN)
518	506 (15;28)	517 (5;5)	γ (CC)
461	450 (2;4)	510 (28;14)	γ (CC)
435	424 (19;63)	465 (2;3)	γ $(CC)_{chain}$
	405 (0;2)	422 (7;16)	δ $(CC)_{ring}$
	381 (1;2)	404 (0;0)	Δ (CCN)
361	361 (1;5)	376 (1;2)	Δ (CCC) + Δ (CSC)
	331 (1;1)	354 (3;3)	Γ (CCC)
314	314 (4;5)	299 (5;1)	Δ (CCC) + Δ (CSC)
	230 (0;1)	276 (0;4)	τ $(CH_3)_{ring}$
218	222 (1;0)	252 (1;1)	τ (CH_3)
	204 (0;0)	224 (0;2)	τ $(CH_3)_{chain}$
	170 (0;0)	209 (0;1)	τ $(CH_3)_{chain}$
118	159 (0;8)	190 (3;1)	τ $(CH_3)_{chain}$
82	97 (2;5)	139 (1;1)	Skeletal mode
	64 (1;4)	114 (2;1)	Skeletal mode
	56 (4;2)	62 (3;2)	Skeletal mode
	50 (0;2)	34 (3;6)	Skeletal mode
	31 (1;3)	27 (1;1)	Skeletal mode

[a] B3LYP/6-31G** level; wavenumbers above 400 cm^{-1} are scaled by 0.9614 [28] (IR intensities in km mol^{-1}; Raman scattering activities in Å amu^{-1}). [b] Atoms are numbered according to Fig. 2, irrespective of the type of atom (O or S); δ and γ stand for in-plane and out-of-plane deformations, respectively; Δ and Γ stand for in-plane and out-of-plane skeletal deformations, respectively.

studies aiming at the identification of synthetic precursors of drugs of abuse by vibrational spectroscopy methods is very scarce. The present work intends to develop this field of research. In fact, the described results allow us to evaluate Raman spectroscopy, enabling rapid and non-destructive measurements, as a most promising tool for Forensic Sciences, as a screening method for the determination of the composition profiles of illicit substances, as well as for tracking clandestine laboratories. Actually, it was shown that even chemically similar intermediates are easily distinguished by this technique. It can also surpass other analytical methods currently used in criminal prosecutions once it allows the concomitant identification of both the active compound and its by-products. The method has the additional advantage of permitting its extension to the main metabolites of the amphetamine-like drugs presently investigated.

Although analysis of multiple illicit preparations will still need to be carried out, in order to ensure reproducibility of the technique, it will hopefully be possible, in the near future, to rely on a Raman database that will constitute an invaluable tool, for both forensic control and toxicological studies.

Acknowledgements

N. Milhazes is grateful to FCT for a fellowship (PRAXIS XXI/BD/18520/98). Thanks are also due to Laboratório Associado CICECO (University of Aveiro, Portugal) for access to the FT-Raman spectrometer, and to Ana M. Amado, for obtaining these spectra.

References

1 A. G. M. Barret and G. Graboski, *Chem. Rev.*, 1986, **86**, 751.
2 G. W. Kabalka, L. H. M. Guindi and R. S. Varma, *Tetrahedron*, 1990, **46**(21), 7443.
3 A. García-Torres, R. Cruz-Almanza and L. D. Miranda, *Tetrahedron Lett.*, 2004, **45**, 2085.
4 C. F. Yao, W. C. Chen and Y. M. Lin, *Tetrahedron Lett.*, 1996, **37**(35), 6339.
5 M. Schmidt and K. Eger, *Pharmazie*, 1996, **51**, 11.
6 T. A. Dal Cason, *J. Forensic Sci.*, 1990, **35**(3), 675.
7 K. C. Carter, Y. S. Finnon, N. Nic-Daeid, D. C. Robson and R. Waddell, *Immunopharmacol. Immunotoxicol.*, 2002, **24**(2), 187.
8 A. J. Poortman and E. Lock, *J. Forensic Sci. Int.*, 1999, **100**(3), 221.
9 S. E. J. Bell, D. T. Burns, A. C. Dennis and J. S. Speers, *Analyst*, 2000, **125**, 541.
10 S. E. J. Bell, D. T. Burns, A. C. Dennis, L. J. Matchett and J. S. Speers, *Analyst*, 2000, **125**, 1811.
11 B. Sägmüller, B. Schwarze, G. Brehm and S. Schneider, *Analyst*, 2001, **126**, 2066.
12 K. Faulds, W. E. Smith, D. Graham and R. J. Lacey, *Analyst*, 2002, **127**, 282.
13 T. Vankeirsbilck, A. Vercauteren, W. baeyens, G. van der Weken, F. Verpoort, G. Vergote and J. P. Remon, *Trends Anal. Chem.*, 2002, **21**, 869.
14 R. Calheiros, N. Milhazes, F. Borges and M. P. M. Marques, *J. Mol. Struct.*, 2004, **692**, 91.
15 M. J. Frisch, *et al.*, *Gaussian 98, Revision A.9*, Gaussian Inc., Pittsburgh PA, USA, 1998.
16 T. V. Russo, R. L. Martin and P. J. Hay, *J. Phys. Chem.*, 1995, **99**, 17085.
17 A. Ignaczak and J. A. N. F. Gomes, *Chem. Phys. Lett.*, 1996, **257**, 609.
18 F. A. Cotton and X. Feng, *J. Am. Chem. Soc.*, 1997, **119**, 7514.

19 A. Ignaczak and J. A. N. F. Gomes, *J. Electroanal. Chem.*, 1997, **420**, 209.
20 T. Wagener and G. Frenking, *Inorg. Chem.*, 1998, **37**, 1805.
21 F. A. Cotton and X. Feng, *J. Am. Chem. Soc.*, 1998, **120**, 3387.
22 C. Lee, W. Yang and R. G. Parr, *Phys. Rev.*, 1988, **B37**, 785.
23 B. Miehlich, A. Savin, H. Stoll and H. Preuss, *Chem. Phys. Lett.*, 1989, **157**, 200.
24 A. D. Becke, *Phys. Rev.*, 1988, **A38**, 3098.
25 A. D. Becke, *J. Chem. Phys.*, 1993, **98**, 5648.
26 P. C. Hariharan and J. A. Pople, *Theor. Chim. Acta*, 1973, **28**, 213.
27 M. M. Francl, W. J. Pietro, W. J. Hehre, J. S. Binkley, M. S. Gordon, D. J. DeFrees and J. A. Pople, *J. Chem. Phys.*, 1982, **77**, 3654.
28 A. P. Scott and L. Radom, *J. Phys. Chem.*, 1996, **100**, 16502.
29 C. Peng, P. Y. Ayala, H. B. Schlegel and M. J. Frisch, *J. Comput. Chem.*, 1996, **17**, 49.
30 A. By, G. Neville and H. F. Shurvell, *J. Forensic Sci.*, 1992, **37**, 503.
31 R. E. Clavijo, R. Araya-Maturana, B. K. Cassels and B. Weiss-López, *Spectrochim. Acta, Part A*, 1996, **50**(12), 2105.
32 F. J. Ramírez and J. T. López Navarrete, *Vib. Spectrosc.*, 1993, **4**, 321.
33 R. Hargitai, P. G. Szalay, G. Pongor and G. Fogarasi, *J. Mol. Struct. (THEOCHEM)*, 1994, **306**, 293.
34 Y. Haas, S. Kendler, E. Zingher, H. Zuckermann and S. Zilberg, *J. Chem. Phys.*, 1995, **103**, 37.
35 S. J. Greaves and W. W. Griffith, *Spectrochim. Acta, Part A*, 1991, **47**, 133.
36 M. Gerhards, W. Perl, S. Schumm, U. Henrichs, C. Jacoby and K. Kleinermanns, *J. Chem. Phys.*, 1996, **104**, 9362.
37 S. M. Fiuza, E. Besien, N. Milhazes, F. Borges and M. P. M. Marques, *J.Mol. Struct.*, 2004, **693**(1–3), 103–118.
38 E. Besien and M. P. M. Marques, *J. Mol. Struct. (THEOCHEM)*, 2003, **625**, 265.

8.3 Derivados do β-nitroestireno como potenciais agentes antibacterianos: um estudo de relação estrutura – propriedades físico-químicas – actividade.

Artigo reproduzido da revista *Bioorganic & Medicinal Chemistry* (2006) 14: 4078-4088, com permissão da Elsevier, Ltd.

Available online at www.sciencedirect.com
SCIENCE DIRECT®
Bioorganic & Medicinal Chemistry
ELSEVIER
Bioorganic & Medicinal Chemistry 14 (2006) 4078–4088

β-Nitrostyrene derivatives as potential antibacterial agents: A structure–property–activity relationship study

Nuno Milhazes,[a,b,c] Rita Calheiros,[d] M. Paula M. Marques,[d,e] Jorge Garrido,[f] M. Natália D. S. Cordeiro,[g,h] Cátia Rodrigues,[g,i] Sandra Quinteira,[g,i] Carla Novais,[g,i] Luísa Peixe[g,i] and Fernanda Borges[b,d,*]

[a]*CEQOFFUP*
[b]*Departamento de Química Orgânica, Faculdade de Farmácia, Universidade do Porto, 4050-047 Porto, Portugal*
[c]*Instituto Superior Ciências da Saúde, Norte, 4585-116 Gandra, PRD, Portugal*
[d]*Unidade I&D 'Química-Física Molecular'*
[e]*Departamento de Bioquímica, Faculdade de Ciências e Tecnologia, Universidade de Coimbra, 3001-401 Coimbra, Portugal*
[f]*Departamento de Engenharia Química, Instituto Superior de Engenharia do Porto, Rua S. Tomé, 4200-485 Porto, Portugal*
[g]*REQUIMTE*
[h]*Departamento de Química, Faculdade de Ciências, Universidade do Porto, Portugal*
[i]*Departamento de Microbiologia, Faculdade de Farmácia, Universidade do Porto, 4050-047 Porto, Portugal*

Received 22 November 2005; revised 26 January 2006; accepted 3 February 2006
Available online 23 February 2006

Abstract—A multidisciplinary project was developed, combining the synthesis of a series of β-nitrostyrene derivatives and the determination of their physicochemical parameters (redox potentials, partition coefficients), to the evaluation of the corresponding antibacterial activity. A complete conformational analysis was also performed, in order to get relevant structural information. Subsequently, a structure–property–activity (SPAR) approach was applied, through linear regression analysis, aiming at obtaining a putative correlation between the physicochemical parameters of the compounds investigated and their antibacterial activity (both against standard strains and clinical isolates). The β-nitrostyrene compounds displayed a lower activity towards all the tested bacteria relative to the β-methyl-β-nitrostyrene analogues. This was observed particularly for the 3-hydroxy-4-methoxy-β-methyl-β-nitrostyrene (**IVb**) against the Gram-positive bacteria (*Staphylococcus aureus*, *Enterococcus faecalis* and *Enterococcus faecium*). The SPAR results revealed the existence of a clear correlation between the redox potentials and the antibacterial activity of the series of β-nitrostyrene derivatives under study.
© 2006 Elsevier Ltd. All rights reserved.

1. Introduction

Over the last few years, compounds comprising a β-nitrostyrene moiety have been recognized to have a series of relevant biological activities. In fact, some β-nitrostyrene derivatives have recently been tested as pro-apoptotic anticancer agents and the β-nitrostyrene moiety was identified as the pharmacophore for this activity.[1] These compounds have also been described as highly potent and selective human telomerase inhibitors[2] as well as cytotoxic for human cancer cell lines.[3] Moreover, it was shown that they are able to downregulate the production of some interleukins, thus affecting the immune response in humans.[3] The nitrovinyl side chain attached to the aromatic ring was recognized to be an essential chemical feature in this type of compounds and a critical conformational pattern for their biological activity.[1,4]

Although the antifungic and antibacterial properties of this type of compounds have been studied since the 1940s, the work in this area during the last decade is rather scarce. In general, the nitrostyrene derivatives were found to be more effective against Gram-positive than Gram-negative bacteria.[5–7]

Keywords: β-Nitrostyrene derivatives; Antibacterial activity; Redox potentials; Structure–property–activity relationship.
* Corresponding author. Tel.: +351 22 2078900; fax: +351 222003977; e-mail: fborges@ff.up.pt

0968-0896/$ - see front matter © 2006 Elsevier Ltd. All rights reserved.
doi:10.1016/j.bmc.2006.02.006

Drug discovery studies have been significantly intensified in recent years, aiming at the search for more effective antibacterial agents displaying activity against Gram-positive and Gram-negative bacteria resistant to the antimicrobials currently used.[8,9] The search for novel chemotherapeutic agents, as well as the attempt to modify and improve the currently available ones, has been a priority mainly as a consequence of the rapid spread of multidrug-resistant bacterial pathogens. The development of new antibacterial drugs is presently based on structure–activity relationship (SAR), structure–property–activity relationship (SPAR) and quantitative structure–activity relationship (QSAR) studies.[9,10]

The aim of the present work is to be aware of the significance of β-nitrostyrene as a putative pharmacophore for antibacterial activity. The antibacterial activity of a series of compounds was evaluated against several type strains and clinical isolates of different bacterial species pathogenic to humans. Simultaneously, relevant physicochemical parameters, such as redox potentials (E_p) and partition coefficients (log P), were determined and/or calculated. A complete conformational analysis of the β-nitrostyrene derivatives under study was also performed through theoretical methods—ab initio molecular orbital calculations—gathering information of the utmost relevance for correlating structural features with the physicochemical properties and antimicrobial activity of this class of compounds.

The compounds studied are chemically related to the parent compound with slight modifications in their aromatic substitution pattern: β-nitrostyrene (**Ia**), 3,4-dihydroxy-β-nitrostyrene (**IIa**), 3,4-dimethoxy-β-nitrostyrene (**IIIa**), 3-hydroxy-4-methoxy-β-nitrostyrene (**IVa**), 4-hydroxy-3-methoxy-β-nitrostyrene (**Va**) and 3,4-methylenedioxy-β-nitrostyrene (**VIa**) (Table 1). In addition, another series of compounds was synthesized, displaying a methyl group in the β-carbon of the vinyl side chain, the aromatic part being kept unchanged. The following compounds were thus obtained: β-methyl-β-nitrostyrene (**Ib**), 3,4-dihydroxy-β-methyl-β-nitrostyrene (**IIb**), 3,4-dimethoxy-β-methyl-β-nitrostyrene (**IIIb**), 3-hydroxy-4-methoxy-β-methyl-β-nitrostyrene (**IVb**), 4-hydroxy-3-methoxy-β-methyl-β-nitrostyrene (**Vb**) and 3,4-methylenedioxy-β-methyl-β-nitrostyrene (**VIb**) (Table 1).

Table 1. β-Nitrostyrene and β-methyl-β-nitrostyrene derivatives synthesized in the present work

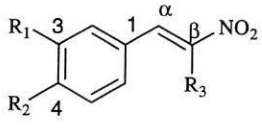

Compound	R_1	R_2	R_3
Ia	H	H	H
Ib	H	H	CH_3
IIa	OH	OH	H
IIb	OH	OH	CH_3
IIIa	OCH_3	OCH_3	H
IIIb	OCH_3	OCH_3	CH_3
IVa	OH	OCH_3	H
IVb	OH	OCH_3	CH_3
Va	OCH_3	OH	H
Vb	OCH_3	OH	CH_3
VIa	$-OCH_2O-$		H
VIb	$-OCH_2O-$		CH_3

2. Results and discussion

2.1. Chemistry

β-Nitrostyrene and β-methyl-β-nitrostyrene derivatives were prepared by a nitroaldol condensation reaction (Henry reaction).[11] The compounds were synthesized by the reaction of the corresponding benzaldehydes—with the same aromatic substitution pattern of the desired product—and nitromethane or nitroethane, respectively, for β-nitrostyrenes and β-methyl-β-nitrostyrenes, using ammonium acetate as the catalyst (Scheme 1). These experimental conditions led to moderate/ high yields. The final products were identified by NMR (^{1}H NMR and ^{13}C NMR), FT-IR and MS-EI spectroscopic techniques. The purity of the target compounds was determined by two different HPLC systems (see Section 4). The structures of the synthesized compounds are depicted in Table 1.

Several β-nitrostyrene derivatives were synthesized in order to study the influence of different aromatic substitution patterns, which confer diverse electronic environments, in the antibacterial activity. In this kind of systems, the nitro group is relatively distant from the aromatic ring and conjugated with an ethylenic double bond, thus allowing long-distance transmission of electronic effects.[12] One methyl group was also added to the β-carbon of the double bond, to verify the influence of conformational and steric parameters on the redox and antibacterial profiles of this chemical family.

2.2. Conformational analysis

In order to establish the effect of the structural preferences of β-nitrostyrene derivatives on their biological activity, a complete conformational analysis was carried out, through theoretical (ab initio) methods. The effects of three structural parameters on the overall stability of these molecules were investigated: (i) relative orientation of the hydroxy and/or methoxy group(s) in the aromatic ring; (ii) orientation of the benzene and the nitro group relative to the double bond, C_α=C_β, defining either a Z or an E configuration; (iii) position of the NO_2 and

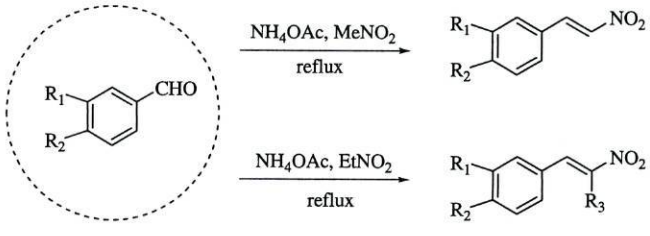

Scheme 1.

methyl group (in β-methyl-β-nitrostyrenes) relative to the ring. For all the geometries obtained calculation of the harmonic vibrational frequencies was also performed, allowing to determine which ones were real energy minima in the potential energy surface.

Since the more substituted β-nitrostyrene derivatives display a higher degree of freedom, several low energy conformers were calculated for them. Two stable geometries were obtained for compounds **Ia** and **Ib** (only one of them being populated at room temperature), 4 conformers were found for **VIa** and **VIb**, 8 were determined for **Va**, 10 for **IIb**, 11 for **IVb** and 12 for **IIa**, **IIIa**, **IIIb**, **IVa** and **Vb** (two of these having significant populations at room temperature). Figure 1 comprises the most stable structures calculated for each of the compounds presently studied.

The conformational behaviour of these phenolic compounds is mainly determined by electronic effects, as well as by the possibility of occurrence of (C)H···O intramolecular hydrogen bonds, which are medium strength, directional interactions (with a preference for linearity) known to be relevant for the overall stability of this kind of systems.[13] The most stable calculated structures were found to display a planar or quasi-planar geometry and an *E* conformation, which corresponds to a more effective π-electron delocalization, as well as to a minimization of repulsive effects, relative to the *Z* conformers. In fact, even for those compounds where two conformers exist at room temperature, they differ only in the value of the C_1–C_α torsion angle: either 0° or 180°. By comparing the β-nitrostyrenes with the β-methyl-β-nitrostyrenes, it was verified that the almost perfect planarity detected for the former is lost upon methyl substitution in the double bond C_β, the aromatic ring being tilted relative to the carbon side chain, the angle around C_1–C_α changing from 0° to 28°. Concerning the relative orientation of the ring substituent groups, it was found that it is identical whenever two OHs or one OH and one OMe are present, in order to allow the formation of intramolecular hydrogen bonds. When there are two OMe substituents, an opposite orientation is favoured (Fig. 1), in view of the minimization of $OCH_3\cdots H_3CO$ steric repulsions.

2.3. Antibacterial activity

The antibacterial properties of the β-nitrostyrene derivatives investigated were measured against selected type strains of Gram-positive (*Staphylococcus aureus* ATCC 29213 and *Enterococcus faecalis* ATCC 29212) and Gram-negative (*Escherichia coli* ATCC 25922 and *Pseudomonas aeruginosa* ATCC 27853) bacteria. *Salmonella typhimurium* FFUP1 and *Acinetobacter baumannii* FFUP10 are clinical isolates susceptible to all antibiotics, according to CLSI (formerly NCCLS) recommendations.[14]

Table 2 comprises the in vitro results of antibacterial activity for the β-nitrostyrenes under study, expressed as minimum inhibitory concentrations (MICs). The lowest antibacterial activity was observed for the β-nitrostyrene series, with MICs ranging from 128 to ⩾512 mg/L. In general, from the activity measured for the β-methyl-β-nitrostyrenes it is possible to conclude that the inclusion of a methyl group in the molecule's side chain leads to an increase of the inhibitory effect—MICs are between 16 and 256 mg/L. This activity enhancement due to the methyl substitution was found to be more pronounced for Gram-positive bacteria (*S. aureus* and *Enterococcus* spp.)—MICs ranging from 16 to 32 mg/L. Among the β-methyl-β-nitrostyrenes, compound **IVb** displayed the highest activity against Gram-positive

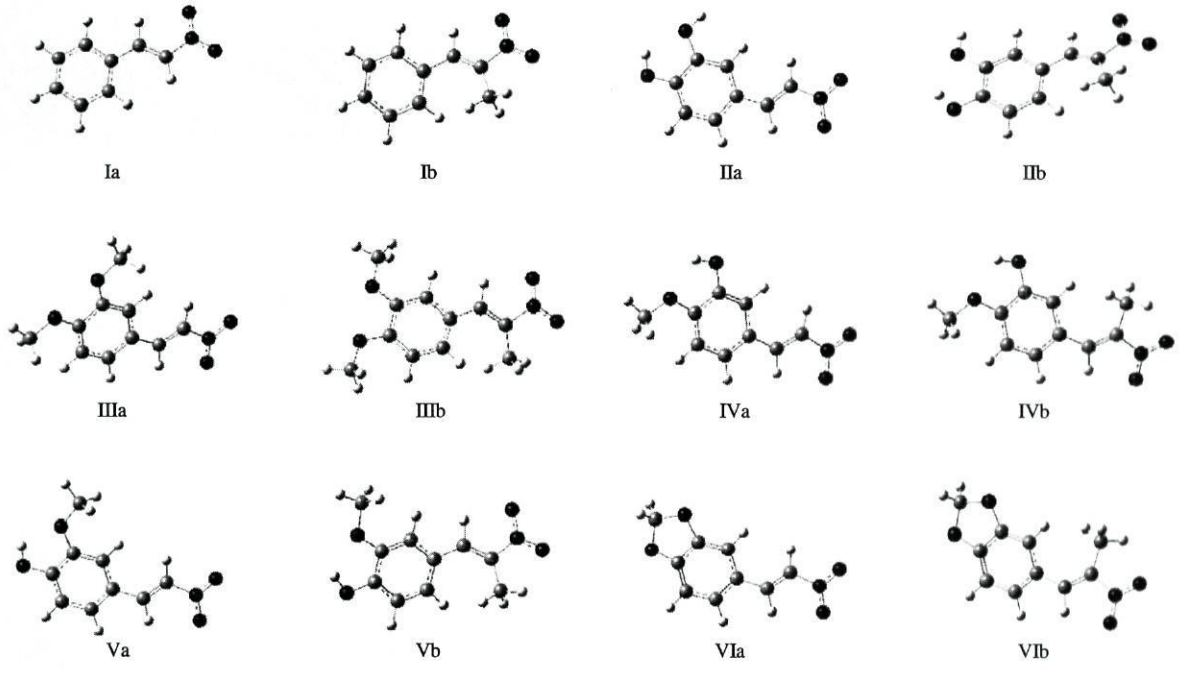

Figure 1. Schematic representation of the most stable geometries calculated (B3LYP/6-31G**) for the β-nitrostyrene derivatives under study.

Table 2. In vitro antibacterial activity of the β-nitrostyrene derivatives against several bacterial strains

Bacterial strain	Minimum inhibitory concentration, MIC (mg/L)											
	Ia	**Ib**	**IIa**	**IIb**	**IIIa**	**IIIb**	**IVa**	**IVb**	**Va**	**Vb**	**VIa**	**VIb**
Escherichia coli ATCC 25922	256	128	256	64	⩾512	256	512	128	512	256	128	256
Salmonella typhimurium FFUP1	256	128	256	64	⩾512	256	512	128	512	256	128	256
Pseudomonas aeruginosa ATCC 27853	256	256	256	256	512	256	256	256	512	256	128	256
Acinetobacter baumannii FFUP10	256	128	256	64	512	256	256	128	256	256	128	256
Enterococcus faecalis ATCC 29212	256	64	256	64	512	32	256	16	256	32	128	32
Staphylococcus aureus ATCC 29213	128	64	256	64	512	32	256	16	256	32	128	32

bacteria. Interestingly, compound **IIb** showed the highest activity against all the tested Gram-negative bacteria (MIC of 64 mg/L), except for *P. aeruginosa*.

The antibacterial activity of the compounds under study was also evaluated against clinical isolates with different resistance profiles to several antimicrobial agents, including sulfonamide-resistant *Salmonella* and ampicillin, aminoglycoside, tetracycline, macrolide and glycopeptide-resistant *Enterococcus* (Table 3). The results obtained corroborate previously reported patterns observed for these type strains. It may then be concluded that the activity of β-nitrostyrene derivatives against antibiotic-resistant *Salmonella* and *Enterococcus* is not affected by their resistance mechanisms, which are capable of inactivating several antimicrobial agents.

Based on the presently obtained results, a series of other compounds based on the same structural templates were designed, aiming at the screening of their antibacterial activity. These derivatives display different aromatic ring substituents (changing their number and polarity degree), thus promoting changes in their electronic characteristics and lipophilicity. Neither of these chemical modifications led to an increase of the activity (data not shown). In order to check the relevance of the nitro group in the antimicrobial activity of this kind of systems, the amine analogues of some of the β-nitrostyrene and β-methyl-β-nitrostyrenes presently studied were synthesized and tested. In addition, various saturated analogues were also obtained, in order to check the relevance of the ethylenic double bond on the antibacterial properties. In both cases, no significant activity was observed (data not shown). These results reinforce the mechanistic hypothesis proposed in the present work.

2.4. Electrochemical and partition coefficient measurements

As the antibacterial activity and the mechanism of action of the nitro compounds, commonly used in therapy, are largely a function of their redox potential, it was found important to study the physicochemical properties of the synthesized β-nitrostyrene derivatives (Table 1).[15,16]

Thus, the standard redox potentials were determined at physiological pH 7.3, using differential pulse polarography, as well as cyclic and square wave voltammetry, with a glassy carbon working electrode.

A well-defined cathodic peak can be observed at physiological pH for all the compounds studied using differential pulse polarography (Fig. 2). This wave is due to a four-electron, four-proton reduction of the nitro group yielding the corresponding hydroxylamine derivative, according to the following equation:[12,17]

$$R_1R_2\text{–Ph–CH=}CR_3\text{–}NO_2 + 4e^- + 4H^+ \rightarrow R_1R_2\text{–Ph–CH=}CR_3\text{–NHOH} + H_2O$$

Cyclic voltammograms were recorded at different sweep rates. All compounds were found to produce a well-defined and irreversible peak at physiological pH (Fig. 3). This peak corresponds to the above-described wave observed by differential pulse polarography. From the dependence of the peak current on the sweep rate, it was possible to conclude that the process follows a mixed diffusion–adsorption control, since the experimentally obtained slopes ($d\log I_p/d\log v$) display values between 0.5 and 1.[18]

Table 3. In vitro antibacterial activity of the β-nitrostyrene derivatives against several clinical isolates

Clinical isolates	Minimum inhibitory concentration, MIC (mg/L)											
	Ia	**Ib**	**IIa**	**IIb**	**IIIa**	**IIIb**	**IVa**	**IVb**	**Va**	**Vb**	**VIa**	**VIb**
Salmonella typhimurium FFUP40	256	128	256	64	⩾512	256	512	128	512	256	128	256
Salmonella enteritidis 09 FF-D	256	128	256	64	⩾512	256	512	128	512	256	128	256
Enterococcus faecalis H 318	256	64	256	64	512	32	256	16	256	32	128	32
Enterococcus faecalis H 318	256	64	256	64	512	32	256	16	256	32	128	32
Enterococcus faecalis H 181A	256	64	256	64	512	32	256	16	256	32	128	32
Enterococcus faecalis 536540	256	64	256	64	512	32	256	16	256	32	128	32
Enterococcus faecium Med150	256	64	256	64	512	32	256	16	256	32	128	32
Enterococcus faecium Med100 F3	128	64	256	64	512	32	256	16	256	32	128	32
Enterococcus faecium KE77F2	128	64	256	64	512	32	256	32	256	32	128	32

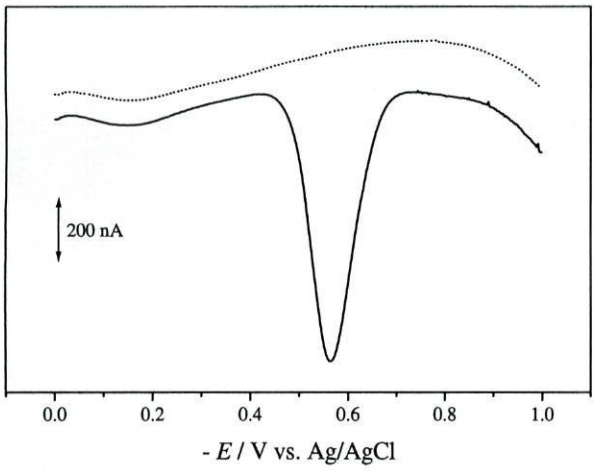

Figure 2. Differential pulse voltammogram for reduction of **VIb**, in pH 7.3 supporting electrolyte, in the absence (· · · · · ·) and presence (—) of 100 μM **VIb**. Scan rate 5 mV s^{-1}.

The results obtained are in agreement with the data reported for other β-nitrostyrene derivatives.[12,17] The shifts detected in the standard redox potential values (Table 4) for the different β-nitrostyrene derivatives are probably due to two distinct substituent effects: (i) substitution of H_β by a methyl group; (ii) different *meta* and *para* substitutions on the aromatic ring.

The redox potential values presented in Table 4 evidence that in all cases the β-methyl-β-nitrostyrene derivatives are reduced at more negative potentials than their corresponding β-nitrostyrenes. Hence, the reduction potential seems to be highly sensitive to a methyl substitution in the β-position. A shift of several tens of millivolts towards more negative potentials is observed when going from β-nitrostyrene to β-methyl-β-nitrostyrene derivatives, which can be attributed to a lack of planarity due to β-methyl substitution.[12] In fact, this distortion of the coplanar arrangement in β-nitrostyrenes leads to a decrease of the resonance interaction between the electroactive nitro group and the aromatic ring, thus causing the observed shift towards negative potentials.[12] This conformational change upon β-methyl substitution is corroborated, in the present study, by the theoretical results that yielded a deviation of about 28° between the planar β-nitrostyrenes and the corresponding β-methyl-β-nitrostyrenes. Also, when such kind of distortion takes place an accumulation of charge on the C_α atom was verified—for example, from +0.050 to −0.008 for compounds **Ia** and **Ib**, respectively—which is probably due to the less effective electronic delocalization to the nitro group in the latter.

The substitution on the aromatic ring in *meta* and especially in *para* position also has a marked effect on the redox potentials. In fact, an increase in the electron-donor properties of the *para* substituent significantly increases the magnitude of the reduction potential, that is, reduction is unlikely to occur (Table 4). As expected, this effect is more pronounced in the β-nitrostyrenes than in the β-methyl-β-nitrostyrenes, due to the decrease in the conjugation coupled with the increase in the C_1–C_α torsion angle,[12] also predicted by the ab initio calculations. Although the increase in the electron-donor properties of the *meta* substituent influences the reduction potential of the compounds, this effect is less pronounced than the one resulting from a *para*-substitution. Moreover, it is more significant for β-nitrostyrenes than for the β-methyl-β-nitrostyrenes, as expected.

In view of better understanding of the overall properties of the compounds, the lipophilicity, expressed as the octanol–water partition coefficient and herein called log *P*, was calculated according to Parham et al.[19] Log *P* between 1.5 and 2.5 were obtained (Table 4).

2.5. Structure–property–activity relationship (SPAR)

In this work, two types of bioisosteric replacements (modifications in the substitution pattern of both the unsaturated side chain and the aromatic ring) were performed in the parent compound—β-nitrostyrene—and the physicochemical properties, as well as antibacterial activity of the series, were examined in order to perform structure–property–activity relationship studies. The chemical structure of each compound was analyzed through three types of parameters: steric interference, electronic distribution and hydrophobicity, since these appear to significantly influence other biological activities.[20,21]

In these SPAR studies, the antimicrobial activities obtained for the nitrostyrene compounds against the *S. aureus* ATCC 29213 and *E. faecalis* ATCC 29212 strains were represented as log 1/MIC. These values were then plotted against E_p and log *P* (Figs. 4 and 5, respectively). These results strongly suggest a correlation between antibacterial activity and redox potential. In turn, no correlation was found between antibacterial activity and lipophilicity. A statistical treatment of the redox potential and partition coefficient results was performed, in view of achieving a better understanding of these findings. An analysis of variance test was carried out, in order to compare the different E_p and log *P* values for the β-nitrostyrenes and the β-methyl-β-nitrostyrenes. Since the experimental values of *F* (between 1.1 and 2.6) were always lower than the theoretical value ($F_{5,5} = 7.1$; $p = 0.05$), it was concluded that there were no significant differences between the variances obtained for those two series of compounds, for neither of the two parameters studied. A comparison of the experimental mean values for the two series of nitrostyrene derivatives was also performed, using the *t* test. Comparison of the redox potentials of β-nitrostyrenes and β-methyl-β-nitrostyrenes yielded *t* test values ($t = 4.2$) higher than the theoretical one ($t = 2.6$; $p = 0.05$). There was no statistical evidence linking the presence of a β-methyl group to a significant effect on the partition coefficient value. Therefore, it may be concluded that the redox potential might be an important parameter ruling the antibacterial activity of β-nitrostyrene derivatives. In fact, it was verified that the more negative the E_p the stronger the antibacterial promoting effect.

In the light of the results presently obtained, it may be suggested that the mode of action of this kind of β-nitro-

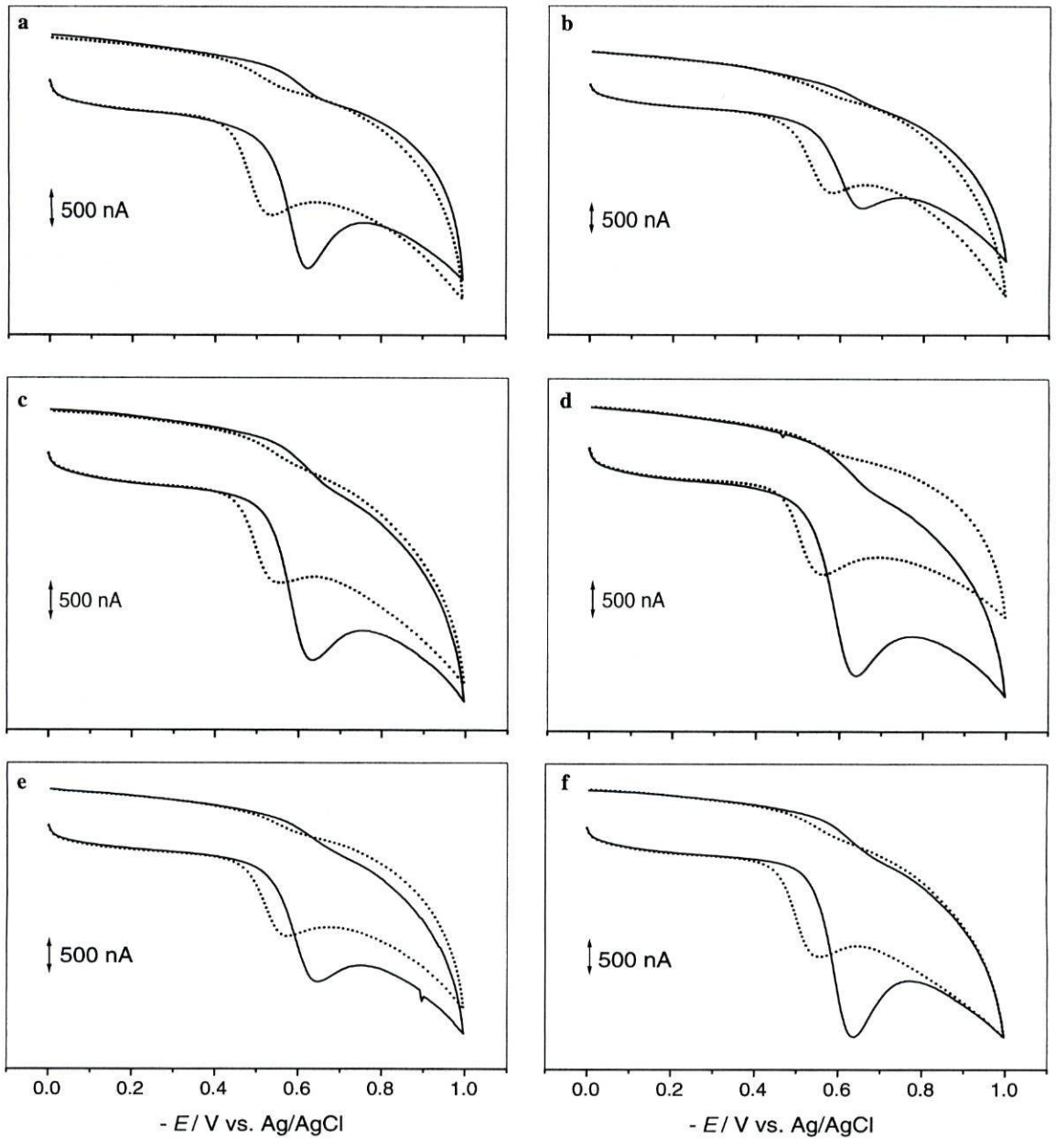

Figure 3. Cyclic voltammograms for several β-nitrostyrene (· · · · · ·) and β-methyl-β-nitrostyrene derivatives (—), in 100 μM solution, at physiological pH. (a) **Ia**, **Ib**; (b) **IIa**, **IIb**; (c) **IIIa**, **IIIb**; (d) **IVa**, **IVb**; (e) **Va**, **Vb**; (f) **VIa**, **VIb**. Scan rate 75 mV s^{-1}.

styrene derivatives is closely related to their electrophilicity, thus being a consequence of their ability to accept electrons, which enables the reduction of the nitro group. The antimicrobial action of nitro compounds is generally believed to result from a 4-electron reduction of the nitro group, carried on by bacterial nitroreductases, to short-lived redox active intermediates, like hydroxylamine adducts, known to be biologically active.[15,16,22,23]

A possible explanation for the higher antimicrobial activity verified for compound **IIb** (one of the β-methyl-β-nitrostyrene derivatives) against some of the Gram-negative bacteria, including members of the *Enterobacteriaceae* family, may be its rather high hydrophilicity (calculated log*P* value of 1.51). In fact, these bacterial strains are known to uptake hydrophilic drugs (<650 Da) through porine channels located on their outer membranes.[24] As shown in Figure 1 and Table 4, the conformational and chemical characteristics of compound **IIb** are in complete accordance with these requisites. Nevertheless, further work is needed in order to prove this hypothesis.

3. Conclusions

The increasing resistance to available antibiotics against clinically important bacteria represents a serious problem in public health which requires the development of new therapeutic alternatives.

The results on the antibacterial activity of β-nitrostyrene derivatives, namely β-methyl-β-nitrostyrenes, towards

Table 4. Redox potential and partition coefficient values for the β-nitrostyrene and β-methyl-β-nitrostyrene derivatives studied in this work

Compound	E_p (V)	ΔE_p[a] (mV)	Log*P*
Ia	−0.455	92	2.28
Ib	−0.547		2.40
IIa	−0.497	77	1.46
IIb	−0.574		1.51
IIIa	−0.471	87	2.34
IIIb	−0.558		2.50
IVa	−0.477	87	1.78
IVb	−0.564		2.11
Va	−0.492	77	1.79
Vb	−0.569		2.15
VIa	−0.473	92	1.85
VIb	−0.565		2.07

[a] E_p difference between the β-nitrostyrenes and the corresponding β-methyl-β-nitrostyrenes.

standard strains suggest that these could constitute a group of promising agents for the most clinically relevant Gram-positive bacteria, *S. aureus* and *Enterococcus* spp. This propensity is in accordance with previously obtained results with similar compounds.[5–7] The high selectivity exhibited by these systems is unequivocally related to their structural features.

Even though further research must be conducted in order to study other physicochemical parameters, the redox potential value seems to be a crucial parameter for the displayed antimicrobial activity. It was verified that the conformational behaviour of these molecules is mainly determined by the stabilizing effect of π-electron delocalization, which is reflected in the most stable geometries calculated for the β-nitrostyrene derivatives, and is in accordance with the electrochemical data.

The results gathered along this work provide a rational approach that will hopefully allow the design of selective and effective antibacterial agents. The β-nitrostyrene family seems to represent a novel class of antibacterial agents possessing a surprisingly small pharmacophore. Changes in the ethylenic side chain of the β-nitrostyrenes must be performed, namely in the length and volume of its substituents, in order to check its influence in the activity versus electrochemical properties.

4. Experimental

4.1. Chemicals

β-Nitrostyrene (**Ia**), ammonium acetate, nitroethane and nitromethane were purchased from Sigma–Aldrich

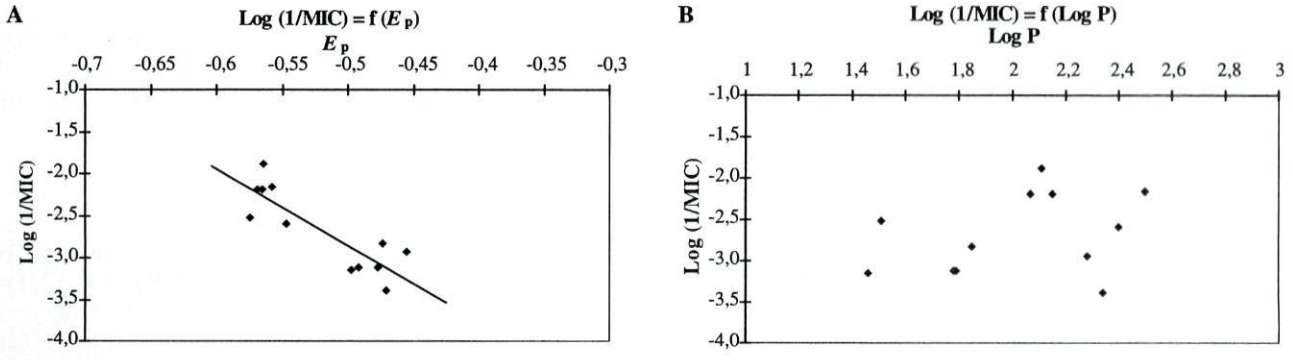

Figure 4. Regression plots of log(1/MIC) towards *Staphylococcus aureus* ATCC 29213, for the β-nitrostyrene derivatives tested: (A) standard redox potential values at physiological pH; (B) log*P* values.

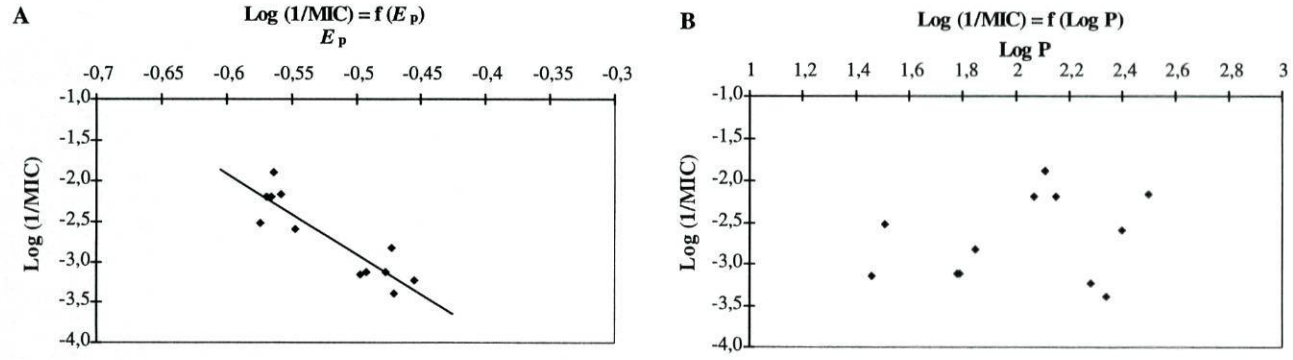

Figure 5. Regression plots of log(1/MIC) towards *Enterococcus faecalis* ATCC 29212, for the β-nitrostyrene derivatives tested: (A) standard redox potential values at physiological pH; (B) log*P* values.

Química SA. (Sintra, Portugal). All other reagents and solvents (pro analysis grade) were acquired from Merck (Lisbon, Portugal). Deionized water (conductivity <0.1 μS cm^{-1}) was used in all experiments. Trypticase soy broth was obtained from Oxoid (Basingstone, UK) and Mueller–Hinton II from Biomérieux (Marcy L'Etoile, France). All reagents were used without further purification.

4.2. Analysis

^1H and ^{13}C NMR data were acquired, at room temperature, on a Brüker AMX 300 spectrometer operating at 300.13 and 75.47 MHz, respectively. Dimethylsulfoxide-d_6 was used as a solvent; chemical shifts are expressed in δ (ppm) values, relative to tetramethylsilane (TMS) (as internal reference); coupling constants (J) are given in Hz. Assignments were also made from Distortionless Enhancement by Polarization Transfer (DEPT) experiments (underlined values). Electron impact mass spectra (EI-MS) were obtained on a VG AutoSpec instrument; data are reported as *m/z* (% of relative intensity for the most important fragments). Melting points were measured on a Köfler microscope (Reichert Thermovar) and are uncorrected.

The purity of the final products (higher than 98%) was verified using two different high-performance liquid chromatography (HPLC) systems, one equipped with UV and the other with an electrochemical detector. HPLC-UV chromatograms were obtained in a Jasco instrument (pumps model 880-PU and solvent mixing model 880-30, Tokyo, Japan), equipped with a Nucleosil RP-18 column (250 mm × 4.6 mm, 5 μm, Macherey-Nagel, Düren, Germany) and UV detection at 214 nm (Jasco model 875-UV). The mobile phase was acetonitrile/water, at a flow rate of 1 mL/min. A linear gradient of acetonitrile from 10% to 100% during a period of 35 min was used. The chromatographic data were processed in a Compaq computer, fitted with CSW 1.7 software (DataApex, Czech Republic).

A Waters 2690 Alliance system equipped with a CONCORDE Electrochemical Detector (Waters Corporation, Milford, USA). The electrochemical cell was a VT-03 flow cell (Antec Leyden, Zoeterwoude, Netherlands) with a confined wall-jet design, in a three-electrode configuration: a 2 mm diameter glassy carbon working electrode, an in situ Ag/AgCl reference electrode and a stainless steel auxiliary electrode. The electrochemical detector was operated in reductive amperometric mode with the working potentials between −450 and −600 mV. The HPLC separation was carried out in a reverse-phase LC-18-S Supelcosil analytical column (150 mm × 4.6 mm, 5 μm, Supelco, Bellefonte, USA). A 50 mM phosphate buffer of pH 6.8 with 6% MeOH was used as mobile phase, in isocratic mode at 1 mL/min flow rate. Chromatograms were acquired in a Millenium 32 Chromatography Manager (Waters Corporation, Milford, USA).

4.3. General synthetic procedure and structural elucidation

The method of Parker et al.,[25] slightly modified, was used for the synthesis of the compounds. The benzaldehyde with the same aromatic substitution pattern of the desired final product (25.0 mmol) and ammonium acetate (6.5 mmol) were dissolved in nitromethane (50 mL)—for the β-nitrostyrene derivatives (**IIIa**, **IVa**, **Va** and **VIa**)—or in nitroethane (50 mL)—for the β-methyl-β-nitrostyrene derivatives (compounds **IIIb**, **IVb** and **Vb**), and refluxed for 6 h. The reactions were followed by thin-layer chromatography (TLC). After cooling the reaction mixtures to room temperature, the solvents were partially evaporated, diluted with diethyl ether and washed twice with water. The organic layer was dried over anhydrous magnesium sulfate, filtered and concentrated. The remaining residues were recrystallized from diethyl ether/petroleum ether (40–60 °C) or from methanol/water.

The synthesized compounds were identified by both NMR and EI-MS. In the present study, the nitro compounds were systematically characterized, although some of them had been previously reported.[26–30] The syntheses of the remaining compounds used in this study (**Ib**, **IIa**, **IIb** and **VIb**) are described elsewhere.[31,32]

4.3.1. 3,4-Dimethoxy-β-nitrostyrene (IIIa). Yield 77%; ^1H NMR δ: 3.82 (3H, s, 3-OCH_3), 3.83 (3H, s, 4-OCH_3), 7.06 (1H, d, J = 8.4, H(5)), 7.43 (1H, d, J = 8.4, H(6)), 7.49 (1H, s, H(2)), 8.07 (1H, d, J = 13.4, H(α)), 8.22 (1H, d, J = 13.5, H(β)); ^{13}C NMR δ: 55.8 (4-OCH_3), 55.9 (3-OCH_3), 111.2, 111.8 C(2) and C(5), 123.0 C(1), 125.9 C(6), 136.0 C(α), 140.1 C(β), 149.2 C(4), 152.7 C(3); EI-MS *m/z* (%): 209 ($M^{+\cdot}$, 100), 162 (53), 147 (19), 119 (15), 91 (11), 77 (11), 63 (7); mp 142–144 °C.

4.3.2. 3,4-Dimethoxy-β-methyl-β-nitrostyrene (IIIb). Yield 68%; ^1H NMR δ: 2.44 (3H, s, CH_3), 3.80 (3H, s, 3-OCH_3), 3.82 (3H, s, 4-OCH_3), 7.08 (1H, d, J = 8.5, H(5)), 7.22 (1H, s, H(2)), 7.23 (1H, d, J = 8.5, H(6)), 8.08 (1H, s, H(α)); ^{13}C NMR δ: 14.0 CH_3, 55.6 (4-OCH_3), 55.7 (3-OCH_3), 111.8, 113.9 C(2) and C(5), 124.3 C(6), 124.4 C(1), 133.8 C(α), 145.6 C(β), 148.7 C(4), 150.7 C(3); EI-MS *m/z* (%): 223 ($M^{+\cdot}$, 100), 176 (78), 165 (22), 161 (37), 146 (47), 131 (46), 119 (36), 103 (37), 91 (47), 77 (38), 65 (34); mp 71–72 °C.

4.3.3. 3-Hydroxy-4-methoxy-β-nitrostyrene (IVa). Yield 92%; ^1H NMR δ: 3.84 (3H, s, OCH_3), 7.02 (1H, d, J = 8.4, H(5)), 7.24 (1H, d, J = 2.0, H(2)), 7.32 (1H, dd, J = 8.4; 2.1, H(6)), 8.01 (2H, s, H(α), H(β)), 9.35 (1H, br s, O*H*); ^{13}C NMR δ: 55.8 (OCH_3), 112.0, 115.6 C(2) and C(5), 122.9 C(1), 123.6 C(6), 135.6 C(α), 139.9 C(β), 146.8 C(3), 151.6 C(4); EI-MS *m/z* (%): 195 ($M^{+\cdot}$, 100), 148 (53), 133 (44), 105 (25), 89 (31), 77 (25), 63 (14); mp 158–161 °C.

4.3.4. 3-Hydroxy-4-methoxy-β-methyl-β-nitrostyrene (IVb). Yield 97%; ^1H NMR δ: 2.40 (3H, s, CH_3), 3.83 (3H, s, OCH_3), 7.04 (1H, d, J = 8.2, H(5)), 7.06–7.10

(2H, m, H(2), H(6)), 7.98 (1H, s, H(α)), 9.39 (1H, br s, O*H*); ^{13}C NMR δ: 14.0 CH_3, 55.6 (OCH_3), 112.1, 116.9 C(2) and C(5), 123.5 C(6), 124.5 C(1), 133.7 C(α), 145.2 C(β), 146.6 C(3), 149.8 C (4); EI-MS *m/z* (%): 209 ($M^{+\cdot}$, 100), 162 (56), 147 (53), 131 (23), 119 (29), 103 (75), 91 (50), 83 (62), 77 (31), 65 (29); mp 79–81 °C.

4.3.5. 4-Hydroxy-3-methoxy-β-nitrostyrene (Va). Yield 91%; ^{1}H NMR δ: 3.82 (3H, s, OCH_3), 6.84 (1H, d, $J = 8.2$, H(5)), 7.30 (1H, dd, $J = 8.2$; 1.9, H(6)), 7.47 (1H, d, $J = 1.8$, H(2)), 8.02 (1H, d, $J = 13.4$, H(α)), 8.16 (1H, d, $J = 13.4$, H(β)), 10.15 (1H, br s, O*H*); ^{13}C NMR δ: 55.8 (OCH_3), 112.2, 115.8 C(2) and C(5), 121.5 C(1), 126.0 C(6), 134.9 C(α), 140.3 C(β), 148.2 C(4), 151.5 C(3); EI-MS *m/z* (%): 195 ($M^{+\cdot}$, 100), 148 (77), 133 (46), 105 (28), 89 (38), 78 (28), 63 (19); mp 168–171 °C.

4.3.6. 4-Hydroxy-3-methoxy-β-methyl-β-nitrostyrene (Vb). Yield 95%; ^{1}H NMR δ: 2.44 (3H, s, CH_3), 3.81 (3H, s, OCH_3), 6.89 (1H, d, $J = 8.2$, H(5)), 7.12 (1H, dd, $J = 8.2$; 1.9, H(6)), 7.20 (1H, d, $J = 1.9$, H(2)), 8.05 (1H, s, H(α)), 9.85 (1H, br s, O*H*); ^{13}C NMR δ: 14.0 CH_3, 55.7 (OCH_3), 114.8, 115.9 C(2) and C(5), 123.0 C(1), 124.8 C(6), 134.2 C(α), 144.7 C(β), 147.7 C(4), 149.2 C(3); EI-MS *m/z* (%): 209 ($M^{+\cdot}$, 100), 162 (81), 147 (53), 131 (33), 119 (30), 103 (84), 91 (56), 77 (36), 65 (32); mp 97–99 °C.

4.3.7. 3,4-Methylenedioxy-β-nitrostyrene (VIa). Yield 91%; ^{1}H NMR δ: 6.09 (2H, s, CH_2), 7.00 (1H, d, $J = 8.0$, H(5)), 7.34 (1H, dd, $J = 8.0$; 1.7, H(6)), 7.46 (1H, d, $J = 1.6$, H(2)), 8.01 (1H, d, $J = 13.5$, H(α)), 8.07 (1H, d,$J = 13.5$, H(β)); ^{13}C NMR δ: 102.3 CH_2, 107.8, 109.2 C(2) and C(5), 124.6 C(1), 128.0 C(6), 136.4 C(α), 139.9 C(β), 148.5 C(4), 151.2 C(3); EI-MS *m/z* (%): 193 ($M^{+\cdot}$, 100), 146 (92), 117 (17), 89 (70), 71 (24), 63 (46); mp 164–165 °C.

4.4. Ab initio MO calculations

The ab initio calculations—full geometry optimization and calculation of the harmonic vibrational frequencies—were performed using the GAUSSIAN 98W program,[33] within the Density Functional Theory (DFT) approach, in order to properly account for the electron correlation effects. The widely employed hybrid method denoted by B3LYP,[34–39] which includes a mixture of HF and DFT exchange terms and the gradient-corrected correlation functional of Lee, Yang and Parr,[40,41] as proposed and parameterized by Becke,[42,43] was used, along with the double-zeta split valence basis set 6-31G**.[44,45]

Molecular geometries were fully optimized by the Berny algorithm, using redundant internal coordinates:[46] The bond lengths to within ca. 0.1 pm and the bond angles to within ca. 0.1°. The final root-mean-square (rms) gradients were always less than 3×10^{-4} hartree bohr^{-1} or hartree radian^{-1}. No geometrical constraints were imposed on the molecules under study. The ZPE scaling was employed for all minima in the potential energy surface.

4.5. Antibacterial activity

4.5.1. Test strains and medium. The antibacterial activity, expressed as MIC values (minimum inhibitory concentration), was determined on both clinical isolates and bacterial strains obtained from the American Type Culture Collection (ATCC) and from the Microbiology Laboratory of Faculty of Pharmacy of University of Porto (FFUP). All bacterial strains were maintained as frozen stocks at −80 °C in protected vials. The stock cultures were propagated overnight in trypticase soy broth at 35 °C, before experimental use.

The Mueller–Hinton II culture medium, containing beef infusion 300 g/L, bio-Case 17.5 g/L, starch 1.5 g/L and agar 17 g/L, was used in the antibacterial assays.

4.5.2. Antibacterial assays. The antibacterial activity of the compounds was evaluated through the agar dilution procedure outlined by the National Committee for Clinical Laboratory Standards (NCCLS).[14] Stock solutions of the β-nitrostyrene derivatives were prepared either in ethanol or water depending on the compounds solubility, and dilutions were carried out with sterilized distilled water. Different concentrations were obtained by 2-fold plate-dilution of a stock containing 1280 mg/L of test substance, ranging from 16 to 512 mg/L, prepared immediately before use and sterilized by filtration through a 0.2 μm membrane filter.

The inoculated plates were incubated overnight at 35 °C. All the experiments were conducted in triplicate. The lowest concentration of the compounds that prevented visible growth was considered to be the MIC value. The solvent was found to have no effect on the microorganisms, for all the concentrations tested (data not shown).

4.6. Electrochemical determinations

4.6.1. Preparation of solutions. Ten millimole stock solutions of the β-nitrostyrene derivatives were prepared by dissolving an appropriate amount in ethanol. The polarographic working solutions were prepared, in the electrochemical cell, by diluting 100 μL of the stock solution in 10 mL of supporting electrolyte, in order to get a final concentration of 0.1 mM.

The pH 7.3 supporting electrolyte was prepared by diluting 6.2 mL of 0.2 M dipotassium hydrogen phosphate and 43.8 mL of 0.2 M potassium dihydrogen phosphate to 100 mL.

4.6.2. Voltammetric measurements. Differential pulse polarograms, cyclic and square wave voltammograms were obtained in a PalmSens potentiostat/galvanostat (Palm Instruments, The Netherlands) and a one-compartment glass electrochemical cell. A 2 mm diameter glassy carbon working electrode (GCE), a platinum wire counterelectrode and an Ag/AgCl saturated KCl reference electrode were used. pH measurements were carried out in a Metrohm E520 pH-meter with a glass electrode (Metrohm, Switzerland).

All measurements were performed at room temperature and purified nitrogen was used for oxygen displacement.

4.7. Log *P* calculations

Estimated partition coefficients (log*P*) were calculated according to the procedure of Parham et al.[19] This method uses an artificial neural network (ANN) analysis based on several property descriptors, which was trained with a large data set including more than 2000 compounds. Property descriptors encompass *Electrotopological state* (E-state) structure descriptors that encode the electron accessibility for each atom (i.e., the potential for non-covalent intermolecular interaction), *Molecular connectivity* χ indices which encode skeletal variation information and K shape indices describing the overall shape of the molecule.

4.8. Statistical analysis

The reported results are means of at least three independent determinations, with a divergence of not more than one MIC value.

Acknowledgements

N.M. and R.C. acknowledge financial support from FCT—PhD fellowships PRAXIS XXI/BD/18520/98 and SFRH/BD/16520/2004.

References and notes

1. Kaap, S.; Quentin, I.; Tamiru, D.; Shaheen, M.; Eger, K.; Steinfelder, H. *J. Biochem. Pharmacol.* **2003**, *65*, 603.
2. Kim, J. H.; Kim, J. H.; Lee, G. E.; Lee, J. E.; Chung, I. K. *Mol. Pharmacol.* **2003**, *63*, 1117.
3. Carter, K. C.; Finnon, Y. S.; Daeid, N. N.; Robson, D. C.; Waddell, R. *Immunopharmacol. Immunotoxicol.* **2002**, *24*, 187.
4. Doré, J. C.; Viel, C. *Farmaco* **1975**, *2*, 81.
5. Brian, P. W.; Grove, J. F.; McGowan, J. C. *Nature* **1946**, *158*, 876.
6. Worthen, L. R.; Bond, H. W. *J. Pharm. Sci.* **1970**, *59*, 1185.
7. Schales, O.; Graefe, H. A. *J. Am. Chem. Soc.* **1952**, *74*, 4486.
8. Nielsen, S. F.; Boesen, T.; Larsen, M.; Schønning, K.; Kromann, H. *Bioorg. Med. Chem.* **2004**, *12*, 3047.
9. Narasimhan, B.; Belsare, D.; Pharande, D.; Mourya, V.; Dhaka, A. *Eur. J. Med. Chem.* **2004**, *39*, 827.
10. Pires, J. R.; Saito, C.; Gomes, S. L.; Giesbrecht, A. M.; Amaral, A. T. *J. Med. Chem.* **2001**, *44*, 3673.
11. Rosini, G.. In *Comprehensive Organic Synthesis Strategy and Efficiency in Modern Organic Chemistry*; Pergamon Press: Oxford, 1991; Vol. 2, pp 321–339.
12. Squella, J. A.; Sturm, J. C.; Weiss-Lopez, B.; Bontá, M.; Núñez-Vergara, L. J. *J. Electroanal. Chem.* **1999**, *466*, 90.
13. Desiraju, G. R.; Steiner, T. *The Weak Hydrogen Bond in Structural Chemistry and Biology IUCr Monographs on Chrystallography—9*; Oxford University Press: UK, 1999, and references cited therein.
14. National Committee for Clinical Laboratory Standards. Standard methods for dilution antimicrobial susceptibility tests for bacteria that grow aerobically. Approved standard M7-A5. National Committee for Clinical Laboratory Standards, Wayne PA, 2000.
15. Nivinskas, H.; Koder, R. L.; Zilvinas, A.; Sarlauskas, J.; Miller, A. F.; Cenas, N. *Arch. Biochem. Biophys.* **2001**, *385*, 170.
16. Sisson, G.; Goodwin, A.; Raudonikiene, A.; Hughes, N. J.; Mukhopadhyay, A. K.; Berg, D. E.; Hoffman, P. S. *Antimicrob. Agents Chemother.* **2002**, *46*, 2116.
17. Masui, M.; Sayo, M. *Pharm. Bull.* **1956**, *4*, 332.
18. Gosser, D. K. In *Cyclic Voltammetry. Simulation and Analysis of Reaction Mechanisms*; VCH: New York, 1994, Chapter 2.
19. Parham, M.; Hall, L.; Kier, L. In *Accurate Prediction of Log P Using E-State Indices with Neural Network Analysis.* 220th ACS National Meeting, Washington, DC, USA, 2000.
20. Koyama, J.; Morita, I.; Tagahara, K.; Osakai, T.; Hotta, H.; Yang, M. X.; Mukainaka, T.; Nishino, H.; Tokuda, H. *Chem. Pharm. Bull.* **2001**, *49*, 1214.
21. Lima, N. M. F.; Correia, C. S.; Ferraz, P. A. L.; Pinto, A. V.; Pinto, M. C. R. F.; Santana, A. E. G.; Goulart, M. O. F. *J. Braz. Chem. Soc.* **2002**, *13*, 822.
22. McCalla, D. R. In *Mechanism of Action of Antibacterial Agents*; Hahn, F. E., Ed.; Springer-Verlag: Berlin Germany, 1979; pp 176–213.
23. Whiteway, J.; Koziarz, P.; Veall, J.; Sandhu, N.; Kumar, P.; Hoecher, B.; Lambert, I. B. *J. Bacteriol.* **1998**, *180*, 5529.
24. Decad, G. M.; Nikaido, H. *J. Bacteriol.* **1976**, *128*, 325.
25. Parker, M. A.; Marona-Lewika, D.; Kurrasch, D.; Shulgin, A. T.; Nichols, D. E. *J. Med. Chem.* **1998**, *41*, 1001.
26. Gairaud, C. B.; Lappin, G. R. *J. Org. Chem.* **1953**, *18*, 1.
27. Rao, T. V.; Ravishankar, L.; Trivedi, G. K. *Indian J. Chem. Sec. B.* **1990**, *29B*, 207.
28. Traxler, P. M.; Wacker, O.; Bach, H. L.; Geissler, J. F.; Kump, W.; Meyer, T.; Regenass, U.; Roesel, J. L.; Lydon, N. *J. Med. Chem.* **1991**, *34*, 2328.
29. Schmidt, M.; Eger, K. *Pharmazie* **1996**, *51*, 11.
30. Wang, C.; Wang, S. *Synth. Commun.* **2002**, *32*, 3481.
31. Calheiros, R.; Milhazes, N.; Borges, F.; Marques, M. P. M. *J. Mol. Struct.* **2004**, *692*, 91.
32. Milhazes, N.; Borges, F.; Calheiros, R.; Marques, M. P. M. *Analyst* **2004**, *129*, 1106.
33. Frisch, M. J.; Trucks, G. W.; Schlegel, H. B.; Scuseria, G. E.; Robb, M. A.; Cheeseman, J. R.; Zakrzewski, V. G.; Montgomery, J. A., Jr.; Stratmann, R. E.; Burant, J. C.; Dapprich, S.; Millam, J. M.; Daniels, A. D.; Kudin, K. N.; Strain, M. C.; Farkas, O.; Tomasi, J.; Barone, V.; Cossi, M.; Cammi, R.; Mennucci, B.; Pomelli, C.; Adamo, C.; Clifford, S.; Ochterski, J.; Petersson, G. A.; Ayala, P. Y.; Cui, Q.; Morokuma, K.; Malick, D. K.; Rabuck, A. D.; Raghavachari, K.; Foresman, J. B.; Cioslowski, J.; Ortiz, J. V.; Baboul, A. G.; Stefanov, B. B.; Liu, G.; Liashenko, A.; Piskorz, P.; Komaromi, I.; Gomperts, R.; Martin, R. L.; Fox, D. J.; Keith, T.; Al-Laham, M. A.; Peng, C. Y.; Nanayakkara, A.; Challacombe, M.; Gill, P. M. W.; Johnson, B.; Chen, W.; Wong, M. W.; Andres, J. L.; Gonzalez, C.; Head-Gordon, M.; Replogle, E. S.; Pople, J. A. *Gaussian 98, Revision A.9*; Gaussian Inc.: Pittsburgh PA, USA, 1998.
34. Russo, T. V.; Martin, R. L.; Hay, P. J. *J. Phys. Chem.* **1995**, *99*, 17085.
35. Ignaczak, A.; Gomes, J. A. N. F. *Chem. Phys. Lett.* **1996**, *257*, 609.
36. Cotton, F. A.; Feng, X. *J. Am. Chem. Soc.* **1997**, *119*, 7514.
37. Ignaczak, A.; Gomes, J. A. N. F. A. *J. Electroanal. Chem.* **1997**, *420*, 209.

38. Wagener, T.; Frenking, G. *Inorg. Chem.* **1998**, *37*, 1805.
39. Cotton, F. A.; Feng, X. *J. Am. Chem. Soc.* **1998**, *120*, 3387.
40. Lee, C.; Yang, W.; Parr, R. G. *Phys. Rev. B* **1988**, *37*, 785.
41. Miehlich, B.; Savin, A.; Stoll, H.; Preuss, H. *Chem. Phys. Lett.* **1989**, *157*, 200.
42. Becke, A. D. *Phys. Rev. A* **1988**, *38*, 3098.
43. Becke, A. D. *J. Chem. Phys.* **1993**, *98*, 5648.
44. Hariharan, P. C.; Pople, J. A. *Theor. Chim. Acta* **1973**, *28*, 213.
45. Francl, M. M.; Pietro, W. J.; Hehre, W. J.; Binkley, J. S.; Gordon, M. S.; DeFrees, D. J.; Pople, J. A. *J. Chem. Phys.* **1982**, *77*, 3654.
46. Peng, C.; Ayala, P. Y.; Schlege, H. B.; Frisch, M. J. *J. Comput. Chem.* **1996**, *17*, 49.

8.4 Síntese e análise de aminocromos por HPLC com detector de fotodíodos. Determinação de adrenocromo em sangue de rato.

Artigo reproduzido da revista *Biomedical Chromatography* (2003) 17: 6-13, com permissão da John Wiley & Sons, Ltd.

BIOMEDICAL CHROMATOGRAPHY
Biomed. Chromatogr. **17**: 6–13 (2003)
Published online in Wiley InterScience (www.interscience.wiley.com).
DOI: 10.1002/bmc.203

ORIGINAL RESEARCH

Synthesis and analysis of aminochromes by HPLC-photodiode array. Adrenochrome evaluation in rat blood

Fernando Remião[1]*, Nuno Milhazes[2,3], Fernanda Borges[2], Félix Carvalho[1], Maria L. Bastos[1], Francisco Lemos-Amado[4], Pedro Domingues[4] and A. Ferrer-Correia[4]

[1]CEQUP/Serviço de Toxicologia, Faculdade de Farmácia, Universidade do Porto, Rua Aníbal Cunha, 164, 4050-047 Porto, Portugal
[2]CEQOFFUP/Serviço de Química Organica, Faculdade de Farmácia, Universidade do Porto, Rua Aníbal Cunha, 164, 4050-047 Porto, Portugal
[3]Instituto de Ciências de Saúde-Norte, R. Central da Gandra, 1317, Gandra, 4585-116 Paredes, Portugal
[4]Departamento de Química, Universidade de Aveiro, 3810-123 Aveiro, Portugal

Received 15 July 2002; revised 4 September 2002; accepted 11 September 2002

ABSTRACT: The catecholamine oxidation process induces cardiotoxicity and neurotoxicity. Catecholamines can oxidize to aminochromes through autoxidation or by enzymatic or non-enzymatic catalysis. Although some toxic effects seem to be related to the formation of aminochromes there is still scarce information concerning the identification and evaluation of these compounds in *in vivo* models. In this study five catecholamines were oxidized to their respective aminochromes: adrenaline/adrenochrome; noradrenaline/noradrenochrome; dopa/dopachrome; dopamine/dopaminochrome; and isoproterenol/isoprenochrome. The evaluation of the catecholamines oxidation profile was performed by HPLC with photodiode array detection and using either enzymatic (tyrosinase) or non-enzymatic [Ag_2O, $CuSO_4$, $NaIO_4$ and $K_3Fe(CN)_6$] catalytic systems. The $NaIO_4$ was found to be the most efficient oxidant of catecholamines. An isocratic reverse-phase HPLC method was developed to analyse each pair of catecholamine–aminochrome. The analytical system was then applied to the detection of adrenochrome in rat blood at 490 nm. Thus, adrenochrome was administered i.p. to rats and its concentration in whole blood was monitored after 5, 15 and 25 min. Blood treatment for adrenochrome evaluation consists of an acidification for protein precipitation followed by a rapid neutralization. The results showed a rapid decrease of adrenochrome concentration in blood after its administration. The adrenochrome present in blood was characterized by UV and tandem mass spectrometry. Copyright © 2002 John Wiley & Sons, Ltd.

KEYWORDS: catecholamines oxidation; enzymatic oxidation; tyrosinase; non-enzymatic oxidation

INTRODUCTION

The catecholamines oxidation process induces cardiotoxicity (Behonick *et al.*, 2001; Dhalla *et al.*, 2001). In fact, it has been known since 1959 that isoproterenol induces myocardial necrosis in rats (Rona *et al.*, 1959), which was suggested to be related to catecholamine oxidation in *in vivo* (Rupp *et al.*, 1994; Dhalla *et al.*, 1996; Tappia *et al.*, 2001) and *in vitro* studies (Ramos and Acosta, 1989; Remião *et al.*, 2001; Tappia *et al.*, 2001). Furthermore, neurotoxic effects induced by oxidation of the catecholamines in the brain have been described (Smythies and Galzigna, 1998), especially dopamine oxidation, which was reported to be involved in the Parkinson's disease (Keller *et al.*, 2000; Martinez-Alvarado *et al.*, 2001).

The oxidation of catecholamines is initiated with its transformation to *ortho*-semiquinones and then to *ortho*-quinones (Fig. 1; Bindoli *et al.*, 1989). *ortho*-Quinones can undergo an irreversible 1,4-intramolecular cyclisation, a process that involves a nucleophilic attack of the nitrogen atom to the 6-position of the quinone ring, which leads to the formation of unstable leukoaminochromes (Bindoli *et al.*, 1989). Leukoaminochromes are subsequently oxidized to aminochromes, through the intermediate leukoaminochrome-*ortho*-semiquinone. Aminochromes have been reported to induce toxicity and are related to the cardiotoxicity observed after catecholamines administration (Behonick *et al.*, 2001; Dhalla *et al.*, 2001).

Catecholamine oxidation can occur by autoxidation, but this reaction seems to happen very slowly at

*Correspondence to: F. Remião, CEQUP/Serviço de Toxicologia, Faculdade de Farmácia, Universidade do Porto, Rua Aníbal Cunha 164, 4050-047 Porto, Portugal.
E-mail: remiao@ff.up.pt

Abbreviations used: DAD, photodiode array detector; DHMI, 5,6-dihydroxy-*N*-methylindole.

Contract/grant sponsor: FEDER European Comminity Funding; contract/grant number: POCT1/36099/FCB/2000.
Contract/grant sponsor: Project PRAXIS; contract/grant number: XXI/BD/18520/98.

Copyright © 2002 John Wiley & Sons, Ltd.

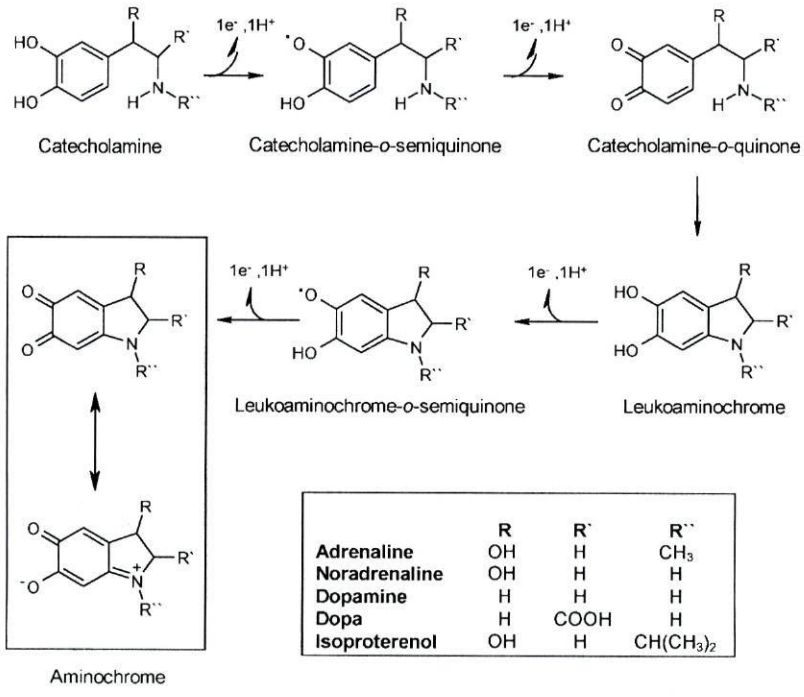

	R	R`	R``
Adrenaline	OH	H	CH_3
Noradrenaline	OH	H	H
Dopamine	H	H	H
Dopa	H	COOH	H
Isoproterenol	OH	H	$CH(CH_3)_2$

Figure 1. Proposed mechanism for catecholamines oxidation to aminochromes (adapted from Bindoli *et al.*, 1989).

physiological pH (Bindoli *et al.*, 1992; Remião *et al.*, 2001). However, this process can be accelerated in physiological conditions by enzymatic or non-enzymatic catalysis. In fact, catecholamines are oxidized by enzymes such as xanthine oxidase (Foppoli *et al.*, 1997), peroxidase (Bindoli *et al.*, 1992), tyrosinase (Heacock, 1959), lipoxygenase (Núñez-Delicado *et al.*, 1996), several copper-containing catechol oxidases (Bindoli *et al.*, 1992), leukocyte myeloperoxidase and heart muscle cytochrome c oxidase (Dhalla *et al.*, 2001), and in the presence of metal cations such as Cu^{2+}, Mn^{2+}, Co^{2+}, Ni^{2+}, Fe^{3+} and several Cu^{2+} and Fe^{3+} chelates (Bindoli *et al.*, 1992). Ferrylmyoglobin (Giulivi and Cadenas, 1998), nitric oxide (Riobó *et al.*, 2002) and ceruloplasmin (plasma protein containing copper; Bindoli *et al.*, 1992) are also able to initiate the oxidation of catecholamines. Although the catecholamines oxidation catalysis and the related aminochromes toxicity have been described, no information concerning direct aminochromes identification and evaluation in *in vivo* models has been reported so far.

In this study two catecholamines, one biogenic (adrenaline) and other synthetic amine (isoproterenol), were oxidized using enzymatic (tyrosinase) and non-enzymatic [Ag_2O, $CuSO_4$, $NaIO_4$ and $K_3Fe(CN)_6$] systems. The oxidation of these catecholamines was monitored by HPLC–photodiode array (HPLC-DAD). The best oxidant system was selected and then applied to oxidize the catecholamines adrenaline, noradrenaline, dopa, dopamine and isoproterenol to their aminochromes adrenochrome, noradrenochrome, dopachrome, dopaminochrome and isoprenochrome, respectively (Fig. 1). An isocratic reverse-phase HPLC-DAD method was developed in order to separate and quantify each pair of catecholamine–aminochrome. The analytical system was then applied to the quantification of adrenochrome in rat blood after its administration to rats. It was necessary to develop a sample preparation suitable for aminochrome analysis in biological samples, which is also described. Finally, the characterization of the adrenochrome in the rat blood was performed by UV and tandem mass spectrometry analysis.

MATERIALS AND METHODS

HPLC-DAD

An HPLC system (Waters model 2690) with a photodiode array detector (Waters model 996) was used. The analytical column was a commercially prepacked reverse-phase cartridge of 244 × 4 mm i.d. containing LiChrospher 100 RP-8 (5 μm) from Merck (Darmstadt, Germany). An isocratic elution was performed at a flow rate of 1 mL min^{-1} and at room temperature. A solution of 95% 10 mM aqueous ammonium acetate (corrected to pH 2.5 with hydrochloric acid) plus 5% acetonitrile was used as mobile phase, which was always filtered through a 0.45 μm membrane (Millipore, Madrid, Spain) and degassed under helium stream. A

Copyright © 2002 John Wiley & Sons, Ltd.

Compaq computer fitted with Millenium[32] software (Waters) processed the chromatographic and spectral data.

Catecholamines oxidation

Non-enzymatic oxidation. To a solution of adrenaline or isoproterenol (1.0 mM) in 5 mL aqueous ammonium acetate buffer (100 μM; corrected to pH 5.8 with hydrochloric acid) 2.0 mM of an inorganic oxidizing agent [Ag_2O, $CuSO_4$, $NaIO_4$ and $K_3Fe(CN)_6$] was added. The solution was then incubated for 2 h at room temperature with slight stirring. The oxidation was monitored at 5 min of incubation and thereafter at every 30 min.

Enzymatic oxidation. To a solution of adrenaline or isoproterenol (1.0 mM) in 5 mL aqueous ammonium acetate buffer (100 μM; corrected to pH 5.8 with hydrochloric acid) 165 U-mL^{-1} of tyrosinase was added. The solution was then incubated for 2 h at room temperature with slight stirring. The oxidation was monitored at 5 min of incubation and thereafter at every 30 min. Protein precipitation of the enzymatic reaction mixtures was performed by sample dilution with methanol (1:1) before HPLC analysis.

Catecholamines oxidation analysis. The oxidation of catecholamines was monitored by HPLC-DAD. Chromatograms were analysed at 279 nm, which corresponds to the maximum absorption wavelength of catecholamines. The percentage of the catecholamines oxidation was calculated as percent decrease in peak area over a specified time period.

Synthesis and analysis of aminochromes

The oxidation of the catecholamines adrenaline, noradrenaline, dopa, dopamine and isoproterenol to their respective aminochromes adrenochrome, noradrenochrome, dopachrome, dopaminochrome and isoprenochrome was performed using a nonenzymatic system. Each catecholamine (1 mM) was oxidized to the respective aminochrome by $NaIO_4$ (2 mM) in aqueous ammonium acetate buffer (100 μM; corrected to pH 5.8 with hydrochloric acid). The reactions were conducted at room temperature with vigorous shaking for 1 min. Samples were immediately injected into the HPLC system. Chromatograms were analysed at 490 nm. The complete oxidation of catecholamines was confirmed through the spectrometry at 279 nm. The UV spectrum of each aminochrome was also checked in each chromatogram. The aminochrome fractions were collected and their structures were confirmed by mass spectrometry through their MS/MS fragmentation pattern (Lemos-Amado *et al.*, 2001).

Adrenochrome evaluation in rat blood

Adrenochrome (32 mg kg^{-1}) was administered (i.p.) to adult male Wistar rats, weighing 300–350 g. After ethyl-ether anesthesia, heparinized blood samples were collected from vena cava at 5, 15 and 25 min after adrenochrome administration.

In order to perform HPLC analysis of the blood, 100 μL of heparinized blood were added to 100 μL of perchloric acid (10%) and centrifuged for 15 s at 16000*g*. The supernatant (100 μL) was immediately neutralized with $KHCO_3$ 0.76 M (75 μL) and centrifuged for 15 s at 16000*g*. The supernatant (100 μL) was injected into the HPLC system and adrenochrome was detected and quantified at 490 nm.

Standard curves of adrenochrome were obtained by HPLC analysis of 0.75, 1.5, 3.0, 6.0 and 12 μM of adrenochrome standard. The linearity was verified for the studied concentrations and correlation coefficients were higher than 0.999.

Mass spectrometry

Electrospray ionization (ESI-MS) and tandem mass spectra (ESI-MS/MS) were acquired with a Q-TOF 2 mass spectrometer (Micromass, Manchester). The instrument resolution was set at 9500 (50% peak valley). The capillary needle voltage was 3000 V and the source temperature was maintained at 150°C. Nitrogen was used as the nebulizer gas and argon was used as the collision gas. Cone voltage was set at 30 V for ESI-MS and ESI-MS/MS. Collision-induced dissociation spectra were acquired by selecting the desired ion with the quadrupole section of the mass spectrometer and colliding it in the collision cell with argon gas (measured pressure in the penning gage $\sim 6 \times 10^{-5}$) using a collision energy of 20–25 eV. The TOF analyser identified the resulting product

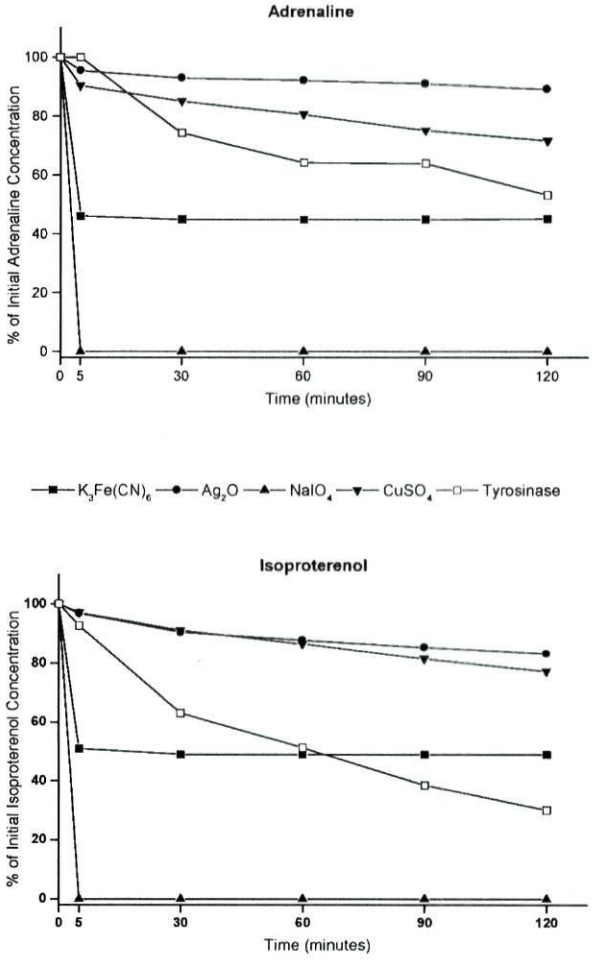

Figure 2. Adrenaline and isoproterenol oxidation profile using different enzymatic (tyrosinase) and nonenzymatic [Ag_2O, $CuSO_4$, $NaIO_4$ and $K_3Fe(CN)_6$] systems.

Copyright © 2002 John Wiley & Sons, Ltd.

ions. HPLC-ESI-MS and HPLC-ESI-MS/MS were performed using the same general MS conditions, increasing the desolvation temperature to 400°C. Data acquisition was carried out with a Micromass MassLynkx 3.4 data system.

The HPLC was connected to the Q-TOF with a home-made splitter, using the optimized conditions, and the flow adjusted to 100 μL min^{-1}.

RESULTS AND DISCUSSION

Figure 2 shows the oxidation profile of a biological (adrenaline) and a synthetic (isoproterenol) catecholamine obtained with different non-enzymatic and enzymatic systems. For the same concentration of the inorganic oxidant it was found that $NaIO_4$ completely oxidized both catecholamines in 5 min. With the other agents, either of nonenzymatic or enzymatic origin, the rate of the reactions was slower and incomplete.

All catecholamines were then oxidized with $NaIO_4$, which was found to be the fastest and most efficient oxidant of catecholamines (Fig. 2). An HPLC-DAD methodology was developed in order to analyze and quantify all the catecholamines and respective aminochromes under study (Fig. 3). The maximum absorption wavelength for the catecholamines is 279 nm and for the aminochromes 220, 305 and 490 nm. The limit of detection for adrenaline, in aqueous ammonium acetate

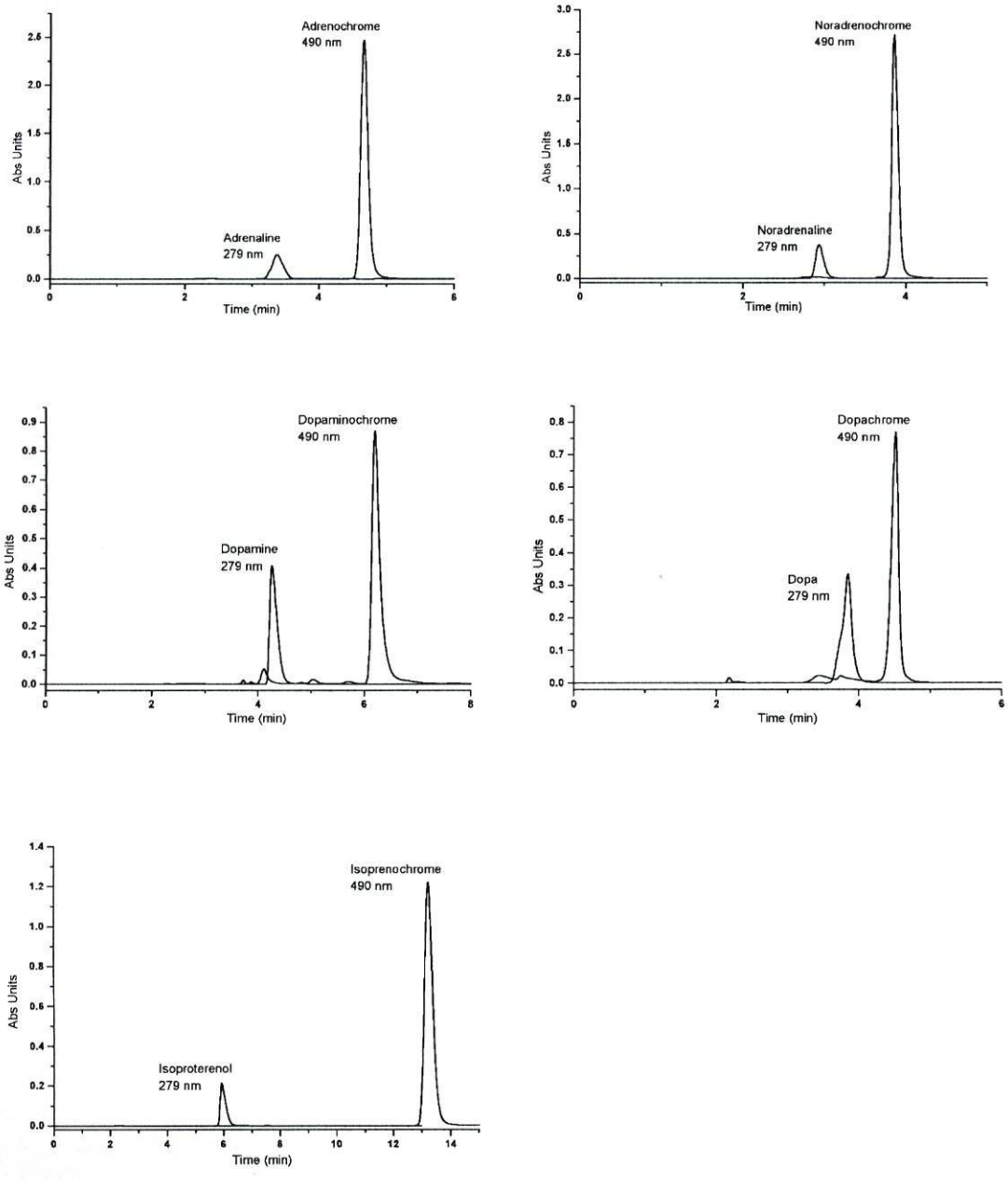

Figure 3. Chromatograms of the catecholamines (1 mM) and respective aminochromes.

Copyright © 2002 John Wiley & Sons, Ltd.

buffer, was 1.6 pmol (in column) at 279 nm. The limit of detection for adrenochrome, in aqueous ammonium acetate buffer, was 0.1, 0.5 and 10 pmol (in column) at 220, 305 and 490 nm, respectively. It is noteworthy that the detection at 220 nm led to a higher sensitivity of the adrenochrome analysis. However, an improvement in specificity is found at 305 or 490 nm for this compound. Because aminochromes are in general not chemically stable and standards are not available, it was necessary to characterize the peaks obtained on the chromatograms. In the UV analysis, the UV spectra of all the aminochromes were similar to the spectrum of adrenochrome standard. Additionally, the aminochromes were characterised using tandem mass spectrometry in collected fractions from HPLC system, by applying a general fragmentation pattern characteristic of this class of compounds (Lemos-Amado *et al.*, 2001).

The analytical methodology developed was applied to evaluate aminochromes in blood. It is noteworthy that a stepwise preparation of the sample was essential to perform this qualitative and quantitative analysis. Different processes were assayed in order to remove proteins, such as protein precipitation by perchloric acid, acetonitrile and methanol, and protein withdrawal by Ultrafree-MC® centrifugal filter devices. It was found that aminochromes, such as adrenochrome, are extremely unstable in acidic medium, being rapidly transformed by perchloric acid (5%) to a colourless compound (probably a leukoderivative). The use of acetonitrile (2:1) for protein precipitation also destroyed the adrenochrome and with methanol (2:1) the results were not reproducible. However, the addition of perchloric acid (5%, final concentration) to adrenochrome and isoprenochrome aqueous solutions (0.1 mM) followed by a rapid (less than 1 min) neutralization to pH 6–7 with $KHCO_3$ (0.33 M) allowed recoveries of 103.5 ± 1.3 and $105.5 \pm 3.1\%$ ($n = 4$), respectively. After neutralization, aminochromes were stable during several minutes. Interestingly, a similar procedure was previously described for sample preparation in adrenochrome evaluation in suspensions of rat polymorphonuclear leucocytes (Matthews *et al.*, 1985), but it was reported not to be applicable for the measurement of adrenochrome in plasma (Dhalla *et al.*, 1989). However, in our studies, spiking serum with adrenochrome (25 μM), followed by perchloric acid addition, sample centrifugation and neutralization, allowed adrenochrome recoveries of $102.6 \pm 1.7\%$ ($n = 5$). The same treatment was performed in whole blood and adrenochrome recovery was $107.3 \pm 2.5\%$ ($n = 3$). Unfortunately, it was found that adrenochrome is rapidly destroyed in the neutralized supernatant from blood samples. Thus, the sample injection into the HPLC system must be done immediately after its preparation.

It was also tried to use Ultrafree-MC® centrifugal filter devices for protein removal. However, this led to very low levels of adrenochrome recovery (data not shown). This can be explained by the fact that in biological samples aminochromes are bound in the tissues (Fliegel *et al.*, 1985), especially to the thiol groups of proteins (Bindoli *et al.*, 1992). The good recovery levels of adrenochrome in biological samples treated with perchloric acid could indicate that this acid destroys aminochrome–protein adducts.

Catecholamines can be also analyzed in biological samples after protein precipitation in acidic medium (Lakshmana and Raju, 1997; Remião *et al.*, 2001). The neutralization of acidic samples, immediately followed by HPLC injection, did not interfere with the catecholamines levels in samples (data not shown). Thus, the described procedure enables the simultaneous analysis of each catecholamine and respective aminochrome in biological samples.

In order to apply this procedure to evaluate adrenochrome in biological samples, adrenochrome was administered (i.p.) to rats in a dose of 32 mg kg^{-1}. Blood samples were collected after 5, 15 and 25 min and treated

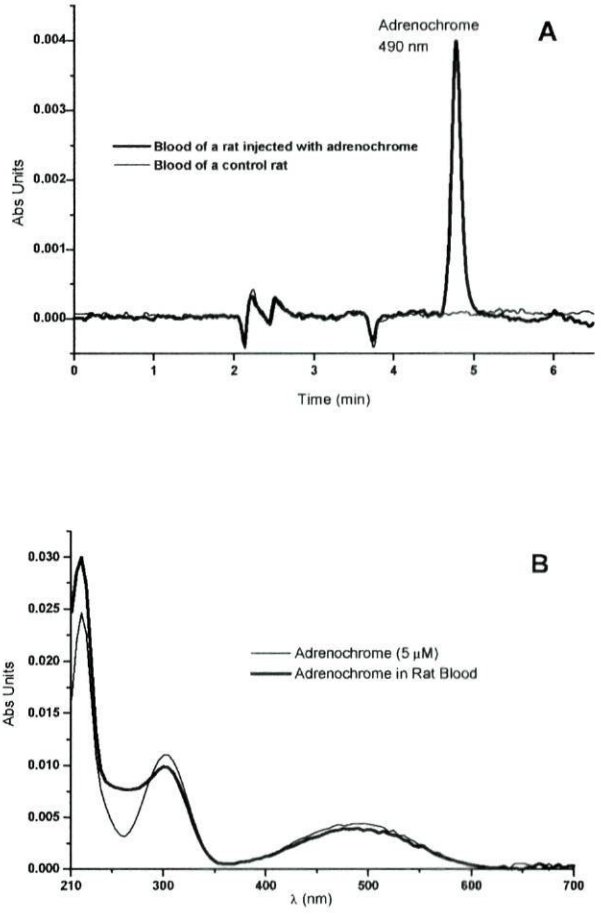

Figure 4. (A) Chromatograms of blood samples from control rats and treated rats (32 mg kg^{-1} of adrenochrome), obtained at 490 nm. (B) UV spectra of adrenochrome standard and adrenochrome in rat blood.

Copyright © 2002 John Wiley & Sons, Ltd.

as described above. This dose of adrenochrome was already used in a previous *in vivo* study to evaluate adrenochrome cardiotoxicity in rats (Singal *et al.*, 1982). Doses higher than 40 mg kg^{-1} cause the death of the rats (Beamish *et al.*, 1981).

Figure 4(A) shows the chromatograms of blood samples from control rats and treated rats, obtained at 490 nm. The characterization of adrenochrome found in blood was performed by UV and tandem mass spectrometry. The comparative analysis of the UV spectra of adrenochrome detected in the rat blood and of the adrenochrome standard (5 μM) shows that they have a very similar profile [Fig. 4(B)]. However, a higher absorbance was observed at 258 nm in the spectrum of the adrenochrome present in rat blood, which results from an interference present in all studied samples from rat blood. The UV spectrum of this interference showed no absorbance either at 305 or 490 nm, thus it did not interfere in adrenochrome quantification.

The characterization of the adrenochrome was also performed by HPLC-ESI-MS and by HPLC-ESI-MS/MS. The adrenochrome was identified on HPLC-ESI-MS chromatogram of the treated sample of rat blood by comparing the retention time and by using the molecular weight of the protonated molecule, *m/z* 180 [Fig. 5(A) and (B)]. The sensitivity achieved with MS was similar to that found using the DAD detector. Further identification was done by performing HPLC-ESI-MS/MS of the ion at *m/z* 180 and by comparison with the spectra of the standard acquired in the same experimental conditions, as can be seen on Fig. 6 (A and B), following the general fragmentation pattern of these compounds (Lemos-Amado *et al.*, 2001).

The results of adrenochrome quantification in whole blood after its administration to rats are presented in Fig. 7. The determinations were performed in whole blood because aminochromes have the capacity to bind to proteins and, therefore, the rejection of blood elements could result in adrenochrome loss. After 5, 15 and 25 min of adrenochrome administration the concentration of adrenochrome in blood was 16.4 ± 2.9, 6.0 ± 1.6 and 2.4 ± 1.6 μM (Mean ± SD, $n = 5$), respectively (Fig. 7). These results show a rapid decrease of adrenochrome concentration in blood, which is in accordance with the *in vivo* toxic effects reported by Singal *et al.* (1982). In that study, adrenochrome, after i.v. injection, rapidly induced ultrastructural and cardiovascular changes (in 5–10 min), which decreased in severity after this time (Singal *et al.*, 1982). The main effects reported included swelling of mitochondria and sarcotubular system, intracellular and perinuclear oedema, hypercontraction of myofibrils, partial separation of the intercalated disk and depression of heart rate and blood pressure. The results are also in accordance with previous studies, which report the fast adrenolutin appearance in blood and urine of rats (Dhalla *et al.*, 1989), as well as in tissues and blood of rabbits

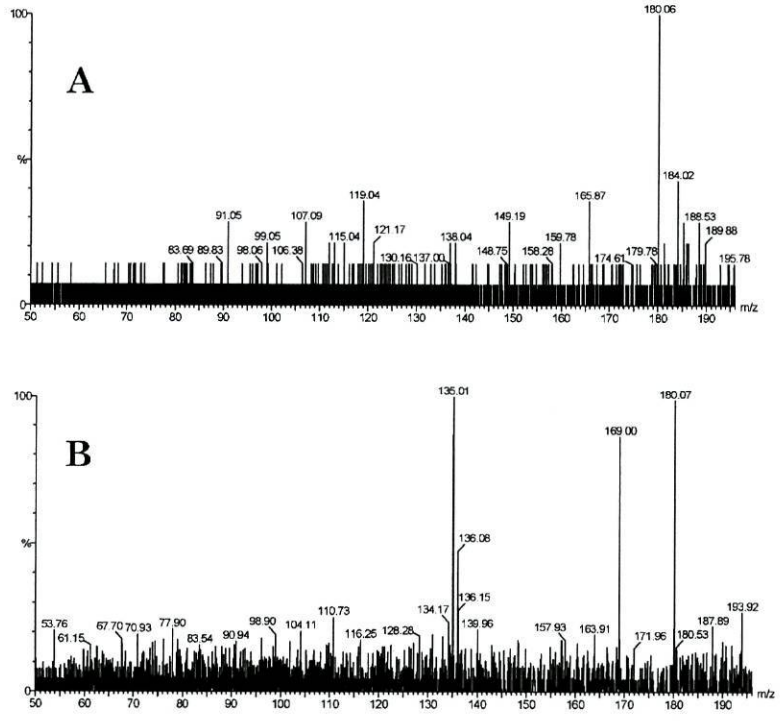

Figure 5. HPLC-ESI-MS spectrum of: (A) adrenochrome standard solution (5 μM); (B) rat blood sample.

Copyright © 2002 John Wiley & Sons, Ltd.

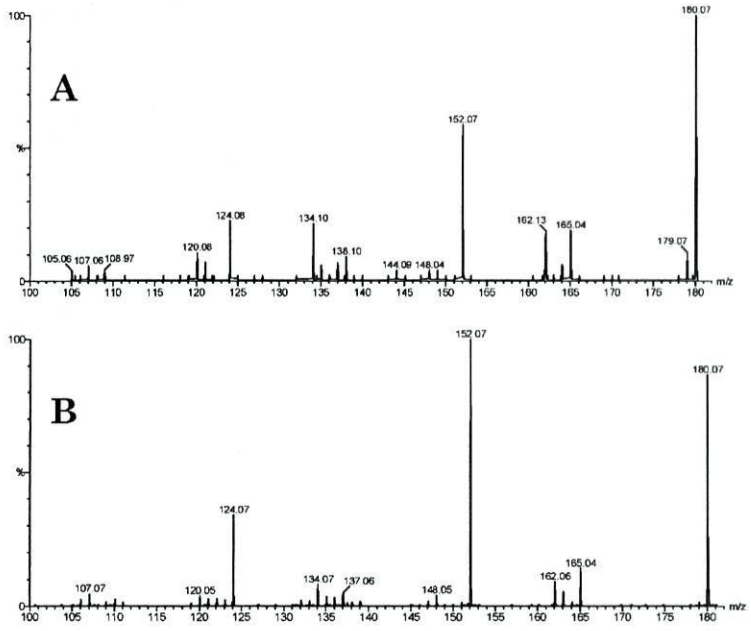

Figure 6. HPLC-ESI-MS/MS spectrum of the protonated molecule of m/z 180 obtained from: (A) adrenochrome standard solution (5 μM); (B) rat blood sample.

(Fischer and Landtsheer, 1950), after administration of adrenochrome. A similar work reported the rapid appearance of sulfate conjugates of adrenolutin and of 5,6-dihydroxy-*N*-methylindole (DHMI) in urine of rats after adrenochrome administration (Noval *et al.*, 1962). Adrenochrome can also be incorporated in tissues, such as myocardium, where it binds in an irreversible way (Fliegel *et al.*, 1985). Thus, it seems that adrenochrome rapidly disappears from blood by tissue uptake or by rearrangement and metabolism to adrenolutin and DHMI. Adrenolutin has been measured in mammalian plasma, which is an evidence for the adrenochrome formation in the evaluated tissues (Dhalla *et al.*, 2001). However, the toxic effects induced by catecholamines oxidation processes are mainly related to aminochromes. Adrenochrome and isoproterenol oxidation products have been reported to induce cell damage, contractile failure and impairment of mitochondrial energy production in perfused rat heart (Dhalla *et al.*, 2001). Adrenochrome and oxidised adrenaline solutions were reported to inhibit monoamine oxidase (Dhalla *et al.*, 2001), alkaline phosphatase (Dhalla *et al.*, 2001) and adenylyl cyclase (Ebina *et al.*, 1997) in a variety of tissues. Dopa, dopamine and isoproterenol oxidation products were also reported to inhibit *in vitro* creatine kinase and glutathione reductase (Miura *et al.*, 1999; Remião *et al.*, 1999). Thus, the development of this methodology allows a direct quantification of adrenochrome in blood or tissues and the correlation of its level with the observed toxic effects.

CONCLUSION

In all studied catalytic systems, $NaIO_4$ was found to be the most efficient oxidant of catecholamines. An isocratic reverse-phase HPLC-DAD methodology was developed in order to separate and quantify catecholamines and their respective aminochromes in blood. A sample treatment procedure for aminochrome evaluation in biological samples was also developed and applied to the detection of adrenochrome in rat blood. All the chromatographic data was validated by UV and tandem mass spectrometry.

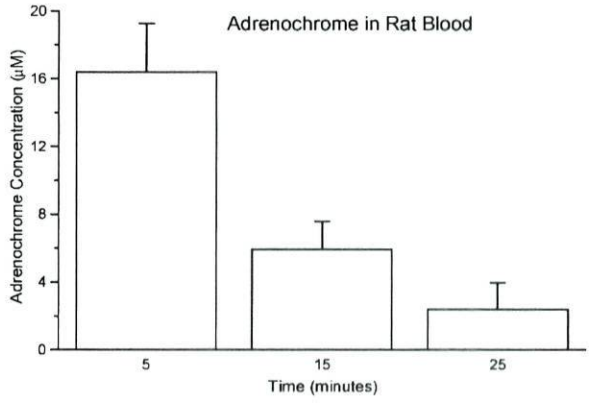

Figure 7. Concentration of adrenochrome (mean ± SD, $n = 5$) in rat blood at 5, 15 and 25 min after administration of 32 mg kg^{-1} of adrenochrome (i.p.).

Copyright © 2002 John Wiley & Sons, Ltd.

In the *in vivo* study, the adrenochrome concentration in rat blood rapidly decreases after its administration.

Acknowledgements

This work was supported by a project from FCT and POCTI, Portugal, by FEDER European Community funding (project POCTI/36099/FCB/2000) and by project PRAXIS XXI/BD/18520/98.

REFERENCES

Beamish RE, Dhillon KS, Singal PK and Dhalla NS. Protective effect of sulfinpyrazone against catecholamine metabolite adrenochrome-induced arrhythmias. *American Heart Journal* 1981; **102**: 149.

Behonick GS, Novak MJ, Nealley EW and Baskin SI. Toxicology update: the cardiotoxicity of the oxidative stress metabolites of catecholamines (aminochromes). *Journal of Applied Toxicology* 2001; **21**: S15.

Bindoli A, Rigobello MP and Galzigna L. Toxicity of aminochromes. *Toxicology Letters* 1989; **48**: 3.

Bindoli A, Rigobello MP and Deeble DJ. Biochemical and toxicological properties of the oxidation products of catecholamines. *Free Radical Biology and Medicine* 1992; **13**: 391.

Dhalla KS, Ganguly PK, Rupp H, Beamish RE and Dhalla NS. Measurement of adrenolutin as an oxidation product of catecholamines in plasma. *Molecular and Cellular Biochemistry* 1989; **87**: 85.

Dhalla KS, Rupp H, Beamish RE and Dhalla NS. Mechanisms of alterations in cardiac membrane Ca^{2+} transport due to excess catecholamines. *Cardiovascular Drugs and Therapy* 1996; **10**: 231.

Dhalla NS, Sasaki H, Mochizuki S, Dhalla KS, Liu X and Elimban V. Catecholamine-induced cardiomyopathy. In Cardiovascular Toxicity, Acosta D (ed.). Raven Press: New York, 2001; 269.

Ebina T, Toya Y, Oka N, Schwencke C, Kawabe J-i and Ishikawa Y. Isoform-specific regulation of adenylyl cyclase by oxidized catecholamines. *Journal of Molecular and Cellular Cardiology* 1997; **29**: 1247.

Fischer P and Landtsheer L. Métabolisme de l'adrénochrome et du trihydroxyméthylindole chez le lapin. *Experimentia* 1950; **6**: 305.

Fliegel L, Takeo S, Beamish RE and Dhalla NS. Adrenochrome uptake and subcellular distribution in the isolated perfused rat heart. *Canadian Journal of Cardiology* 1985; **1**: 122.

Foppoli C, Coccia R, Cini C and Rosei MA. Catecholamines oxidation by xanthine oxidase. *Biochimica et Biophysica Acta* 1997; **1334**: 200.

Giulivi C and Cadenas E. Oxidation of adrenaline by ferrylmyoglobin. *Free Radical Biology and Medicine* 1998; **25**: 175.

Heacock RA. The chemistry of adrenochrome and related compounds. *Chemical Review* 1959; **59**: 181.

Keller JN, Huang FF, Dimayuga ER and Maragos WF. Dopamine induces proteasome inhibition in neural PC12 cell line. *Free Radical Biology and Medicine* 2000; **29**: 1037.

Lakshmana MK and Raju TR. An isocratic assay for norepinephrine, dopamine and 5-hydroxytrypyamine using their native fluorescent by high-performance liquid chromatography with fluorescence detection in discrete brain areas of rat. *Analytical Biochemistry* 1997; **246**: 166.

Lemos-Amado F, Domingues P, Ferrer-Correia A, Remião F, Milhazes N, Borges F, Carvalho FD and Bastos ML. Electrospray tandem mass spectrometry of aminochromes. *Rapid Communications in Mass Spectrometry* 2001; **15**: 2466.

Martinez-Alvarado P, Dagnino-Subiabre A, Paris I, Metodiewa D, Welch CJ, Olea-Azar C, Ceviedes P, Ceviedes R and Segura-Aguilar J. Possible role of slasolinol quinone methide in the decrease of RCSN-3 cell survival. *Biochemical and Biophysical Research Communications* 2001; **283**: 1069.

Matthews SB, Henderson AH and Campbell AK. The adrenochrome pathway: the major route for adrenalin catabolism by polymorphonuclear leucocytes. *Journal of Molecular and Cellular Cardiology* 1985; **17**: 339.

Miura T, Muraoka S and Fugimoto Y. Inactivation of creatine kinase induced by dopa and dopamine in the presence of ferrylmyoglobin. *Chemical-Biological Interactions* 1999; **123**: 51.

Noval JJ, Sohler A, Stackhouse SP and Bryan AC. Metabolism of adrenochrome in experimental animals. *Biochemical Pharmacology* 1962; **1**: 467.

Núñez-Delicado E, Pérez-Gilabert M, Sánchez-Ferrer A and García-Carmona F. Hydroperoxidase activity of lipoxygenase: a kinetic study of isoproterenol oxidation. *Biochimica et Biophysica Acta* 1996; **1293**: 17.

Ramos K and Acosta D. Cytotoxic actions of isoproterenol in cardiac cells: protective effects of antioxidants. In CRC Handbook of Free Radicals and Antioxidants in Biomedicine, Vol. 2, Miquel J, Quintanilha AT and Weber H (eds). CRC Press: Boca Raton, PL. 1989; 177.

Remião F, Carmo H, Carvalho F and Bastos ML. Inhibition of glutathione reductase by isoproterenol oxidation products. *Journal of Enzyme Inhibition* 1999; **15**: 47.

Remião F, Carmo H, Carvalho F and Bastos ML. Copper enhances isoproterenol toxicity in isolated rat cardiomyocytes: effects on oxidative stress. *Cardiovascular Toxicology* 2001; **1**: 195.

Riobó NA, Schopfer FJ, Boveris AD, Cadenas E and Poderoso JJ. The reaction of nitric oxide with 6-hydroxydopamine: implications for Parkinson's disease. *Free Radical Biology and Medicine* 2002; **32**: 115.

Rona G, Chappel CI, Balazs T and Gaudry R. An infarct-like myocardial lesion and other toxic manifestations produced by isoproterenol in the rat. *Archives of Pathology* 1959; **67**: 443.

Rupp H, Dhalla KS and Dhalla NS. Mechanisms of cardiac cell damage due to catecholamines: significance of drugs regulating central sympathetic outflow. *Journal of Cardiovascular Pharmacology* 1994; **24** (Suppl. 1): S16.

Singal PK, Dhillon KS, Beamish RE, Kapur N and Dhalla NS. Myocardial cell damage and cardiovascular changes due to I.V. infusion of adrenochrome in rats. *British Journal of Experimental Pathology* 1982; **63**: 167.

Smythies J and Galzigna L. The oxidative metabolism of catecholamines in the brain: a review. *Biochimica et Biophysica Acta* 1998; **1380**: 159.

Tappia PS, Hata T, Hozaima L, Sandhu MS, Panagia V and Dhalla NS. Role of oxidative stress in catecholamine-induced changes in cardiac sarcolemmal Ca^{2+} transport. *Archives of Biochemistry and Biophysics* 2001; **387**: 85.

Copyright © 2002 John Wiley & Sons, Ltd.

8.5 Caracterização electroquímica e espectroscópica de drogas do tipo anfetamínico: aplicação à detecção da 3,4-metilenodioximetanfetamina (MDMA) e dos seus precursores sintéticos.

Electrochemical and spectroscopic characterisation of amphetamine-like drugs: Application to the screening of 3,4-methylenedioxymethamphetamine (MDMA) and its synthetic precursors

Nuno Milhazes[a,b,c], Pedro Martins[d], Eugenio Uriarte[d], Jorge Garrido[e,f], Rita Calheiros,[e,f] M. Paula M. Marques[e,g] and Fernanda Borges[b,e,*]

[a] *CEQOFFUP/* [b] *Departamento de Química Orgânica, Faculdade de Farmácia, Universidade do Porto, Portugal*

[c] *Instituto Superior de Ciências da Saúde - Norte, Gandra, Paredes, Portugal*

[d] *Departamento de Química Orgánica, Facultade de Farmacia, Universidad de Santiago de Compostela, España*

[e] *Unidade I&D "Química-Física Molecular";* [f] *Departamento de Engenharia Química, ISEP, Instituto Politécnico do Porto, Portugal;* [g] *Departamento de Bioquímica, Faculdade de Ciências e Tecnologia, Universidade de Coimbra, Portugal*

* To whom correspondence should be addressed: Departamento de Química Orgânica, Faculdade de Farmácia, Universidade do Porto, 4050-047 Porto, Portugal. Tel: +351222078900. Fax: +351222003977. E-mail: fborges@ff.up.pt

Abstract

A complete physicochemical characterisation of MDMA and its synthetic precursors MDA, 3,4-methylenedioxybenzaldehyde (piperonal) and 3,4-methylenedioxy-β-methyl-β-nitrostyrene was carried out through voltammetric assays and Raman spectroscopy combined to theoretical (DFT) calculations. The former allowed to obtain important analytical redox data, concluding that the oxidative mechanism of the *N*-demethylation of MDMA involves the removal of an electron from the amino-nitrogen atom, leading to the formation of a primary amine and an aldehyde. The vibrational spectroscopic experiments enable to afford a rapid and reliable detection of this type of compounds, since they yield characteristic spectral patterns that lead to an unequivocal identification.

Moreover, the rational synthesis of the drug of abuse 3,4-methylenedioxymethamphetamine (MDMA or "ecstasy") from one of its most relevant precursors 3,4-methylene-dioxyamphetamine (MDA), is reported. In addition, several approaches for the *N*-methylation of MDA, a limiting synthetic step, were attempted and the overall yields compared.

Keywords

MDMA; Raman spectroscopy; Redox potentials; DFT calculations; Synthesis

Introduction

The amphetamine analogues 3,4-methylenedioxymethamphetamine (MDMA, "ecstasy") and 3,4-methylenedioxyamphetamine (MDA) are popular recreational drugs mainly due to their stimulant effects on the central nervous system and increased sense of well-being [1-4]. These compounds are ring-substituted phenethylamines, structurally related to both psychomotor stimulant amphetamines and the hallucinogen mescaline. MDMA is nowadays a commonly misused drug, thus giving rise to a serious public health problem repeatedly associated with serotoninergic neurotoxicity [4-6].

All methylenedioxy-containing amphetamines became very popular after modification of the MDA structure in clandestine laboratories, by replacement of one or two hydrogens in the nitrogen atom by alkyl groups, yielding several distinct compounds with high potential for abuse. In fact, the simple addition of a *N*-methyl group is responsible for a decrease in the temporal course of action of the drug to less than half, as well as for a reduction (or even a disappearance) of the hallucinogenic effects associated to MDA [1].

MDA, besides other compounds, is frequently described as an impurity in the MDMA synthetic process. It is also produced metabolically by *N*-demethylation of MDMA, hence becoming its major metabolite in a short time after ingestion. This biotransformation step is thought to proceed through a carbinolamine intermediate, formed by cytochrome P-450 mediated oxidation of the α-carbon to the *N*-methyl group, or through *N*-oxidation followed by rearrangement to a primary amine [7,8]. Accordingly, the knowledge of conceptual biotransformation, in which oxidation reactions play a major role [9], is absolutely critical to understand the toxicity of this kind of compounds.

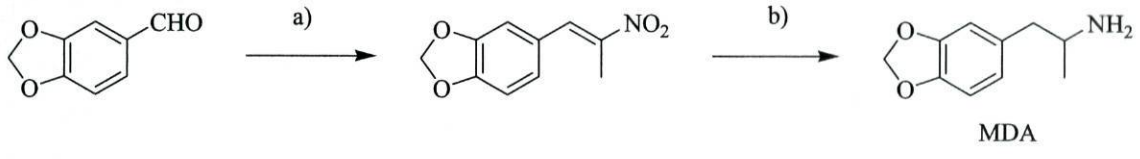

Fig. 1 General procedure for the synthesis of MDA. Chemical conditions: a) $EtNO_2$, NH_4CH_3COO, reflux; b) $LiAlH_4$, THF, reflux.

The present work reports the total synthesis of MDA and MDMA. Firstly, the preparation of MDA was based on a well-known synthetic procedure, often described in

the literature as one of the main routes for the manufacture of amphetamines [10-12], that relies upon the synthesis of the appropriate β-methyl-β-nitrostyrene precursor (Fig. 1). Secondly, several different pathways for *N*-methylation of MDA were investigated (Fig. 2), since this step is known to be limiting.

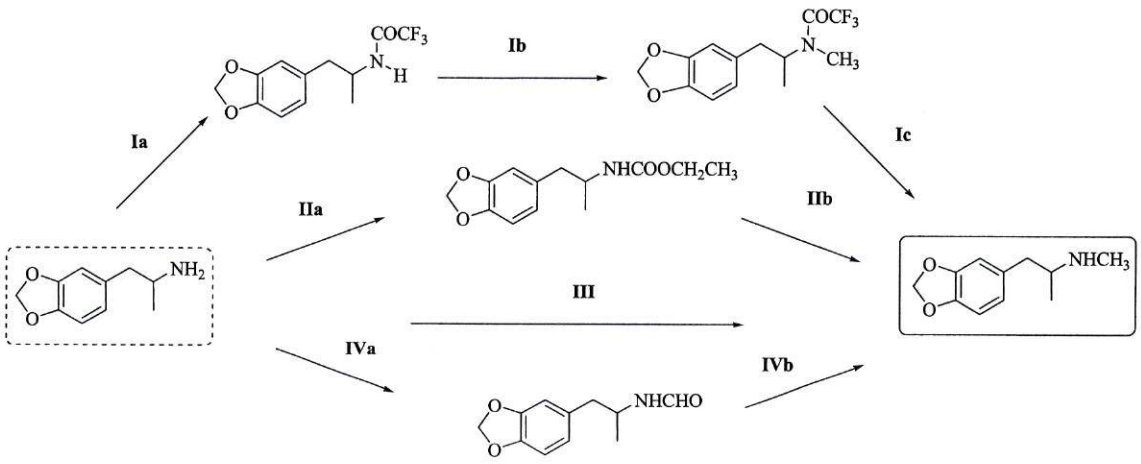

Fig. 2 Strategies used for the synthesis of MDMA using MDA as starting material. Method **I** - **Ia**: $O(COCF_3)_2$, Pyr, CH_2Cl_2; 0 °C, 2 h. **Ib**: NaH, CH_3I, DMF; 20 °C, 10 h. **Ic**: Cs_2CO_3, MeOH, H_2O; Δ, 2 h (overall yield: 41.6%). Method **II** - **IIa**: $ClCOOC_2H_5$, NaOH, H_2O; 0 °C, 1.5 h. **IIb**: $LiALH_4$, THF; Δ, 13 h (overall yield: 51.7%). Method **III**: HCHO, $NaBH_3CN$, MeOH, AcOH; rt, 3 h (overall yield: 33.3%). Method **IV** - **IVa**: $HCOOC_2H_5$; Δ, N_2, 6 h. **IVb**: $LiAlH_4$, THF; Δ, N_2, 4 h (overall yield: 37.1%).

The oxidative electroactivity of MDMA and its synthetic precursors MDA, 3,4-methylenedioxybenzaldehyde (piperonal) and 3,4-methylenedioxy-β-methyl-β-nitrostyrene (Fig. 1) was studied using voltammetric techniques. Besides the putative analytical interest, the results thus gathered can hopefully help to clarify the hypothetical *in vivo* *N*-demethylation oxidation process. Actually, MDMA metabolism is known to comprise one or more oxidative pathways [13].

Furthermore, a conformational characterisation of MDMA and MDA was carried out through Raman spectroscopic experiments combined to quantum mechanical (DFT) calculations. Although there are some reported studies on the Raman analysis of amphetamine-like compounds [14-21], these experiments have only focused on particular regions of the vibrational spectra.

Experimental

Chemicals

Ethyl formate, lithium aluminum hydride (1 M solution in THF), pyridine, trifluoroacetic anhydride, formaldehyde (37% solution in water), sodium cyanoborohydride, sodium hydride (60% dispersion in mineral oil), methyl iodide, ethyl chloroformate, cesium carbonate and all the dry solvents were purchased from Sigma-Aldrich Química S.A. (Sintra, Portugal). All other reagents and solvents (*pro analysis* grade) were acquired from Merck (Lisbon, Portugal). All reagents were used without further purification. Deionised water (conductivity < 0.1 μS cm^{-1}) was used in all experiments.

Synthesis

Structural Elucidation

^{1}H and ^{13}C-NMR data were acquired, at room temperature, on a Brüker AMX 300 spectrometer operating at 300.13 and 75.47 MHz, respectively. Dimethylsulfoxide-d_6 was used as a solvent; chemical shifts being expressed in δ (ppm) values relative to tetramethylsilane (TMS) (as internal reference); coupling constants (J) are in Hz. Spectral assignments were also made from DEPT (Distortionless Enhancement by Polarization Transfer) experiments (underlined values). Electron impact mass spectra (EI-MS) were obtained on a VG AutoSpec instrument; data are reported as *m/z* (% of relative intensity for the most important fragments). Melting points were measured on a Köfler microscope (Reichert Thermovar) and are uncorrected. All the intermediates of the following syntheses were identified by mass spectroscopy and were found to be the described compounds.

Chromatographic Conditions

The analytical control was performed by thin-layer chromatography (TLC) on plates precoated with silica gel 60 F_{254} as stationary phase (0.2 mm as layer thickness) and the following mobile phases: petroleum ether/diethyl ether/ formic acid (5:5:0.1); chloroform/acetone/formic acid (8:2:0.1); chloroform/methanol/formic acid (7:3:0.1). The spots were visualised under UV detection (254 and 366 nm) and iodine vapour.

The purity of the final products (> 98% purity) was verified using a high-performance liquid chromatography (HPLC) system equipped with UV detector. HPLC-UV

chromatograms were obtained in a Jasco instrument (pumps model 880-PU and solvent mixing model 880-30, Tokyo, Japan), equipped with a Nucleosil RP-18 column (250 mm × 4.6 mm, 5 μm, Macherey-Nagel, Düren, Germany), and UV detection at 280 nm (Jasco model 875-UV). pH 3 phosphate buffer/methanol (6:1) was used as the mobile phase, in isocratic flow rate of 1.2 mL/min. The chromatographic data was processed in a Compaq computer, fitted with CSW 1.7 software (DataApex, Czech Republic).

Synthesis of MDA (3,4-methylenedioxyamphetamine)

MDA was synthesised by an adaptation of a previous described method (Fig. 1) [11]. Briefly, a Henry reaction between nitroethane and piperonal (3,4-methylenedioxybenzaldehyde) was performed through basic catalysis of ammonium acetate followed by water elimination. The resulting β-methyl-β-nitrostyrene derivative was then reduced to the corresponding phenethylamine (MDA) by lithium aluminium hydride. The obtained free base oil was used straightforward into the next syntheses.

(R,S)-3,4-Methylenedioxyamphetamine hydrochloride (MDA). ^{1}H NMR δ: 1.10 (3H, *d*, C$\underline{H}_3$), 2.60 (1H, *dd*, *J*=13.4; 8.5, C$\underline{H}_2$), 2.89 (1H, *dd*, *J*=13.4; 5.2, C$\underline{H}_2$), 3.35 (1H, *m*, C$\underline{H}$), 5.99 (2H, *s*, OC$\underline{H}_2$O), 6.62 (1H, *dd*, *J*=7.8; 1.2, H(6)), 6.74 (1H, *d*, *J*=1.2, H(2)), 6.78 (1H, *d*, *J*=7.9, H(5)), 8.08 (3H, b*s*, N$\underline{H}_3^+$); ^{13}C NMR δ: 17.6 $\underline{C}$H$_3$, 39.7 $\underline{C}$H$_2$, 48.0 $\underline{C}$H, 100.8 (O$\underline{C}$H$_2$O), 108.3, 109.5 C(2) and C(5), 122.4 C(6), 130.4 C(1), 146.0 C(3), 147.4 C(4); EI-MS *m/z* (%): 179 ($M^{+\bullet}$, 3), 162 (4), 136 (100), 105 (12), 82 (8), 77 (35), 65 (5), 58 (8); mp 186-188 °C.

Synthesis of 3,4-methylenedioxymethamphetamine (MDMA, "ecstasy")

Method I:

Ia) *N*-Trifluoroacetyl-3,4-methylenedioxyamphetamine

MDA as a free base (3.55 g, 19.8 mmol) was dissolved in dry dichloromethane (30 mL), under nitrogen, with the following addition of pyridine (2.3 mL, 28.5 mmol). The solution was ice-cooled and trifluoroacetic anhydride (3.8 mL, 27.3 mmol) was added dropwise to the reaction vessel. The mixture was allowed to reach room temperature and stirred for more 2 h. The solution was washed with water (30 mL) and the organic layer dried ($MgSO_4$) and evaporated under reduced pressure. The obtained residue (5.17 g, 18.8 mmol) was purified by column chromatography (silica gel; petroleum ether/diethyl ether (7:3)).

Ib) *N*-Trifluoroacetyl-3,4-methylenedioxymethamphetamine

N-trifluoroacetyl-3,4-methylenedioxyamphetamine (5.17 g, 18.8 mmol) was dissolved in DMF (25 mL) and a 60% dispersion in mineral oil of sodium hydride (0.80 g, 33.3 mmol) was added to the solution. The reaction was stirred during 2 h at room temperature. Then methyl iodide (1.3 mL, 20.9 mmol) was added and the mixture was stirred for further 8 h. After this time the reaction medium was transferred to a vessel containing a 0.1 M solution of acetic acid (15 mL). The product was extracted with dichloromethane (3x50 mL) and the organic phase was dried ($MgSO_4$) and evaporated under reduced pressure. The product was subsequently purified by CC to remove the mineral oil (silica gel; dichloromethane/ethyl acetate in different proportions) (3.34 g, 11.5 mmol).

Ic) 3,4-Methylenedioxymethamphetamine (MDMA)

To a solution of *N*-trifluoroacetyl-3,4-methylenedioxymethamphetamine (3.34 g, 11.5 mmol) in a mixture of methanol/water (1:1) (30 mL) cesium carbonate (8.48 g, 26.0 mmol) was added and the resulting mixture was refluxed for 1.5 h. After partial evaporation of the solvent and sequential addition of water (70 mL), the compound was extracted with ethyl acetate (2×100 mL). The solvent was dried over magnesium sulfate and evaporated. The residue was recrystallised with methanol acidified with HCl and the MDMA hydrochloride was obtained as white solid product after addition of diethyl ether (1.89 g, overall yield: 41.6%).

(R,S)-3,4-Methylenedioxymethamphetamine hydrochloride (MDMA) ^{1}H NMR δ: 1.08 (3H, *d*, $C\underline{H}_3$), 2.54 (3H, *s*, $NC\underline{H}_3$), 2.56 (1H, *dd*, *J*=13.4; 8.7, $C\underline{H}_2$), 3.04 (1H, *dd*, *J*=13.4; 4.5, $C\underline{H}_2$), 3.33 (1H, *m*, C<u>H</u>), 5.99 (2H, *s*, $OC\underline{H}_2O$), 6.70 (1H, *dd*, *J*=8.0; 1.6, H(6)), 6.86 (1H, *d*, *J*=1.6, H(2)), 6.87 (1H, *d*, *J*=7.9, H(5)), 8.78 (2H, b*s*, $N\underline{H}_2^+$); ^{13}C NMR δ: 14.8 $\underline{C}H_3$, 29.4 $N\underline{C}H_3$, 37.7 $\underline{C}H_2$, 55.1 <u>C</u>H, 100.7 $O\underline{C}H_2O$, 108.1, 109.3 C(2) and C(5), 122.2 C(6), 130.6 C(1), 146.3 C(3), 147.7 C(4); EI-MS *m/z* (%): 193 ($M^{+\bullet}$, 9), 178 (12), 163 (10), 135 (100), 105 (25), 89 (28), 83 (16), 77 (98); mp 148-150 °C.

Method II:

IIa) *N*-Carbethoxy-3,4-methylenedioxyamphetamine

MDA (0.81 g, 4.5 mmol) as a free base was dissolved in water (30 mL) at 0 °C. A solution of NaOH (0.3 g) in water (2.5 mL) was then added to the reaction with following addition of ethyl chloroformate (0.5 mL, 5.3 mmol). The suspension was stirred at 0 °C for 2 h and the reaction was then stopped by extraction with

dichloromethane (3×100 mL). The organic layer was dried (Na_2SO_4) and the solvent was evaporated to obtain the corresponding carbamate (0.95 g, 3.8 mmol).

IIb) 3,4-Methylenedioxymethamphetamine (MDMA)

The carbamate (0.95 g, 3.8 mmol) was dissolved in THF (15 mL) and this solution was slowly added to lithium aluminium hydride (12 mmol) suspended in THF (25 mL), under N_2. The reaction was stirred, heated under reflux for 10 h and then allowed to cool to room temperature. The excess of $LiAlH_4$ was decomposed and the reaction quenched by smooth addition of cold water/ice with vigorous stirring. The inorganic residue was removed by vacuum filtration; the solvent was dried over anhydrous magnesium sulphate, evaporated, the residue diluted with diethyl ether and extracted with aqueous HCl (3×100 mL of a 2 M solution). The acidic extract was alkalinised with a NaOH solution and extracted with diethyl ether (3×100 mL). The organic layer was dried over anhydrous magnesium sulphate, filtered and concentrated to yield a light coloured oil turned into a white solid of MDMA hydrochloride by the addition of ethereal HCl (0.53 g, overall yield: 51.7%).

Method III:

MDA (2.00 g, 11.7 mmol) as a free base was dissolved in methanol (50 mL) acidified with acetic acid until pH 5. Formaldehyde (1 mL of a 37% solution in water, 12.3 mmol) and sodium cyanoborohydride (0.98 g, 15.6 mmol) were then slowly added to the solution. The reaction was stirred at room temperature during 3 h. After that the solvent was evaporated and the resulting yellowish oil was dissolved in methanol, the solution was acidified with HCl and diethyl ether was added until insolubilisation. A white solid identified as MDMA hydrochloride was obtained (0.89 g, yield: 33.3%).

Method IV:

IVa) *N*-Formyl-3,4-methylenedioxyamphetamine

MDA (1.59 g, 8.9 mmol) as a free base was suspended in ethyl formate (50 mL) and the ensuing mixture was heated to reflux providing a homogeneous solution. After 6 h, the excess of ethyl formate was removed under reduced pressure, and the resulting yellow solid of the formamide (1.59 g, 7.7 mmol) was identified and used without further purification in the next reaction.

IVb) 3,4-Methylenedioxymethamphetamine (MDMA)

A solution of *N*-formyl-3,4-methylenedioxyamphetamine (1.59 g, 7.7 mmol) in anhydrous tetrahydrofuran (25 mL) was added dropwise to a stirred solution of lithium aluminium hydride (15 mmol) in anhydrous tetrahydrofuran (35 mL), while cooling

with ice-water in an inert environment (N_2). The mixture was allowed to warm up to room temperature and then refluxed for more 4 h. After cooling and decomposing the hydride excess by the caution addition of water, the precipitated inorganic salts were eliminated by filtration. The combined organic solutions were dried over sodium sulphate and concentrated to yield a yellow oil that was dissolved in methanol and acidified with an ethereal solution of HCl to obtain a almost white solid identified as MDMA (0.76 g, overall yield: 37.1%).

Electrochemical measurements

For the electrochemical measurements, 10 mM stock solutions of MDMA, MDA, 3,4-methylenedioxy-β-methyl-β-nitrosyrene and piperonal were made by dissolving an appropriate amount of compound in water or ethanol, depending on their solubility. The voltammetric working solutions were prepared, in the electrochemical cell, by diluting 100 μL of the stock solution in 10 mL of supporting electrolyte, in order to get a final concentration of 0.1 mM.

The pH 7.3 supporting electrolyte used in the voltammetric determinations was prepared by diluting 6.2 mL of 0.2 M dipotassium hydrogen phosphate and 43.8 mL of 0.2 M potassium dihydrogen phosphate to 100 mL.

Voltammetric studies were performed using an Autolab PGSTAT 12 potentiostat/galvanostat (Eco-Chemie, Netherlands) and a one-compartment glass electrochemical cell. Voltammetric curves were recorded at room temperature using a three-electrode system. A glassy carbon working electrode (GCE) (d = 2 mm), a platinum wire counter electrode and an Ag/AgCl saturated KCl reference electrode were used. A Metrohm E520 pH-meter with glass electrode was used for the pH measurements (Metrohm, Switzerland).

Quantum Mechanical Calculations

The quantum mechanical calculations – geometry optimisation and calculation of the harmonic vibrational frequencies – were performed using the GAUSSIAN 98W program [22], within the Density Functional Theory (DFT) approach in order to properly represent the electron correlation effects. The B3LYP hybrid method, which includes a mixture of HF and DFT exchange terms and the gradient-corrected correlation functional of Lee, Yang and Parr [23,24] as proposed and parameterised by Becke [25,26], was used, along with the double-zeta split valence basis set 6-31G* [27].

Molecular geometries were fully optimised by the Berny algorithm, using redundant internal coordinates [28]: the bond lengths to within *ca.* 0.1 pm and the bond angles to within *ca.* 0.1°. The final root-mean-square (rms) gradients were always less than 3×10^{-4} hartree.bohr^{-1} or hartree.radian^{-1}. No geometrical constraints were imposed on the molecules under study.

Frequency calculations were run, at the B3LYP/6-31G* level, for all the energy minima obtained for the molecules under study. In view of accounting for the anharmonicity, wavenumbers above 400 cm^{-1} were scaled using a factor of 0.9614 according to Scott and Radom [29], before comparing them with the experimental data.

Raman Spectroscopy

The Raman spectra were obtained at room temperature, on a triple monochromator Jobin-Yvon T64000 Raman system (0.640 m, *f*/7.5), with holographic gratings of 1800 grooves.mm^{-1}. The detection system was a non-intensified CCD (Charge Coupled Device). The entrance slit was set to 200 μm and the slit between the premonochromator and the spectrograph was opened to 14.0 mm. The 514.5 nm line of an Ar^+ laser (Coherent, model Innova 300) was used as the excitation radiation, providing between 10 and 50 mW at the sample position. Samples were sealed in Kimax glass capillary tubes of 0.8 mm inner diameter. Under the above-mentioned conditions, the error in wavenumbers was estimated to be within 1 cm^{-1}.

Results and discussion

Chemistry

The synthesis of MDMA from MDA is outlined in Fig. 1 and the related structural elucidation data is presented in the experimental section.

In general, amines can be *N*-alkylated through several pathways by the use of a key property of the nitrogen atom, its nucleophilicity. The alkylation methods are usually indirect, since the reaction of amines with haloalkanes is usually slow and not clean. Indeed, the *N*-methylation of a primary amine frequently results in a mixture of the secondary and the tertiary amine. Due to this difficulty four indirect alkylation processes were designed, experimented and compared (methods I-IV), aiming at an improvement of the overall yield and of the purity of the final product.

Briefly, in the first procedure (method I), a simple modification of the direct method was chosen, in which a trifluoroacetyl group is used to generate an acetamide derivative (N-$COCF_3$, N-TFA). This group is readily attached to the nitrogen atom by reaction of the primary amine with trifluoroacetic anhydride ($(CF_3CO)_2O$) in the presence of a base (triethylamine or pyridine), at low temperature [30,31]. Then, after *N*-alkylation with methyl iodide, the resulting *N*-methyltrifluoroacetamide is easily cleaved (*N*-deacylation) in basic conditions [30].

On the other hand, method II is based on the synthesis of a carbamate intermediate (NCOOR), a classic example of protecting group for amines. The most common one is the ethylcarbamate ($NCOOCH_2CH_3$), a group obtained by reaction of the amine with ethyl chloroformate in the presence of a base (Method II). This group is usually reduced by most of hydrides, like $LiAlH_4$, giving the corresponding *N*-methylamines [32].

Method III seemed an attractive approach to MDMA synthesis from MDA since it corresponds to a one-pot reaction in which MDA is treated with an aldehyde (formaldehyde) in the presence of sodium cyanoborohydride as a catalyst. In these synthetic conditions the amine group undergoes a reductive methylation [31,33].

Method IV is based on a *N*-formylation of the primary amine (MDA) with ethyl formate (HCO_2Et) providing the corresponding formamide intermediate (IVa) which after reduction with lithium aluminum hydride gave the *N*-methyl compound (MDMA) [34,35] in relative good yields.

It worth mentioning that the synthesised amines were isolated and used in the analytical assays after obtention of their hydrochloride salts. However, prior to the *N*-

methylation, the regeneration of the base from its salt form must be conducted after alkalinisation with ammonia. This step is important since the lone pair of electrons on the nitrogen was unavailable to the usual reactions involving amines (alkylation and/or oxidation).

Electrochemical Oxidation

To increase the understanding of the redox profile of the drugs, important for the advance of the knowledge of molecular toxicological mechanisms and the development of new analytical assays, the electrochemical behaviour of MDMA, MDA and their synthetic precursors 3,4-methylenedioxybenzaldehyde (piperonal) and 3,4-methylenedioxy-β-methyl-β-nitrostyrene was studied at physiological pH, at a glassy carbon working electrode (GCE) using differential pulse, cyclic and square wave voltammetry.

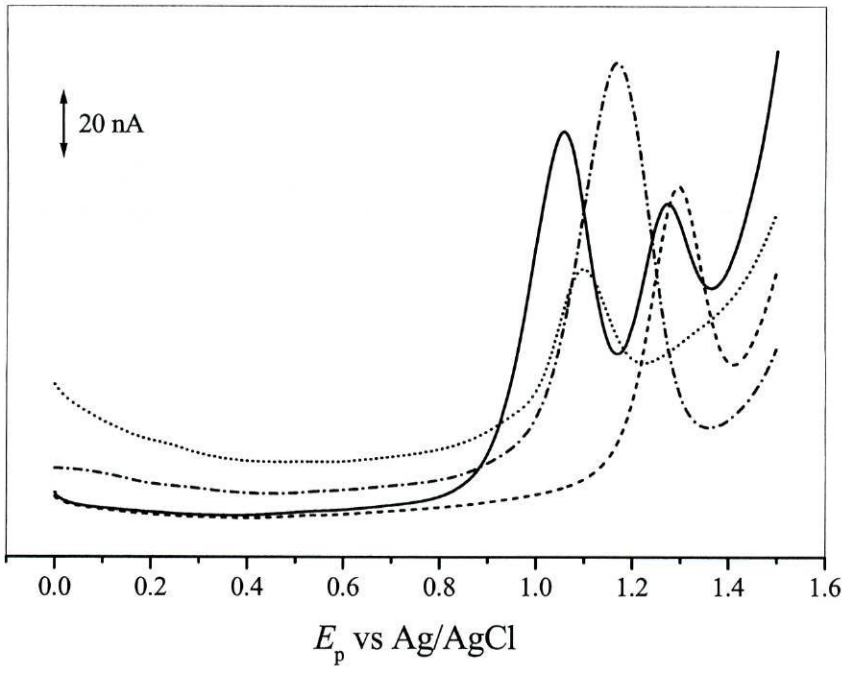

Fig. 3 Differential pulse voltammograms for 0.1 mM solutions of (—) MDMA, (·····) MDA, (----) 3,4-methylenedioxybenzaldehyde and (—·—) 3,4-methylenedioxy-β-methyl-β-nitrostyrene, in physiological pH 7.3 supporting electrolyte. Scan rate: 5 mV s^{-1}.

For MDMA, two well-defined anodic peaks can be observed at physiological pH using differential pulse voltammetry (Fig. 3). The first oxidation peak, E_p = +1.05 V, is probably due to the removal of one electron from the aromatic nucleus. The second

wave, E_p = +1.26 V, corresponds to the oxidation of the secondary amine present in the MDMA molecule. Cyclic voltammograms were also recorded at different sweep rates. Two well-defined and irreversible peaks were observed for MDMA at physiological pH (Fig. 4). These peaks correspond to the above-described waves observed by differential pulse voltammetry.

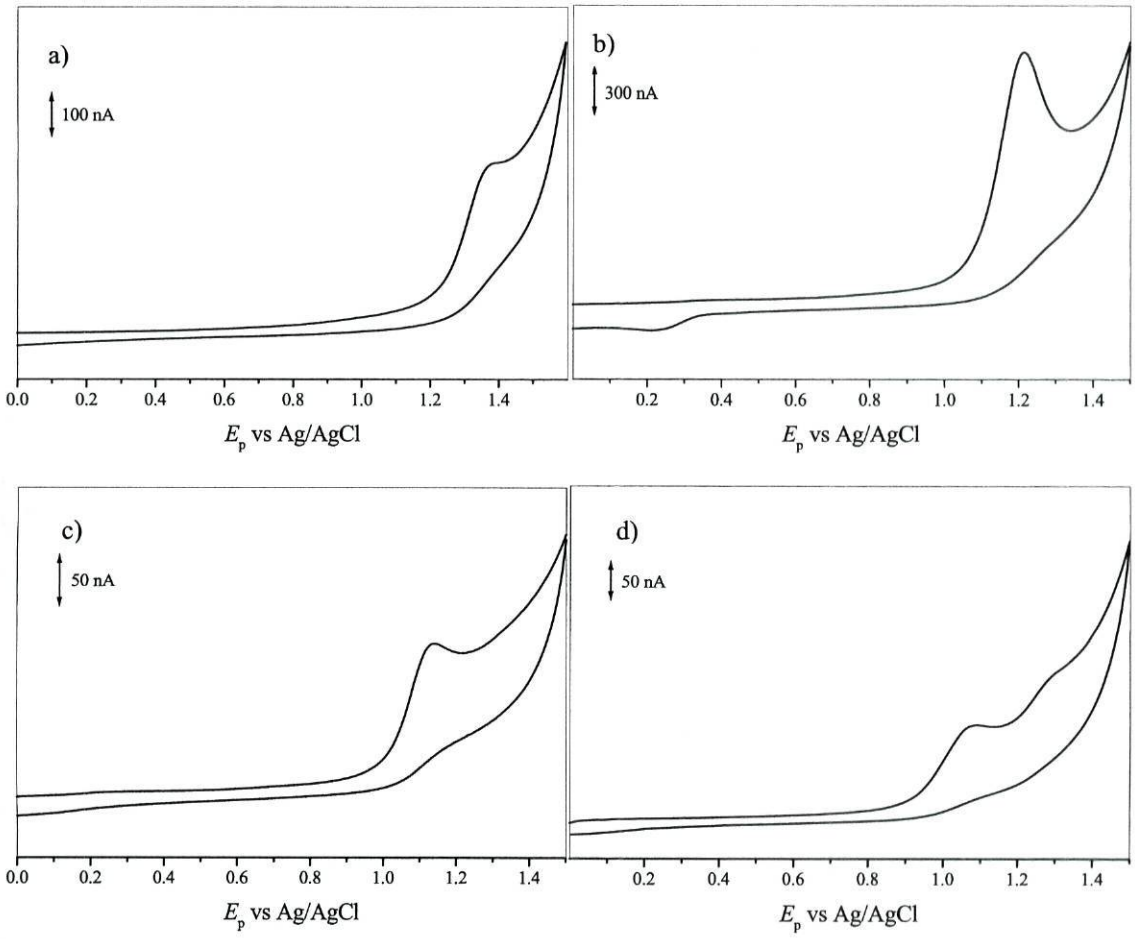

Fig. 4 Cyclic voltammograms for 0.1 mM solutions of (a) 3,4-methylenedioxybenzaldehyde, (b) 3,4-methylenedioxy-β-methyl-β-nitrostyrene (c) MDA and (d) MDMA, in physiological pH 7.3 supporting electrolyte. Scan rate: 50 mV s^{-1}.

The electrochemical study of MDMA synthetic impurities, MDA, 3,4-methylenedioxybenzaldehyde (piperonal) and 3,4-methylenedioxy-β-methyl-β-nitrostyrene enabled to reinforce the established mechanistical hypothesis that the groups involved in the oxidation of MDMA are the aromatic electrophore and the secondary amine. For these compounds, only a single and well-defined anodic oxidation wave is noticed at physiological pH (Fig. 4), that can be attributed to the removal of one electron from the aromatic nucleus. The only structural difference between MDMA and

MDA lies in the amine group, MDMA has a secondary and MDA a primary amine group. Thus, the second wave observed for MDMA could only be related with the oxidation of the secondary amine group. The appearance of a peak at this E_p value resulting from the oxidation of aliphatic secondary amines has also been described in the literature for other aliphatic amines [36,37]. Authors' previous work with compounds structurally related with MDMA, also showed the occurrence of an anodic wave that has been undoubtedly attributed to the oxidation of the secondary amine [37]. A detailed oxidative study of MDA showed that the E_p for the anodic observed wave was shifted to more negative potentials with increasing pH, corresponding to a process involving the same number of electrons and protons (data not presented). Then, a mechanism could be postulated for the oxidation of the secondary amine, which is similar to the proposal for biological transformation, involving the abstraction of an electron from the lone-pair on the nitrogen, followed by a rapid proton loss to form a neutral radical, which, after electron withdrawal, is hydrolysed to a primary amine and an aldehyde [38,39].

The first peak observed for MDMA, E_p = +1.05 V, ascribed to the oxidation of the aromatic electrophore also occurs for MDA, E_p = +1.06 V. The inexistence of other groups in the molecule capable of being oxidised could itself justify this attribution. In addition, it could be found in literature some studies involving compounds possessing similar functionalities that present a wave at similar potentials to that establish for MDMA and MDA and that were also directly related to the oxidation of the aromatic ring [40,41]. The results obtained suggest an EC mechanism with a one-electron transfer leading to the formation of a cation radical and a subsequent chemical reaction of this species. The formation of a carbocation it could be justified in this case due to the stabilizing effect of the methylenedioxy group [40].

Besides the importance of redox data for toxicological studies, in which metabolism is an important pathway, it is noteworthy its importance for analytical forensic assays in which an electrochemical detector is often used due to its sensibility and selectivity (*e.g.* HPLC).

Conformational Analysis

The geometry optimisation carried out for both MDA and MDMA ("ecstasy") hydrochlorides allowed to obtain their low energy conformers represented in Fig. 5. The corresponding theoretical vibrational spectra were yielded by the harmonic frequency

calculations (which also confirmed these geometries as real minima in the potential energy surface). In MDA and MDMA the unsaturated aliphatic ($C_7C_8N_{10}$) side chain was found to be almost perpendicular relative to the coplanar aromatic and methylenedioxy rings – ($C_2C_1C_7C_8$) equal to 73.9° for "ecstasy" and 75.4° for MDA (Table 1) – thus minimising steric repulsions between the C_8-methyl and aromatic hydrogens (H_{15} or H_{18}).

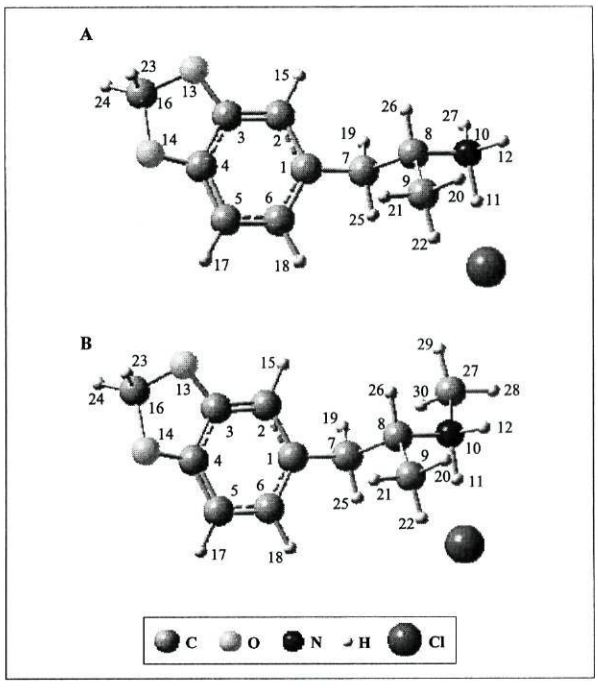

Fig. 5 Schematic representation of the most stable calculated (B3LYP/6-31G*) conformers for the hydrochloride salts of 3,4-methylenedioxyamphetamine (MDA) (A) and 3,4-methylenedioxymethamphetamine (MDMA) (B). (The atom numbering is included).

N-methylation of MDA, yielding its *N*-methyl analogue "ecstasy" (MDMA), occurs in a *trans* position relative to the methyl group in C_8 (($C_9C_8N_{10}C_{27}$)=-171.5°, Fig. 5), in order to avoid repulsion effects between the two adjacent CH_3 groups. Moreover, inclusion of the methyl group in the terminal amino moiety of the molecule is associated to a slight decrease of the ($C_1C_7C_8C_9$) dihedral – from 64.6° in MDA to 62.6° in "ecstasy" – coupled to an increase of ($C_1C_7C_8N_{10}$) – from -175.6° in MDA to -177.6° in "ecstasy" (Table 1). *N*-methylation also leads to a slight variation of the relative orientation of the C_8–C_9 bond relative to the plane of the rings – ($C_9C_8C_1C_6$)= -26.4° in MDA to -29.9° in MDMA – as well as to a reorientation of the amino group –

($C_7C_8N_{10}H_{11}$) and ($C_7C_8N_{10}H_{12}$) equal to -61.2° and 179.5° in MDA *vs* -57.0° and -170.7° in "ecstasy" (Table 1).

Table 1 Relevant calculated (B3LYP/6-31G*) geometric parameters for the most stable conformers of MDA and MDMA.

	MDA	MDMA
[a] μ (D)	8.4	8.8
bond lengths / pm		
[b] C_1-C_2	141.4	141.4
C_3-C_4	139.4	139.4
C_5-C_6	140.8	140.8
C_1-C_7	151.4	151.5
C_7-C_8	154.4	154.4
C_8-C_9	152.7	152.9
C_3-O_{13}	137.4	137.4
C_4-O_{14}	137.4	137.5
C_{16}-O_{13}	143.3	143.3
C_8-N_{10}	150.3	150.9
C_{27}-N_{10}	-	148.2
C_2-H_{15}	108.6	108.6
C_{16}-H_{23}	109.4	109.4
C_7-H_{19}	110.0	109.7
C_8-H_{26}	109.8	109.9
C_9-H_{20}	109.7	109.7
C_9-H_{21}	109.2	109.2
N_{10}-H_{11}	122.0	116.3
N_{10}-H_{12}	102.2	102.2
C_{27}-H_{28}	-	109.2
C_{27}-H_{29}	-	109.4
bond angles / degrees		
C_6-C_1-C_2	119.7	119.7
C_6-C_1-C_7	120.5	120.6
C_1-C_7-C_8	113.2	112.8
C_7-C_8-C_9	113.9	113.2
O_{13}-C_{16}-O_{14}	108.1	108.0
C_4-C_3-O_{13}	109.7	109.7
C_3-O_{13}-C_{16}	105.7	105.6
C_7-C_8-N_{10}	107.6	109.7
C_8-N_{10}-C_{27}	-	117.3
C_1-C_7-H_{19}	109.4	108.9
C_7-C_8-H_{26}	109.3	109.5
C_8-C_9-H_{20}	111.1	111.2
O_{13}-C_{16}-H_{23}	109.4	109.4
N_{10}-C_{27}-H_{28}	-	108.3
N_{10}-C_{27}-H_{29}	-	110.8
H_{20}-C_9-H_{21}	107.9	107.9
H_{23}-C_{16}-H_{24}	110.9	111.0
dihedral angles / degrees		
C_1-C_2-C_3-C_4	0.0	-0.1
C_3-C_2-C_1-C_7	-179.4	-179.8
C_2-C_1-C_7-C_8	75.4	73.9
C_1-C_7-C_8-C_9	64.6	62.6
C_1-C_7-C_8-N_{10}	-175.6	-177.6
C_7-C_8-N_{10}-C_{27}	-	65.2
C_7-C_8-N_{10}-H_{11}	-61.2	-57.0
C_7-C_8-N_{10}-H_{12}	179.5	-170.7
C_2-C_3-O_{13}-C_{16}	174.2	173.6
C_3-O_{13}-C_{16}-O_{14}	10.6	11.6

C_3-O_{13}-C_{16}-H_{23}	129.6	130.7
C_6-C_1-C_2-H_{15}	-179.1	-179.1
C_6-C_1-C_7-H_{19}	134.9	132.3
C_1-C_7-C_8-H_{26}	-58.7	-60.5
C_7-C_8-C_9-H_{20}	-177.9	-177.3
C_8-N_{10}-C_{27}-H_{28}	-	171.3

[a] $D=1/3x10^{-2}$ Cm. [b] Atoms are numbered according to Fig. 5.

Table 2 Selected experimental (solid state) and calculated (B3LYP/6-31G*) Raman wavenumbers (cm^{-1}) for the most stable conformer of "ecstasy" (MDMA).

Experimental	[a]Calculated	[b]Approximate description
	3339	ν (NH_2)
	3105	ν (C^5H)
3083	3082	ν (C^2H)
	3079	ν (C^5H) + ν (C^6H)
3060	3072	ν ($C^{27}H_3$)
3054	3044	ν ($C^{27}H_3$)
3023	3038	ν (C^9H_3)
2994	2997	ν ($C^{16}H_2$)
2981	2992	ν (C^7H_2)
1634		ν $(CC)_{ring}$
1611	1617	ν $(CC)_{ring}$
	1546	ω (NH_2)
1516	1514	t ($C^{16}H_2$)
	1512	r (NH_2)
1459	1458	r ($C^{27}H_3$) + r (C^9H_3) + t (C^7H_2)
1443	1440	r ($C^{27}H_3$) + sciss (NH_2)
1403	1395	γ ($C^{27}H_3$) + γ (C^9H_3) + sciss ($C^{16}H_2$) + r (NH_2)
1371	1367	t (C^7H_2)
1249	1243	ω (CH_2) + δ (C^8H) + t (NH_2)
1199	1204	t (CH_2) + r (NH_2)
1196	1178	r ($C^{16}H_2$)
1102	1108	ω ($C^{16}H_2$)
1094	1095	t (CH_2) + δ $(CH)_{ring}$
1081	1084	sciss ($C^{16}H_2$) + r ($C^{27}H_3$)
1040	1054	r (C^9H_3) + r ($C^{27}H_3$)
1023	1030	δ (OCO)
931	939	δ (OCO)
927	916	δ (OCO)
888	896	r (CH_3) + r (CH_2) + r (NH_2) + δ (C^5H) + δ (C^6H)

869	868	r (NH_2)
855	852	r (CH_3) + r (NH_2)
829	837	δ (C^2H)
814	810	δ (C^8H)
801	780	δ $(CH)_{ring}$
777	758	ν (C=C) + ν (CO)
725	706	ν $(CO)_{ring}$
717	690	ν (C=C)
633	617	Δ $(CCC)_{ring}$
606	594	Δ $(CCC)_{ring}$
535	522	Δ $(CCC)_{ring}$
479	481	Γ (CCC) + Γ (CCN)
449	448	Γ (COC) + Γ (CCC) + Γ (CCN)
411	416	Γ (COC) + Γ (CCC) + Γ (CCN)
381	380	Γ (COC) + Γ (CCC)
341	368	Γ (COC) + Γ (C^8NC^{27})
267	254	τ (C^9H_3)
252	241	τ (C^9H_3) + Γ (COC)
	214	τ (C^9H_3)
193	193	τ ($C^{27}H_3$)

[a]Wavenumbers above 400 cm^{-1} are scaled by a factor of 0.9614[P6]. [b]Atoms are labeled according to Fig. 5; δ – in-plane deformation; γ – out-of-plane deformation; Δ – in-plane deformation of skeleton atoms; Γ – out-of-plane deformation of skeleton atoms; ν – stretching; ν_s – symmetric stretching; ν_{as} – antisymmetric stretching; r – rocking; sciss – scissoring; t – twisting; τ – torsion; ω – wagging.

Raman Spectroscopy

The Raman spectra of MDA and MDMA are represented in Fig. 6 (from 100 to 1750 cm^{-1}), along with the spectra of their synthetic precursors 3,4-methylene-dioxybenzaldehyde (piperonal) and 3,4-methylenedioxy-*β*-methyl-*β*-nitrostyrene. The corresponding vibrational wavenumbers were assigned in the light of the theoretical results presently carried out (Table 2) and the spectroscopic data previously reported for *β*-methyl-*β*-nitrostyrene derivatives [42-45] and similar compounds [46-52].

As previously verified [42], Raman spectroscopy showed to be quite adequate for a rapid and reliable characterisation of this type of systems. In fact, the spectral patterns obtained in this work allow an unequivocal identification of the amphetamine MDA and the corresponding *N*-methyl derivative MDMA ("ecstasy") (Figs. 6 and 7). The former displays typical Raman bands at 836/861 cm^{-1} (CH_2 in-plane deformation, δ(CH_2)/CH_2

wagging, $\omega(CH_2)$), 985 - 965 cm^{-1} (NH_3 rocking, $r(NH_3)$), 1024 cm^{-1} (OCO ring deformation, $\delta(OCO)$), 1310/1319 cm^{-1} (NH_3 in-plane deformation, $\delta(NH_3)$), and 1355 cm^{-1} ($r(NH_3)$). MDMA, in turn, presents characteristic signals at 381-479 cm^{-1} (skeletal CCC, COC and CCN out-of-plane deformations, Γ(CCC/COC,CCN)), 855 cm^{-1} (NH_2 rocking, $r(NH_2)$), 888/1040/1081 cm^{-1} (rocking of the N-methyl group, $r(CH_3)$), 1199 cm^{-1} (NH_2 twisting, $t(NH_2)$), and 1443 cm^{-1} (NH_2 scissoring, $sciss(NH_2)$) (Table 2).

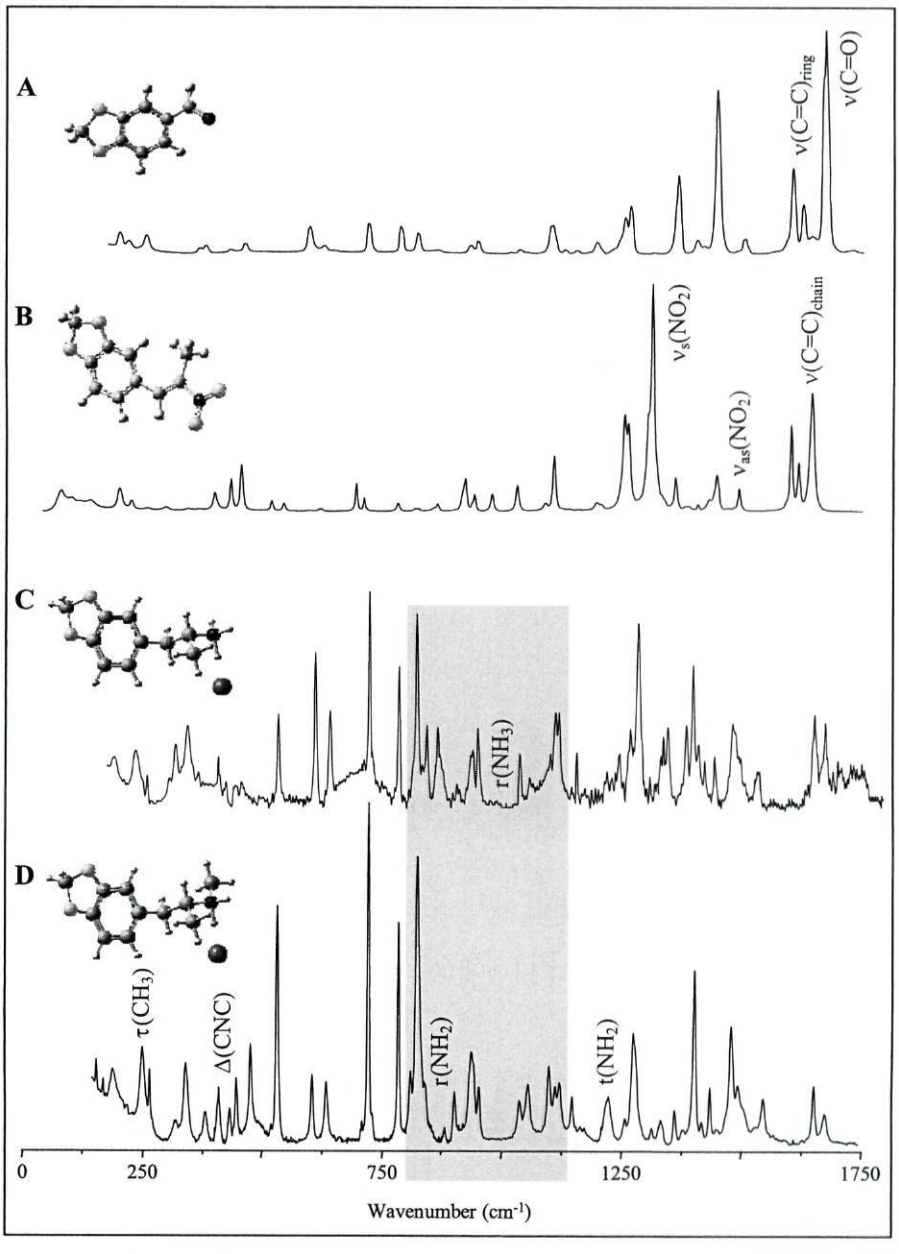

Fig. 6 Experimental Raman spectra (100–1750 cm^{-1}, solid state, at 25°C) for piperonal (A), 3,4-methylenedioxy-β-methyl-β-nitrostyrene (B), 3,4-methylenedioxyamphetamine hydrochloride (MDA) (C), 3,4-methylenedioxymethamphetamine hydrochloride (MDMA) (D). (δ – in-plane deformation; Δ – in-plane deformation of skeleton atoms; ν – stretching; ν_s – symmetric stretching; ν_{as} – antisymmetric stretching; r – rocking; t – twisting; τ – torsion. Atoms are represented as in Fig. 5. The shaded area is expanded in Fig. 7).

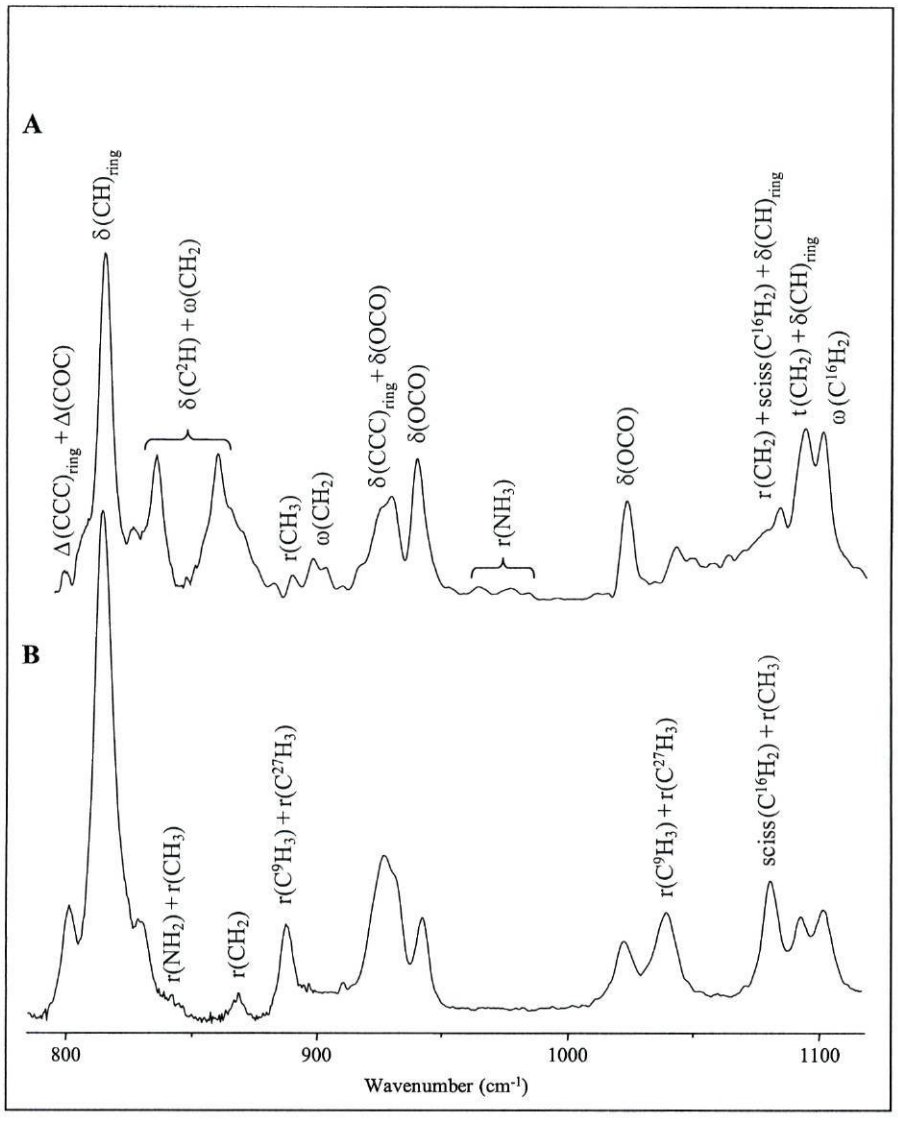

Fig. 7 Experimental Raman spectra (780–1120 cm^{-1}, solid state, at 25°C) for MDA (A) and "ecstasy" (B) hydrochlorides. (Atoms are numbered according to Fig. 5. δ – in-plane deformation; γ – out-of-plane deformation; r – rocking; ω – wagging; sciss – scissoring; t – twisting).

The NH_3 stretching (for MDA) is calculated at 3405 cm^{-1}, while $\nu(NH_2)$ (for "ecstasy") is calculated at 3339 cm^{-1}. Since no significative intramolecular hydrogen-type interactions may occur in these molecules, the NH_2/NH_3 stretching vibrations can only be affected by interaction with the chloride counterion, which may explain why they are not detected in the experimental Raman spectra (added to the typical low intensity of these modes in Raman). Apart from the amino group stretching modes, a quite good agreement was found between the experimental and calculated frequencies for both MDA and MDMA (Fig. 8).

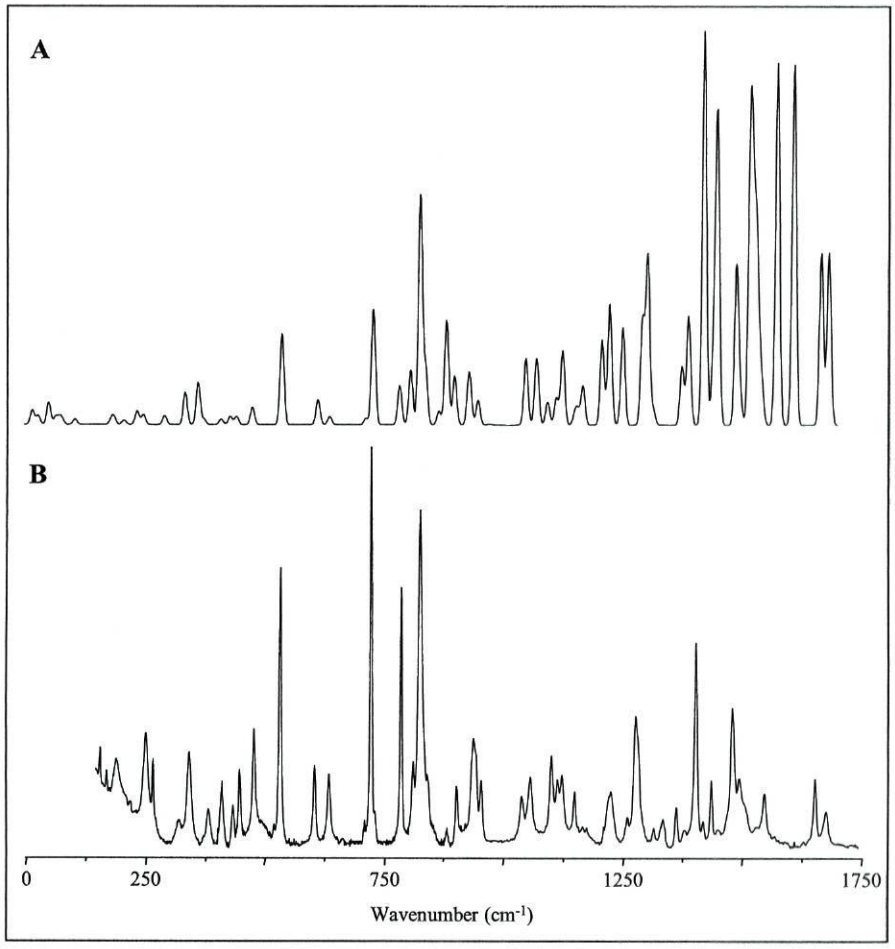

Fig. 8 Calculated (A) *versus* experimental (B) Raman spectra (0–1750 cm^{-1}) for 3,4-methylenedioxymethamphetamine hydrochloride.

Raman spectroscopy was described to be a valuable technique for a complete characterisation of drugs of abuse, either in seizure or biological samples. In that way it was applied to easily identify MDA and MDMA, as well as to differentiate them from their synthetic precursors piperonal and 3,4-methylenedioxy-β-methyl-β-nitrostyrene, through the signals at 1445 cm^{-1} (aldehyde deformation, δ(CH)) and 1647 cm^{-1} (chain C=C stretching, ν(C=C)) – typical of piperonal – and at 1316 cm^{-1} (symmetric stretching of the nitro group, $\nu_s(NO_2)$) and 1672 cm^{-1} (carbonyl stretching, ν(C=O)) – characteristic of 3,4-methylenedioxy-β-methyl-β-nitrostyrene (Fig. 6).

This study is, to the authors' knowledge, the first attempt to perform a complete Raman spectral assignment of these amphetamine-like systems, based on a structural analysis carried out by theoretical methods. It follows a similar conformational analysis performed for β-methyl-β-nitrostyrenes [42], which are synthetic precursors of several amphetamines. These compounds can be detected as impurities or side-products in

illicitly produced MDMA [21,53], which are likely to lead to severe adverse effects when contaminated with such products.

Conclusion

The results of this work evidence a reliable interplay between different areas of research (synthesis, electrochemistry and spectroscopy, coupled with DFT calculations) which all together allow to get insight into the physicochemical properties of a drug of abuse (MDMA) and its synthetic impurities, obtaining valuable information for forensic or toxicological studies.

The development of new synthetic strategies for *N*-methylation is of the utmost importance, both chemically and toxicologically. In fact, the pharmacological and toxicological profile of a drug is often a consequence of its metabolism, being N-methylation one of the most important pathways. For instance, *N*-methylated metabolites of amphetamine-like drugs of abuse (*e.g.* 3,4-dihydroxymethamphetamine) were found to be important to understand the toxicological profile of "ecstasy", at a molecular level [54,55].

In the present work, along with the development of synthetic strategies of *N*-methylation the characterisation of the compounds was performed by electrochemical assays, as well as by Raman spectroscopy experiments and quantum mechanical (DFT) calculations. From the voltammetric results it was verified that the main anodic waves of the oxidation profiles of the compounds under study are associated to the formation of a cationic methylenedioxyphenyl radical. Moreover, it was concluded that MDMA oxidative *N*-demethylation process is found to be associated to the removal of an electron from the corresponding amino-nitrogen atom, yielding a primary amine and an aldehyde. The same oxidative pattern was found for "ecstasy" synthetic impurities.

The vibrational (Raman) spectra, interpreted in the light of DFT calculations, allowed to achieve a rapid and unequivocal identification of the compounds investigated, which is of the utmost relevance for clinical, forensic and toxicological purposes. Raman spectroscopy has lately been shown to be a valuable tool for an unambiguous detection of amphetamine-like products [14,17]. Actually, this technique provides a spectral fingerprint of the compounds tested and can thus be used to identify even chemically similar intermediates, as well as to trace back the precursor materials

and the synthetic pathways employed in the preparation of the samples. In a near future, one will hopefully be able to rely on a Raman database for both forensic and toxicological studies.

Acknowledgements

NM acknowledges financial support from FCT – PhD fellowship PRAXIS XXI/BD/18520/98, I&D Nº 226/94 and POCTI (QCA III). RC also acknowledges financial support from FCT - PhD fellowship SFRH/BD/16520/2004.

References

[1] D. E. Nichols, A. J. Hoffman, R. Oberiender, P. Jacob and A. T. Shulgin, Derivatives of 1-(1,3-benzodioxol-5-yl)-2-butanamine: representatives of a novel therapeutic class. J. Med. Chem. 29 (1986) 2009-2015.

[2] D. E. Nichols, Differences between the mechanism of action of MDMA, MBDB, and the classic hallucinogens. Identification of a new therapeutic class: entactogens. J. Psychoactive Drugs 18 (1986) 305-313.

[3] D. L. Martinez-Price, K. Krebs-Thomson and M. A. Geyer, Behavioral psychopharmacology of MDMA and MDMA-like drugs: A review of human and animal studies. Addict. Res. Theory 10 (2002) 43-67.

[4] K. M. Hegadoren, G. B. Baker and M. Bourin, 3,4-Methylenedioxy analogues of amphetamine: Defining the risks to humans. Neurosci. Biobehav. Rev. 23 (1999) 539-553.

[5] G. A. Ricaurte, A. L. Martello, J. L. Katz and M. B. Martello, Lasting effects of (+-)-3,4-methylenedioxymethamphetamine (MDMA) on central serotonergic neurons in nonhuman primates: neurochemical observations. J. Pharmacol. Exp. Ther. 261 (1992) 616-622.

[6] U. D. McCann, V. Eligulashvili and G. A. Ricaurte, (±)3,4-Methylenedioxymethamphetamine ('ecstasy')-induced serotonin neurotoxicity: Clinical studies. Neuropsychobiology 42 (2000) 11-16.

[7] R. L. Fitzgerald, R. V. Blanke, J. A. Rosecrans and R. A. Glennon, Stereochemistry of the metabolism of MDMA to MDA. Life Sci. 45 (1989) 295-301.

[8] K.-P. Kreth, K.-A. Kovar, M. Schwab and U. M. Zanger, Identification of the human cytochromes P450 involved in the oxidative metabolism of "Ecstasy"-related designer drugs. Biochem. Pharmacol. 59 (2000) 1563-1571.

[9] A. P. Kulkarni, Role of biotransformation in conceptal toxicity of drugs and other chemicals. Curr. Pharm. Des. 7 (2001) 833-857.

[10] T. A. Dal Cason, An evaluation of the potential for clandestine manufacture of 3,4-methylenedioxyamphetamine (MDA) analogs and homologs. J. Forensic Sci. 35 (1990) 675-697.

[11] M. A. Parker, D. Marona-Lewicka, D. Kurrasch, A. T. Shulgin and D. E. Nichols, Synthesis and pharmacological evaluation of ring-methylated derivatives of 3,4-(methylenedioxy)amphetamine (MDA). J. Med. Chem. 41 (1998) 1001-1005.

[12] M. Swist, J. Wilamowski and A. Parczewski, Determination of synthesis method of ecstasy based on the basic impurities. Forensic Sci. Int. 152 (2005) 175-184.

[13] H. H. Maurer, J. Bickeboeller-Friedrich, T. Kraemer and F. T. Peters, Toxicokinetics and analytical toxicology of amphetamine-derived designer drugs ('Ecstasy'). Toxicol. Lett. 112-113 (2000) 133-142.

[14] S. E. J. Bell, D. T. Burns, A. C. Dennis and J. S. Speers, Rapid analysis of ecstasy and related phenethylamines in seized tablets by Raman spectroscopy. Analyst 125 (2000) 541-544.

[15] S. E. J. Bell, D. T. Burns, A. C. Dennis, L. J. Manchett and J. S. Speers, Composition profiling of seized ecstasy tablets by Raman spectroscopy. Analyst 125 (2000) 1811-1815.

[16] B. Sägmüller, B. Schwarze, G. Brehm and S. Schneider, Application of SERS spectroscopy to the identification of (3,4-methylenedioxy)amphetamine in forensic samples utilizing matrix stabilized silver halides. Analyst 126 (2001) 2066-2071.

[17] K. Faulds, W. E. Smith, D. Graham and R. J. Lacey, Assessment of silver and gold substrates for the detection of amphetamine sulfate by surface enhanced Raman scattering (SERS). Analyst 127 (2002) 282-286.

[18] S. E. J. Bell, L. J. Barrett, D. T. Burns, A. C. Dennis and J. S. Speers, Tracking the distribution of "ecstasy" tablets by Raman composition profiling: A large scale feasibility study. Analyst 128 (2003) 1331-1335.

[19] B. Sägmüller, B. Schwarze, G. Brehm, G. Trachta and S. Schneider, Identification of illicit drugs by a combination of liquid chromatography and surface-enhanced Raman scattering spectroscopy. J. Mol. Struct. 661-662 (2003) 279-290.

[20] P. Gimeno, F. Besacier and H. Chaudron-Thozet, Optimization of extraction parameters for the chemical profiling of 3,4-methylenedioxymethamphetamine (MDMA) tablets. Forensic Sci. Int. 132 (2003) 182-194.

[21] N. N. Daéid and R. J. H. Waddell, The analytical and chemometric procedures used to profile illicit drug seizures. Talanta 67 (2005) 280-285.

[22] M. J. Frisch *et al.* Gaussian 98, Revision A.9, Gaussian Inc., Pittsburgh PA, USA, 1998.

[23] C. Lee, W. Yang and R. G. Parr, Development of the Colle-Salvetti correlation-energy formula into a functional of the electron density. Phys. Rev. B37 (1988) 785-789.

[24] B. Miehlich, A. Savin, H. Stoll and H. Preuss, Results obtained with the correlation energy density functionals of Becke and Lee, Yang and Parr. Chem. Phys. Lett. 157 (1989) 200-206.

[25] A. D. Becke, Density-functional exchange-energy approximation with correct asymptotic behaviour. Phys. Rev. A38 (1988) 3098-3100.

[26] A. D. Becke, Density-functional thermochemistry. III. The role of exact exchange J. Chem. Phys. 98 (1993) 5648-5652.

[27] P. C. Hariharan and J. A. Pople, The influence of polarization functions on molecular orbital hydrogenation energies. Theor. Chim. Acta 28 (1973) 213-222.

[28] C. Peng, P. Y. Ayala, H. B. Schlegel and M. J. Frisch, Using redundant internal coordinates to optimize equilibrium geometries and transition states. J. Comp. Chem. 17 (1996) 49-56.

[29] A. P. Scott and L. Radom, Harmonic vibrational frequencies: An evaluation of Hartree-Fock, Møller-Plesset, quadratic configuration interaction, density functional theory, and semiempirical scale factors. J. Phys. Chem. 100 (1996) 16502-16513.

[30] B. M. Sykes, G. J. Atwell, A. Hogg, W. R. Wilson, C. J. O'Connor and W. A. Denny, *N*-Substituted 2-(2,6-Dinitrophenylamino)propanamides: Novel prodrugs that release a primary amine via nitroreduction and intramolecular cyclization. J. Med. Chem. 42 (1999) 346-355.

[31] E. Hammarberg, G. Nordvall, R. Leideborg, M. Nylöf, S. Hanson, L. Johansson, S.-O. Thorberg, B.-R. Tolf, E. Jerning, G. T. Svantesson, N. Mohell, C. Ahlgren, A. Westlind-Danielsson, I. Csöregh and R. Johansson, Synthesis of novel 5-substituted 3-amino-3,4-dihydro-2*H*-1-benzopyran derivatives and their interactions with the 5-HT_{1A} receptor. J. Med. Chem. 43 (2000) 2837-2850.

[32] C. G. Chavdarian, D. Karashima, N. Castagnoli and H. K. Hundley, Oxidative and cardiovascular studies on natural and synthetic catecholamines. J. Med. Chem. 21 (1978) 548-554.

[33] A. F. Abdel-Magid, K. G. Carson, B. D. Harris, C. A. Maryanoff and R. D. Shah, Reductive amination of aldehydes and ketones with sodium triacetoxyborohydride. Studies on direct and indirect reductive amination procedures. J. Org. Chem. 61 (1996) 3849-3862.

[34] A. Adejare, F. Gusovsky, W. Padgett, C. R. Creveling, J. W. Daly and K. L. Kirk, Syntheses and adrenergic activities of ring-fluorinated epinephrines. J. Med. Chem. 31 (1988) 1972-1977.

[35] S. Lu, B. Herbert, G. Haufe, K. W. Laue, W. L. Padgett, O. Oshunleti, J. W. Daly and K. L. Kirk, Syntheses of (*R*)- and (*S*)-2- and 6-fluoronorepinephrine and (*R*)- and (*S*)-2- and 6-fluoroepinephrine: Effect of stereochemistry on fluorine-induced adrenergic selectivities. J. Med. Chem. 43 (2000) 1611-1619.

[36] M. Masui, H. Sayo and Y. Tsuda, Anodic oxidation of amines. Part I. Cyclic voltammetry of aliphatic amines at a stationary glassy-carbon electrode. J. Chem. Soc. B (1968) 973-976.

[37] J. M. P. J. Garrido, C. D. Matos, F. Borges, T. R. A. Macedo and A. M. Oliveira-Brett, Voltammetric oxidation of drugs of abuse III. Heroin and metabolites. Electroanalysis 16 (2004) 1497-1502.

[38] M. Masui and H. Sayo, Anodic oxidation of amines. Part II. Electrochemical dealkylation of aliphatic tertiary amines. J. Chem. Soc. B (1971) 1593-1596.

[39] A. Adenier, M. M. Chehimi, I. Gallardo, J. Pinson and N. Vilà, Electrochemical Oxidation of Aliphatic Amines and Their Attachment to Carbon and Metal Surfaces. Langmuir 20 (2004) 8243-8253.

[40] J. A. Squella, B. K. Cassels, M. Arata, M. P. Bavestrello and L. J. Nunez-Vergara, Electrochemical oxidation of methylenedioxyamphetamines. Talanta 40 (1993) 1379-1384.

[41] J. M. P. J. Garrido, C. D. Matos, F. Borges, T. R. A. Macedo and A. M. Oliveira-Brett, Voltammetric oxidation of drugs of abuse II. Codeine and metabolites. Electroanalysis 16 (2004) 1427-1433.

[42] N. Milhazes, F. Borges, R. Calheiros and M. P. M. Marques, Identification of synthetic precursors of amphetamine-like drugs using Raman spectroscopy and *ab initio* calculations: β-Methyl-β-nitrostyrene derivatives. Analyst 129 (2004) 1106-1117.

[43] R. E. Clavijo, R. Araya-Maturana, B. K. Cassels and B. Weiss-López, Infrared spectra of nitrostyrene derivatives. Spectrochim. Acta 50A (1994) 2105-2115.

[44] A. By, G. Neville and H. F. Shurvell, Fourier transform infrared/raman differentiation and characterization of *cis*- and *trans*-2,5-dimethoxy-4,β-dimethyl-β-nitrostyrenes: Precursors to the street drug STP. J. Forensic Sci. 37, (1992) 503-512.

[45] R. Calheiros, N. Milhazes, F. Borges and M. P. M. Marques, β-Nitrostyrene derivatives—a conformational study by combined Raman spectroscopy and ab initio MO calculations. J. Mol. Struct. 692 (2004) 91-106.

[46] S. J. Greaves and W. W. Griffith, Vibrational spectra of catechol, catechol-d_2 and -d_6 and the catecholate monoanion. Spectrochim. Acta 47A (1991) 133-140.

[47] F. J. Ramírez and J. T. López Navarrete, Normal coordinate and rotational barrier calculations on 1,2-dihydroxybenzene. Vib. Spec. 4 (1993) 321-334.

[48] R. Hargitai, P. G. Szalay, G. Pongor and G. Fogarasi, Scaled quantum mechanical (SQM) force field and vibrational assignment for styrene. J. Mol. Struct. (THEOCHEM) 306 (1994) 293-311.

[49] Y. Haas, S. Kendler, E. Zingher, H. Zuckermann and S. Zilberg, $S_0 \leftrightarrow S_1$ transition of *trans*-β-methyl styrene: Vibronic structure and dynamics. J. Chem. Phys. 103 (1995) 37-47.

[50] M. Gerhards, W. Perl, S. Schumm, U. Henrichs, C. Jacoby and K. Kleinermanns, Structure and vibrations of catechol and catechol·$H_2O(D_2O)$ in the S_0 and S_1 state. J. Chem. Phys. 104 (1996) 9362-9375.

[51] E. Besien and M. P. M. Marques, Ab initio conformational study of caffeic acid. J. Mol. Struct. (THEOCHEM) 625 (2003) 265-275.

[52] S. M. Fiuza, E. Besien, N. Milhazes, F. Borges and M. P. M. Marques, Conformational analysis of a trihydroxylated derivative of cinnamic acid—a

combined Raman spectroscopy and Ab initio study. J. Mol. Struct. 693 (2004) 103-118.

[53] P. Gimeno, F. Besacier, M. Bottex, L. Dujourdy and H. Chaudron-Thozet, A study of impurities in intermediates and 3,4-methylenedioxymethamphetamine (MDMA) samples produced via reductive amination routes. Forensic Sci. Int. 155 (2005) 141-157.

[54] M. Carvalho, F. Remião, N. Milhazes, F. Borges, E. Fernandes, M.C. Monteiro, M.J. Gonçalves, V. Seabra, F. Amado, F. Carvalho, M.L. Bastos, Metabolism is required for the expression of ecstasy-induced cardiotoxicity in vitro. Chem. Res. Toxicol. 17 (2004) 623-632.

[55] M. Carvalho, N. Milhazes, F. Borges, E. Fernandes, T. J. Monks, F. Carvalho, M.L. Bastos, Hepatotoxicity of 3,4-methylenedioxyamphetamine and α-methyldopamine in isolated rat hepatocytes: formation of glutathione conjugates Arch. Toxicol. 78 (2004) 16-24.

8.6 Síntese e perfil de citotoxicidade da 3,4-metilenodioximetanfetamina ("ecstasy") e seus metabolitos em células PC12 indiferenciadas: uma provável relação estrutura – toxicidade.

Artigo reproduzido da revista *Chemical Research in Toxicology* (2006) 19: 1294-1304, com permissão da American Chemical Society.

Chem. Res. Toxicol. **2006,** *19,* 1294−1304

Synthesis and Cytotoxic Profile of 3,4-Methylenedioxymethamphetamine ("Ecstasy") and Its Metabolites on Undifferentiated PC12 Cells: A Putative Structure−Toxicity Relationship

Nuno Milhazes,[†,‡] Teresa Cunha-Oliveira,[§] Pedro Martins,[∥] Jorge Garrido,[⊥,#] Catarina Oliveira,[§] A. Cristina Rego,[§] and Fernanda Borges*[,∥,⊥]

CEQOFFUP, Faculdade de Farmácia, Universidade do Porto, 4050-047 Porto, Portugal, Instituto Superior Ciências da Saúde-Norte, 4585-116 Gandra, PRD, Portugal, Instituto de Bioquímica, Faculdade de Medicina e Centro de Neurociências e Biologia Celular de Coimbra, Universidade de Coimbra, 3004-504 Coimbra, Portugal, Departamento de Química Orgânica, Faculdade de Farmácia, Universidade do Porto, 4050-047 Porto, Portugal, Unidade I&D "Química-Física Molecular", and Departamento de Engenharia Química, Instituto Superior de Engenharia do Porto, IPP, Porto, Portugal

Received June 7, 2006

The toxicological and redox profiles of MDMA and its major metabolites (MDA, α-methyldopamine, *N*-methyl-α-methyldopamine, 6-hydroxy-α-methyldopamine, 3-methoxy-α-methyldopamine) were studied to establish a structure-toxicity relationship and determine their individual contribution to cell death induction by apoptosis and/or necrosis. The results of the comparative toxicity study, using undifferentiated PC12 cells, strongly suggest that the metabolites possessing a catecholic group are more toxic to the cells than MDMA and metabolites with at least one protected phenolic group. Redox studies reveal that an oxidative mechanism seems to play an important role in metabolite cytotoxicity. Nuclear features of apoptosis and/or necrosis show that most of the metabolites, particularly *N*-methyl-α-methyldopamine, induce cell death by apoptosis, largely accompanied by necrotic features. No significant differences were found between MDMA and the metabolites, concerning overall characteristics of cell death. These results may be useful to ascertain the contribution of metabolism in MDMA neurotoxicity molecular mechanisms.

Introduction

3,4-Methylenedioxymethamphetamine (MDMA, "ecstasy", **16**) is a ring-substituted phenethylamine derivative widely used as a recreational drug. The abuse of this group of amphetamine-like designer drugs is increasing among young adults, being at present a serious public health problem (*1*, *2*). The toxicity related to the misuse of this drug is extensively reported in recent literature, but the molecular mechanisms involved remain largely unknown. Among several biological targets, the neurotoxic (*3*), nephrotoxic (*4*), hepatotoxic (*5*), and cardiovascular (*6*) effects of MDMA were extensively studied *in vitro* and *in vivo*.

The research on the biotransformation reactions of xenobiotics, which play a major role in influencing the nature, intensity, and duration of wanted and unwanted effects, is an important task in the medicinal chemistry field (*7*). A majority of the investigation has been based on the overall effects induced by the use of the drug, but little attention has been given to the putative activities of the metabolites themselves. Several recent studies suggest that part of the toxicity ascribed to MDMA can be related to the formation of metabolites with higher activity (*8*−*10*). Several MDMA metabolic pathways have been proposed and reported (*11*−*12*), with the *N*-demethylation to 3,4-methylenedioxyamphetamine (MDA, **11**), also as a recreational drug, and the simultaneous or subsequent *O*-demethylenation to 3,4-dihydroxyamphetamine (α-methyldopamine, α-MeDA, **19**) and 3,4-dihydroxymethamphetamine (*N*-methyl-α-methyldopamine, *N*-Me-α-MeDA, **21**) being the most significant ones. It has also been assumed that the catecholic compounds **19** and **21** can undergo subsequent *O*-methylation mediated by catechol *O*-methyltranferase (COMT) to 4-hydroxy-3-methoxyamphetamine (3-methoxy-α-methyldopamine, 3-*O*-Me-α-MeDA, **13**) and 4-hydroxy-3-methoxymethamphetamine (Figure 1).

Aromatic hydroxylation has also been established as an important biotransformation step in *in vivo* metabolism of MDMA in rats. This reaction can occur at the remaining positions of the aromatic ring, but the one occurring at C_6 is the most reactive one. The resulting compound 2,4,5-trihydroxyamphetamine (6-hydroxy-α-methyldopamine, 6-OH-α-MeDA, **20**) is structurally similar to 6-hydroxydopamine (a potent neurotoxin obtained by *in vivo* aromatic hydroxylation of dopamine) (*13*, *14*). All compounds possessing a catecholic group can undergo further conjugation with other molecules like sulfate, glucuronide and thiol-containing endogenous substances (glutathione, cysteine, and *N*-acetylcysteine).

Animals exposed to MDMA show acute and long-term neurotoxic effects, causing irreversible damage to the central nervous system. Characterization of the *in vivo* and *in vitro* MDMA-induced neurotoxicity was widely accomplished (*15*−*17*), although the molecular mechanisms involved remain to be fully elucidated. Previously published studies suggested that bioactivation occurs after the administration of amphetamines, mediating a series of neurotoxic effects (*18*−*20*).

* Corresponding author. Tel: +351222078900. Fax: +351222003977. E-mail: fborges@ff.up.pt.
† CEQOFFUP, Universidade do Porto.
‡ Instituto Superior Ciências da Saúde - Norte.
§ Universidade de Coimbra.
∥ Departamento de Química Orgânica, Universidade do Porto.
⊥ Unidade I&D "Química-Física Molecular".
Instituto Superior de Engenharia do Porto.

10.1021/tx060123i CCC: $33.50 © 2006 American Chemical Society
Published on Web 09/07/2006

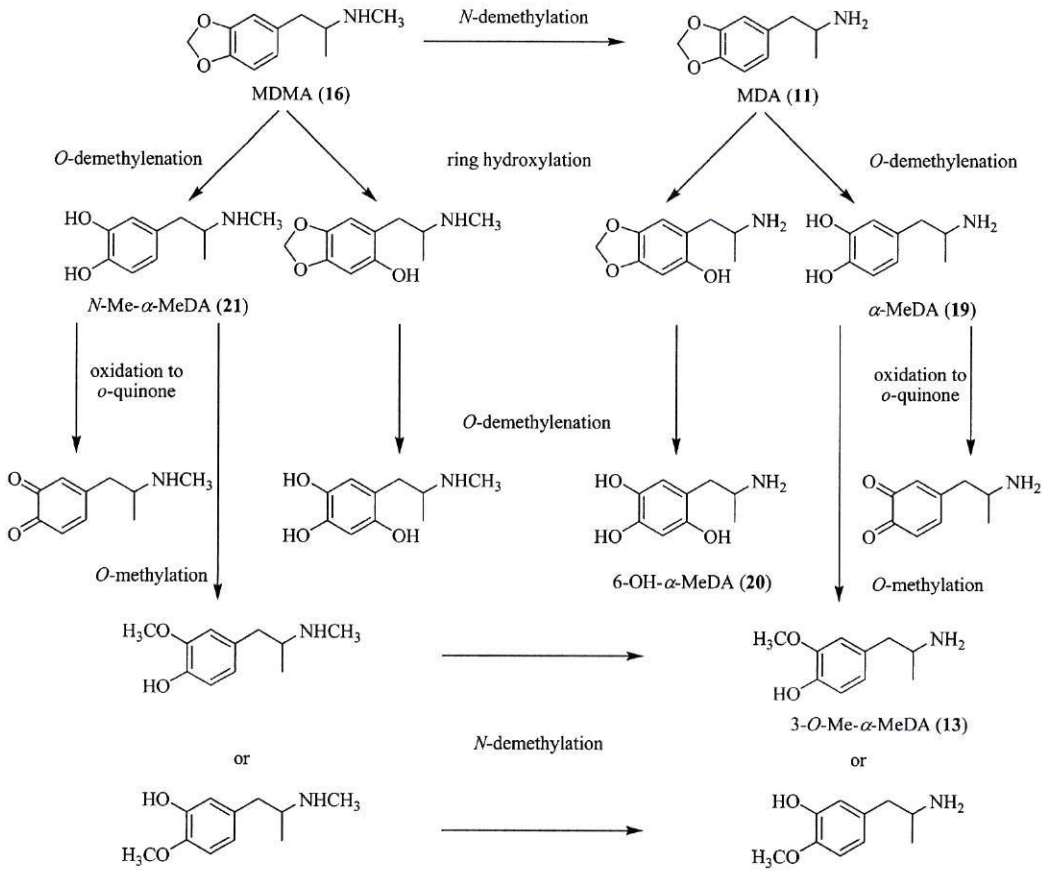

Figure 1. Proposed major metabolic pathways of MDMA; the numbered compounds correspond to the metabolites synthesized and used in the toxicological assays.

MDMA is a monoaminergic neurotoxin in both serotonin (5HT) and dopamine nerve terminals, depending on the animal species and conditions of administration. The neurotoxicity has been largely associated to a modification of the serotonergic function, namely, through an acute release of serotonin from central neurons, followed by prolonged depletion and structural neuronal damage (*21*–*23*). There is also considerable evidence that MDMA shows marked effects on dopamine release and can damage dopamine axon terminals, which could play a major role in some behavioral, mental, and thermal changes in animals (*24*, *25*).

Cell death by apoptosis or necrosis has been proposed to be involved in amphetamine-induced neurodegeneration (*26*, *27*). The activation of these pathways seems to be closely related to the occurrence of oxidative stress in the cellular medium, through redox cycles, which is intimately linked to the metabolism of MDMA and catecholamine (auto)oxidation (*10*, *28*).

Nonconjugated metabolites of MDMA are present in blood, brain, liver, feces, and urine for a 24-hour period following drug administration (*11*). It is generally accepted that one or more metabolites of MDMA or MDA may be responsible for neurotoxic effects because direct intracerebral injection of the drugs failed to reproduce the neurotoxicity revealed after peripheral administration (*29*). As MDMA does not seem to be neurotoxic, the evaluation of the metabolite's toxic effects is essential for the elucidation of the molecular mechanisms involved. However, there is controversy regarding the specific role of the metabolites. Intracerebroventricular administration of α-MeDA, *N*-Me-α-MeDA, and 3-*O*-Me-α-MeDA failed to produce the same neurotoxic features on central serotoninergic and dopaminergic systems induced by peripherally administered MDMA (*18*, *30*); nonetheless, other neurochemical effects were determined, and alterations were detected for the same metabolites, specially for 6-OH-α-MeDA (*18*, *31*, *32*).

In order to examine the hypothesis that the metabolites can contribute to the neurotoxicity of the parent compound, the cytotoxic potential of MDMA and five of its metabolites was investigated. The research project includes the synthesis of the main described metabolites of MDMA through standard synthetic methods and the evaluation of their cytotoxic profiles by using undifferentiated PC12 cells in culture, a well-established *in vitro* model of catecholaminergic neurons (*33*–*35*). Cell viability was assessed after incubation for 24 h with increasing concentrations of the compounds in order to determine the IC_{50} values. Because oxidative pathways have been proposed to play an important role in the toxicity profile of this type of compounds, the relationship between the redox profile and cytotoxicity was also studied. Accordingly, to get new insights on the molecular mechanisms underlying the biological activities, the redox properties of the drug and metabolites were determined using different electrochemical techniques.

Because MDMA-induced cell damage is related to programmed cell death in serotoninergic and neocortical neurons (*36*, *37*), assays of chromatin fragmentation/condensation were performed in PC12 cells in order to define drug-induced cell death as apoptotic and/or necrotic. To the best of our knowledge, there are no reports of apoptosis-like events induced by the MDMA metabolites in dopaminergic-like neurons.

Experimental Procedures

Materials and Solutions. PC12 cells were obtained from ATCC (Manassas, VA). 3,4-Dihydroxybenzaldehyde, 3,4-dimethoxybenzaldehyde, 4-hydroxy-3-methoxybenzaldehyde, 2,4,5- trimethoxy-

benzaldehyde, bromochloromethane, potassium carbonate, benzyl chloride, cesium carbonate, ammonium acetate, nitroethane, anhydrous magnesium sulfate, lithium aluminum hydride (1 M solution in tetrahydrofuran), ethyl chloroformate, boron tribromide (1 M solution in dichloromethane), 10% platinum in carbon, RPMI 1640 medium (modified with L-glutamine and 25 mM HEPES), streptomycin, penicillin, MTT, poly-L-lysine and propidium iodide, and all dry solvents were purchased from Sigma-Aldrich Química S.A. (Sintra, Portugal). Syto-13 was obtained from Molecular Probes (Eugene, OR). Horse serum and fetal bovine serum were purchased from BioChrom KG (Berlin, Germany). All other reagents and solvents were *pro analysis* grade and were acquired from Merck (Lisbon, Portugal). Deionized water (conductivity $<0.1\ \mu S\ cm^{-1}$) was used in all experiments. The gases, hydrogen, argon and nitrogen, were of the highest grade available. All reagents were used without further purification.

To perform electrochemical measurements, 10 mM stock solutions of the compounds were made by dissolving an appropriate amount in water. The voltammetric working solutions were prepared, in an electrochemical cell, by diluting 100 μL of the stock solution in 10 mL of supporting electrolyte to get a final concentration of 0.1 mM. The pH 7.3 supporting electrolyte, used for voltammetric determinations, was prepared by diluting 6.2 mL of 0.2 M dipotassium hydrogen phosphate and 43.8 mL of 0.2 M potassium dihydrogen phosphate to 100 mL.

Apparatus and Other Analytical Conditions. ^{1}H and ^{13}C NMR data were acquired, at room temperature, on a Brüker AMX 300 spectrometer operating at 300.13 and 75.47 MHz, respectively. Chemical shifts are expressed in δ (ppm) values, relative to tetramethylsilane (TMS) (as internal reference); coupling constants (J) are given in Hz. Dimethyl sulfoxide-d_6 was used as solvent unless specified in spectroscopic data. Assignments were also made from DEPT (distortionless enhancement by polarization transfer) experiments (values in italic). Electron impact mass spectra (EI-MS) were obtained on a VG AutoSpec instrument; data are reported as m/z (% of relative intensity for the most important fragments). Melting points were measured on a Köfler microscope (Reichert Thermovar) and were uncorrected. Analytical thin-layer chromatography (TLC) was carried out on 0.2 mm silica gel 60 F254 plates.

The purity of the final products (>95% purity) was verified using two different high-performance liquid chromatography (HPLC) systems, one equipped with a UV detector (DAD) and the other with an electrochemical detector. First, chromatograms were obtained in an HPLC/DAD system, a Jasco instrument (pumps model 880-PU and solvent mixing model 880-30, Tokyo, Japan), equipped with a commercially prepacked Nucleosil RP-18 analytical column (250 mm × 4.6 mm, 5 μm, Macherey-Nagel, Düren, Germany), and UV detection (Jasco model 875-UV) at the maximum wavelength determined by the analysis of the UV spectrum of each compound. The isocratic mobile phase consisted of 10 mM aqueous ammonium acetate (adjusting the final pH to 3 with hydrochloric acid) with 10% acetonitrile, at a flow rate of 1 mL/min at room temperature. The chromatographic data was processed in a Compaq computer, fitted with CSW 1.7 software (DataApex, Czech Republic).

A Waters 2690 Alliance system equipped with a CONCORDE Electrochemical Detector (Waters Corporation, Milford, USA) was also used. The electrochemical cell was a VT-03 flow cell (Antec Leyden, Zoeterwoude, Netherlands) with a confined wall-jet design in a three-electrode configuration: a 2 mm diameter glassy carbon working electrode, an *in-situ* Ag/AgCl reference electrode, and a stainless steel auxiliary electrode. The electrochemical detector was operated in oxidative amperometric mode with the working potentials between −100 mV and +1200 mV. The HPLC separation was carried out in a reverse phase LC-18-S Supelcosil analytical column (150 mm × 4.6 mm, 5 μm, Supelco, Bellefonte, USA); 100 mM sodium acetate (pH 4.3)/methanol (10:3) was used as mobile phase, in isocratic mode at 1 mL/min flow rate. Chromatograms were acquired in a Millenium 32 Chromatography Manager (Waters Corporation, Milford, USA).

Electrochemical data were obtained using an Autolab PGSTAT 12 potentiostat/galvanostat (Eco-Chemie, Netherlands) and a one-compartment glass electrochemical cell. Voltammetric curves were recorded at room temperature using a three-electrode system. A glassy carbon working electrode (GCE) (d = 2 mm), a platinum wire counter electrode, and an Ag/AgCl saturated KCl reference electrode were used. A Metrohm E520 pH-meter with glass electrode was used for pH measurements (Metrohm, Switzerland).

Synthesis of Metabolites. Synthesis of Aldehydes 1 and 5. 3,4-Methylenedioxybenzaldehyde (1). Because piperonal (**1**) is not commercially available in Portugal, it was synthesized by an adaptation of a previously described procedure (*38*). The dioxole ring was closed after the reaction of the starting material 3,4-benzaldehyde with bromochloromethane and using cesium carbonate as a catalyst.

3,4-Dibenzyloxybenzaldehyde (5). Briefly, 3,4-benzaldehyde or protocatechualdehyde (5.0 g, 36.2 mmol) was dissolved in *N,N*-dimethylformamide (DMF) (80 mL). Potassium carbonate (20.0 g, 144.9 mmol) and benzyl chloride (9.6 mL, 83.5 mmol) were then added to the solution, and the resulting suspension was stirred and refluxed for 5 h. The remaining residue was filtered and the solution poured on cold water/ice and acidified with HCl (pH 4). The yellow precipitate produced was filtered, washed with cold water, and identified as compound **5** (yield: 96%). The spectroscopic data is in accordance with an article published earlier (*39*).

General Synthetic Procedure for Obtaining β-Methyl-β-nitrostyrenes (6−10). The synthetic method used to obtain these compounds was an adaptation of references published earlier (*38*, *40*, *41*) with only minor modifications. The corresponding benzaldehyde (**1**−**5**), with the aromatic substitution pattern of the target compound, (30.0 mmol) and ammonium acetate (7.5 mmol) were dissolved in nitroethane (50 mL) and refluxed for 6 h. After cooling the reaction mixtures to room temperature, the solvent was partially evaporated, diluted with diethyl ether, and washed twice with 100 mL of water. The organic layers were dried over anhydrous magnesium sulfate, filtered, and concentrated. The remaining residues were recrystallized from diethylether/petroleum ether (40−60 °C) or from methanol/water to yield yellow to orange solids.

The reactions were all followed by thin layer chromatography (TLC). The synthesized β-methyl-β-nitrostyrene derivatives (**6**−**10**) were identified by both NMR and EI-MS. The compounds were systematically characterized in this work, even though some of them had been previously reported (*11*, *42*, *43*). The data of the remaining compound used in this study (**6**) is described elsewhere (*44*).

3,4-Dimethoxy-β-methyl-β-nitrostyrene (7). Yield 95%; ^{1}H NMR δ: 2.44 (3H, *s*, CH_3), 3.80 (3H, *s*, 3-OCH_3), 3.82 (3H, *s*, 4-OCH_3), 7.08 (1H, *d*, J = 8.5, H (5)), 7.22 (1H, *s*, H (2)), 7.23 (1H, *d*, J = 8.5, H (6)), 8.08 (1H, *s*, H(α)); ^{13}C NMR δ: *14.0* CH_3, *55.6* (4-OCH_3), *55.7* (3-OCH_3), *111.8*, *113.9* C (2) and C (5), *124.3* C (6), 124.4 C (1), *133.8* C(α), 145.6 C(β), 148.7 C (4), 150.7 C (3); EI-MS m/z (%): 223 ($M^{+\bullet}$, 100), 176 (78), 165 (22), 161 (37), 146 (47), 131 (46), 119 (36), 103 (37), 91 (47), 77 (38), 65 (34); mp 71−72 °C (lit (*43*). mp 72−74 °C).

4-Hydroxy-3-methoxy-β-methyl-β-nitrostyrene (8). Yield 98%; ^{1}H NMR δ: 2.44 (3H, *s*, CH_3), 3.81 (3H, *s*, OCH_3), 6.89 (1H, *d*, J = 8.2, H (5)), 7.12 (1H, *dd*, J = 8.2; 1.9, H (6)), 7.20 (1H, *d*, J = 1.9, H (2)), 8.05 (1H, *s*, H(α)), 9.85 (1H, b*s*, O*H*); ^{13}C NMR δ: *14.0* CH_3, *55.7* (OCH_3), *114.8*, *115.9* C (2) and C (5), 123.0 C (1), *124.8* C (6), *134.2* C(α), 144.7 C(β), 147.7 C (4), 149.2 C (3); EI-MS m/z (%): 209 ($M^{+\bullet}$, 100), 162 (81), 147 (53), 131 (33), 119 (30), 103 (84), 91 (56), 77 (36), 65 (32); mp 97−99 °C (lit (*42*). mp 100−101 °C).

2,4,5-Trimethoxy-β-methyl-β-nitrostyrene (9). Yield 92%; ^{1}H NMR δ: 2.39 (3H, *s*, CH_3), 3.74 (3H, *s*, 2-OCH_3), 3.88 (6H, *s*, 4- and 5-OCH_3), 6.79 (1H, *s*, H (3)), 7.01 (1H, *s*, H (6)), 8.20 (1H, *s*, H(α)); ^{13}C NMR δ: 14.1 CH_3, 56.0, 56.2, 56.4 (3×OCH_3), 97.5 C (3), 111.1, 113.3 C (1) and C (6), 128.8 C(α), 142.5 C (2), 145.1 C(β), 152.5 C (4), 153.9 C (5); EI-MS m/z (%): 253 ($M^{+\bullet}$, 100), 206 (64), 191 (40), 177 (36), 163 (19), 149 (15), 121 (17), 77 (16), 69 (16); mp 93−95 °C.

3,4-Dibenzyloxy-β-Methyl-β-nitrostyrene (10). Yield 79%; ^{1}H NMR δ: 2.32 (3H, *s*, CH_3), 5.20 (2H, *s*, 3-OCH_2), 5.22 (2H, *s*, 4-OCH_2), 7.20 (2H, *m*, H (2) and H (5)), 7.33–7.45 (11H, *m*, phenyl and H (6)), 8.03 (1H, *s*, H(α)); ^{13}C NMR δ: *13.9* CH_3, *69.8*, *70.0* (2×CH_2), *113.9, 116.2* C (2) and C (5), 124.6 C (1), *124.9* C (6), *127.6-128.5* (10×*C*HAr), *133.5 C*(α), 136.9 (2×*C*Ar), 145.7 C(β), 147.8 C (3), 150.1 C (4); EI-MS *m/z* (%): 375 ($M^{+\bullet}$, 20), 284 (8), 181 (10), 91 (100), 65 (13); mp 107–109 °C (lit (*45*). mp 103–105 °C).

General Synthetic Procedure for the Reduction of Nitrostyrene Intermediates. The method applied for the synthesis of compounds **11**–**15** was a modification of those described earlier (*40*, *45*). Therefore, a solution of the appropriate β-methyl-β-nitrostyrene derivative (**6**–**10**) (8 mmol) in anhydrous tetrahydrofuran (THF) (30 mL) was added dropwise to a stirred suspension of lithium aluminum hydride (20 mmol) in anhydrous THF (50 mL) under nitrogen (N_2). The reaction was stirred, heated under reflux for 4 h, and then allowed to cool to room temperature. The excess $LiAlH_4$ was decomposed and the reaction quenched by the smooth addition of cold water/ice with vigorous stirring. The inorganic residue was removed by vacuum filtration; the solvent was dried under anhydrous magnesium sulfate, evaporated, and the residue diluted with diethyl ether and extracted with aqueous HCl (3 × 100 mL of a 2 M solution). The acidic extract was alkalinized with a NaOH solution and extracted with diethyl ether (3 × 100 mL). The organic layer was dried over anhydrous magnesium sulfate, filtered and concentrated to yield light brown oils.

When necessary for the systematic characterization of the compounds, the phenethylamine derivatives were isolated as salts (due mainly to their stability and simple of handling). Hence, the hydrochloride salts were prepared by acidifying the remaining residues with methanolic or ethanolic HCl and diluting with diethyl ether to obtain a white or almost white solid.

The identification of several of the amphetamine derivatives (**11**–**15**) had been previously reported (*10, 11, 43, 45*–*48*). Nevertheless, some structural data was insufficiently accomplished, and the spectroscopic characterization was thoroughly performed in this work. For the accurate ^{1}H NMR assignment of the (CH_2CH)CH_3 group in all of the amphetamine derivatives, the spectra were also acquired in $CDCl_3$ and D_2O.

(*R,S*)-3,4-Dimethoxyamphetamine Hydrochloride (12). Yield 56%; ^{1}H NMR δ: 1.11 (3H, *d*, CH_3), 2.61 (1H, *dd*, *J* = 13.4; 8.7, CH_2), 2.93 (1H, *dd*, *J* = 13.4; 5.4, CH_2), 3.36 (1H, *m*, *CH*), 3.72 (3H, *s*, 3-OCH_3), 3.75 (3H, *s*, 4-OCH_3), 6.73 (1H, *dd*, *J* = 8.1; 1.8, H (6)), 6.85 (1H, *d*, *J* = 1.8, H (2)), 6.89 (1H, *d*, *J* = 8.2, H (5)), 8.11 (3H, b*s*, NH_3^+); ^{13}C NMR δ: *17.6* CH_3, *39.6* CH_2, *48.0 CH*, *55.4*, *55.5* (2×OCH_3), *111.8*, *112.9* C (2) and C (5), *121.2* C (6), 129.0 C (1), 147.6 C (3), 148.7 C (4); EI-MS *m/z* (%): 195 ($M^{+\bullet}$, 5), 162 (7), 152 (95), 137 (17), 121 (6), 107 (14), 91 (12), 83 (100), 65 (15); mp 146–148 °C (lit (*43*). mp 145–148 °C).

(*R,S*)-4-Hydroxy-3-methoxyamphetamine Hydrochloride (13). Yield 35%; ^{1}H NMR δ: 1.10 (3H, *d*, CH_3), 2.56 (1H, *dd*, *J* = 13.5; 8.6, CH_2), 2.86 (1H, *dd*, *J* = 13.4; 5.5, CH_2), 3.38 (1H, *m*, *CH*), 3.75 (3H, *s*, 3-OCH_3), 6.60 (1H, *dd*, *J* = 8.0; 1.8, H (6)), 6.72 (1H, *d*, *J* = 8.0, H (5)), 6.79 (1H, *d*, *J* = 1.8, H (2)), 7.99 (3H, b*s*, NH_3^+), 8.91 (1H, b*s*, 4-*OH*); ^{13}C NMR δ: *17.7* CH_3, *39.5* CH_2, *48.2 CH*, *55.5* (OCH_3), *113.2*, *115.5* C (2) and C (5), *121.5* C (6), 127.3 C (1), 145.4 C (4), 147.6 C (3); EI-MS *m/z* (%): 181 ($M^{+\bullet}$, 7), 138 (100), 122 (19), 94 (20), 89 (12), 77 (13), 65 (12); mp 245 °C (dec) (lit (*48*). mp 244–246 °C).

(*R,S*)-3,4,5-Trimethoxyamphetamine Hydrochloride (14). Yield 70%; ^{1}H NMR δ: 1.09 (3H, *d*, CH_3), 2.64 (1H, *dd*, *J* = 13.3; 8.4, CH_2), 2.86 (1H, *dd*, *J* = 13.3; 5.7, CH_2), 3.35 (1H, *m*, *CH*), 3.69 (3H, *s*, 6-OCH_3), 3.77 (3H, *s*, 3-OCH_3), 3.78 (3H, *s*, 4-OCH_3), 6.68 (1H, *s*, H (2)), 6.79 (1H, *s*, H (5)), 7.94 (3H, b*s*, NH_3^+); ^{13}C NMR δ: 17.8 CH_3, 34.3 CH_2, 47.0 *CH*, 55.8, 56.1, 56.3 (3×OCH_3), 98.2 C (5), 115.3, 115.7 C (1) and C (2), 142.4 C (6), 148.6 C (3), 151.6 C (4); EI-MS *m/z* (%): 225 ($M^{+\bullet}$, 11), 182 (100), 167 (32), 151 (15), 139 (8); mp 193–195 °C.

(*R,S*)-3,4-Dibenzyloxyamphetamine Hydrochloride (15). Yield 56%; ^{1}H NMR δ: 1.08 (3H, *d*, CH_3), 2.59 (1H, *dd*, *J* = 13.4; 8.8, CH_2), 2.93 (1H, *dd*, *J* = 13.4; 5.8, CH_2), 3.39 (1H, *m*, *CH*), 5.13 (2H, *s*, 3-OCH_2), 5.15 (2H, *s*, 4-OCH_2), 6.77 (1H, *dd*, *J* = 8.2; 1.8, H (6)), 7.00 (1H, *d*, *J* = 1.8, H (2)), 7.20 (1H, *d*, *J* = 8.2, H (5)), 7.33–7.50 (10H, *m*, phenyl), 8.07 (3H, b*s*, NH_3^+); ^{13}C NMR : 17.6 CH_3, 39.6 CH_2, 48.0 *CH*, 70.0 (2×OCH_2), 114.5, 115.6 C (2) and C (5), 121.9 C (6), 127.6–128.4 (10×*C*HAr), 129.6 C (1), 137.3, 137.4 (2×*C*Ar), 147.1 C (3), 148.1 C (4); EI-MS *m/z* (%): 348 ($M^{+\bullet}$, 5), 181 (12), 91 (100), 65 (14); mp 130–132 °C (lit (*45*). mp 130–133 °C).

General Synthetic Procedure for the N-Methylation of the Amphetamine Derivatives. Compounds **16**, **17**, and **18** were synthesized according to a synthetic route published earlier (*47*). The preparation of these secondary amines, starting from the respective primary amines, was preformed by a two-step reaction pathway, in which the intermediate was a carbamate derivative. The amine hydrochlorides (**11**, **12**, and **15**) (4.5 mmol) were dissolved in water (30 mL) at 0 °C. A solution of NaOH (0.3 g) in water (2.5 mL) was then added to the reaction followed by the addition of ethylchloroformate (0.5 mL, 5.3 mmol). The suspension was stirred at 0 °C for 3 h, and the reaction was then stopped by extraction with 3 × 100 mL of dichloromethane. The organic layer was dried, and the solvent was evaporated to obtain the corresponding urethane (R-NHCOOEt) (yields around 85%). These compounds were then reduced to the methylated amine by reaction with $LiAlH_4$. Briefly, the carbamates (4.1 mmol) were dissolved in THF (15 mL), and this solution was slowly added to lithium aluminum hydride (12 mmol) suspended in THF (25 mL), under N_2. The reaction was stirred and heated under reflux for 10 h. The quenching of the reaction, purification procedure, and the salification were performed by the same technique used in the previous reaction step. The purified compounds were fully characterized with the following structural features.

(*R,S*)-3,4-Dimethoxymethamphetamine Hydrochloride (17). Yield 55%; ^{1}H NMR δ: 1.09 (3H, *d*, CH_3), 2.54 (3H, *s*, NCH_3), 2.56 (1H, *dd*, *J* = 13.2; 8.2, CH_2), 3.07 (1H, *dd*, *J* = 13.2; 4.5, CH_2), 3.35 (1H, *m*, *CH*), 3.72 (3H, *s*, 3-OCH_3), 3.75 (3H, *s*, 4-OCH_3), 6.74 (1H, *dd*, *J* = 8.2; 1.8, H (6)), 6.86 (1H, *d*, *J* = 1.8, H (2)), 6.90 (1H, *d*, *J* = 8.2, H (5)), 8.90 (2H, b*s*, NH_2^+); ^{13}C NMR δ: *15.0* CH_3, *29.6* NCH_3, *37.9* CH_2, *55.3 CH*, *55.4* (2×OCH_3), *111.8*, *112.9* C (2) and C (5), *121.3* C (6), 128.8 C (1), 147.7 C (3), 148.7 C (4); EI-MS *m/z* (%): 210 ($M^{+\bullet}$, 6), 152 (16), 107 (5), 72 (7), 58 (100); mp 118–120 °C (lit (*43*). mp 117–119 °C).

(*R,S*)-3,4-Dibenzyloxymethamphetamine Hydrochloride (18). Yield 42%; ^{1}H NMR δ: 1.04 (3H, *d*, CH_3), 2.53 (3H, *s*, NCH_3), 2.55 (1H, *dd*, *J* = 13.2; 8.4, CH_2), 3.03 (1H, *dd*, *J* = 13.2; 4.3, CH_2), 3.35 (1H, *m*, *CH*), 5.10 (2H, *s*, 3-OCH_2), 5.12 (2H, *s*, 4-OCH_2), 6.75 (1H, *dd*, *J* = 8.2; 1.9, H (6)), 6.99 (1H, *d*, *J* = 2.0, H (2)), 7.01 (1H, *d*, *J* = 8.2, H (5)), 7.29–7.46 (10H, *m*, phenyl), 8.74 (2H, b*s*, NH_2^+); ^{13}C NMR δ: *15.0* CH_3, *29.7* NCH_3, *37.9* CH_2, *55.3 CH*, *70.1* (2×OCH_2), *114.5, 115.7* C (2) and C (5), *121.9* C (6), *127.5-128.4* (10×*C*HAr), 129.4 C (1), 137.2, 137.4 (2×*C*Ar), 147.2 C (3), 148.1 C (4); EI-MS *m/z* (%): 361 ($M^{+\bullet}$, 5), 304 (22), 181 (4), 91 (46), 65 (7), 58 (100); mp 152–155 °C.

General Synthetic Procedure for the O-Demethylation. The process of *O*-demethylation to obtain the phenolic derivatives (**19**–**21**) was based on a method described earlier (*47*, *49*). The first step was the transformation of the hydrochloride salts in the respective free base amines, by dissolving them in water, making them alkaline with NH_3 solution, and extracting with dichloromethane. The di or trihydroxilated compounds **12**, **14**, and **17** (4.5 mmol) were then dissolved in anhydrous dichloromethane (50 mL) in an inert atmosphere (N_2) and at −60 °C. To this solution, boron tribromide (13 mL of 1 M solution in dichloromethane, 13 mmol) was added, and the reaction was kept at − 60 °C for 10 min and then allowed to reach room temperature for 4 h. The reaction was quenched by cautious addition of methanol (10 mL), and the solvent evaporated yielding a residue of the hydrobromide salt. Compound **19** was obtained as an almost white solid after recrystallization with acetonitrile. Compound **20** was recrystallized from dichloromethane as a white solid that quickly turns into a

dark oil at room temperature and when exposed to air. The data obtained was in accordance with that described in the literature (*10*−*13*).

(*R*,*S*)-3,4-Dihydroxyamphetamine Hydrobromide (19). Yield 57%; ^{1}H NMR δ: 1.08 (3H, *d*, CH_3), 2.46 (1H, *dd*, J = 13.4; 8.8, CH_2), 2.77 (1H, *dd*, J = 13.4; 5.4, CH_2), 3.30 (1H, *m*, *CH*), 6.46 (1H, *dd*, J = 8.0; 1.9, H (6)), 6.59 (1H, *d*, J = 1.9, H (2)), 6.68 (1H, *d*, J = 8.0, H (5)), 7.78 (3H, bs, NH_3^+), 8.85 (2H, bs, 2×*OH*); ^{13}C NMR δ: *17.6* CH_3, *39.6* CH_2, *48.3* *CH*, *115.7*, *116.5* C (2) and C (5), *119.9* C (6), 127.2 C (1), 144.2 C (3), 145.2 C (4); EI-MS *m*/*z* (%):168 ($M^{+\bullet}$, 8), 151 (12), 124 (42), 123 (70), 107 (8), 84 (62), 80 (62), 79 (21), 77 (97), 66 (100); mp 189−192 °C (lit (*10*). mp 193−195 °C).

(*R*,*S*)-2,4,5-Trihydroxyamphetamine Hydrobromide (20). Yield 65%; ^{1}H NMR δ: 1.06 (3H, *d*, CH_3), 2.50 (1H, *dd*, J = 13.3; 8.6, CH_2), 2.70 (1H, *dd*, J = 13.3; 5.5, CH_2), 3.38 (1H, *m*, *CH*), 6.34 (1H, *s*, H (2)), 6.44 (1H, *s*, H (5)), 7.74 (3H, bs, NH_3^+), 8.80 (3H, bs, 3×*OH*); ^{13}C NMR δ: *17.8* CH_3, *34.7* CH_2, *47.3* *CH*, *103.7* C (5), 112.3 C (1), *117.9* C (2), 137.6 C (6), 144.6 C (3), 147.9 C (4); EI-MS *m*/*z* (%): 183 ($M^{+\bullet}$, 4), 163 (14), 140 (5), 84 (77), 66 (100).

General Synthetic Procedure for the O-Debenzylation. The synthesis was carried out by catalytic hydrogenolysis of compounds **15** and **18** as described earlier (*46*). In a flask containing Argon and 10% Pd/C (300 mg) previously wetted with dry methanol, a solution of **15** and **18** (2.5 mmol) in methanol (30 mL) was added. The mixture was then hydrogenated catalytically in a PARR pump, at room temperature and at 40 psi until no more hydrogen was consumed, and the reaction ended (approximately 2 h). The suspension was filtered by suction to eliminate Pd/C, and methanol was partially evaporated, HCl was added to form the hydrochloride salt of the catecholic compounds. Acetonitrile was used as the recrystallization solvent and compound **21** was obtained as a light brownish oil and used directly.

(*R*,*S*)-3,4-Dihydroxymethamphetamine Hydrochloride (21). Yield 72%; ^{1}H NMR δ: 1.06 (3H, *d*, CH_3), 2.49 (3H, *s*, NCH_3), 2.53 (1H, *dd*, J = 13.2; 8.3, CH_2), 2.98 (1H, *dd*, J = 13.2; 4.2, CH_2), 3.33 (1H, *m*, *CH*), 6.45 (1H, *dd*, J = 8.0; 1.9, H (6)), 6.60 (1H, *d*, J = 1.9, H (2)), 6.67 (1H, *d*, J = 8.0, H (5)), 8.03 (2H, bs, 2×*OH*), 8.92 (2H, bs, NH_2^+); ^{13}C NMR δ: *14.9* CH_3, *29.6* NCH_3, *37.8* CH_2, *55.6* *CH*, *115.8*, *116.7* C (2) and C (5), *120.0* C (6), 127.3 C (1), 144.1 C (3), 145.3 C (4); EI-MS *m*/*z* (%): 180 ($M^{+\bullet}$, 8), 166 (13), 151 (6), 123 (57), 105 (12), 91 (11), 86 (100), 77 (53), 66 (24).

Biological Methods. Culture of Undifferentiated PC12 Cells. PC12 cells, derived from a pheochromocytoma of the rat adrenal medulla, were cultured in RPMI 1640 medium (with l-glutamine and HEPES) supplemented with 10% (v/v) horse serum, 5% (v/v) fetal bovine serum (FBS), 50 U/mL penicillin, and 50 mg/mL streptomycin (final pH at about 7.4), as described before (*50*).

Cultures were preserved in 75 cm^2 flasks at 37 °C in a humidified incubator containing 95% air and 5% CO_2, and passed at least twice a week. The cells were plated on poly-L-lysine-coated multiwells at a density of 100 000 cells/cm^2 for MTT assays. In what is related with the study of chromatin condensation, the cells were plated in coverslips pre-coated with poly-L-lysine at a density of 180 000 cells/cm^2. The cells were additionally incubated with MDMA and its metabolites (placed as aqueous solutions) for more 24 h.

Analysis of Cell Viability. Cell viability was measured by the 3-(4,5-dimethylthiazol-2-yl)-2,5-diphenyltetrazolium bromide (MTT) reduction assay (*51*). Following the incubation of the cells for 24 h with the tested compounds, they were washed with sodium solution (in mM:140 NaCl, 5 KCl, 1 $MgCl_2$, 1 NaH_2PO_4, 1.5 $CaCl_2$, 5.6 glucose, and 20 HEPES (pH 7.4)) and incubated further with 0.2 mL of MTT solution (0.5 mg/mL dissolved in sodium solution containing 1.0 mM of $CaCl_2$) for 2.5 h. The blue formazan precipitate, produced after the reduction of MTT by cellular dehydrogenases, was resuspended and dissolved after addition of 0.2 mL of acidic isopropanol (0.04 M of HCl). The capacity of treated cells in reducing the tetrazolium salt was expressed as a percentage of absorbance in control cells (ELISA microplate reader at 570 nm).

Analysis of Chromatin Condensation. The fluorescent probes SYTO-13 and PI (propidium iodide) were used to evaluate the morphological evidence of cell death by necrosis and/or apoptosis, after preincubation of the cells with the compounds in a concentration close to IC_{50}.

Necrosis and apoptosis were evaluated concomitantly on cultured PC12 cells after double fluorescence staining using vital fluorescence dyes SYTO-13 (a permeant intercalating probe that labels RNA and DNA in living cells with an UV-excited green-colored emission) and propidium iodide (a nonpermeant intercalating probe, which is excluded from viable cells with an UV-excited red emission). Normal nuclei exhibited loose chromatin colored green by SYTO-13; apoptotic nuclei exhibited condensed green-colored chromatin (postapoptotic necrosis or secondary apoptosis (*52*) was characterized by nuclei exhibiting the same apoptotic morphological features, but with red colored chromatin); necrotic cells exhibited red-colored nuclei with loose chromatin.

The cells were loaded for 3 min with sodium solution containing SYTO-13 (4 μM) and PI (4 μg/mL). The cells were then visualized and counted by fluorescence microscopy in a Nikon diaphot microscope equipped with a Xenon lamp and a FX 64 Omega Optical triple filter. Apoptotic and necrotic cells were scored by counting at least 200 nuclei in four or more random different fields in triplicates from three different experiments.

Statistical Analysis. Data presented are the mean ±SEM from the number of experiments indicated in the Figure legends, performed in triplicate. For the comparison of MTT reduction between treated cells and controls, we performed one-way statistical analysis of variance (ANOVA) followed by the Tukey−Kramer post-hoc test. For the analysis of chromatin condensation, statistical analysis was performed by the Kruskal−Wallis test followed by the Mann−Whitney multiple comparison with Bonferroni correction. In both cases, significance was accepted at $p < 0.05$.

Results and Discussion

Chemistry. MDMA and its major metabolites are ring-substituted phenethylamine derivatives structurally related to psychomotor stimulant amphetamines and the hallucinogen mescaline.

The total synthesis of the drug and its main metabolites was based on the general pathway presented in Figure 2.

Briefly, the synthesis of the target compounds was performed in a straightforward manner, starting from the appropriate substituted benzaldehydes (**1**−**5**), which were converted into the corresponding phenylisopropylamines (**11**−**15**) *via* β-methyl-β-nitrostyrenes (**6**−**10**) intermediates. First, a Knoevenagel condensation between the aldehyde, with the corresponding aromatic substitution pattern, and nitroethane was carried out, yielding the nitrostyrene derivatives (*53*). These compounds were then reduced to the unsaturated primary amines by lithium aluminum hydride ($LiAlH_4$). When necessary, the subsequent *N*-methylation of the amphetamine derivatives **11**, **12**, and **15** was accomplished by a two-step reaction path, beginning with the treatment with ethylchloroformate to provide the *N*-formyl derivatives followed by a reduction with $LiAlH_4$ to yield the designed *N*-methylated products (**16**−**18**). Finally and in order to obtain the phenolic amphetamine analogous (**19**−**21**), compounds **12**, **14**, and **17** were *O*-demethylated after reaction with boron tribromide (BBr_3).

Prior to the characterization procedures and biological assays, all of the compounds containing an amine group were converted to their hydrochloride or hydrobromide salts, according to the employed synthetic route and/or stability of the final compound.

Derivative **13** (4-hydroxy-3-methoxyamphetamine), as a hydrochloride, was also prepared in fairly good yield by

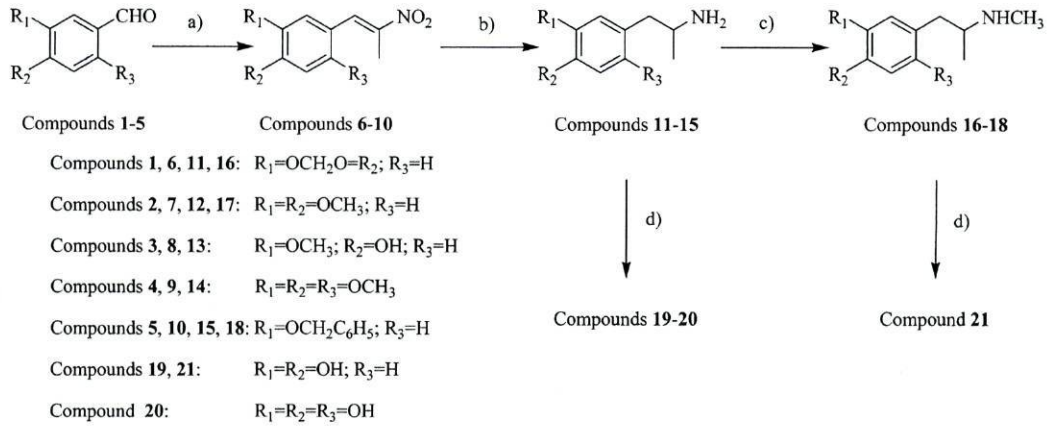

Figure 2. General synthetic procedure for MDMA and its metabolites. Chemical conditions: (a) $EtNO_2$, NH_4CH_3COO, reflux; (b) $LiAlH_4$, THF, reflux; (c) 1. $ClCOOC_2H_5$, H_2O, NaOH, 0 °C; 2. $LiAlH_4$, THF, reflux; (d) for the methylated compounds (**12**, **14**, **17**): BBr_3, CH_2Cl_2, −60 °C; for the benzylated compounds (**15**, **18**): H_2, Pd/C, MeOH. See Experimental Procedures.

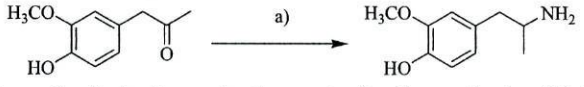

Figure 3. Reductive amination route for the synthesis of 3-*O*-Me-α-MeDA (**13**). Chemical conditions: (a) ammonium acetate (NH_4CH_3COO) and sodium cyanoborohydride ($NaCNBH_3$) in methanol (24 h/rt/N_2/pH 6).

reductive amination of the ketone 4-hydroxy-3-methoxyphenylacetone (Figure 3) (*10*).

The synthetic approach leading to the phenolic compounds **19**–**21** requires protection/deprotection steps to prevent alleged side reactions. Because the process of deprotection and following purification seems to be a limitative key step of the designed synthetic procedure, it was interesting to study different strategies to synthesize compounds **19** and **21** with the main goal of improving the overall yield. For the protection of the catechol of the starting material (3,4-dihydroxybenzaldehyde), the following protecting groups were used: benzyl (Bn or -$CH_2C_6H_5$), methoxymethyl (MOM), tetrahydropyranyl (THP), and di-*tert*-butyldichlorosilyl (DTBS) ethers (*54*). The yields of these protection reactions were not significantly different, except for benzylic ether, which seems to be a good alternative because the benzylated benzaldehyde was obtained in good yield, and the deprotected final amines (α-MeDA and *N*-Me-α-MeDA) can be easily achieved by hydrogenolysis (a selective, apparently smoother and cleaner reaction compared to that of boron tribromide demethylation; see Experimental Procedures) (Figure 4).

All of the synthesized compounds were identified by both NMR and electron impact mass spectroscopy (EI-MS), and their purity was confirmed using the HPLC systems reported in Experimental Procedures.

Biological Assays: Analysis of Cell Viability. The putative neurotoxic effects of this series of compounds were evaluated by two different types of assays: (i) analysis of PC12 cell viability after incubation with increasing concentrations of the tested compounds and (ii) analysis of chromatin fragmentation/condensation after incubation of PC12 cells with a concentration close to the respective IC_{50} values (concentration of the drug that decreases cell viability by 50%). The cell line selected for the cytotoxicity studies is derived from a catecholamine-secreting tumor (pheochromocytoma) of rat adrenal medulla, which upon exposure to nerve growth factor (NGF) differentiates into a neuronal phenotype similar to that of the postganglionic sympathetic (catecholaminergic) nerve-like cell (*34*). Undifferentiated PC12 cells are commonly used for the screening of cytotoxicity and to study the disruption by neurotoxicants related to various aspects of neuronal physiology and biochemistry (*55*, *56*). It is worthwhile to mention that undifferentiated PC12 cells release more dopamine and less acetylcholine than differentiated cells (*34*).

Studies of cell toxicity were performed by analyzing cell-reducing capacity through the examination of the ability of these cells to reduce MTT (3-(4,5-dimethylthiazol-2-il)-2,5-diphenyltetrazolium). The MTT measures the reducing capacity of the cells, a parameter dependent upon the maintenance of cellular metabolic function, thus reflecting cell viability and/or proliferation. This tetrazolium salt (yellow and soluble) is reduced to formazan (blue and insoluble) by active cellular dehydrogenases. The number of metabolically viable cells in the culture was directly correlated with the amount of formazan dye formed.

Changes in cell viability caused by exposure to MDMA or its five metabolites were evaluated and compared as shown in Figure 5. All of the compounds induced a dose-dependent decrease in cell viability after 24 h of incubation; however, the catechol-containing metabolites (**19**–**21**) were considerably more toxic to PC12 cells because their IC_{50} values are significantly lower than the ones of MDA and MDMA, as determined by the analysis of all of the IC_{50} values: IC_{50} ~158 μM (*N*-Me-α-MeDA) < IC_{50} ~247 μM (6-OH-α-MeDA) < IC_{50} ~416 μM (α-MeDA) ≪ IC_{50} ~3365 μM (MDA) < IC_{50} ~4464 μM (MDMA) < IC_{50} ~7526 μM (3-*O*-Me-α-MeDA), decreasing order of toxicity. The range of concentrations achieved is believed to occur *in vivo* after repeated drug usage (*57*).

Evaluation of Necrosis and Apoptosis. Apoptosis has been shown to play a key role in the cytotoxic effects of many drugs, including amphetamine derivatives (*36*, *37*). However, the precise role of apoptosis in the toxic effects of MDMA and its metabolites in dopaminergic cells has not been fully accomplished. Thus, upon analysis of cell viability, we attempted to characterize cell death as apoptotic and/or necrotic, by studying the morphological changes of the nuclei.

We analyzed the fragmentation/condensation of chromatin, a characteristic feature of apoptosis, by using the SYTO-13/PI assay. Apoptotic cells resulted in shrunken, brightly green fluorescent nuclei due to SYTO-13 labeling, showing condensed chromatin with high fluorescence compared with nonapoptotic cells. Simultaneous labeling with propidium iodide (PI), a non-permeable fluorescent dye, excluded from the living cells, allowed the detection of nucleic acids in intact nuclei of membrane-damaged cells (red fluorescence), characteristic of necrotic cell death. Late or secondary apoptosis was characterized by SYTO-13 plus PI labeling of fragmented/condensed nuclei.

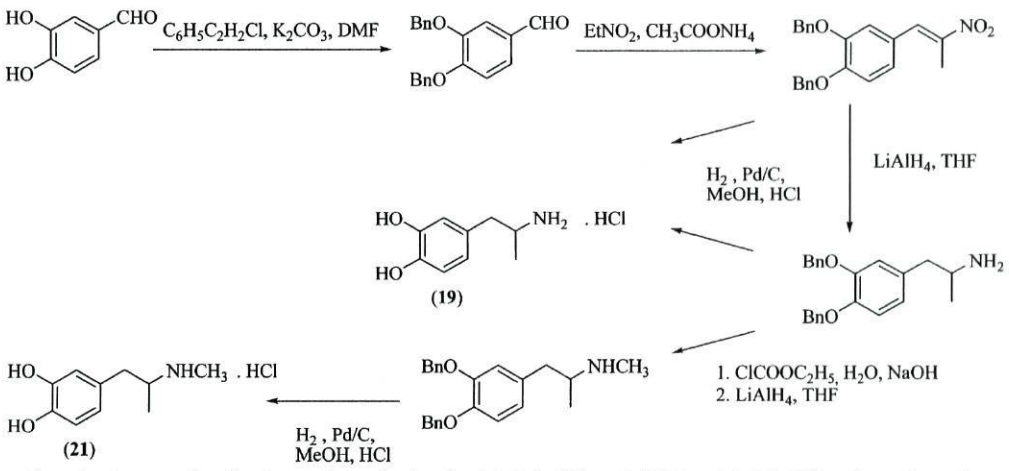

Figure 4. Proposed synthetic strategies for the total synthesis of α-MeDA (**19**) and *N*-Me-α-MeDA (**21**) using a benzyl group to protect the catechol.

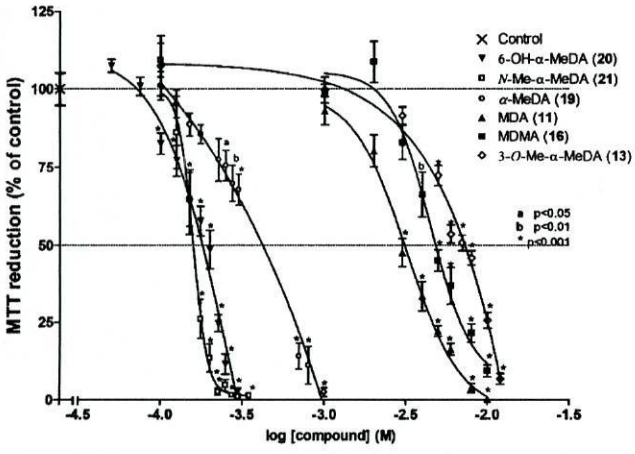

Figure 5. Dose–response curves of MDMA and metabolite-induced cytotoxicity. PC12 cells were incubated with increasing concentrations of the compounds for 24 h, and the toxic effects were evaluated by the MTT reduction assay (percentage of MTT reduction relative to the control). Data are the mean ± SEM of at least three experiments performed in triplicate.

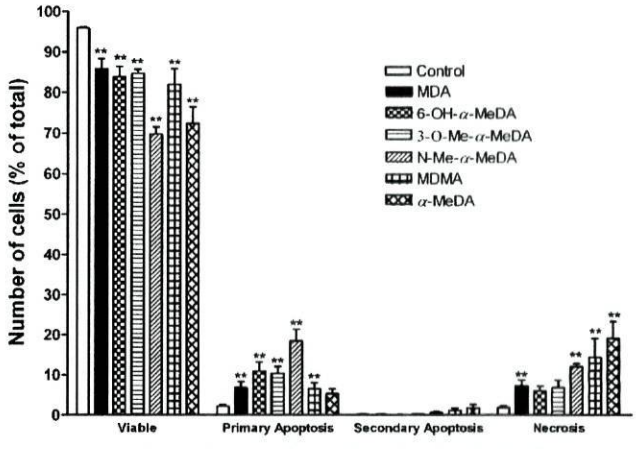

Figure 6. Analysis of chromatin condensation in PC12 cells exposed to the six compounds: *N*-Me-α-MeDA, 6-OH-α-MeDA, α-MeDA (300 μM each), MDA, MDMA, and 3-*O*-Me-α-MeDA (3 mM each) incubated for 24 h. SYTO-13 and propidium iodide (PI) were used to evaluate apoptotic or necrotic cell death. Data are the mean ± SEM of three experiments performed in triplicate. Statistical significance compared to the control (in the absence of the drug): $^{**}p < 0.01$ with Bonferroni correction is considered very significant.

To determine the fraction of fragmented/condensed nuclei, PC12 cells were incubated with the compounds for 24 h in concentrations in the vicinity of the IC_{50} values as determined in Figure 5. Under these conditions, there was a decrease by 15 to 30% in the number of viable cells (Figure 6). It should be noted that the loss of cell-reducing capacity (ascertained by the MTT assay) may not correspond immediately to cell death, as evidenced by the SYTO13/PI assay. Cells may have lost metabolic activity before showing evidence of a loss of membrane integrity or nuclear fragmentation or condensation.

All of the compounds tested, with the exception of α-MeDA, induced fragmentation and condensation of chromatin and, therefore, apoptosis when compared to the control, as observed by the labeling with SYTO-13 (Figure 6). MDMA, MDA, *N*-Me-α-MeDA, and α-MeDA revealed an increase of necrotic cell death compared to the control.

By comparing the relative proportion of the cells showing features of necrosis and apoptosis for each compound, it is important to highlight that although in a relatively small percentage *N*-Me-α-MeDA causes cell death mainly by apoptosis (by 6%), MDMA (by 8%) and α-MeDA (by 13.7%) cause cell death mostly by necrosis, whereas the other compounds did not induce a predominant type of cell death.

Comparison of features of apoptosis and necrosis observed for MDMA and its metabolites revealed no significant differences between the groups and, therefore, no major changes in the profile of cell death evoked by all of the compounds tested.

Structure–Oxidation–Toxicity Relationships. Because cytotoxic effects are frequently ascribed to be related to the occurrence of redox reactions, standard redox potentials of MDMA and its metabolites were determined in order to establish the relationship between the observed cytotoxicity and the oxidative profile. The electrochemical behavior of the compounds was studied at physiological pH 7.3, at a glassy carbon working electrode (GCE) using differential pulse, cyclic, and square wave voltammetry.

From the analysis of the electrochemical data of the drug and metabolites, it was possible to clearly distinguish two sets of compounds (Figure 7): one containing the metabolites with a catecholic group (α-MeDA (**19**), 6-OH-α-MeDA (**20**), *N*-Me-α-MeDA (**21**)) and the other including the compounds with a substituted catechol function (MDA (**11**), 3-*O*-Me-α-MeDA (**13**), MDMA (**16**)).

For 6-OH-α-MeDA (**20**), *N*-Me-α-MeDA (**21**), and α-MeDA (**19**), two well-defined anodic peaks were observed at physiological pH using differential pulse voltammetry (Figure 7a). The first peak is related to the oxidation of the catechol group to *o*-quinone and occurs at $E_p = -0.11$ V for compound **20**

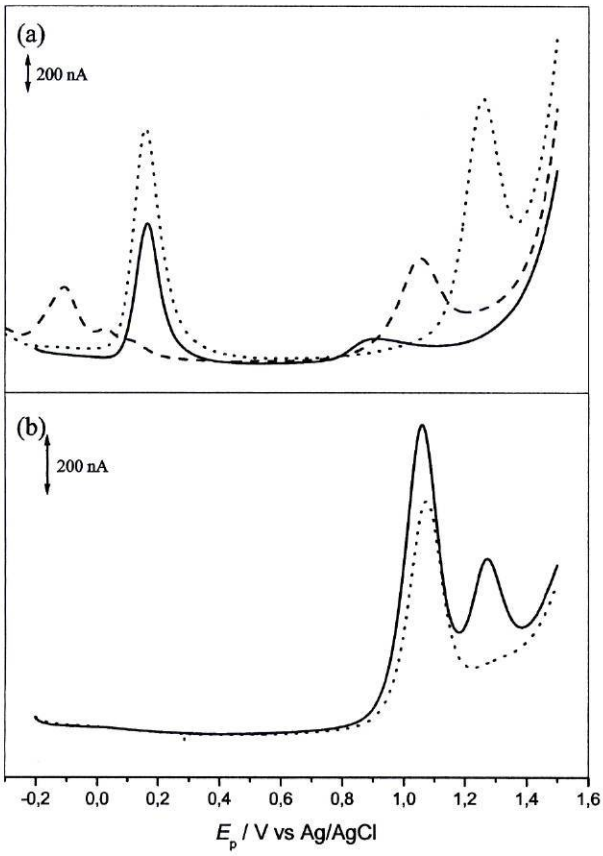

Figure 7. Differential pulse voltammograms in pH 7.3 phosphate supporting electrolyte of 0.1 mM solutions of (a) (---) 6-OH-α-MeDA, (·····) *N*-Me-α-MeDA and (—) α-MeDA; (b) (—) MDMA and (·····) MDA. Scan rate 5 mVs^{-1}.

and +0.16 V for compounds **19** and **21**. Cyclic and square wave voltammograms recorded for these compounds clearly show the reversible character of this first electron-transfer oxidation reaction, which is consistent with the formation of quinonoid structures. The second anodic wave occurring at more positive potentials (Figure 7a) could be due to the oxidation of the quinone side-chain. MDMA (**16**) presents two well-defined anodic peaks at physiological pH using differential pulse voltammetry (Figure 7b). The first, E_p = +1.06 V, is due to the removal of one electron from the aromatic ring with the formation of a radical cation stabilized by the substituents, and the second peak, E_p = +1.27 V, could be attributed to the oxidation of the secondary amine present in the structure. MDA (**11**) showed only a single and well-defined anodic wave at physiological pH, E_p = +1.07 V (Figure 7b) attributed also to the removal of one electron from the aromatic ring, the same oxidation process as in MDMA. For 3-*O*-Me-α-MeDA (**13**), a well-defined anodic peak is observed at physiological pH using differential pulse voltammetry (Figure 8). This peak, E_p = +0.43 V, is due to the oxidation of the phenolic group. An indistinct second wave also appears at *ca.* +1.15 V (Figure 8), which might correspond to the formation of the radical aromatic cation.

Regarding the redox potentials obtained for the compounds, which are summarized in Table 1, it is possible to depict a clear correlation: all of the catechol-containing metabolites are more easily oxidized and remarkably more cytotoxic (Figure 5), a feature that could be intrinsically related with the *in situ* formation of electrophilic quinones. In fact, the obtained electrochemical data allow us to show that the catecholic metabolites share a common oxidative profile with the formation of quinones as primary oxidation products, which are highly

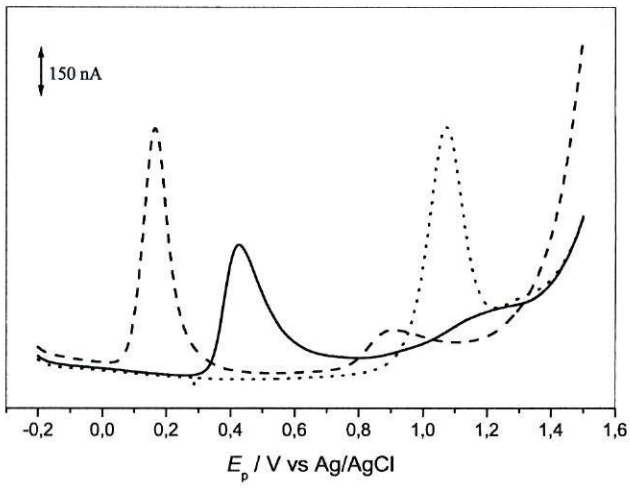

Figure 8. Differential pulse voltammograms in pH 7.3 phosphate supporting electrolyte of 0.1 mM solutions of (---) α-MeDA, (·····) MDA and (—) 3-*O*-Me-α-MeDA. Scan rate 5 mVs^{-1}.

Table 1. Redox Potential Values of MDMA and Its Metabolites

compound	peak	E_p/V vs Ag/AgCl
α-MeDA (**19**)	I	0.16
	II	0.89
6-OH-α-MeDA (**20**)	I	−0.11
	II	1.05
N-Me-α-MeDA (**21**)	I	0.16
	II	1.25
3-*O*-Me-α-MeDA (**13**)	I	0.43
	II	1.15
MDMA (**16**)	I	1.06
	II	1.27
MDA (**11**)	I	1.07

reactive with respect to nucleophiles. The quinones can undergo an intracyclization process through the amine group of the side-chain, as an available nucleophile, leading to the formation of leucoaminochromes. Subsequently, these heterocyclic compounds can be easily oxidized to aminochromes. Moreover, the high predisposition to oxidation of these catecholic compounds, traduced by its redox potential, can also result in its autoxidation, leading to the formation of extracellular hydrogen peroxide and consequently to an increase in cytotoxicity.

Conclusion

The obtained data clearly indicate that some of the metabolites of MDMA cause stronger effects on PC12 cells than the parent compound, as shown by the analysis of their cytotoxic profiles. Given the large ammount of data implicating MDMA in neurodegeneration, the present results support the hypothesis that the mechanism of neurotoxicity can be related with biotransformation after the administration of the drug.

Although *N*-Me-α-MeDA, 6-OH-α-MeDA, and α-MeDA have not been undoubtedly established as *in vivo* neurotoxic metabolites of MDMA, it was demonstrated that these metabolites can account for the toxic properties of this drug. Note that *N*-Me-α-MeDA, a metabolite that attains human plasma concentrations similar to those of MDMA (*58*), was the most toxic metabolite, a result that is in agreement with toxicological data obtained in cardiomyocytes and hepatocytes (*9*, *59*). It is possible that adducts of these catecholic-containing compounds and major oxidative metabolites of MDMA could be generated and participate in its toxic effects (*60*–*62*).

Comparing the cytotoxicity of 6-OH-α-MeDA and α-MeDA, we conclude that the introduction of an hydroxyl group at the

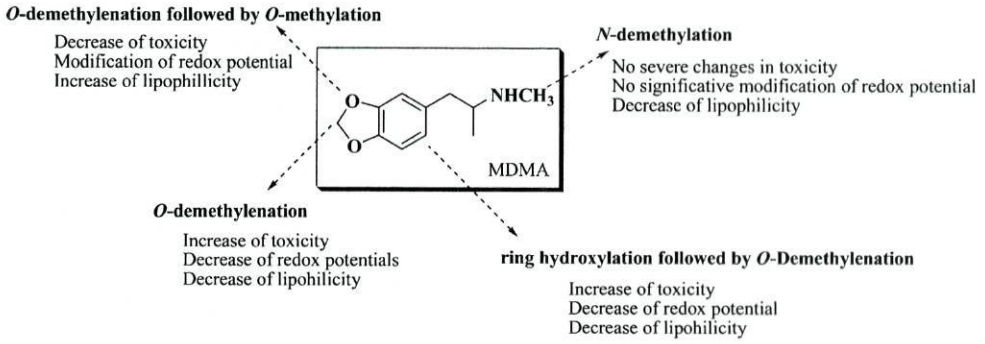

Figure 9. Consequences of structural modifications on toxicity and physicochemical properties of "ecstasy" (MDMA) and its metabolites.

ortho position to the amine side chain leads to an increase in cytotoxic properties. 6-OH-α-MeDA was previously described as neurotoxic because it has structural similarities with 6-hydroxydopamine, a potent neurotoxin that causes long-term alterations in central monoaminergic systems (*13*, *19*).

All compounds that possess a substituent in the catechol group seem to be less toxic than those with free aromatic hydroxyl groups. The ability of these latter compounds to form reactive *o*-quinones, leading to the formation of reactive species, is thought to represent a critical step in their toxicity, as suggested by previous studies (*63*, *64*). Furthermore, the oxidation of the metabolites to their respective aminochromes, which are toxic, must also be taken in consideration (*9*). Electrochemical results fully support and explain the differences observed in terms of the cytotoxicity of the compounds.

N-Methylation enhances cytotoxicity on PC12 cells. In contrast, O-methylation of the catecholamine-type compounds seems to be a detoxification step in the metabolism of MDMA because the resulting compound (3-*O*-Me-α-MeDA) is significantly less toxic than the parent compound and the catecholic precursors that will undergo O-methylation by the action of COMT.

It is important to notice that the experimental IC_{50} values obtained in the present work (ranging from 150 to 7000 μM) are in agreement with other similar published *in vitro* studies (*59*, *61*, *62*), particularly for the more toxic metabolites.

It was undoubtedly established that metabolism leads to changes of the redox potential of the parent compound. However, the authors believe that another physicochemical parameter, namely, lipophilicity, also contributes to its toxicity because a correlation was found between the partition coefficients of the metabolites and their toxicity as depicted in Figure 9.

The data on chromatin fragmentation/condensation reveal that the majority of MDMA metabolites significantly increase cell death by apoptosis. Programmed cell death was previously proposed to be involved in the neurotoxic effects of MDMA because the drug induces apoptosis on serotonergic and neocortical neurons (*36*, *37*). If one compares the metabolites and the drugs used recreationally (MDMA and MDA), the overall effects of the compounds as apoptosis inducers are quite similar, and their toxic effects in undifferentiated PC12 cells seem to be associated with the induction of apoptotic cell death. Nevertheless, it is important to note that some metabolites also led to significant death by necrosis. Accordingly, further experimental approaches are needed to clarify the precise cytotoxic mechanisms.

Systemic metabolism of MDMA seems to be needed for the occurrence of neurotoxicity, but the nature of any putative toxic metabolite is still unknown. Because drug metabolites are usually more hydrophilic than their parent drug, specific transporters are presumably needed to take up the neurotoxic metabolite into the brain (*10*, *23*). These results provide evidence that the metabolism of MDMA is a key factor for its toxicity and may prove to be useful in elucidating the amphetamine-like drug's putative activities.

Acknowledgment. N.M. and T.O. acknowledge financial support from FCT−Ph.D. fellowships PRAXIS XXI/BD/18520/98 and SFRH/BD/10910/2002. N.M. also acknowledges FCT-I&D N° 226/94 and POCTI (QCA III) for their support.

References

(1) Strote, J., Lee, J. E., and Wechsler, H. (2002) Increasing MDMA use among college students: Results of a national survey. *J. Adolesc. Health 30*, 64−72.

(2) Schifano, F., Oyefeso, A., Corkeri, J., Cobain, K., Jambert-Gray, R., Martinotti, G., and Ghodse, A. H. (2003) Death rates from ecstasy (MDMA, MDA) and polydrug use in England and Wales 1996−2002. *Hum. Psychopharmacol. Clin. Exp. 18*, 519−524.

(3) Meyer, J. S., Grande, M., Johnson, K., and Ali, S. F. (2004) Neurotoxic effects of MDMA ("ecstasy") administration to neonatal rats. *Int. J. Dev. Neurosci. 22*, 261−271.

(4) Cunningham, M. (1997) Ecstasy-induced rhabdomyolysis and its role in the development of acute renal failure. *Intensive Crit. Care Nurs. 13*, 216−223.

(5) Montiel-Duarte, C., Ansorena, E., López-Zabalza, M. J., Cenarruzabeitia, E., and Iraburu, M. J. (2004) Role of reactive oxygen species, glutathione and NF-κ B in apoptosis induced by 3, 4-methylenedioxymethamphetamine ("Ecstasy") on hepatic stellate cells. *Biochem. Pharmacol. 47*, 1151−1156.

(6) O'Cain, P. A., Hletko, S. B., Ogden, B. A., and Varner, K. J. (2000) Cardiovascular and sympathetic responses and reflex changes elicited by MDMA. *Physiol. Behav. 70*, 141−148.

(7) Testa, B., and Soine, W. (2003) Principles of Drug Metabolism. In *Burger's Medicinal Chemistry and Drug Discovery*, (Abraham, D. J., Ed.) 6th ed., Vol. 2, pp 431−498, Wiley-Interscience, Hoboken, NJ.

(8) Forsling, M. L., Fallon, J. K., Shah, D., Tilbrook, G. S., Cowan, D. A., Kicman, A. T., and Hutt, A. J. (2002) The effect of 3, 4-methylenedioxymethamphetamine (MDMA, "ecstasy") and its metabolites on neurohypophysial hormone release from the isolated rat hypothalamus. *Br. J. Pharmacol. 135*, 649−656.

(9) Carvalho, M., Remião, F., Milhazes, N., Borges, F., Fernandes, E., Monteiro, M. C., Gonçalves, M. J., Seabra, V., Amado, F., Carvalho, F., and Bastos, M. L. (2004) Metabolism is required for the expression of Ecstasy-induced cardiotoxicity in vitro. *Chem. Res. Toxicol. 17*, 623−632.

(10) Monks, T. J., Jones, D. C., Bai, F., and Lau, S. S. (2004) The role of metabolism in 3, 4-(±)-methylenedioxyamphetamine and 3, 4-(±)-methylenedioxymethamphetamine (ecstasy) toxicity. *Ther. Drug Monit. 26*, 132−136.

(11) Lim, H. K., and Foltz, R. L. (1988) In vivo and in vitro metabolism of 3, 4-(methylenedioxy)methamphetamine in the rat: Identification of metabolites using an ion trap detector. *Chem. Res. Toxicol. 1*, 370−378.

(12) Lim, H. K., and Foltz, R. L. (1991) Ion trap tandem mass spectrometric evidence for the metabolism of 3, 4-(methylenedioxy)methamphetamine to the potent neurotoxins 2,4,5-trihydroxymethamphetamine and 2,4,5-trihydroxyamphetamine. *Chem. Res. Toxicol. 4*, 626−632.

(13) Ma, S., Lin, L., Raghavan, R., Cohenour, P., Lin, P. Y. T., Bennett, J., Lewis, R. J., Enwall, E. L., Kostrzewa, R., Lehr, R. E., and Blank, C. L. (1995) In vivo and in vitro studies on the neurotoxic potential of 6-hydroxydopamine analogs. *J. Med. Chem. 38*, 4087−4097.

(14) Hayes, J., Tipton, K. F., Bianchi, L., and Della Corte, L. (2001) Complexities in the neurotoxic actions of 6-hydroxydopamine in relation to the cytoprotective properties of taurine. *Brain Res. Bull. 55*, 239–245.

(15) Colado, M. I., Williams, J. L., and Green, A. R. (1995) The hyperthermic and neurotoxic effects of "ecstasy" (MDMA) and 3, 4-methylenedioxyamphetamine (MDMA) in the Dark Agouti (DA) rat, a model of the CYP2D6 poor metabolizer phenotype. *Br. J. Pharmacol. 115*, 1281–1289.

(16) Armstrong, B. D., and Noguchi, K. K. (2004) The neurotoxic effects of 3, 4-methylenedioxymethamphetamine (MDMA) and methamphetamine on serotonin, dopamine, and GABA-ergic terminals: An in-vitro autoradiographic study in rats. *Neurotoxicology 25*, 905–914.

(17) Itzhak, Y., and Achat-Mendes, C. (2004) Methamphetamine and MDMA (ecstasy) neurotoxicity: 'of mice and men'. *IUBMB Life 56*, 249–255.

(18) Johnson, M., Elayan, I., Hanson, G. R., Foltz, R. L., Gibb, J. W., and Lim, H. K. (1992) Effects of 3, 4-dihydroxymethamphetamine and 2, 4, 5-trihydroxymethamphetamine, two metabolites of 3, 4-methylenedioxymethamphetamine, on central serotonergic and dopaminergic systems. *J. Pharmacol. Exp. Ther. 261*, 447–453.

(19) Zhao, Z., Castagnoli, N., Jr., Ricaurte, G. A., Steele, T., and Martello, M. (1992) Synthesis and neurotoxicological evaluation of putative metabolites of the serotonergic neurotoxin 2-(methylamino)-1-[3,4-(methylenedioxy)phenyl]propane [(methylenedioxy)methamphetamine]. *Chem. Res. Toxicol. 5*, 89–94.

(20) Bai, F., Lau, S. S., and Monks, T. J. (1999) Glutathione and N-acetylcysteine conjugates of α-methyldopamine produce serotonergic neurotoxicity: Possible role in methylenedioxyamphetamine-mediated neurotoxicity. *Chem. Res. Toxicol. 12*, 1150–1157.

(21) Ricaurte, G., Bryan, G., Strauss, L., Seiden, L., and Schuster, C. (1985) Hallucinogenic amphetamine selectively destroys brain serotonin nerve terminals. *Science 229*, 986–988.

(22) Ricaurte, G. A., Martello, A. L., Katz, J. L., and Martello, M. B. (1992) Lasting effects of (±)3,4-methylenedioxymethamphetamine (MDMA) on central serotonergic neurons in nonhuman primates: Neurochemical observations. *J. Pharmacol. Exp. Ther. 261*, 616–622.

(23) Lyles, J., and Cadet, J. L. (2003) Methylenedioxymethamphetamine (MDMA, ecstasy) neurotoxicity: Cellular and molecular mechanisms. *Brain Res. Rev. 42*, 155–168.

(24) Colado, M. I., Camarero, J., Mechan, A. O., Sanchez, V., Esteban, B., Elliot, J. M., and Green, A. R. (2001) A study of the mechanisms involved in the neurotoxic action of 3, 4-methylenedioxymethamphetamine (MDMA, 'ecstasy') on dopamine neurones in mouse brain. *Br. J. Pharmacol. 134*, 1711–1723.

(25) Colado, M. I., O'Shea, E., and Green, A. R. (2004) Acute and long-term effects of MDMA on cerebral dopamine biochemistry and function *Psychopharmacology 173*, 249–263.

(26) Davidson, C., Gow, A. J., Lee, T. H., and Ellinwood, E. H. (2001) Methamphetamine neurotoxicity: necrotic and apoptotic mechanisms and relevance to human abuse treatment. *Brain Res. Rev. 36*, 1–22.

(27) Jiménez, A., Jordá, E. G., Verdaguer, E., Pubill, D., Sureda, F. X., Canudas, A. M., Escubedo, E., Camarasa, J., Camins, A., and Pallàs, M. (2004) Neurotoxicity of amphetamine derivatives is mediated by caspase pathway activation in rat cerebellar granule cells. *Toxicol. Appl. Pharmacol. 196*, 223–234.

(28) Jayanthi, S., Ladenheim, B., Andrews, A. M., and Cadet, J. L. (1999) Overexpression of human copper/zinc superoxide dismutase in transgenic mice attenuates oxidative stress caused by methylenedioxymethamphetamine (ecstasy). *Neuroscience 91*, 379–1387.

(29) Esteban, B., O'Shea, E., Camarero, J., Sanchez, V., Green, A. R., and Colado, M. I. (2001) 3,4-Methylededioxymethamphetamine induces monoamino release, but not toxicity, when administered centrally at a concentration occuring following a peripherally injected neurotoxic dose. *Psychopharmacology 154*, 251–260.

(30) McCann, U., and Ricaurte, G. A. (1991) Major metabolites of (±)3, 4-methylenedioxyamphetamine (MDA) do not mediate its toxic effects on brain serotonin neurons. *Brain Res. 545*, 279–282.

(31) Yeh, S. Y., and Hsu, F.-L. (1991) The neurochemical and stimulatory effects of putative metabolites of 3,4-methylenedioxyamphetamine and 3,4-methylenedioxymethamphetamine in rats. *Pharmacol. Biochem. Behav. 39*, 787–790.

(32) Elayan, I., Gibb, J. W., Hanson, G. R., Foltz, R. L., Lim, H. K., and Johnson, M. (1992) Long-term alteration in the central monoaminergic systems of the rat by 2,4,5-trihydroxyamphetamine but not by 2-hydroxy-4,5-methylenedioxymethamphetamine or 2-hydroxy-4,5-methylenedioxyamphetamine. *Eur. J. Pharmacol. 221*, 281–288.

(33) Greene, L. A., and Tischler, A. S. (1982) PC12 pheochromocytoma cultures in neurobiological research. *Adv. Cell. Neurobiol. 3*, 373–414.

(34) Shafer, T. J., and Atchison, W. D. (1991) Transmitter, ion channel and receptor properties of pheochromocytoma (PC12) cells: A model for neurotoxicological studies. *Neurotoxicology 12*, 473–492.

(35) Lein, P., Silbergeld, E., Locke, P., and Goldberg, A. M. (2005) In vitro and other alternative approaches to developmental neurotoxicity testing (DNT). *Environ. Toxicol. Pharmacol. 19*, 735–744.

(36) Simantov, R., and Tauber, M. (1997) The abused drug MDMA (ecstasy) induces programmed death of human serotonergic cells. *FASEB J. 11*, 141–146.

(37) Stumm, G., Schlegel, J., Schäfer, T., Würz, C., Mennel, H. D., Krieg, J.-C., and Vedder, H. (1999) Amphetamines induce apoptosis and regulation of bcl-x splice variants in neocortical neurons. *FASEB J. 13*, 1065–1072.

(38) Parker, M. A., Marona-Lewicka, D., Kurrasch, D., Shulgin, A. T., and Nichols, D. E. (1998) Synthesis and pharmacological evaluation of ring-methylated derivatives of 3, 4-(methylenedioxy)amphetamine (MDA). *J. Med. Chem. 41*, 1001–1005.

(39) Naito, Y., Sugiura, M., Yamaura, Y., Fukaya, C., Yokoyama, K., Nakagawa, Y., Ikeda, T., Senda, M., and Fujita, T. (1991) Quantitative structure-activity relationship of catechol derivatives inhibiting 5-lipoxygenase. *Chem. Pharm. Bull. 39*, 1736–1745.

(40) Johnson, M. P., Frescas, S. P., Oberlender, R., and Nichols, D. E. (1991) Synthesis and pharmacological examination of 1-(3-methoxy-4-methylphenyl)-2-aminopropane and 5-methoxy-6-methyl-2-aminoindan: Similarities to 3,4-(methylenedioxy)methamphetamine (MDMA). *J. Med. Chem. 34*, 1662–1668.

(41) Monte, A. P., Marona-Lewicka, D., Cozzi, N. V., and Nichols, D. E. (1993) Synthesis and pharmacological examination of benzofuran, indan, and tetralin analogues of 3,4-(methylenedioxy)amphetamine. *J. Med. Chem. 36*, 3700–3706.

(42) Gairaud, C. B., and Lappin, G. R. (1953) The synthesis of ω-nitrostyrenes. *J. Org. Chem. 18*, 1–3.

(43) Morgan, P. H., and Beckett, A. H. (1975) Synthesis of some N-oxygenated products of 3,4-dimethoxyamphetamine and its N-alkyl derivatives. *Tetrahedron 31*, 2595–2601.

(44) Milhazes, N., Borges, F., Calheiros, R., and Marques, M. P. M. (2004) Identification of synthetic precursors of amphetamine-like drugs using Raman spectroscopy and *ab initio* calculations: β-Methyl-β-nitrostyrene derivatives. *Analyst 129*, 1106–1117.

(45) Ensslin, H. K., Maurer, H. H., Gouzoulis, E., Hermle, L., and Kovar, K.-A. (1996) Metabolism of racemic 3,4-methylenedioxyethylamphetamine in humans: Isolation, identification, quantification, and synthesis of urinary metabolites. *Drug Metab. Dispos. 24*, 813–820.

(46) Marshall, K. S., and Castagnoli, N. (1973) Absolute configuration of α-methyldopamine formed metabolically from α-methyldopa in man. *J. Med. Chem. 16*, 266–270.

(47) Chavdarian, C. G., Karashima, D., Castagnoli, N., and Hundley, H. K. (1978) Oxidative and cardiovascular studies on natural and synthetic catecholamines. *J. Med. Chem. 21*, 548–554.

(48) de Boer, D., Tan, L. P., Gorter, P., van de Wall, R. M. A., Kettenes-van den Bosch, J. J., Bruijn, E. A., and Maes, R. A. A. (1997) Gas chromatographic/mass spectrometric assay for profiling the enantiomers of 3,4-methylenedioxymethamphetamine and its chiral metabolites using positive chemical ionization ion trap mass spectrometry. *J. Mass Spectrom. 32*, 1236–1246.

(49) Bartholow, R. M., and Walaszek, E. J. (1976) 2,3-Dihydroxyphenethanolamine as an adrenergic agent. *J. Med. Chem. 19*, 189–190.

(50) Oliveira, M. T., Rego, A. C., Morgadinho, M. T., Macedo, T. R. A., and Oliveira, C. R. (2002) Toxic effects of opioid and stimulant drugs on undifferentiated PC12 cells. *Ann. N.Y. Acad. Sci. 965*, 487–496.

(51) Mosmann, T. (1983) Rapid colorimetric assay for cellular growth and survival: Application to proliferation and cytotoxicity assays. *J. Immunol. Methods 65*, 55–63.

(52) Nicotera, P., and Melino, G. (2004) Regulation of the apoptosis-necrosis switch. *Oncogene 23*, 2757–2765.

(53) Calheiros, R., Milhazes, N., Borges, F., and Marques, M. P. M. (2004) β-Nitrostyrene derivatives - a conformational study by combined Raman spectroscopy and ab initio MO calculations. *J. Mol. Struct. 692*, 91–106.

(54) Greene, T. W., and Wuts, P. G. M., Eds. (1999) Protective Groups in Organic Synthesis, 3rd ed., John Wiley & Sons, Inc., NY.

(55) Fornai, F., Lenzi, P., Frenzilli, G., Gesi, M., Ferrucci, M., Lazzeri, G., Biagioni, F., Nigro, M., Falleni, A., Giusiani, M., Pellegrini, A., Blandini, F., Ruggieri, S., and Paparelli, A. (2004) DNA damage and ubiquitinated neuronal inclusions in the substantia nigra and striatum of mice following MDMA (ecstasy). *Psychopharmacology (Berlin) 173*, 353–363.

(56) Hanrott, K., Gudmunsen, L., O'Neill, M. J., and Wonnacott, S. (2006) 6-Hydroxydopamine-induced apoptosis is mediated via extracellular auto-oxidation and caspase 3-dependent activation of protein kinase Cδ. *J. Biol. Chem. 281*, 5373–5382.

(57) Ricaurte, G. A., Yuan, J., and McCann, U. D. (2000) (±)3, 4-Methylenedioxymethamphetamine ('ecstasy')-induced serotonin neurotoxicity: studies in animals. *Neuropsychobiology 42*, 5–10.

(58) Segura, M., Ortuño, J., Farré, M., McLure, J. A., Pujadas, M., Pizarro, N., Llebaria, A., Joglar, J., Roset, P. N., Segura, J., and de la Torre, R. (2001) 3, 4-Dihydroxymethamphetamine (HHMA). A major in vivo 3, 4-methylenedioxymethamphetamine (MDMA) metabolite in humans. *Chem. Res. Toxicol. 14*, 1203−1208.

(59) Carvalho, M., Remião, F., Milhazes, N., Borges, F., Fernandes, E., Carvalho, F., and Bastos, M. L. (2004) The toxicity of *N*-methyl-α-methyldopamine to freshly isolated rat hepatocytes is prevented by ascorbic acid and *N*-acetylcysteine. *Toxicology 200*, 193−203.

(60) Miller, R. T., Lau, S. S., and Monks, T. J. (1995) Metabolism of 5-(glutathione-S-yl)-α-methyldopamine following intracerebroventricular administration to male Sprague-Dawley rats. *Chem. Res. Toxicol. 8*, 634−641.

(61) Carvalho, M., Hawsworth, G., Milhazes, N., Borges, F., Monks, T. J., Fernandes, E., Carvalho, F., and Bastos, M. L. (2002) Role of metabolites in MDA (ecstasy) induced nephrotoxicity: an *in vitro* study using rat and human renal proximal tubular cells. *Arch. Toxicol. 76*, 581−588.

(62) Carvalho, M., Milhazes, N., Borges, F., Fernandes, E., Monks, T. J., Carvalho, F., and Bastos, M. L. (2004) Hepatoxicity of 3, 4-methylenedioxyamphetamine and α-methyldopamine in isolated hepatocytes: formation of glutathione conjugates. *Arch. Toxicol. 78*, 16−24.

(63) Bolton, J. L., Trush, M. A., Penning, T. M., Dryhurst, G., and Monks, T. J. (2000) Role of quinones in toxicology. *Chem. Res. Toxicol. 13*, 135−160.

(64) Chichirau, A., Flueraru, M., Chepelev, L. L., Wright, J. S., Willmore, W. G., Durst, T., Hussain, H. H., and Charron, M. (2005) Mechanism of cytotoxicity of catechols and a naphthalenediol in PC12-AC cells: the connection between extracellular autoxidation and molecular electronic structure. *Free Radical Biol. Med. 38*, 344−355.

TX060123I

PARTE III

CONCLUSÕES, REFERÊNCIAS E ANEXOS

9. CONCLUSÕES

Segundo os objectivos propostos inicialmente, o trabalho constante desta dissertação permitiu extrair as seguintes conclusões:

i) Nesta dissertação foram estudados os perfis de citotoxicidade e potenciais redox da MDMA e dos seus principais metabolitos de fase I (MDA, α-MeDA, N-Me-α-MeDA, 6-OH-α-MeDA e 3-*O*-Me-α-MeDA). Os resultados obtidos sugerem que os metabolitos que possuem um grupo catecol livre são significativamente mais tóxicos (valores de IC_{50} cerca de dez vezes mais baixos) para as células PC12 indiferenciadas (um modelo para estudos *in vitro* da toxicidade monoaminérgica) do que a MDMA e os seus metabolitos que possuem pelo menos um dos hidroxilos fenólicos substituídos. A *O*-desmetilenação e a hidroxilação aromática levam a um aumento da citotoxicidade, enquanto que o processo de *O*-metilação diminui a toxicidade dos compostos.

Nos estudos de condensação da cromatina, verificou-se que a maior parte dos compostos induz fragmentação e condensação da cromatina nas células, que revelam, por isso, características de apoptose (principalmente quando expostas a N-Me-α-MeDA), quando comparada com o controlo, como se observa pela marcação com SYTO-13. Estas características também são acompanhadas por uma necrose acentuada. Não foram encontradas diferenças significativas no que diz respeito ao perfil de morte celular, quando se comparam os diversos metabolitos e a própria MDMA.

O metabolismo da MDMA conduz a modificações significativas do potencial redox ao longo das suas vias de biotransformação. Os estudos dos potenciais redox dos metabolitos demonstram que existe um mecanismo oxidativo inerente à toxicidade da MDMA, sendo possível distinguir nitidamente duas séries de compostos: uma dos metabolitos contendo a função catecol (α-MeDA, N-Me-α-MeDA e 6-OH-α-MeDA) e outro constituído pela MDMA e os seus outros metabolitos, MDA e 3-*O*-Me-α-MeDA. Os primeiros são mais facilmente oxidáveis, e também mais tóxicos, facto que pode estar relacionado com a formação *in situ* de quinonas electrofílicas.

Todos os resultados observados neste trabalho podem contribuir para a elucidação do mecanismo molecular da neurotoxicidade da MDMA, visto que o

consumo de MDMA está associado a processos neurodegenerativos, embora sejam necessários mais ensaios complementares de toxicidade. Este trabalho permitiu, no entanto, estabelecer claramente que é obrigatória a bioactivação da MDMA, para esta manifestar citotoxicidade em células PC12. A N-Me-α-MeDA revelou ser o metabolito mais citotóxico, o que está de acordo com os trabalhos efectuados anteriormente em cardiomiócitos e hepatócitos (Carvalho *et al.*, 2004a; Carvalho *et al.*, 2004b).

No sentido de aprofundar a caracterização físico-química dos metabolitos, foi calculado o log*P* dos compostos. As correlações da lipofilia com a toxicidade vão ser aprofundadas em futuros trabalhos. Numa análise preliminar pode concluir-se que os metabolitos menos lipofílicos são mais tóxicos do que aqueles que possuem uma lipofilia mais acentuada (Gulaboski *et al.*, 2007).

ii) A análise conformacional completa dos derivados do β-nitroestireno e do β-metil-β-nitroestireno, por espectroscopia de Raman e cálculos de mecânica quântica, revelou que o comportamento conformacional deste tipo de compostos é maioritariamente determinado pelo efeito estabilizador da deslocalização dos electrões π. Estes compostos existem predominantemente sob a forma dos seus confórmeros *E* e possuem uma forte tendência para uma geometria planar devido à presença do sistema altamente conjugado, excepto quando existe impedimento estérico. Além dos efeitos electrostáticos, as preferências conformacionais destes compostos também são determinadas pela formação de interacções de hidrogénio intramoleculares, do tipo (C)H···O e (O)H···O, de força intermédia, e pela minimização dos efeitos repulsivos. Os desvios observados à planaridade dos β-nitroestirenos devem-se ao impedimento estérico dos grupos substituintes.

A optimização dos parâmetros geométricos dos nitroestirenos, juntamente com o cálculo das frequências harmónicas vibracionais correspondentes, e o estudo dos perfis de energia potencial para várias rotações internas dos compostos, permitem uma atribuição completa dos espectros de Raman das amostras no estado sólido e possibilitando a sua identificação inequívoca.

Para além da importância analítica, este tipo de análise, que conjuga métodos espectroscópicos com cálculos teóricos, pode ainda fornecer informação molecular relevante para ser usada no estabelecimento de relações estrutura – actividade ou estrutura – toxicidade.

iii) Os pressupostos anteriores também se aplicam aos derivados do β-metil-β-nitroestireno, que correspondem a intermediários de uma das vias sintéticas mais comuns na obtenção de drogas contendo o núcleo anfetamínico. Os espectros de Raman destes compostos possuem características específicas, o que se pode traduzir na sua aplicabilidade numa identificação espectroscópica rápida e inequívoca destas substâncias. Os resultados obtidos permitem propor a aplicação da espectroscopia de Raman como uma ferramenta analítica importante em análises de rotina de anfetaminas apreendidas, possibilitando detectar a presença de intermediários e precursores de síntese e assim estudar o perfil químico destas substâncias ilícitas. A espectroscopia de Raman pode, por exemplo, ser usada para diferenciar a MDMA dos seus precursores sintéticos, como o piperonal, o 3,4-metilenodioxi-β-metil-β-nitroestireno e a MDA através dos sinais característicos destes compostos.

iv) O estudo da influência das características estruturais, dos potenciais redox e dos coeficientes de partilha na actividade antibacteriana de uma série de β-nitroestirenos, foi efectuado com sucesso. Os análogos β-metil-β-nitroestirenos apresentaram actividade significativa contra bactérias Gram-positivas, enquanto que os respectivos β-nitroestirenos manifestaram uma actividade antibacteriana menos pronunciada. A presença do grupo nitro e da dupla ligação conjugada foi considerada fundamental para a actividade, visto que os análogos reduzidos não apresentam actividade antibacteriana significativa. De salientar que os análogos insaturados (redução da ligação dupla), as aminas correspondentes (redução apenas do grupo nitro) e outros nitroestirenos, com substituintes volumosos no núcleo aromático, não exibiram actividade contra as bactérias testadas.

Uma das possíveis justificações para a diferença de actividade entre os β-nitroestirenos e os β-metil-β-nitroestirenos pode estar na capacidade dos primeiros serem reduzidos a potenciais menos negativos do que os análogos β-metilados. Esta alteração é devida à diminuição da planaridade do sistema causada pelo grupo metilo e consequente diminuição do efeito de ressonância entre o grupo nitro e o anel aromático. Por outro lado, a substituição por um substituinte doador de electrões em posição *para* no anel aromático influencia marcadamente a actividade, facto que pode estar relacionado com uma maior dificuldade de redução do composto.

As propriedades físico-químicas foram relacionadas com a actividade, através de análise de regressão linear, concluindo-se que existe uma correlação entre os potenciais redox e

a actividade antimicrobiana. Estes resultados demonstram que o mecanismo de acção dos derivados do β-nitroestireno está relacionado com a sua capacidade de redução do grupo nitro. O sistema enzimático responsável pela redução do grupo nitro, as nitrorredutases bacterianas, parece ser fundamental para a actividade antibacteriana destes compostos, traduzindo-se na formação de intermediários extremamente reactivos que a podem justificar.

Apesar de serem necessários mais estudos, os resultados apresentados neste trabalho permitiram concluir que os derivados do β-nitroestireno e do β-metil-β-nitroestireno constituem um grupo de compostos com uma actividade antibacteriana relevante contra *Staphylococcus aureus* e algumas espécies de *Enterococcus*. Estes estudos podem ser importantes no planeamento racional e no desenvolvimento de novos antibióticos mais activos e selectivos, tendo como base este sistema, que apresenta um farmacóforo relativamente pequeno.

v) No que respeita à síntese e análise de aminocromos, a partir da oxidação das catecolaminas (adrenalina, noradrenalina, dopamina, isoprenalina e dopa) desenvolveu-se um trabalho que permite a síntese, detecção e quantificação directa destes produtos de oxidação. A metodologia instituída é baseada em HPLC em fase reversa com detecção por fotodíodos e permite a análise de todos os conjuntos catecolamina-aminocromo estudados.

De todos os sistemas oxidantes testados no estudo do perfil de oxidação das catecolaminas – hexacianoferrato (III) de potássio, óxido de prata (I), sulfato de cobre (II), periodato de sódio, tirosinase, o $NaIO_4$ demonstrou ser o mais eficaz.

A metodologia desenvolvida revelou-se extremamente sensível e também pouco susceptível a interferências de outros compostos. Esta foi aplicada à determinação de adrenocromo em sangue de rato e poderá ser também proposta para a detecção de outros aminocromos noutras matrizes biológicas, usando o tratamento da amostra aqui preconizado.

10. REFERÊNCIAS

Abreu, F.C.; Goulart, M.O.F.; Brett, A.M.O. (2002) Detection of the damage caused to DNA by niclosamide using an electrochemical DNA-biosensor. *Biosens. Bioelectron.* 17: 913-919.

Aptula, A.O.; Patlewicz, G.; Roberts, D.W. (2005) Skin sensitization: reaction mechanistic applicability domains for structure-activity relationships. *Chem. Res. Toxicol.* 18: 1420-1426.

Avdeef, A.; Testa, B. (2002) Physicochemical profiling in drug research: a brief survey of the state-of-the-art of experimental techniques. *Cell. Mol. Life Sci.* 59: 1681-1689.

Bai, F.; Lau, S.S.; Monks, T.J. (1999) Glutathione and N-acetylcysteine conjugates of α-methyldopamine produce serotonergic neurotoxicity. Possible role in methylenedioxyamphetamine-mediated neurotoxicity. *Chem. Res. Toxicol.* 12: 1150-1157.

Ballini, R.; Bosica, G. (1997) Nitroaldol reaction in aqueous media: an important improvement of the Henry reaction. *J. Org. Chem.* 62: 425-427.

Barreiro, E.J.; Silva, J.F.M.; Fraga, C.A.M. (1996) Noções básicas do metabolismo de fármacos. *Quim. Nova* 19: 641-650.

Barret, A.G.M.; Graboski, G.G. (1986) Conjugated nitroalkenes: versatile intermediates in organic synthesis. *Chem. Rev.* 86: 751-762.

Battaglia, G.; Brooks, B.P.; Kulsakdinum, C.; Sousa, E.B. (1988) Pharmacologic profile of MDMA (3,4-methylenedioxymethamphetamine) at various brain recognition sites. *Eur. J. Pharmacol.* 149: 159-163.

Becke, A.D. (1988) Density-functional exchange-energy approximation with correct asymptotic behavior. *Phys. Rev. A* 38: 3098-3100.

Becke, A.D. (1993) Density-functional thermochemistry. III. The role of exact exchange. *J. Chem Phys.* 98: 5648-5652.

Behonick, G.S.; Novak, M.J.; Nealley, E.W.; Baskin, S.I. (2001) Toxicology update: the cardiotoxicity of the oxidative stress metabolites of catecholamines (aminochromes). *J. Appl. Toxicol.* 21: S15-S22.

Bell, S.E.J.; Burns, D.T.; Dennis, A.C.; Matchett, L.J.; Speers, J.S. (2000a) Composition profiling of seized ecstasy tablets by Raman spectroscopy. *Analyst* 125: 1811-1815.

Bell, S.E.J.; Burns, D.T.; Dennis, A.C.; Speers, J.S. (2000b) Rapid analysis of ecstasy and related phenethylamines in seized tablets by Raman spectroscopy. *Analyst* 125: 541-544.

Benigni, R. (2005) Structure-activity relationship studies of chemical mutagens and carcinogens: mechanistic investigations and prediction approaches. *Chem. Rev.* 105: 1767-1800.

Bindoli, A.; Rigobello, M.P.; Deeble, D.J. (1992) Biochemical and toxicological properties of the oxidation products of catecholamines. *Free Radical Biol. Med.* 13: 391-405.

Bindoli, A.; Rigobello, M.P.; Galzigna, L. (1989) Toxicity of aminochromes. *Toxicol. Lett.* 48: 3-20.

Błachut, D.; Wojtasiewicz, K.; Czarnocki, Z. (2002) Identification and synthesis of some contaminants present in 4-methoxyamphetamine (PMA) prepared by the Leuckart method. *Forensic Sci. Int.* 127: 45-62.

Bouchard, G.; Carrupt, P.A.; Testa, B.; Gobry, V.; Girault, H.H. (2001) The apparent lipophilicity of quaternary ammonium ions is influenced by Galvani potential difference, not ion-pairing: a cyclic voltammetry study. *Pharm. Res.* 18: 702-708.

Bouchard, G.; Carrupt, P.A.; Testa, B.; Gobry, V.; Girault, H.H. (2002) Lipophilicity and solvation of anionic drugs. *Chem. Eur. J.* 8: 3478-3484.

Boyland, E.; Chasseaud, L.F. (1969) The role of glutathione and glutathione S-transferases in mercapturic acid biosynthesis. *Adv. Enzymol.* 32: 173-219.

Brian, P.W.; Grove, J.F.; McGowan, J.C. (1946) Fungistatic activity of ethylenic and acetylenic compounds. *Nature* 158: 876.

Brunmark, A.; Cadenas, E. (1989) Redox and addition chemistry of quinoid compounds and its biological implications. *Free Radic. Biol. Med.* 7: 435-477.

Buchwald, P.; Bodor, N. (1998) Octanol-water partition: searching for predictive models. *Curr. Med. Chem.* 5: 353-380.

Butaye, P.; Cloeckaert, A.; Schwarz, S. (2003) Mobile genes coding for efflux-mediated antimicrobial resistance in Gram-positive and Gram-negative bacteria. *Int. J. Antimicrob. Agents* 22: 205-210.

By, A.; Neville, G.A.; Shurvell, H.F. (1992) Fourier transform infrared/Raman differentiation and characterization of *cis*- and *trans*-2,5-dimethoxy-4,β-dimethyl-β-nitrostyrenes: precursors to the street drug STP *J. Forensic Sci.* 37: 503-512.

Carter, K.C.; Finnon, Y.S.; Daeid, N.N.; Robson, D.C.; Waddell, R. (2002) The effect of nitrostyrene on cell proliferation and macrophage immune responses. *Immunopharmacol. Immunotoxicol.* 24: 187-197.

Carvalho, L.A.E.B.; Marques, M.P.M.; Tomkinson, J. (2006) Drug-excipient interactions in ketoprofen – a vibrational spectroscopy study. *Biopolymers* 82: 420-424.

Carvalho, M.; Hawksworth, G.; Milhazes, N.; Borges, F.; Monks, T.J.; Fernandes, E.; Carvalho, F.; Bastos, M.L. (2002) Role of metabolites in MDMA (ecstasy)-induced nephrotoxicity: an in vitro study using rat and human renal proximal tubular cells. *Arch. Toxicol.* 76: 581-588.

Carvalho, M.; Remião, F.; Milhazes, N.; Borges, F.; Fernandes, E.; Carvalho, F.; Bastos, M.L. (2004a) The toxicity of *N*-methyl-α-methyldopamine to freshly isolated rat hepatocytes is prevented by ascorbic acid and *N*-acetylcysteine. *Toxicology* 200: 193-203.

Carvalho, M.; Remião, F.; Milhazes, N.; Borges, F.; Fernandes, E.; Monteiro, M.C.; Gonçalves, M.J.; Seabra, V.; Amado, F.; Carvalho, F.; Bastos, M.L. (2004b) Metabolism is required for the expression of Ecstasy-induced cardiotoxicity in vitro. *Chem. Res. Toxicol.* 17: 623-632.

Cavier, R.; Alladé, I.; Bouvier, P.; Colau, R.; Doré, J.-C.; Viel, C. (1978) Activité amoebicide et trichomonacide *in vitro* de β-nitrostyrènes, d'α-nitrostilbènes et d'analogues α ou β-substitués. *Ann. Pharm. Fr.* 36: 607-620.

Chase, D.B. (1986) Fourier transform Raman spectroscopy. *J. Am. Chem. Soc.* 108: 7485-7488.

Chavdarian, C.G.; Karashima, D.; Castagnoli, N.; Hundley, H.K. (1978) Oxidative and cardiovascular studies on natural and synthetic catecholamines. *J. Med. Chem.* 21: 548-554.

Cheynier, V.; Moutounet, M. (1992) Oxidative reactions of caffeic acid in model systems containing polyphenol oxidase. *J. Agric. Food Chem.* 40: 2038-2044.

Cheynier, V.F.; Van Hulst, M.W.J. (1988) Oxidation of trans-caftaric acid and 2-S-glutathionylcaftaric acid in model solutions. *J. Agric. Food Chem.* 36: 10-15.

Chichirau, A.; Flueraru, M.; Chepelev, L.L.; Wright, J.S.; Willmore, W.G.; Durst, T.; Hussain, H.H.; Charron, M. (2005) Mechanism of cytotoxicity of catechols and a naphtalenediol in PC12-AC cells: the connection between extracellular autoxidation and molecular electronic structure. *Free Radic. Biol. Med.* 38: 344-355.

Cho, A.K.; Hiramatsu, M.; Di Stefano, E.W.; Chang, A.S.; Jender, D.J. (1990) Stereochemical differences in the metabolism of 3,4-methylenedioxymethamphetamine *in vivo* and *in vitro*: a pharmacokinetic analysis. *Drug Metab. Dispos.* 18: 686-691.

Christophersen, A. (2000) Amphetamine designer drugs – an overview and epidemiology. *Toxicol. Lett.* 15: 127-131.

Chu, T.; Kumagai, Y; Di Stefano, E.W.; Cho, A.K. (1996) Disposition of methylenedioxymethamphetamine and three metabolites in the brains of different rat strains and their possible roles in acute serotonin depletion. *Biochem. Pharmacol.* 51: 789-796.

Cillier, J.J.L.; Singleton, V.L. (1989) Nonenzymic autoxidative phenolic browning reactions in a caffeic acid model system. *J. Agric. Food Chem.* 37: 890-896.

Cillier, J.J.L.; Singleton, V.L. (1990) Caffeic acid autoxidation an the effects of thiol. *J. Agric. Food Chem.* 38: 1789-1796.

Cillier, J.J.L.; Singleton, V.L. (1991) Characterization of the products of nonenzymic autoxidative phenolic reactions in a caffeic acid model system. *J. Agric. Food Chem.* 39: 1298-1303.

Clavijo, R.E.; Araya-Maturana, R.; Cassels, B.K.; Weiss-López, B. (1994) Infrared spectra of nitrostyrene derivatives. *Spectrochim. Acta* 50A: 2105-2115.

Coates, A.; Hu, Y.; Page, C. (2002) The future challenges facing the development of new antimicrobial drugs. *Nat. Rev. Drug Discov.* 1: 895-910.

Cole, J.C.; Sumnall, H.R. (2003) Altered states: the clinical effects of ecstasy. *Pharmacol. Ther.* 98: 35-38.

Costa, C.; Bertazzo, A.; Allegri, G.; Toffano, G.; Curcuruto, O.; Traldi, P. (1992) Melanin biosynthesis from dopamine. II. A mass spectrometric and collisional spectroscopic investigation. *Pigment Cell Res.* 5: 122-131.

Cotton, F.A.; Feng, X. (1997) Density functional theory study of transition-metal compounds containing metal-metal bonds. 1. Molecular structures of dinuclear compounds by complete geometry optimization. *J. Am. Chem. Soc.* 119: 7514-7520.

Cotton, F.A.; Feng, X. (1998) Density functional theory study of transition-metal compounds containing metal-metal bonds. 2. Molecular structures and vibrational spectra of dinuclear tetracarboxylate compounds of Molybdenum and Rhodium. *J. Am. Chem. Soc.* 120: 3387-3397.

Cronin, M.T.D.; Dearden, J.C.; Duffy, J.C.; Edwards, R.; Manga, N.; Worth, A.P.; Worgan, A.D.P. (2002) The importance of hydrophobicity and electrophilicity descriptors in mechanistically-based QSARs for toxicological endpoints. *SAR QSAR Environ. Res.* 13: 167-176.

Cronin, M.T.D.; Schultz, T.W. (2001) Development of quantitative structure-activity relationships for the toxicity of aromatic compounds to *Tetrahymena pyriformis*: comparative assessment of the methodologies. *Chem. Res. Toxicol.* 14: 1284-1295.

Cutmore, E.A.; Skett, P.W. (1993) Application of Fourier transform Raman spectroscopy to a range of compounds of pharmaceutical interest. *Spectrochim. Acta* 49A: 809-818.

Daéid, N.N.; Waddell, R.J.H. (2005) The analytical and chemometric procedures used to profile illicit drug seizures. *Talanta* 67: 280-285.

Dal Cason, T.A. (1990) An evaluation of the potential for clandestine manufacture of 3,4-methylenedioxyamphetamine (MDA) analogs and homologs. *J. Forensic Sci.* 35: 675-697.

De la Torre, R.; Farré, M.; Ortuño, J.; Mas, M.; Brenneisen, R.; Roset, P.N.; Segura, J.; Cami, J. (2000) Non-linear pharmacokinetics of MDMA ("ecstasy") in humans. *Br. J. Clin. Pharmacol.* 49: 104-109.

De la Torre, R.; Farré, M.; Roset, P.N.; Pizarro, N.; Abanades, S.; Segura, M.; Segura, J.; Cami, J. (2004) Human pharmacology of MDMA. Pharmacokinetics, metabolism, and disposition. *Ther. Drug Monit.* 26: 137-144.

Demicheli, G.; Maggi, R.; Mazzacani, A.; Righi, P.; Sartori, G.; Bigi, F. (2001) Supported organic catalysts: synthesis of (*E*)-nitrostyrenes from nitroalkanes and aromatic aldehydes over propylamine supported on MCM-41 silica as a reusable catalyst. *Tetrahedron Lett.* 42: 2401-2403.

Dhalla, K.S.; Ganguly, P.K.; Rupp, H.; Beamish, R.E.; Dhalla, N.S. (1989) Measurement of adrenolutin as an oxidation product of catecholamines in plasma. *Mol. Cell. Biochem.* 87: 85-92.

Dhalla, N.S.; Yates, J.C.; Lee, S.L.; Singh, A. (1978) Functional and subcellular changes in the isolated rat heart perfused with oxidized isoproterenol. *J. Mol. Cell. Cardiol.* 10: 31-41.

Doré, J.C.; Viel, C. (1975) Recherches en chimiotherapie antitumorale. Activité cytotoxique et antitumorale de β-nitrostyrènes et de composés nitrovinyliques dérivés. *Farmaco* 30: 81-109.

Downing, J. (1986) The psychological and physiological effects of MDMA on normal volunteers. *J. Psychoactive Drugs* 18: 335-340.

Eadsforth, C.V.; Moser, P. (1983) Assessment of reverse-phase chromatographic methods for determining partition coefficients. *Chemosphere* 12: 1459-1475.

Edelbach, D.J.; Lodge, K.B. (2000) Insights into the measurement of the octanol-water partition coefficient from experiments with acrylate esters. *Phys. Chem. Chem. Phys.* 2: 1763-1771.

Eisenhofer, G.; Aneman, A.; Hooper, D.; Rundqvist, B.; Friberg, P. (1996) The organ production, hepatic metabolism, and renal elimination of norepinephrine metabolites in humans. *J. Neurochem.* 66: 1565-1573.

Eisenhofer, G.; Kopin, I.J.; Goldstein, D.S. (2004) Catecholamine metabolism: a contemporary view with implications for physiology and medicine. *Pharmacol. Rev.* 56: 331-349.

Elayan, I.; Gibb, J.W.; Hanson, G.R.; Foltz, R.L.; Lim, H.K.; Johnson, M. (1992) Long-term alteration in the central monoaminergic systems of the rat by 2,4,5-trihydroxyamphetamine but not by 2-hydroxy-4,5-methylenedioxymethamphetamine or 2-hydroxy-4,5-methylenedioxyamphetamine. *Eur. J. Pharmacol.* 221: 281-288.

Ellis, G.; Hendra, P.J.; Hodges, C.M.; Jawari, T.; Jones, C.H.; Le Barazer, P.; Passingham, C.; Royaud, I.A.M.; Sánchez-Blázquez, A.; Warnes, G.M. (1989) Routine analytical Fourier transform Raman spectroscopy. *Analyst* 114: 1061-1066.

Ensslin, H.K.; Maurer, H.H.; Gouzoulis, E.; Hermle, L.; Kovar, K.A. (1996) Metabolism of racemic 3,4-methylenedioxyethylamphetamine in humans. Isolation, identification, quantification, and synthesis of urinary metabolites. *Drug Metab. Dispos.* 24: 813-820.

Erhardt, P.W. (1999) Drug metabolism data: past, present and future considerations. Em *Drug metabolism-databases and high-throughput testing during drug design and development* P.W. Erhardt (Ed.), pp. 2-15, IUPAC/Blackwell, Boston, Estados Unidos da América.

Erhardt, P.W. (2002) Medicinal chemistry in the new millennium. A glance into the future. *Pure Appl. Chem.* 74: 703-785.

Esteban, B.; O'Shea, E.; Camarero, J. Green, A.R.; Colado, M.I. (2001) 3,4- Methylenedioxymethamphetamine induces monoamine release, but not toxicity, when administered centrally at a concentration occurring following a peripherally injected neurotoxic dose. *Psychopharmacology* 154: 251-260.

Evans, D.C.; Watt, A.P.; Nicoll-Griffith, D.A.; Baillie, T.A. (2004) Drug-protein covalent adducts: an industry perspective on minimizing the potential for drug bioactivation in drug discovery and development. *Chem. Res. Toxicol.* 17: 3-16.

Fadda, G.; Spanu, T.; Ardito, F.; Taddei, C.; Santangelo, R.; Siddu, A.; Ciccaglione, D. (2004) Antimicrobial resistance among non-fermentative Gram-negative bacilli isolated from the respiratory tracts of italian inpatients: a 3-year surveillance study by the Italian Epidemiological Survey. *Int. J. Antimicrob. Agents* 23: 254-261.

Fathi, A.R.; Krautheim, A.; Kaap, S.; Eger, K.; Steinfelder, H.J. (2000) Michael adducts of ascorbic acid as inhibitors of protein phosphatase 2A and inducers of apoptosis. *Bioorg. Med. Chem. Lett.* 10: 1605-1608.

Fears, R. (1986) Lipophilic xenobiotic conjugates: the pharmacological and toxicological consequences of the participation of drugs and other foreign compounds as substrates in lipid biosynthesis *Prog. Lip. Res.* 24: 177-195.

Fiuza, S.M.; Van Besien, E.; Milhazes, N.; Borges, F.; Marques, M.P.M. (2004) Conformational analysis of a trihydroxylated derivative of cinnamic acid - a combined Raman spectroscopy and ab initio study. *J. Mol. Struct.* 693: 103-118.

Foppoli, C.; Coccia, R.; Cini, C.; Rosei, M.A. (1997) Catecholamines oxidation by xanthine oxidase. *Biochim. Biophys. Acta* 1334: 200-206.

Freeman, S.; Alder, J.F. (2002) Arylethylamine psychotropic recreational drugs: a chemical perspective. *Eur. J. Med. Chem.* 37: 527-539.

Fujita, T. (1997) Recent success stories leading to commercializable bioactive compounds with the aid of traditional QSAR procedures. *Quant. Struct.-Act. Relat.* 16: 107-112.

Gairaud, C.B.; Lappin, G.R. (1953) The synthesis of ω-nitrostyrenes. *J. Org. Chem.* 18: 1-3.

Garbow, J.R.; Gaede, B.J. (1990) A new method for the analysis of granular pesticide formulations. *J. Agric. Food Chem.* 38: 996-999.

Garrido, J.M.P.J.; Delerue-Matos, C.; Borges, F.; Macedo, T.R.A.; Oliveira-Brett, A.M. (2004a) Voltammetric oxidation of drugs of abuse. I. Morphine and metabolites. *Electroanalysis* 16: 1419-1426.

Garrido, J.M.P.J.; Delerue-Matos, C.; Borges, F.; Macedo, T.R.A.; Oliveira-Brett, A.M. (2004b) Voltammetric oxidation of drugs of abuse. II. Codeine and metabolites. *Electroanalysis* 16: 1427-1433.

Garrido, J.M.P.J.; Delerue-Matos, C.; Borges, F.; Macedo, T.R.A.; Oliveira-Brett, A.M. (2004c) Voltammetric oxidation of drugs of abuse. II. Heroin and metabolites. *Electroanalysis* 16: 1497-1502.

Gimeno, P.; Besacier, F.; Chaudron-Thozet, H. (2003) Optimization of extraction parameters for the chemical profiling of 3,4-methylenedioxymethamphetamine (MDMA) tablets. *Forensic Sci. Int.* 132: 182-194.

Gimeno, P.; Besacier, F.; Chaudron-Thozet, H.; Girard, J.; Lamotte, A. (2002) A contribution to the chemical profiling of 3,4-methylenedioxymethamphetamine (MDMA) tablets. *Forensic Sci. Int.* 127: 1-44.

Giulivi, C.; Cadenas, E. (1998) Oxidation of adrenaline by ferrylmyoglobin. *Free Radical Biol. Med.* 25: 175-183.

Gökçe, M.; Utku, S.; Berçin, E.; Özçelik, B.; Karaoğlu, T.; Noyanalpan, N. (2005) Synthesis and in vitro antimicrobial and cytotoxicity activities of 2-[(2-nitro-1-phenylalkyl)thio]benzoic acid derivatives. *Turk. J. Chem.* 29: 207-217.

Graham, D.G. (1978) Oxidative pathways for catecholamines in the genesis of neuromelanin and cytotoxic quinones. *Mol. Pharmacol.* 14: 633-643.

Green, A.R.; Mechan, A.O.; Elliott, J.M.; O'Shea, E.; Colado, M.I. (2003) The pharmacology and clinical pharmacology of 3,4-methylenedioxymethamphetamine (MDMA, "ecstasy"). *Pharmacol. Rev.* 55: 463-508.

Green, D.E.; Richter, D. (1937) Adrenaline and adrenochrome. *Biochem. J.* 31: 596-616.

Green, D.R.; Kroemer, G. (2004) The pathophysiology of mitochondrial cell death. *Science* 305: 626-629.

Greer, G.R.; Tolbert, R. (1986) Subjective reports of the effects of MDMA in a clinical setting. *J. Psychoactive Drugs* 18: 319-327.

Greer, G.R.; Tolbert, R. (1998) A method of conducting therapeutic sessions with MDMA. *J. Psychoactive Drugs* 30: 371-379.

Gulaboski, R.; Cordeiro, M.N.D.S.; Milhazes, N.; Garrido, J.; Borges, F.; Jorge, M.; Pereira, C.M.; Bogeski, I.; Morales, A.H.; Naumoski, B.; Silva, A.F. (2007) Evaluation of the lipophilic properties of opioids, amphetamine-like drugs and metabolites through electrochemical studies at the interface between two immiscible solutions. *Anal. Biochem.* no prelo.

Hamilton-Miller, J.M.T. (2004) Antibiotic resistance from two perspectives: man and microbe. *Int. J. Antimicrob. Agents* 23: 209-211.

Hanaki, H.; Yamaguchi, Y.; Nomura, S.; Haraga, I.; Nagayama, A.; Sunakawa, K. (2004) Method of detecting β-lactam antibiotic induced vancomycin resistant MRSA (BIVR). *Int. J. Antimicrob. Agents* 23: 1-5.

Hansch, C.; Fujita, T. (1964) ρ-σ-π Analysis. A method for the correlation of biological activity and chemical structure. *J. Am. Chem. Soc.* 86: 1616-1626.

Hansch, C.; Muir, R.M.; Fujita. T.; Maloney, P.P.; Geiger, F.; Streich, M. (1963) The correlation of biological activity of plant growth regulators and chloromycetin derivatives with Hammet constants and partition coefficients. *J. Am. Chem. Soc.* 85: 2817-2824.

Harley-Mason, J. (1948) The structure of adrenochrome and its reduction products. *Experientia* 4: 307-308.

Hawley, M.D.; Tatawawadi, S.V.; Piekarski, S.; Adams, R.N. (1967) Electrochemical studies of the oxidation pathways of catecholamines. *J. Am. Chem. Soc.* 89: 447-450.

Heacock, R.A. (1959) The chemistry of adrenochrome and related compounds. *Chem. Rev.* 59: 181-237.

Heacock, R.A. (1965) The aminochromes. *Adv. Heterocycl. Chem.* 5: 205-290.

Hendra, P.J.; Wilson, H.M.M.; Wallen, P.J.; Wesley, I.J.; Bentley, P.A.; Arruebarrena-Baez, M.; Haigh, J.A.; Evans, P.A.; Dyer, C.D.; Lehnert, R.; Pellow-Jarman, M.V. (1995) Routine analytical Fourier transform Raman spectroscopy. Part 2: an updated review. *Analyst* 120: 985-991.

Hermle, L.; Spitzer, M.; Borchardt, D.; Kovar, K.-A.; Gouzoulis, E. (1993) Psychological effects of MDE in normal subjects. Are entactogens a new class of psychoactive agents? *Neuropsychopharmacology* 8: 171-176.

Herráez-Hernández, R.; Campíns-Falcó, P.; Verdú-Andrés, J. (2001) Sensitive determination of methylenedioxylated amphetamines by liquid chromatography. *Analyst* 126: 581-586.

Hiramatsu, M.; Kumagai, Y.; Unger, S.E.; Cho, A.K. (1990) Metabolism of methylenedioxymethamphetamine: formation of dihydroxymethamphetamine and a quinone identified as its glutathione adduct. *J. Pharmacol. Exp. Ther.* 254: 521-527.

Hrbac, J.; Kohen, R. (2000) Biological redox activity: its importance, methods for its quantification and implication for health and disease. *Drug Dev. Res.* 50: 516-527.

Huether, G.; Zhou, D.; Rüther, E. (1997) Causes and consequences of the loss of serotonergic presynapses elicited by the consumption of 3,4-methylenedioxymethamphetamine (MDMA, "ecstasy") and its congeners. *J. Neural Transm.* 104: 771-794.

Ignaczak, A.; Gomes, J.A.N.F. (1996) Interaction of halide ions with copper: the DFT approach. *Chem. Phys. Lett.* 257: 609-615.

Jiménez, A.; Jordá, E.G.; Verdaguer, E.; Pubill, D.; Sureda, F.X.; Canudas, A.M.; Escubedo, E.; Camarasa, J.; Camins, A.; Pallàs, M. (2004) Neurotoxicity of amphetamine derivatives is mediated by caspase pathway activation in rat cerebellar granule cells. *Toxicol. Appl. Pharmacol.* 196: 223-234.

Johnson, M.; Elayan, I.; Hanson, G.R.; Foltz, R.L.; Gibb, J.W.; Lim, H.K. (1992) Effects of 3,4-dihydroxymethamphetamine and 2,4,5-trihydroxymethamphetamine, two metabolites of 3,4-methylenedioxymethamphetamine, on central serotonergic and dopaminergic systems. *J. Pharmacol. Exp. Ther.* 261: 447-453.

Johnson, M.P.; Hoffman, A.H.; Nichols, D.E. (1986) Effects of the enantiomers of MDA, MDMA and related analogues on [^{3}H]-serotonin and [^{3}H]-dopamine release from superfused rat brain slices. *Eur. J. Pharmacol.* 132: 269-276.

Kaap, S.; Quentin, I.; Tamiru, D.; Shaheen, M.; Eger, K.; Steinfelder, H.J. (2003) Structure activity analysis of the pro-apoptotic, antitumor effect of nitrostyrene adducts and related compounds. *Biochem. Pharmacol.* 65: 603-610.

Kalgutkar, A.S.; Soglia, J.R. (2005) Minimising the potential for metabolic activation in drug discovery. *Exp. Opin. Drug Metab. Toxicol.* 1: 91-142.

Kazius, J.; McGuire, R.; Bursi, R. (2005) Derivation and validation of toxicophores for mutagenicity prediction. *J. Med. Chem.* 48: 312-320.

Kerns, E.H.; Di, L. (2003) Pharmaceutical profiling in drug discovery. *Drug Discov. Today* 8: 316-323.

Kerr, J.F. (1971) Shrinkage necrosis: a distinct mode of cellular death. *J. Pathol.* 105: 13-20.

Kerr, J.F.; Wyllie, A.H.; Currie, A.R. (1972) Apoptosis: a basic biological phenomenon with wide-ranging implications in tissue kinetics. *Br. J. Cancer* 26: 239-257.

Kim, J.H.; Kim, J.H.; Lee, G.E.; Lee, J.E.; Chung, I.K. (2003) Potent inhibition of human telomerase by nitrostyrene derivatives. *Mol. Pharmacol.* 63: 1117-1124.

Kovacic, P.; Becvar, L.E. (2000) Mode of action of anti-infective agents: focus on oxidative stress and electron transfer. *Curr. Pharm. Des.* 6: 143-167.

Koyama, J.; Morita, I.; Tagahara, K.; Osakai, T.; Hotta, H.; Yang, M.X.; Mukainaka, T.; Nishino, H.; Tokuda, H. (2001) Correlation with redox potentials and inhibitory effects on Epstein-Barr virus activation of azaanthraquinones. *Chem. Pharm. Bull.* 49: 1214-1216.

Kraemer, T.; Maurer, H.H. (2002) Toxicokinetics of amphetamines: metabolism and toxicokinetic data of designer drugs, amphetamine, methamphetamine, and their N-alkyl derivatives. *Ther. Drug Monit.* 24: 277-289.

Kreth, K.; Kovar, K.; Schwab, M.; Zanger, U.M. (2000) Identification of the human cytochromes P450 involved in the oxidative metabolism of "ecstasy"-related designer drugs. *Biochem. Pharmacol.* 59: 1563-1571.

Kroemer, G.; El-Deiry, W.S.; Golstein, W.S.; Peter, M.E.; Vaux, D.; Vandenabeele, P.; Zhivotovsky, B.; Blagosklonny, M.V.; Malorni, W.; Knight, R.A.; Piacentini, M.; Nagata, S.; Melino, G. (2005) Classification of cell death: recommendations of the nomenclature committee on cell death. *Cell Death Differ.* 12: 1463-1467.

Kuwahara, Y.; Ômura, H.; Tanabe, T. (2002) 2-nitroethenylbenzenes as natural products in millipede defense secretions. *Naturwissenschaften* 89: 308-310.

Lawrence, N.S.; Beckett, E.L.; Davis, J.; Compton, R.G. (2002) Advances in the voltammetric analysis of small biologically relevant compounds. *Anal. Biochem.* 303: 1-16.

Lein, P.; Silbergeld, E.; Locke, P.; Goldberg, A.M. (2005) In vitro and other alternative approaches to developmental neurotoxicity testing (DNT). *Environ. Toxicol. Pharmacol.* 19: 735-744.

Lemos-Amado, F.; Domínguez, P.; Ferrer-Correia, A.; Remião, F.; Milhazes, N.; Borges, F.; Carvalho, F.D.; Bastos, M.L. (2001) Electrospray tandem mass spectrometry of aminochromes. *Rapid Commun. Mass Spectrom.* 15: 2466-2471.

Liechti, M.E.; Baumann, C.; Gamma, A.; Vollenweider, F.X. (2000) Acute psychological effects of 3,4-methylenedioxymethamphetamine (MDMA, "ecstasy") are attenuated by serotonin uptake inhibitor citalopram. *Neuropsychopharmacology* 22: 513-521.

Lien, E.J.; Hansch, C.; Anderson, S.M. (1968) Structure-activity correlations for antibacterial agents on Gram-positive and Gram-negative cells. *J. Med. Chem.* 11: 430-441.

Lim, H.K.; Foltz, R.L. (1988) In vivo and in vitro metabolism of 3,4-(methylenedioxy)methamphetamine in the rat: identification of metabolites using an ion trap detector. *Chem. Res. Toxicol.* 1, 370-378.

Lim, H.K.; Foltz, R.L. (1991) Ion trap tandem mass spectrometric evidence for the metabolism of 3,4-(methylenedioxy)methamphetamine to the potent neurotoxins 2,4,5-trihydroxymethamphetamine and 2,4,5-trihydroxyamphetamine. *Chem. Res. Toxicol.* 4: 626-632.

Lima, N.M.F.; Correia, C.S.; Ferraz, P.A.L.; Pinto, A.V.; Pinto, M.C.R.F.; Santana, A.E.G.; Goulart, M.O.F. (2002) Molluscicidal hydroxynaphthoquinones and derivatives: correlation between their redox potentials and activity against *Biomphalaria glabrata*. *J. Braz. Chem. Soc.* 13: 822-829.

Lin, L.Y.; Di Stefano, E.W.; Schmitz, D.A.; Hsu, L.; Ellis, S.W.; Lennard, M.S.; Tucker, G.T.; Cho, A.K. (1997) Oxidation of methamphetamine and methylenedioxymethamphetamine by CYP2D6. *Drug Metab. Dispos.* 25: 1059-1064.

Lombardo, F.; Shalaeva, M.Y.; Tupper, K.A.; Goa, F.; Abraham, M.H. (2000) $ElogP_{oct}$: a tool for lipophilicity determination in drug discovery. *J. Med. Chem.* 43: 2922-2928.

Lurie, I.S.; Bailey, C.G.; Anex, D.S.; Bethea, M.J.; McKibben, T.D.; Casale, J.F. (2000) Profiling of impurities in illicit methamphetamine by high-performance liquid chromatography and capillary chromatography. *J. Chromatogr. A* 870: 53-68.

Lyles, J.; Cadet, J.L. (2003) Methylenedioxymethamphetamine (MDMA, ecstasy) neurotoxicity: cellular and molecular mechanisms. *Brain Res. Rev.* 42: 155-168.

Maurer, H.H. (1996) On the metabolism and the toxicological analysis of methylenedioxyphenylalkylamine designer drugs by gas chromatography-mass spectrometry. *Ther. Drug Monit.* 18: 465-470.

Maurer, H.H.; Bickeboeller-Friedrich, J.; Kraemer, T.; Peters, F.T. (2000) Toxicokinetics and analytical toxicology of amphetamine-derived designer drugs ("ecstasy"). *Toxicol Lett.* 112-113: 133-142.

Mayer, J.; Testa, B. (1994) Stereoselectivity in metabolic reactions of toxication and detoxication. Em *Pharmacokinetics of drugs* P.G. Welling, L.P. Balant (Eds.), pp. 209-231, Springer, Berlim, Alemanha.

McCann, U.D.; Eligulaschvili, V.; Ricaurte, G.A. (2000) (±)3,4-Methylenedioxymethamphetamine ("ecstasy")-induced serotonin neurotoxicity: clinical studies. *Neuropsychobiology* 42: 11-16.

McCann, U.D.; Ricaurte, G.A. (1991) Major metabolites of (±)3,4-methylenedioxyamphetamine (MDA) do not mediate its toxic effects on brain serotonin neurons. *Brain Res.* 545: 279-282.

McKinney, J.D.; Richard, A.; Waller, C.; Newman, M.C.; Gerberick, F. (2000) The practice of structure-activity relationships in toxicology. *Toxicol. Sci.* 56: 8-17.

Michel, P.P.; Hefti, F. (1990) Toxicity of 6-hydroxydopamine and dopamine for dopaminergic neurons in culture. *J. Neurosci. Res.* 76: 428-435.

Mikami, Y.; Yazawa, K.; Maeda, A.; Uno, J.; Kubo, A.; Saito, N.; Kawakami, N. (1991) Antifungal activity of SL-1, a beta-nitrostyrene type pigment and its synthetic congeners. *J. Antibiot.* 44: 1454-1456.

Miller, R.T.; Lau, S.S.; Monks, T.J. (1995) Metabolism of 5-(glutathion-S-yl)-α-methyldopamine following intracerebroventricular administration to male Sprague-Dawley rats. *Chem. Res. Toxicol.* 8: 634-641.

Misra, H.P.; Fridovich, I. (1972) The role of superoxide anion in the autoxidation of epinephrine and a single assay for superoxide dismutase. *J. Biol. Chem.* 247: 3170-3175.

Monks, T.J.; Hanzlik, P.; Cohen, G.M.; Ross, D.; Graham, D.G. (1992) Quinone chemistry and toxicity. *Toxicol. Appl. Pharmacol.* 112: 2-16.

Monks, T.J.; Jones, D.C.; Bai, F.; Lau, S.S. (2004) The role of metabolism in 3,4-(±)-methylenedioxyamphetamine and 3,4-(±)-methylenedioxymethamphetamine (ecstasy) toxicity. *Ther. Drug Monit.* 26: 132-136.

Monks, T.J.; Lau, S.S. (1997) Biological reactivity of polyphenolic-glutathione conjugates. *Chem. Res. Toxicol.* 10: 1296-1313.

Moore, K.A.; Mozayani, A.; Fierro, M.F.; Poklis, A.; (1996) Distribution of 3,4-methylenedioxymethamphetamine (MDMA) and 3,4-methylenedioxyamphetamine (MDA) stereoisomers in a fatal poisoning. *Forensic Sci. Int.* 83: 111-119.

Morgan, M.J. (2000) Ecstasy (MDMA): a review of its possible persistent psychological effects. *Psychopharmacology* 152: 230-248.

Mori, A.; Ishiyama, I.; Akita, H.; Suzuki, K.; Mitsuoka, T.; Oishi, T. (1990) Formation of amphetamine from its nitro analogue by anaerobic intestinal bacteria. *Xenobiotica* 20: 629-634.

Narasimhan, B.; Belsare, D.; Pharande, D.; Mourya, V.; Dhake, A. (2004) Esters, amides and substituted derivatives of cinnamic acid: synthesis, antimicrobial activity and QSAR investigations. *Eur. J. Med. Chem.* 39: 827-834.

Nichols, D.E. (1986) Differences between the mechanism of action of MDMA, MBDB, and the classic hallucinogens. Identification of a new therapeutic class: entactogens. *J. Psychoactive Drugs* 18: 305-313.

Nichols, D.E.; Hoffman, A.J.; Oberlender, R.A.; Jacob, P.; Shulgin, A.T. (1986) Derivatives of 1-(1,3-benzodioxol-5-yl)-2-butanamine: representative of a novel therapeutic class. *J. Med. Chem.* 29: 2009-2015.

Núñez-Delicado, E.; Pérez-Gilabert, M.; Sánchez-Ferrer, A.; Garcia-Carmona, F. (1996) Hydroperoxidase activity of lipoxygenase: a kinetic study of isoproterenol oxidation. *Biochim. Biophys. Acta* 1293: 17-22.

O'Brien, P.J. (1991) Molecular mechanisms of quinone toxicity. *Chem. Biol. Interact.* 80: 1-41.

O'Dea, J.; Wojciechowski, M.; Osteryoung, J.; Aoki, K. (1985) Square wave voltammetry at electrodes having a small dimension. *Anal. Chem.* 57: 954-955.

Oberlender, R.; Nichols, D.E. (1988) Drug discrimination studies with MDMA and amphetamine. *Psychopharmacology (Berlin)* 95: 71-76.

Ochs, S.D.; Westfall, T.C.; Macarthur, H. (2005) The separation and quantification of aminochromes using high-pressure liquid chromatography with electrochemical detection. *J. Neurosci. Methods* 142: 201-208.

Orrenius, S.; Zhivotovsky, B. (2006) The future of toxicology – does it matter how cells die? *Chem. Res. Toxicol.* 19: 729-733.

Özkan, S.A.; Uslu, B.; Aboul-Enein, H.Y. (2003) Analysis of pharmaceuticals and biological fluids using modern electroanalytical techniques. *Crit. Rev. Anal. Chem.* 33: 155-181.

Pagliari, A.; Khamis, E.; Trinh, A.; Carrupt, P.A.; Tsai, R.S.; Testa, B. (1995) Structural properties governing retention mechanisms on RP-HPLC stationary phases used for lipophilicity measurements. *J. Liquid Chromatogr.* 18: 1721-1745.

Palhol, F.; Boyer, S.; Naulet, N.; Chabrillat, M. (2002) Impurity profiling of seized MDMA tablets by capillary gas chromatography. *Anal. Bioanal. Chem.* 374: 274-281.

Parham, M.; Hall, L.; Kier, L. (2000) *Accurate prediction of log P using E-state indices with neural network analysis.* 220th ACS National Meeting, Washington, DC, Estados Unidos da América.

Park, J.; Pei, D. (2004) *trans*-β-Nitrostyrene derivatives as slow-binding inhibitors of protein tyrosine phosphatases. *Biochemistry* 43: 15014-15021.

Parker, M.A.; Marona-Lewicka, D.; Kurrasch, D.; Shulgin, A.T.; Nichols, D.E. (1998) Synthesis and pharmacological evaluation of ring-methylated derivatives of 3,4-(methylenedioxy)amphetamine (MDA). *J. Med. Chem.* 41: 1001-1005.

Paula, F.S.; Cioletti, A.G.; Silva Filho, J.F.; Santana, A.E.G.; Santos, A.F.; Goulart, M.O.F.; Vallaro, M.; Fruttero, R. (2003) Electrochemical studies of biologically active arylazoxy compounds. The relationship between redox potentials and molluscicidal activities. *J. Electroanal. Chem.* 544: 25-34.

Pierce, P.A.; Peroutka, S.J. (1988) Ring-substituted amphetamine interactions with neurotransmitter receptor binding sites in human cortex. *Neurosci. Lett.* 95: 208-212.

Ploemen, J.H.T.M; Van Ommen, B.; Haan, A; Schefferlie, J.G.; Van Bladeren, P.J. (1993) *In vitro* and *in vivo* reversible and irreversible inhibition of rat glutathione S-transferase isoenzymes by caffeic acid and its 2-S-glutathionyl conjugate. *Food Chem. Toxicol.* 31: 475-482.

Poortman, A.J.; Lock, E. (1999) Analytical profile of 4-methylthioamphetamine (4-MTA), a new street drug. *Forensic Sci. Int.* 100: 221-233.

Raman, C.V. (1928) A change of wavelength in light scattering. *Nature (London)* 121: 619-620.

Raman, C.V.; Krishnan, K.S. (1928) A new type of secondary radiation. *Nature (London)* 121: 501-502.

Ran, Y.; He, Y.; Yang, G.; Johnson, J.L.H.; Yalkowsky, S.H. (2002) Estimation of aqueous solubility of organic compounds by using the general solubility equation. *Chemosphere* 48: 487-509.

Rastogi, V.K.; Jain, V.; Yadav, R.A.; Singh, C.; Palafox, M.A. (2000) Fourier transform Raman spectrum and ab initio and density functional computations of the vibrational spectrum, molecular geometry, atomic charges and some molecular properties of the anticarcinogenic drug 5-fluorouracil. *J. Raman Spectrosc.* 31: 595-603.

Rauth, A.M.; Melo, T.; Misra, V. (1998) Bioreductive therapies: an overview of drugs and their mechanisms of action. *Int. J. Radiation Oncology Biol. Phys.* 42: 755-762.

Remião, F.; Carmo, H.; Carvalho, F.; Bastos, M.L. (2001) Copper enhances isoproterenol toxicity in isolated rat cardiomyocytes. *Cardiovasc. Toxicol.* 1: 195-204.

Remião, F.; Carvalho, M.; Carmo, H.; Carvalho, F.; Bastos, M.L. (2002) Cu^{2+}-Induced isoproterenol oxidation into isoprenochrome in adult rat calcium-tolerant cardiomyocytes. *Chem. Res. Toxicol.* 15: 861-869.

Ricaurte, G.; Bryan, G.; Strauss, L.; Seiden, L.; Schuster, C. (1985) Hallucinogenic amphetamine selectively destroys brain serotonin nerve terminals. *Science* 229: 986-988.

Ricaurte, G.A.; DeLanney, L.E.; Irwin, I.; Langston, J.W. (1988) Toxic effects of MDMA on central serotonergic neurons in the primate: importance of route and frequency of drug administration. *Brain Res.* 446: 165-168.

Rona, G. (1985) Catecholamine cardiotoxicity. *J. Mol. Cell. Cardiol.* 17: 291-306.

Rudnick, G.; Wall, S.C. (1992) The molecular mechanism of "ecstasy" [3,4-methylenedioxymethamphetamine (MDMA)]: serotonin transporters are targets for MDMA-induced serotonin release. *Proc. Natl. Acad. Sci. USA* 89: 1817-1821.

Rupp, H.; Dhalla, K.S.; Dhalla, N.S. (1994) Mechanisms of cardiac cell damage due to catecholamines: significance of drugs regulating central sympathetic outflow. *J. Cardiovasc. Pharmacol.* 24: S16-S24.

Russel, A.D. (2003) Biocide use and antibiotic resistance: the relevance of laboratory findings to clinical environmental situations. *Lancet Infect. Dis.* 3: 794-803.

Russo, T.V.; Martin, R.L.; Hay, P.J. (1995) Effective Core potentials for DFT calculations. *J. Phys. Chem.* 99: 17085-17087.

Sant'Anna, C.M.R. (2002) Glossário de termos usados no planejamento de fármacos (recomendações da IUPAC para 1997). *Quim. Nova* 25: 505-512.

Sartori, G.; Bigi, F.; Maggi, R.; Sartorio, R.; Macquarrie, D.J.; Lenarda, M.; Storaro, L.; Collucia, S.; Martra, G. (2004) Catalytic activity of aminopropyl xerogels in the selective synthesis of (*E*)-nitrostyrenes from nitroalkanes and aromatic aldehydes. *J. Catal.* 222: 410-418.

Schales, O.; Graefe, H.A. (1952) Arylnitroalkenes: a new group of antibacterial agents. *J. Am. Chem. Soc.* 74: 4486-4490.

Schifano, F.; Oyefeso, A.; Corkeri, J.; Cobain, K.; Jambert-Gray, R.; Martinotti, G.; Ghodse, A.H. (2003) Death rates from ecstasy (MDMA, MDA) and polydrug use in England and Wales 1996-2002. *Hum. Psychopharmacol. Clin. Exp.* 18: 519-524.

Schmidt, M.; Eger, K. (1996) Michael reactions of ascorbic acid, 4th communication: nitrostyrene as a Michael acceptor toward vitamin C. *Pharmazie* 51: 11-16.

Schmitt, M.; Popp, J. (2006) Raman spectroscopy at the beginning of the twenty-first century. *J. Raman Spectrosc.* 37: 20-28.

Schwartz, R.H.; Miller, N.S. (1997) MDMA (ecstasy) and the rave: a review. *Pediatrics* 100: 705-708.

Segura, M.; Ortuño, J.; Farré, M.; McLure, J.A.; Pujadas, M.; Pizarro, N.; Llebaria, A.; Joglar, J.; Roset, P.N.; Segura, J.; De la Torre, R. (2001) 3,4-Dihydroxymethamphetamine (HHMA). A major in vivo 3,4-methylenedioxymethamphetamine (MDMA) metabolite in humans. *Chem. Res. Toxicol.* 14: 1203-1208.

Shafer, T.J.; Atchison, W.D. (1991) Transmitter, ion channel and receptor properties of pheochromocytoma (PC12) cells: a model for neurotoxicological studies. *Neurotoxicology* 12: 473-492.

Sherlock K.; Wolff, K.; Hay, A.W.; Conner, M. (1999) Analysis of illicit ecstasy tablets: implications for clinical management in the accident and emergency department. *J. Accid. Emerg. Med.* 16: 194-197.

Sondermann, N.; Kovar, K.A. (1999) Screening experiments of ecstasy street samples using near infrared spectroscopy. *Forensic Sci. Int.* 106: 147-156.

Souza, D.; Machado, S.A.S.; Avaca, L.A. (2003) Voltametria de onda quadrada. Primeira parte: aspectos teóricos. *Quim. Nova* 26: 81-89.

Squella, J.A.; Bollo, S.; Núñez-Vergara, L.J. (2005) Recent developments in the electrochemistry of some nitro compounds of biological significance. *Curr. Org. Chem.* 9: 565-581.

Squella, J.A.; Sturm, J.C.; Weiss-Lopez, B.; Bontá, M.; Núñez-Vergara, L.J. (1999) Electrochemical study of β-nitrostyrene derivatives: steric and electronic effects on their electroreduction. *J. Electroanal. Chem.* 466: 90-98.

Steele, T.D.; Nichols, D.E.; Yim, G.K.W. (1987) Stereochemical effects of 3,4-methylenedioxymethamphetamine (MDMA) and related amphetamine derivatives on inhibition of uptake of [^{3}H]-monoamines into synaptosomes from different regions of rat brain. *Biochem. Pharmacol.* 36: 2297-2303.

Stone, D.M.; Hanson, G.L.; Gibb, J.W. (1987) Differences in the central serotonergic effects of 3,4-methylenedioxymethamphetamine (MDMA) in mice and rats. *Neuropharmacology* 26: 1657-1661.

Strote, J.; Lee, J.E.; Wechsler, H. (2002) Increasing MDMA use among college students: results of a national survey. *J. Adolesc. Health* 30: 64-72.

Świst, M.; Wilamowski, J.; Parczewski, A. (2005a) Determination of synthesis method of ecstasy based on the basic impurities. *Forensic Sci. Int.* 152: 175-184.

Świst, M.; Wilamowski, J.; Parczewski, A. (2005b) Basic and neutral route specific impurities in MDMA prepared by different synthesis methods. Comparison of impurity profiles. *Forensic Sci. Int.* 155: 100-111.

Świst, M.; Wilamowski, J.; Zuba, D.; Kochana, J.; Parczewski, A. (2005c) Determination of synthesis route of 1-(3,4-methylenedioxyphenyl)-2-propanone (MDP-2-P) based on impurity profiles of MDMA. *Forensic Sci. Int.* 149: 181-192.

Tavares, L.C. (2004) QSAR: a abordagem de Hansch. *Quim. Nova* 27: 631-639.

Testa, B. (1984) Drugs? Drug research? Advances in drug research? Musings of a medicinal chemist. *Adv. Drug Res.* 13:1-58.

Testa, B.; Balmat, A.-L.; Long, A. (2004) Predicting drug metabolism: Concepts and challenges. *Pure Appl. Chem.* 76: 907-914.

Testa, B.; Caron, G.; Crivori, P.; Rey, S.; Reist, M.; Carrupt, P.A. (2000a) Lipophilicity and related molecular properties as determinants of pharmacokinetic behaviour. *Chimia* 54: 672-677.

Testa, B.; Crivori, P.; Reist, M.; Carrupt, P.A. (2000b) The influence of lipophilicity on the pharmacokinetic behavior of drugs: concepts and examples. *Perspect. Drug Discov. Design* 19: 179-211.

Testa, B.; Soine,W. (2003) Principles of drug metabolism. Em *Burger's Medicinal Chemistry and Drug Discovery (6ª Edição)* Abraham, D.J. (Ed.), pp.431-498, vol. 2, Wiley-Interscience, Hoboken, NJ, Estados Unidos da América.

Testa, B.; Vistoli, G.; Pedretti, A. (2005) Musings on ADME predictions and structure-activity relations. *Chem. Biodivers.* 2: 1411-1427.

Titeler, M.; Lyon, R.A.; Glennon, R.A. (1988) Radioligand binding evidence implicates the brain 5-HT_2 receptor as a site of action for LSD and central phenylisopropylamine hallucinogens. *Psychopharmacology* 94: 213-216.

Traxler, P.M.; Wacker, O.; Bach, H.L.; Geissler, J.F.; Kump, W.; Meyer, T.; Regenass, U.; Roesel, J.L.; Lydon, N. (1991) Sulfonylbenzoyl-nitrostyrenes: potential bisubstrate type inhibitors of the EGF-receptor tyrosine protein kinase. *J. Med. Chem.* 34: 2328-2337.

Tucker, G.T.; Lennard, M.S.; Ellis, S.W.; Woods, H.F.; Cho, A.K.; Lin, L.Y.; Hiratsuka, A.; Schmitz, D.A.; Chu, T.Y. (1994) The demethylenation of methylenedioxymethamphetamine ("ecstasy") by debrisoquine hydroxylase (CYP2D6). *Biochem. Pharmacol.* 47: 1151-1156.

Van der Waterbeemd, H.; Smith, D.A.; Beaumont, K.; Walker, D.K. (2001) Property-based design: optimization of drug absorption and pharmacokinetics. *J. Med. Chem.* 44: 1313-1333.

Vankeirsbilck, T; Vercauteren, A; Baeyens, W.; Van der Weken, G; Verpoort, F.; Vergote, G.; Remon, J.P. (2002) Applications of Raman spectroscopy in pharmaceutical analysis. *Trends Anal. Chem.* 21: 869-877.

Varma, R.S.; Dahiya, R.; Kumar, S. (1997) Microwave-assisted Henry reaction: solventless synthesis of conjugated nitroalkenes. *Tetrahedron Lett.* 38: 5131-5134.

Varma, R.S.; Naicker, K.P.; Liesen, P.J. (1998) Selective nitration of styrenes with clayfen and clayan: a solvent-free synthesis of β-nitrostyrenes. *Tetrahedron Lett.* 39: 3977-3980.

Verweij, A.M.A. (1989) Impurities in illicit drug preparations: amphetamine and methamphetamine. *Forensic Sci. Rev.* 1: 1-11.

Verweij, A.M.A. (1992) Impurities in illicit drug preparations: 3,4-(metylenedioxy)amphetamine and 3,4-(metylenedioxy)methylamphetamine. *Forensic Sci. Rev.* 4: 137-146.

Vicini, P.; Zani, F.; Cozzini, P.; Doytchinova, I. (2002) Hydrazones of 1,2-benzisothiazole hydrazides: synthesis, antimicrobial activity and QSAR investigations. *Eur. J. Med. Chem.* 37: 553-564.

Vollenweider, F.X.; Gamma, A.; Liechti, M.; Huber, T. (1998) Psychological and cardiovascular effects and short-term sequelae of MDMA ("ecstasy") in MDMA-naïve healthy volunteers. *Neuropsychopharmacology* 19: 241-251.

Wang, C.; Wang, S. (2002) The rapid synthesis of β-nitrostyrenes under microwave irradiation without solvent. *Synth. Commun.* 32: 3481-3486.

Watanabe, N.; Forman, H.J. (2003) Autoxidation of extracellular hydroquinones is a causative event for the cytotoxicity of menadione and DMN in A539-S cells. *Arch. Biochem. Biophys.* 411: 135-157.

Wermuth, G.C.; Ganellin, C.R.; Lindberg, P.; Mitscher, L.A. (1998) Glossary of terms used in Medicinal Chemistry (IUPAC recommendations 1998). *Pure & Appl. Chem.* 70: 1129-1143.

Williams, D.P.; Naisbitt, D. (2002) Toxicophores: groups and metabolic routes associated with increased safety risk. *Curr. Opin. Drug Discov. Dev.* 5: 104-115.

Woodford, N. (2003) Novel agents for the treatment of resistant Gram-positive infections. *Expert Opin. Invest. Drugs* 12: 117-137.

Worthen, L.R.; Bond, H.W. (1970) Antimicrobial activity of some β-nitrostyrenes. *J. Pharm. Sci.* 59: 1185-1186.

Wring, S.A.; Hart, J.P. (1992) Chemically modified, carbon-based electrodes and their application as electrochemical sensors for the analysis of biologically important compounds. A review. *Analyst* 117: 1215-1229.

Wu, D.; Otton, S.V.; Inaba, T.; Kalow, W.; Sellers, E.M. (1997) Interactions of amphetamine analogs with human liver CYP2D6. *Biochem. Pharmacol.* 53: 1605-1612.

Yao, C.-F.; Chen, W.-C.; Lin, Y.-M. (1996) Reactions of β-nitrostyrenes with Grignard reagents. *Tetrahedron Lett.* 37: 6339-6342.

Yao, C.-F.; Kao, K.-H.; Liu, J.-T.; Chu, C.-M.; Wang, Y.; Chen, W.-C.; Lin, Y.-M.; Lin, W.-W.; Yan, M.-C.; Liu, J.-Y.; Chuang, M.-C.; Shiue, J.L. (1998) Generation of nitroalkanes, hydroximoyl halides and nitrile oxides from the reactions of β-nitrostyrenes with Grignard or organolithium reagents. *Tetrahedron* 54: 791-822.

Yee, Y.C. (2003) Laboratory testing of newer antibiotics against Gram-positive organisms: avoiding false susceptibility and resistance results. *Clin. Microbiol. Newslett.* 25: 9-16.

Zong, W.X.; Thompson, C.B. (2006) Necrotic death as a cell fate. *Genes Dev.* 20: 1-15.

11. ANEXOS

11.1 Hepatotoxicidade da 3,4-metilenodioximetanfetamina e α-metildopamina em hepatócitos isolados de rato: formação de conjugados com a glutationa.

Artigo reproduzido da revista *Archives of Toxicology* (2004) 78: 16-24, com permissão da Springer-Verlag.

Arch Toxicol (2004) 78: 16–24
DOI 10.1007/s00204-003-0510-7

ORGAN TOXICITY AND MECHANISMS

**Márcia Carvalho · Nuno Milhazes · Fernando Remião
Fernanda Borges · Eduarda Fernandes
Francisco Amado · Terrence J. Monks
Félix Carvalho · Maria Lourdes Bastos**

Hepatotoxicity of 3,4-methylenedioxyamphetamine and α-methyldopamine in isolated rat hepatocytes: formation of glutathione conjugates

Received: 2 May 2003 / Accepted: 4 August 2003 / Published online: 28 October 2003
© Springer-Verlag 2003

Abstract The amphetamine designer drugs 3,4-methylenedioxymethamphetamine (MDMA or "ecstasy") and its *N*-demethylated analogue 3,4-methylenedioxyamphetamine (MDA or "love") have been extensively used as recreational drugs of abuse. MDA itself is a main MDMA metabolite. MDMA abuse in humans has been associated with numerous reports of hepatocellular damage. Although MDMA undergoes extensive hepatic metabolism, the role of metabolites in MDMA-induced hepatotoxicity remains unclear. Thus, the aim of the present study was to evaluate the effects of MDA and α-methyldopamine (α-MeDA), a major metabolite of MDA, in freshly isolated rat hepatocyte suspensions. The cells were incubated with MDA or α-MeDA at final concentrations of 0.1, 0.2, 0.4, 0.8, or 1.6 mM for 3 h. The toxic effects induced following incubation of hepatocyte suspensions with these metabolites were evaluated by measuring cell viability, the extent of lipid peroxidation, levels of glutathione (GSH) and glutathione disulfide (GSSG), the formation of GSH conjugates, and the activities of GSSG reductase (GR), GSH peroxidase (GPX), and GSH *S*-transferase (GST). MDA induced a concentration- and time-dependent GSH depletion, but had a negligible effect on lipid peroxidation, cell viability, or on the activities of GR, GPX, and GST. In contrast, α-MeDA (1.6 mM, 3 h) induced a marked depletion of GSH accompanied by a loss on cell viability, and decreases in GR, GPX and GST activities, although no significant effect on lipid peroxidation was found. For both metabolites, GSH depletion was not accompanied by increases in GSSG levels; rather, 2-(glutathion-*S*-yl)-α-MeDA and 5-(glutathion-*S*-yl)-α-MeDA were identified by HPLC-DAD/EC within cells incubated with MDA or α-MeDA. The results provide evidence that one of the early consequences of MDMA metabolism is a disruption of thiol homeostasis, which may result in loss of protein function and the initiation of a cascade of events leading to cellular damage.

Keywords 3,4-Methylenedioxyamphetamine · α-Methyldopamine · Rat hepatocytes · Glutathione conjugates

M. Carvalho (✉) · F. Remião · F. Carvalho · M. L. Bastos
REQUIMTE, Toxicology Department, Faculty of Pharmacy, University of Porto, Rua Aníbal Cunha 164, 4050/047 Porto, Portugal
E-mail: marciacarvalho@ff.up.pt
Fax: +351-22-2003977

N. Milhazes · F. Borges
CEQOFFUP, Organic Chemistry Department, Faculty of Pharmacy, University of Porto, Rua Aníbal Cunha 164, 4050/047 Porto, Portugal

E. Fernandes
REQUIMTE, Physical-Chemistry Department, Faculty of Pharmacy, University of Porto, Rua Aníbal Cunha 164, 4050/047 Porto, Portugal

F. Amado
Department of Chemistry, University of Areiro, 3810/123 Areiro, Portugal

T. J. Monks
Center for Molecular and Cellular Toxicology, College of Pharmacy, University of Texas at Austin, Austin, TX 78712-1074, USA

Introduction

The amphetamine designer drugs 3,4-methylenedioxymethamphetamine (MDMA or "ecstasy") and its *N*-demethylated analogue 3,4-methylenedioxyamphetamine (MDA or "love") have been used as recreational drugs of abuse, mainly among young people, due to their stimulant and hallucinogenic properties. However, MDMA and MDA produce a variety of systemic and organ-specific effects, including serotonergic neurotoxicity (Battaglia et al. 1987; Ricaurte et al. 2000), convulsions, hyperthermia, disseminated intravascular coagulation, rhabdomyolysis, and acute renal failure

(Simpson and Rumack 1981; Henry et al. 1992; Hegadoren et al. 1999; Walubo and Seger 1999). In the past decade, clinical evidence has increasingly shown that the liver is also a target of MDMA toxicity. Jaundice, hepatomegaly, centrilobular necrosis, hepatitis and fibrosis represent some of the adverse effects caused by MDMA in the liver (Henry et al. 1992; Dykhuizen et al. 1995; Khakoo et al. 1995; Ellis et al. 1996; Milroy et al. 1996; Fineschi et al. 1999; Varela-Rey et al. 1999). Various factors probably play a role in MDMA-induced liver toxicity, including the metabolism of MDMA, the increased efflux of neurotransmitters, the oxidation of biogenic amines, and hyperthermia. In fact, our group has shown recently that the toxic effects induced by MDMA in isolated mouse hepatocytes are exacerbated under hyperthermic conditions (Carvalho et al. 2001). However, in spite of the extensive hepatic metabolism of MDMA, the role of metabolites in MDMA-induced hepatotoxicity is still unclear. In view of this, the present work was performed to evaluate the effects of two main MDMA metabolites, MDA and α-methyldopamine (α-MeDA), in freshly isolated rat hepatocytes. MDA is not only a synthetic drug of abuse but it is also an important metabolite of MDMA (Cho et al. 1990). MDMA is metabolized to *N*-methyl-α-MeDA and α-MeDA (Lim and Foltz 1988; Kumagai et al. 1991), and MDA to α-MeDA (Marquardt et al. 1978). *N*-Methyl-α-MeDA and α-MeDA are catechols that can undergo oxidation to the corresponding *ortho*-quinones. Quinones are highly redox-active molecules, which can enter redox cycles through their semiquinone radicals, leading to the formation of reactive oxygen species (ROS), including the superoxide anion, hydrogen peroxide, and the hydroxyl radical. Alternatively, since the reactive *ortho*-quinone intermediates are Michael acceptors, they can promote cellular damage through an alkylation process with biomolecules such as crucial cellular proteins and/or DNA (Bolton et al. 2000). In the presence of glutathione (GSH), the *ortho*-quinone of α-MeDA undergoes conjugation with GSH to form (glutathion-*S*-yl)-α-MeDA adducts (Hiramatsu et al. 1990). The GSH conjugates remain redox active and may be readily oxidized to the *ortho*-quinone thioethers, which can be followed by reductive addition of a second molecule of GSH to yield 2,5-*bis*(glutathion-*S*-yl)-α-MeDA (Miller et al. 1997). It must be stressed that these redox-active metabolites have been recently implicated in the mechanisms underlying MDMA-induced neurotoxicity (Miller et al. 1995, 1997; Bai et al. 1999, 2001) and nephrotoxicity (Carvalho et al. 2002b). To further elucidate the potential role of metabolites in MDMA-elicited hepatotoxicity, we evaluated the effects of MDA and α-MeDA on cell viability, the extent of lipid peroxidation, levels of glutathione and glutathione disulfide (GSSG), the formation of GSH conjugates, and the activities of GSSG reductase (GR), GSH peroxidase (GPX), and GSH *S*-transferase (GST) in isolated rat hepatocytes. Finally, high-performance liquid chromatography methodology with simultaneous combined electrochemical and diode-array analysis (HPLC-DAD/EC) was utilized to identify the GSH conjugates of these metabolites formed within the cells.

Materials and methods

Chemicals

All reagents used in this study were of analytical grade. Collagenase (type I), bovine serum albumin (fraction V), *N*-(2-hydroxyethyl)piperazine-*N'*-(2-ethanesulfonic acid) (HEPES), ethylene glycol-*bis*(β-aminoethyl ether) *N,N,N',N'*-tetraacetic acid (EGTA), reduced GSH, GSSG, GR (EC 1.6.4.2), 2-vinylpyridine, β-nicotinamide adenine dinucleotide phosphate reduced form (β-NADPH), β-nicotinamide adenine dinucleotide reduced form (β-NADH), 5,5'-dithio-*bis*(2-nitrobenzoic acid) (DTNB), pyruvic acid, 2-thiobarbituric acid (TBA), 1-octanesulfonic acid, γ-glutamyl transpeptidase (γ-GT; EC 2.3.2.2) and all the reagents for enzymatic determinations were obtained from Sigma Chemical Company (St. Louis, MO, USA). Chloroacetic acid, citric acid, methanol (gradient grade), perchloric acid, and all other chemicals were obtained from Merck (Darmstadt, Germany). 3,4-Methylenedioxyamphetamine (HCl salt) and α-methyldopamine (HBr salt) were synthesized in the Organic Chemistry Department, Faculty of Pharmacy, Porto University, Portugal. 5-(Glutathion-*S*-yl)-α-MeDA was synthesized in the Center for Molecular and Cellular Toxicology, College of Pharmacy, University of Texas, Austin, USA.

Animals

Male Wistar rats (200–250 g) were obtained from Charles-River Laboratories (Barcelona, Spain). Animals were acclimatized in polyethylene cages, lined with wood shavings, with wire-mesh tops, at an ambient temperature of 20 ± 2°C, humidity between 40 and 60% and 12 h/12 h light/dark cycle. The animals had free access to standard rat chow and drinking water, and were kept in the animal house for at least 1 week prior to use. Surgical procedures for the isolation of hepatocytes were performed under anesthesia and were carried out always between 9:00 a.m. and 10:00 a.m.

Hepatocyte isolation and incubation

Hepatocytes were isolated by collagenase perfusion as previously described (Moldéus et al. 1978). Cell viability at the initiation of the experiments was between 85% and 97%.

Incubations were performed in a shaking water bath (90 oscillations/min) at 37°C, using 10^6 cells/ml in Krebs-Henseleit buffer supplemented with 25 mM HEPES (pH 7.4), and gassed with an air stream of humidified carbogen. Isolated hepatocytes were pre-incubated for 30 min at 37°C and then incubated with MDA chloride or α-MeDA bromide at final concentrations of 0, 0.1, 0.2, 0.4, 0.8, or 1.6 mM. Since α-MeDA is a light-sensitive unstable compound, all incubations were performed under light-protection conditions. Aliquots of the cell suspensions were taken at time zero and at hourly intervals for 3 h for the evaluation of cell viability, lipid peroxidation, GSH and GSSG levels. Selenium-dependent GPX, GR and GST activities were also quantified in cell suspension aliquots taken at time zero and after 3 h of incubation (samples were kept frozen at −80°C until assay, usually within 1 week). At the end of the experiments, aliquots of cell suspensions (10^6 cells) were collected and immediately centrifuged at 300 rpm for 2 min. The pellet was used for detection of GSH conjugates.

Biochemical analysis

Cell viability was determined after isolation by the Trypan blue exclusion test. During the course of the experiments cell viability was determined by the lactate dehydrogenase (LDH) leakage method, randomly confirmed by the Trypan blue exclusion test.

The extent of lipid peroxidation was measured by the thiobarbituric acid reactive substances (TBARS) assay at 535 nm as described before (Carvalho et al. 1997).

The GSH and GSSG contents of cell suspensions were determined by the DTNB–GSSG reductase recycling assay as described by Anderson (1985), with some modifications. Briefly, 200 µl of cell suspension aliquots were precipitated with 200 µl perchloric acid (5% final acid concentration) and centrifuged for 10 min at 13,000 rpm in a refrigerated centrifuge (4°C). After this time, 100 µl acidic supernatant was neutralized with 100 µl 0.76 M $KHCO_3$ and the sample centrifuged for 1 min at 13,000 rpm. Fresh reagent, containing 0.69 mM NADPH and 4 mM DTNB in 72 mM phosphate buffer, was prepared daily. For measurement of total glutathione, 100 µl/well of samples, standards or blank were added in duplicate to 96-well microtiter plates, followed by 65 µl/well of the freshly prepared reagent. Plates were then incubated in a thermomax plate reader (PowerWaveX; Bio-Tek, Winooski, VT, USA) at 30°C for 10 min prior to the addition of 40 µl GR per well (10 IU/ml in phosphate buffer). The stoichmetric formation of 5-thio-2-nitrobenzoic acid (TNB) was followed for 2 min at 415 nm and compared with a standard curve. For the determination of GSSG, aliquots (200 µl) of acidic supernatant were treated with 10 µl 2-vinylpyridine and mixed continuously for 1 h for derivatization of GSH. GSSG was then measured as described above for total glutathione. The GSH levels were calculated by subtracting GSSG content from the total glutathione content ($GSH = GSH_t - 2 \times GSSG$).

For measurement of the activities of selenium-dependent GPX, GR and GST, aliquots of cell suspensions were sonicated for 12 s at medium intensity and then centrifuged at 13,000 rpm for 5 min. GPX, GR, and GST activities were then determined in the supernatant as previously described (Carvalho et al. 2002a).

HPLC-DAD/EC analysis of GSH conjugates

The separation and characterization of GSH conjugates was performed by high-performance liquid chromatography (HPLC), equipped with an electrochemical (EC) and a photodiode array detector (DAD). HPLC analysis was performed using an autosampler injector (Gilson model 231-401), and a Spherisorb RP-18 (5 µm) column (Waters, Milford, MA, USA). A Coulochem II electrochemical detector (ESA, Chelmsford, MA, USA) equipped with a guard cell (ESA 5020) and an analytical cell (ESA 5010) was used. The electrochemical potential settings of the Coulochem II multidetector were: guard cell +0.45 V, detector 1 −0.1 V, and detector 2 +0.35 V. A current of 1–5 µA full-scale was used. A photodiode array detector (Waters model 2690) was placed before the analytical cell and the detection was performed at 292 nm, corresponding to the maximum absorption wavelength of the mono GSH-conjugates. A Compaq computer fitted with Millennium software (Waters) processed the chromatographic and spectral data.

The mobile phase (50 mM citric acid, 0.46 mM 1-octanesulfonic acid and 15% methanol, adjusted to pH 3.0 with 10 M NaOH) was filtered through a 0.45-µm membrane (Millipore, Madrid, Spain) and degassed under a helium stream. An isocratic elution was performed at 1.0 ml/min at room temperature.

Sample aliquots were treated with methanol for precipitation of protein and centrifuged for 10 min at 13,000 rpm. The supernatant was evaporated under a stream of nitrogen and then reconstituted to 150 µl with water. A volume of 100 µl was then injected into the HPLC system. The presence of the conjugates was confirmed by co-chromatography with 2-(glutathion-*S*-yl)-α-MeDA and 5-(glutathion-*S*-yl)-α-MeDA standards.

To strengthen sample peak identification of GSH conjugates, cell samples were sonicated (12 s at medium intensity) and then treated with γ-GT (8 IU in Krebs-Henseleit buffer) for 1 min before precipitation of proteins with methanol. UV spectra of peaks present in samples were obtained to corroborate identification of GSH conjugates.

Synthesis of 2-(glutathion-*S*-yl)-α-MeDA conjugate

A mixture of α-MeDA (2 mM), GSH (10 mM), and tyrosinase (5000 U) in 5 ml potassium phosphate buffer (50 mM, pH 7.4) was incubated for 1 min at 37°C. The reaction was then terminated by addition of 1 ml 15% perchloric acid. The reaction mixture was centrifuged, and 100 µl supernatant was injected into the HPLC-DAD/EC system. The mobile phase consisted of 10 mM ammonium acetate and 10% methanol (adjusted to pH 3.0), at a flow rate of 1.0 ml/min. The HPLC chromatogram revealed the presence of two major peaks corresponding to 2-(glutathion-*S*-yl)-α-MeDA and 5-(glutathion-*S*-yl)-α-MeDA conjugates, with retention times of 8 min and 16 min, respectively. The peak corresponding to 5-(glutathion-*S*-yl)-α-MeDA was confirmed after co-elution with 5-(glutathion-*S*-yl)-α-MeDA standard. Fractions containing 2-(glutathion-*S*-yl)-α-MeDA were collected and the structure confirmed by mass spectrometry (adapted from Miller et al. 1995).

Statistical analysis

Results are presented as means ± SEM (from five to eight experiments of different preparations of hepatocytes). Statistical comparisons between groups were performed by one-way analysis of variance (ANOVA) followed by Scheffé's test. Changes in the studied parameters with time of incubation were evaluated by one-way repeated measures ANOVA (Huynh-Feldt adjustment). Significance was accepted at $P < 0.05$.

Results

The toxic effects induced by MDA or α-MeDA on hepatocyte suspensions were evaluated by measuring cell viability, the extent of lipid peroxidation, levels of GSH, GSSG and total glutathione, and antioxidant enzyme activities. Figure 1 illustrates the viability of hepatocytes incubated with MDA or α-MeDA (both at 0.1–1.6 mM). At all tested concentrations, MDA had a negligible effect on cell viability, as measured by LDH leakage (Fig. 1A). In contrast, α-MeDA at the highest concentration tested (1.6 mM) induced a significant decrease in cell viability (cell death up to 43 ± 5%) after 3 h of incubation (Fig. 1B).

No lipid peroxidation was observed when cells were incubated with MDA or α-MeDA (0.1–1.6 mM, 3-h incubation) as measured by TBARS assay (data not shown). Both MDA and α-MeDA (0.1–1.6 mM) induced a concentration- and time-dependent GSH depletion (Fig. 2A,B, respectively). GSH depletion was clearly more marked for the catechol metabolite at the highest concentration studied. In fact, 1.6 mM MDA caused nearly 42% depletion of GSH after 2 h of incubation, whereas 1.6 mM α-MeDA caused an ~85% depletion of GSH, compared with controls. Differences were not evident at the lower tested concentrations. An important finding was that glutathione depletion induced by MDA

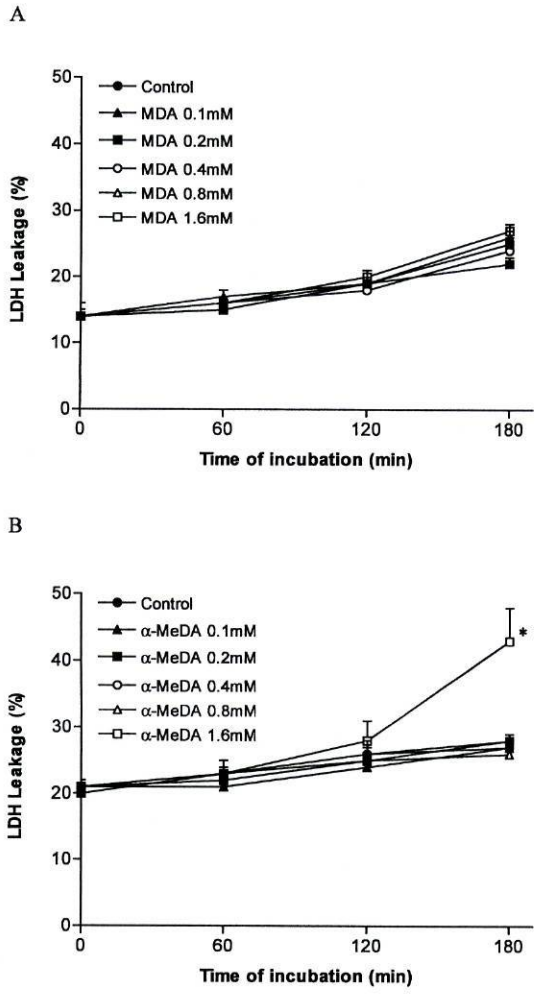

Fig. 1A,B Effect of 3,4-methylenedioxyamphetamine (MDA; **A**) and its major metabolite α-methyldopamine (α-MeDA; **B**) on cell viability of hepatocyte suspensions as measured by percentage of lactate dehydrogenase (LDH) leakage. Data represent means ± SEM, $n = 5$–8; $^{*}P < 0.05$, compared with control

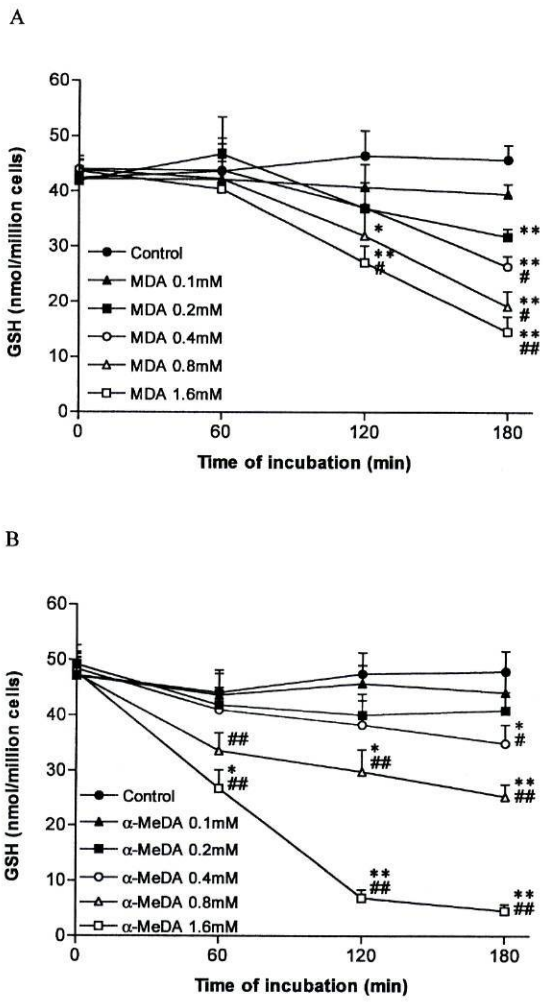

Fig. 2A,B Effect of MDA (**A**) and α-MeDA (**B**) on glutathione (GSH) levels in hepatocyte suspensions. Data represent means ± SEM, $n = 5$–8; $^{*}P < 0.05$, $^{**}P < 0.01$, compared with control; $^{\#}P < 0.05$ and $^{\#\#}P < 0.01$, compared with time zero

or α-MeDA was not due to glutathione oxidation (Fig. 3A,B, respectively). In fact, no significant differences in GSSG levels were found when cells were treated with MDA (0.1–1.6 mM) or α-MeDA (0.1–0.8 mM). It is noteworthy that after the third hour of incubation, GSSG levels were significantly decreased by 1.6 mM α-MeDA, when compared with those of controls. Total glutathione content of cells incubated with 1.6 mM MDA was significantly reduced to 42% of control levels after 3 h of incubation, whereas with 1.6 mM α-MeDA total glutathione levels of cells were significantly reduced to 63% and 72% of control levels after 2 and 3 h of incubation, respectively (data not shown).

One of the aims of the present work was to identify putative GSH conjugates formed within cells incubated with MDA or α-MeDA; thus, an HPLC methodology was implemented to separate and identify these conjugates. In all HPLC-EC analyses of samples obtained from incubations with MDA, a predominant electroactive peak (with retention time of 12.5 min) was detected and identified as α-MeDA after coelution with authentic α-MeDA standard. Within this samples, the HPLC-DAD/EC system also demonstrated the presence of two mono GSH-conjugates in cells treated with 1.6 mM MDA for 3 h. The incubation of hepatocytes with 0.1–1.6 mM α-MeDA for 3 h resulted in a more expressive presence of the two mono GSH-conjugates (Fig. 4). Retention times for the 2-(glutathion-*S*-yl)-α-MeDA and 5-(glutathion-*S*-yl)-α-MeDA conjugates were 10.0 min (Fig. 4A) and 20.5 min (Fig. 4B), respectively, and were confirmed by co-chromatography with authentic standards. The appearance of two peaks in each of the standards and samples is due to the presence of diastereomers. In previous work, using different chromatographic conditions, we were able to completely separate these two peaks and confirm their identity by mass spectrometry (unpublished data). Furthermore, it was observed that the peaks corresponding to the GSH conjugates completely disappeared when samples were treated with γ-GT, an enzyme known to cleave the γ-glutamyl bond of GSH

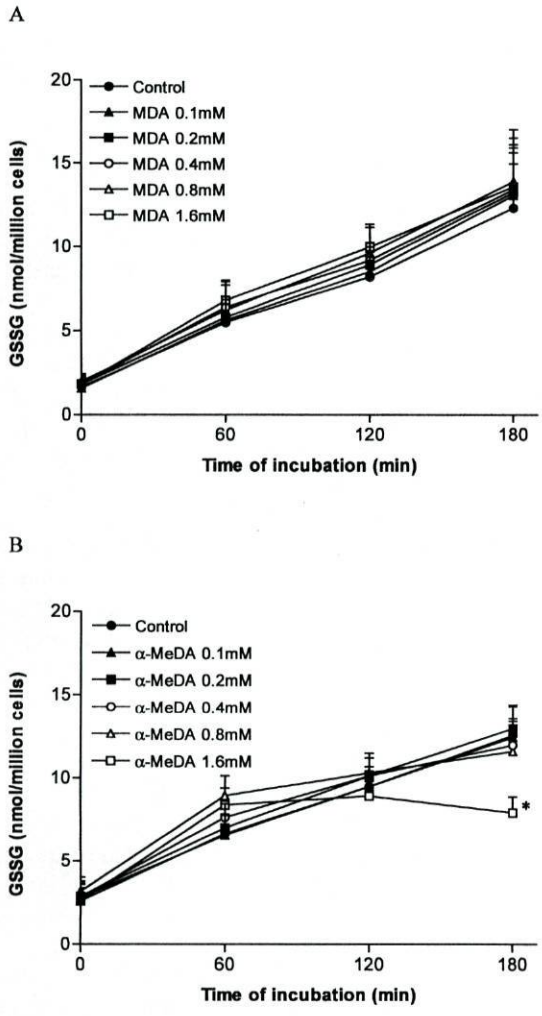

Fig. 3A,B Effect of MDA (**A**) and α-MeDA (**B**) on glutathione disulfide (GSSG) levels in hepatocyte suspensions. Data represent means ± SEM, $n = 5$–8; $^*P < 0.05$, compared with control

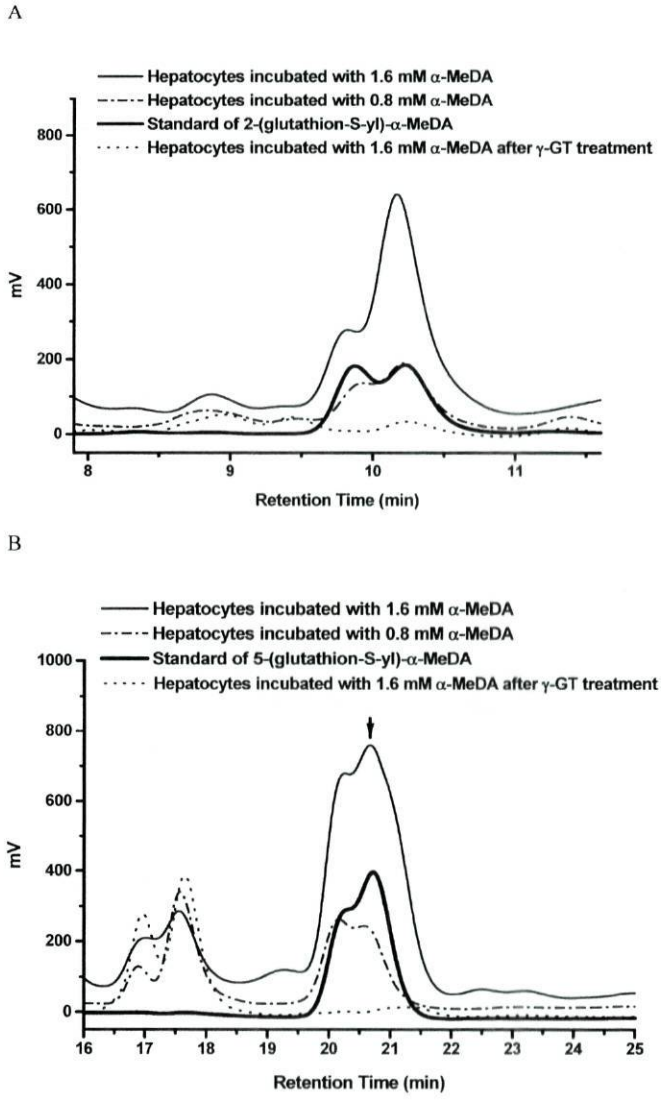

Fig. 4A,B Chromatograms from electrochemical detection HPLC showing the peaks corresponding to the 2-(glutathion-*S*-yl)-α-methyldopamine (**A**) and 5-(glutathion-*S*-yl)-α-methyldopamine (**B**) conjugates formed within cells incubated with 0.8 mM or 1.6 mM α-methyldopamine (α-MeDA) for 3 h, and their respective standards. Peaks obtained from cells incubated with 1.6 mM α-MeDA after treatment with γ-glutamyl transpeptidase (γ-GT) are also presented. Experimental details are stated in "Materials and methods"

(Fig. 4A,B). Although the purpose of the present work was not the quantification of these GSH conjugates, it was observed that 2-(glutathion-*S*-yl)-α-MeDA and 5-(glutathion-*S*-yl)-α-MeDA formation in cells incubated with α-MeDA correlated with decreases in the concentration of α-MeDA in the incubation medium (as shown in Fig. 4A,B by hepatocytes incubated with α-MeDA at a final concentration of 0.8 mM and 1.6 mM). A comparison of the UV spectra of the 5-(glutathion-*S*-yl)-α-MeDA conjugate present in the α-MeDa treated cells with that of the respective standard is shown in Fig. 5. The same UV pattern was also observed for 2-(glutathion-*S*-yl)-α-MeDA conjugate (data not shown). UV spectra of the GSH-conjugate peaks detected in samples exhibited three λ_{max}, at 236 nm, 256 nm and 292 nm, which are characteristic of *S*-glutathionyl conjugates of catecholamines (Spencer et al. 1998).

Finally, the enzymatic activities of GR, GST, and GPX were also evaluated. No significant differences in GR, GPX and GST activities were observed after incubation of hepatocyte suspensions with 0.1–1.6 mM MDA (data not shown). In contrast, the activity of each of these enzymes was significantly lower in samples incubated with 1.6 mM α-MeDA (3 h) than in control samples (Fig. 6). GPX was the most susceptible to inhibition, decreasing to 32% of initial activity, whereas GR and GST activities decreased to only 62% and 55% of initial activity, respectively.

Discussion

MDA is a hepatic-derived metabolite of MDMA (Lim and Foltz 1988). Metabolic activation to a reactive

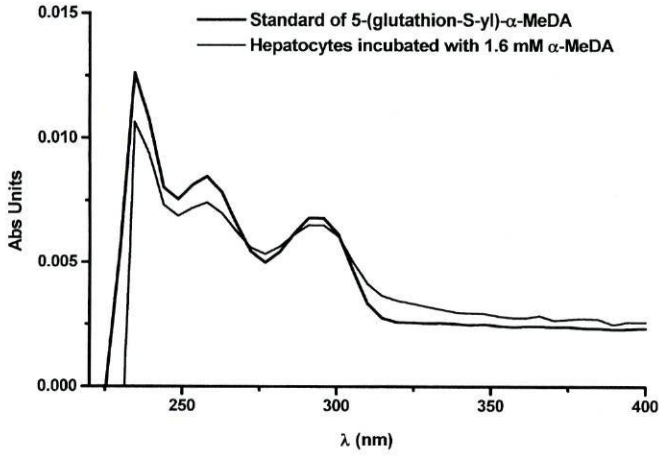

Fig. 5 Comparative UV spectra of the 5-(glutathion-*S*-yl)-α-MeDA conjugate present in hepatocyte suspensions incubated with α-methyldopamine (α-MeDA) and the respective standard

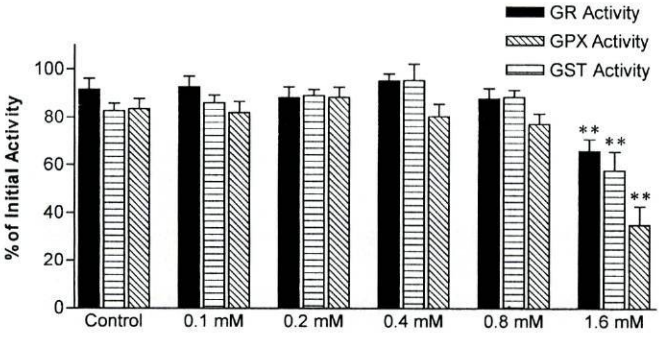

Fig. 6 Percentage of GSSG reductase (GR), GSH peroxidase (GPX) and GSH *S*-transferase (GST) activities in hepatocyte suspensions after 3 h of incubation with α-MeDA, relative to initial activities. Data represent means ±SEM, $n = 7–8$; $^{**}P < 0.01$, compared with control

metabolite capable of conjugating with GSH has been shown for MDMA and MDA (Hiramatsu et al. 1990). MDMA is *N*-demethylated to MDA, and MDA is demethylenated to α-MeDA by cytochromes P450 2D, 2B and 3A1 (Bai et al. 1999; Kreth et al. 2000). α-MeDA undergoes spontaneous oxidation to the corresponding *ortho*-quinone, which is a highly reactive molecule that can redox cycle with its semiquinone radical, leading to the generation of ROS or reactive nitrogen species (see Fig. 7) (Bolton et al. 2000).

Alternatively, the *ortho*-quinone formed by oxidation of α-MeDA is readily conjugated with GSH to form 2-(glutathion-*S*-yl)-α-MeDA and/or 5-(glutathion-*S*-yl)-α-MeDA, which themselves may be readily oxidized to *ortho*-quinones followed by the addition of a second molecule of GSH to form 2,5-*bis*(glutathion-*S*-yl)-α-MeDA (Miller et al. 1997). These thioether conjugates of α-MeDA not only preserve but also enhance the biological activity of the parent compounds. In fact, electrochemical studies indicate that the thioether conjugates of α-MeDA exhibit lower half-wave oxidation potentials than α-MeDA, and thus are potentially more reactive (Bai et al. 1999).

In the present study, a time- and concentration-dependent depletion of GSH was found to occur in rat hepatocytes following exposure to MDA or α-MeDA. The GSH depletion was clearly more marked for the catechol metabolite at the highest concentration studied. The fact that GSH depletion obtained with the lowest concentrations of MDA and α-MeDA was similar indicates that, probably, the effect of MDA is due to its conversion into α-MeDA. In fact, in the present study the metabolism of MDA was observed to occur in hepatocytes since the catechol metabolite α-MeDA and the conjugates of α-MeDA with GSH were detected within cells incubated with MDA. The resulting depletion of GSH has already been reported after MDMA exposure of isolated rat (Beitia et al. 1999) and mouse (Carvalho et al. 2001) hepatocytes. As an endogenous antioxidant, GSH is known to play a crucial protective role against cellular injury, which is due to its oxidant neutralizing, lipid peroxidase and/or tocopheryl-radical regenerating activities (Di Mascio et al. 1991). Thus, GSH depletion may render the cells more exposed to the effects of reactive compounds, ROS and reactive nitrogen species being formed within the cells, leading to deleterious effects in hepatocytes.

Despite changes in GSH homeostasis, incubation of freshly isolated rat hepatocytes with MDA did not result in any modification of cell viability or lipid redox status, suggesting that the lower intracellular GSH concentrations are sufficient to protect hepatocytes against oxidative damage. However, after the marked GSH depletion observed in hepatocyte suspensions incubated with the highest concentration of α-MeDA, concentrations of GSH are insufficient to prevent cell death (Fig. 1). These results are in agreement with previous reports (cited in Reed 1990), which showed that cytotoxicity as measured by lipid peroxidation, cell necrosis, and loss of intracellular enzymes in vivo and in vitro occurs only if the intracellular concentrations of GSH fall below 10–15% of the initial value. It must also be stressed that anorexia, hypoxia, and hyperthermia are well-known physiological conditions induced by MDMA in vivo that may strongly contribute to cell death when GSH is no longer available for protection.

2-(Glutathion-*S*-yl)-α-MeDA and 5-(glutathion-*S*-yl)-α-MeDA, were identified and characterized in freshly isolated rat hepatocytes after incubation with MDA or α-MeDA (Fig. 4). The intracellular formation of GSH conjugates helps to explain the observed decrease in GSH levels without the corresponding enhancement in GSSG levels.

The ability of polyphenolic thioether conjugates to undergo redox cycling and produce ROS provides a rationale for the potential role of these metabolites in MDA and MDMA hepatotoxicity. *N*-Methyl-α-MeDA, a metabolite of MDMA, and α-MeDA, a metabolite of MDA and MDMA, have been implicated in the neurotoxicity of the respective parent amphetamines following their biotransformation into the corresponding thioether conjugates (Miller et al. 1996, 1997; Bai et al.

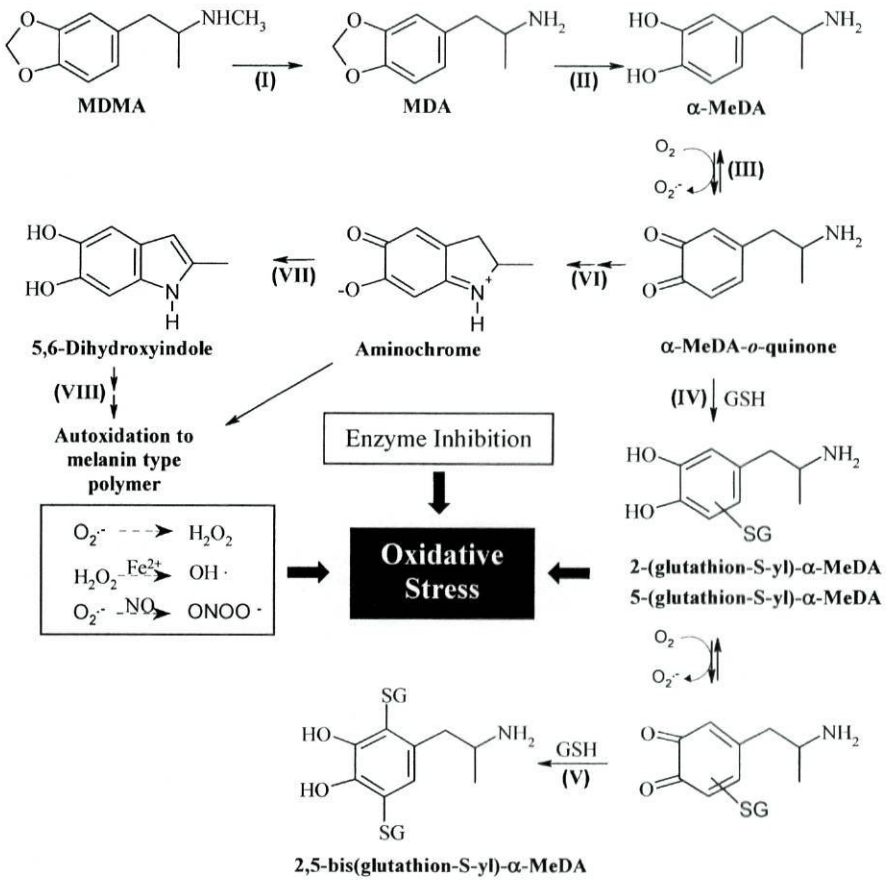

Fig. 7 Schematic presentation of possible metabolic pathway of 3,4-methylenedioxymethamphetamine (MDMA) and 3,4-methylenedioxyamphetamine (MDA) in liver. Microsomal *N*-demethylation of MDMA to MDA (*I*) and demethylenation of MDA to α-methyldopamine (α-MeDA) (*II*) followed by *ortho*-quinone formation (*III*) and glutathione conjugation (*IV*, *V*). On cyclization, the *ortho*-quinone of α-MeDA may give rise to the formation of an aminochrome (*VI*) and related compounds, such as 5,6-dihydroxyindoles (*VII*), which can undergo further oxidation and polymerization to form brown or black insoluble pigments of melanin type (*VIII*)

1999). In fact, when injected directly into brain, MDMA and MDA are not neurotoxic. In contrast, direct injection of 5-(glutathion-*S*-yl)-α-MeDA and 2,5-*bis*(glutathion-*S*-yl)-α-MeDA reproduces the toxicity observed following peripheral administration of MDA (Miller et al. 1996, 1997; Bai et al. 1999).

Consistent with known pathways of catecholamine oxidation, incubation of rat hepatocytes with α-MeDA resulted in the formation of orange-colored aminochromes. Furthermore, as the oxidation progressed, dark brown/black turbidity appeared in the medium, a consequence of melanin-type polymer formation (Bindoli et al. 1992; Zhang and Dryhurst 1994). It was already reported that oxidation of dopamine by tyrosinase gives rise to a black, insoluble polymer only when the concentrations of sulfhydryls such as GSH and cysteine are low relative to those of dopamine (Carstam et al. 1991; Zhang and Dryhurst 1994). Consistent with these reports, the formation of black pigments in the incubation medium of cells incubated with α-MeDA only occurs as a late-stage event, probably resulting from the depleted GSH concentrations (and of the antioxidant defense system) being unable to react with the *ortho*-quinones being formed within cells (with the result of further oxidation of quinones to melanin-type polymers). In fact, α-MeDA-*ortho*-quinone can be further oxidized in a process that involves an irreversible 1,4-intramolecular cyclization reaction, resulting in the formation of aminochromes (colored pigments) and related compounds, such as 5,6-dihydroxyindoles, which eventually leads to the appearance of brown or black insoluble polymers of the melanin type (see Fig. 7) (Bindoli et al. 1989, 1992). Importantly, the catecholamine autoxidation process can be accelerated under physiological conditions by oxidative enzymes, such as xanthine oxidase, peroxidase, lipoxygenase, several copper-containing catechol oxidases, or in presence of metal ions such as Cu^{2+}, Mn^{2+}, Fe^{3+}, and several Cu^{2+} and Fe^{3+} chelates (Bindoli et al. 1992).

Melanins represent a large group of chemically active and potentially toxic substances (Hegedus 2000). In the presence of Fe^{3+}, synthetic melanin can catalyze a Fenton-type reaction, which generates the hydroxyl radical and initiates lipid peroxidation (Ben-Shachar et al. 1991). Thus, future work is therefore clearly required to investigate the toxicity exerted by these polymers in hepatocytes.

Ortho-quinones and aminochromes can interact with various nucleophiles in the cell; of particular importance are the reactions with thiol groups, which are present in cysteine, GSH and proteins. The ability of 1.6 mM α-MeDA to inhibit GR, GPX, and GST activities may thus be related to either the oxidation or alkylation of sulfhydryl groups present within the enzymes' active site. *Ortho*-quinones and aminochromes can inhibit enzymes that possess either a GSH-binding site and/or cysteine residues that are critical for enzyme function (Ommen et al. 1991; Bindoli et al. 1992). Several quinones are

known to cause irreversible inhibition of GST (Ommen et al. 1991; Monks and Lau 1992). The GSTs catalyze the nucleophilic attack of GSH on electrophilic substrates, thereby protecting various cell components from potentially damaging reactive electrophiles (Mannervik and Danielson 1988; Armstrong 1991; van Bladeren 2000). Most GST isoenzymes possess a nucleophilic amino acid, which is rapidily modified by quinones, a reaction that inactivates the enzyme (Ploemen et al. 1991), and the 5-(*S*-glutathionyl) conjugates of dopamine and α-methyldopa inhibit human GSTs (Ploemen et al. 1994). Interestingly, GSH conjugates of several quinones also react rapidly with GST (thereby inactivating the enzyme). Therefore, the presence of a GSH moiety may serve to target the quinone to the enzyme (Ommen et al. 1991). The activity of GR, which catalyzes the NADPH-dependent reduction of GSSG to GSH, is crucial to maintain a high cellular GSH/GSSG ratio. Inhibition of GR and GST by quinones, as well as GR, GPX and GST by aminochromes, has been reported (Remião et al. 1999, 2002).

Taken together, it seems likely that *ortho*-quinones, aminochromes and ROS generated during catecholamine oxidation reactions may all participate in α-MeDA-induced enzyme inhibition. Inhibition of these enzymes can increase the oxidative stress resulting from α-MeDA oxidation.

The toxicity of MDA and α-MeDA in freshly isolated rat hepatocytes has not been previously reported. The present results indicate that oxidative stress may play a part in the first step of MDMA-induced liver damage. The loss of GSH and the modification of enzyme activities by oxidized α-MeDA clearly shows that one of the early consequences of MDMA and MDA metabolism is a disruption of thiol homeostasis, which may result in loss of protein function and initiation of a cascade of events leading to cellular damage. GSH in conjunction with GPX/GR is responsible for the elimination of cellular hydrogen peroxide (H_2O_2) and organic peroxides. Thus, depletion of GSH and/or decreased activity of these enzymes may compromise this pathway, thereby allowing H_2O_2 to accumulate to toxic levels. It must be stressed that hepatic mitochondria are especially vulnerable to this effect since they lack the H_2O_2 metabolizing enzyme catalase (DeLeve and Kaplowitz 1991). Alternatively, the loss of GSH may lead to alterations in normal cellular metabolism and lead to the increased accumulation of ROS.

In conclusion, present findings show that MDA and α-MeDA induce toxicity in freshly isolated rat hepatocytes. The toxic effects are characterized by a loss of GSH homeostasis due to conjugation of GSH with α-MeDA, decreases in the antioxidant enzyme activities, and cell death. Thus, it can be postulated that the metabolism of MDMA and MDA, resulting in the formation of the highly reactive compounds *N*-Me-α-MeDA and α-MeDA, and α-MeDA, respectively, is one of the main causes of their hepatotoxic effects.

Acknowledgements This work was supported by PhD grants from Fundação para a Ciência e Tecnologia (Praxis XXI/BD/20087/99 and Praxis XXI/BD/18520/98) and Programa Operacional Ciência, Tecnologia e Inovação (POCTI), Portugal, in co-participation with Fonds Européen de Développement Régional (FEDER) (project POCTI/36099/FCB/2000). The experiments are declared to comply with the current laws of Portugal.

References

Anderson ME (1985) Determination of glutathione and glutathione disulfide in biological samples. Methods Enzymol 113:548–555

Armstrong RN (1991) Glutathione *S*-transferases: reaction mechanism, structure, and function. Chem Res Toxicol 4:131–140

Bai F, Lau SS, Monks TJ (1999) Glutathione and *N*-acetylcysteine conjugates of α-methyldopamine produce serotoninergic neurotoxicity: possible role in methylenedioxyamphetamine-mediated neurotoxicity. Chem Res Toxicol 12:1150–1157

Bai F, Jones DC, Lau SS, Monks TJ (2001) Serotonergic neurotoxicity of 3,4-(±)-methylenedioxyamphetamine and 3,4-(±)-methylenedioxymethamphetamine (Ecstasy) is potentiated by inhibition of γ-glutamyl transpeptidase. Chem Res Toxicol 14:863–870

Battaglia G, Yeh SY, O'Hearn E, Molliver ME, Kuhar MJ, Sousa EBD (1987) 3,4-Methylenedioxymethamphetamine and 3,4-methylenedioxyamphetamine destroy serotonin terminals in rat brain: quantification of neurodegeneration by measurement of [^{3}H]paroxetine-labeled serotonin uptake sites. J Pharmacol Exp Ther 242:911–916

Beitia G, Cobreros A, Sainz L, Cenarruzabeitia E (1999) 3,4-Methylenedioxymethamphetamine (ecstasy)-induced hepatotoxicity: effect on cytosolic calcium signals in isolated hepatocytes. Liver 19:234–241

Ben-Shachar D, Riederer P, Youdim MB (1991) Iron-melanin interaction and lipid peroxidation: implications for Parkinson's disease. J Neurochem 57:1609–1614

Bindoli A, Rigobello MP, Galzigna L (1989) Toxicity of aminochromes. Toxicol Lett 48:3–20

Bindoli A, Rigobello MP, Deeble DJ (1992) Biochemical and toxicological properties of the oxidation products of catecholamines. Free Radic Biol Med 13:391–405

Bolton JL, Trush MA, Penning TM, Dryhurst G, Monks TJ (2000) Role of quinones in toxicology. Chem Res Toxicol 13:135–160

Carstam R, Brinck C, Hindemith-Augustsson A, Rorsman H, Rosengren E (1991) The neuromelanin of the human substancia nigra. Biochim Biophys Acta 1097:152–160

Carvalho F, Remião F, Soares ME, Catarino R, Queiroz G, Bastos ML (1997) d-Amphetamine-induced hepatotoxicity: possible contribution of catecholamines and hyperthermia to the effect studied in isolated rat hepatocytes. Arch Toxicol 71:429–436

Carvalho M, Carvalho F, Bastos ML (2001) Is hyperthermia the triggering factor for hepatotoxicity induced by 3,4-methylenedioxymethamphetamine (ecstasy)? An in vitro study using freshly isolated mouse hepatocytes. Arch Toxicol 74:789–793

Carvalho M, Carvalho F, Remião F, Pereira MdL, Pires-das-Neves R, Bastos MdL (2002a) Effect of 3,4-methylenedioxymethamphetamine ("ecstasy") on body temperature and liver antioxidant status in mice: influence of ambient temperature. Arch Toxicol 76:166–172

Carvalho M, Hawksworth G, Milhazes N, Borges F, Monks T, Fernandes E, Carvalho F, Bastos ML (2002b) Role of metabolites in MDMA (ecstasy)-induced nephrotoxicity: an in vitro study using rat and human renal proximal tubular cells. Arch Toxicol 76:581–588

Cho AK, Hiramatsu M, Distefano EW, Chang AS, Jenden DJ (1990) Stereochemical differences in the metabolism of 3,4-methylenedioxymethamphetamine in vivo and in vitro: a pharmacokinetic analysis. Drug Metab Dispos 18:686–691

DeLeve LD, Kaplowitz N (1991) Glutathione metabolism and its role in hepatotoxicity. Pharmacol Ther 52:287–305

Di Mascio P, Murphy ME, Sies H (1991) Antioxidant defense systems: the role of carotenoids, tocopherols, and thiols. Am J Clin Nutr 53:194S–200S

Dykhuizen RS, Brunt PW, Atkinson P, Simpson JG, Smith CC (1995) Ecstasy induced hepatitis mimicking viral hepatitis. Gut 36:939–941

Ellis A, Wendon J, Portmann B, Williams R (1996) Acute liver damage and ecstasy ingestion. Gut 38:454–458

Fineschi V, Centini F, Mazzeo E, Turillazzi E (1999) Adam (MDMA) and Eve (MDA) misuse: an immunohistochemical study on three fatal cases. Forensic Sci Int 104:65–74

Hegadoren KM, Baker GB, Bourin M (1999) 3,4-Methylenedioxy analogues of amphetamine: defining the risks to humans. Neurosci Biobehav Rev 23:539–553

Hegedus ZL (2000) The probable involvement of soluble and deposited melanins, their intermediates and the reactive oxygen side-products in human diseases and aging. Toxicology 145:85–101

Henry JA, Jeffreys KJ, Dawling S (1992) Toxicity and deaths from 3,4-methylenedioxymethamphetamine ("ecstasy"). Lancet 340:384–387

Hiramatsu M, Kumagai Y, Unger SE, Cho AK (1990) Metabolism of methylenedioxymethamphetamine: formation of dihydroxymethamphetamine and a quinone identified as its glutathione adduct. J Pharmacol Exp Ther 254:521–527

Khakoo S, Coles C, Armstrong J, Barry R (1995) Hepatotoxicity and accelerated fibrosis following 3,4-methylenedioxymethamphetamine ("ecstasy") usage. J Clin Gastroenterol 20:244–247

Kreth K-P, Kovar K-A, Schwab M, Zanger UM (2000) Identification of the human cytochromes P450 involved in the oxidative metabolism of "ecstasy"-related designer drugs. Biochem Pharmacol 59:1563–1571

Kumagai Y, Lin LY, Schmitz DA, Cho AK (1991) Hydroxyl radical mediated demethylenation of (methylenedioxy)phenyl compounds. Chem Res Toxicol 4:330–334

Lim HK, Foltz RL (1988) In vivo and in vitro metabolism of 3,4-(methylenedioxy)methamphetamine in the rat: identification of metabolites using an ion trap detector. Chem Res Toxicol 1:370–378

Mannervik B, Danielson UH (1988) Glutathione transferases-structure and catalytic activity. CRC Crit Rev Biochem 23:283–337

Marquardt GM, DiStefano V, Ling LL (1978) Metabolism of β-3,4-methylenedioxyamphetamine in the rat. Biochem Pharmacol 27:1503–1505

Miller RT, Lau SS, Monks TJ (1995) Metabolism of 5-(glutathion-*S*-yl)-α-methyldopamine following intracerebroventricular administration to male Sprague-Dawley rats. Chem Res Toxicol 8:634–641

Miller RT, Lau SS, Monks TJ (1996) Effects of intracerebroventricular administration of 5-(glutathion-*S*-yl)-α-methyldopamine on brain dopamine, serotonin, and norepinephrine concentrations in male Sprague-Dawley rats. Chem Res Toxicol 9:457–465

Miller RT, Lau SS, Monks TJ (1997) 2,5-*bis*-(glutathion-*S*-yl)-α-methyldopamine, a putative metabolite of (±)-3,4-methylenedioxyamphetamine, decreases brain serotonin concentrations. Eur J Pharmacol 323:173–180

Milroy CM, Clark JC, Forrest ARW (1996) Pathology of deaths associated with "ecstasy" and "eve" misuse. J Clin Pathol 49:149–153

Moldéus P, Hogberg J, Orrenius S (1978) Isolation and use of liver cells. Methods Enzymol 52:60–71

Monks TJ, Lau SS (1992) Toxicology of quinone-thioethers. Crit Rev Toxicol 22:243–270

Ommen BV, Ploemen JHTM, Bogaards JJP, Monks TJ, Lau SS, Bladeren PJV (1991) Irreversible inhibition of rat glutathione *S*-transferase 1-1 by quinones and their glutathione conjugates. Structure–activity relationship and mechanism. Biochem J 276:661–666

Ploemen JH, Ommen BV, Bladeren PJV (1991) Irreversible inhibition of human glutathione *S*-transferase isoenzymes by tetrachloro-1,4-benzoquinone and its glutathione conjugate. Biochem Pharmacol 41:1665–1669

Ploemen JH, Ommen BV, Haan AD, Venekamp JV, Bladeren PJV (1994) Inhibition of human glutathione *S*-transferases by dopamine, α-methyldopa and their 5-*S*-glutathionyl conjugates. Chem Biol Interact 90:87–99

Reed DJ (1990) Glutathione: toxicological implications. Annu Rev Toxicol 30:603–631

Remião F, Carmo H, Carvalho FD, Bastos ML (1999) Inhibition of glutathione reductase by isoproterenol oxidation products. J Enzyme Inhib 15:47–61

Remião F, Carvalho M, Carmo H, Carvalho FD, Bastos ML (2002) Cu^{2+}-induced isoproterenol oxidation into isoprenochrome in adult rat calcium-tolerant cardiomyocytes. Chem Res Toxicol 15:861–869

Ricaurte GA, Yuan J, McCann UD (2000) (±)3,4-Methylenedioxymethamphetamine ("ecstasy")-induced serotonin neurotoxicity: studies in animals. Neuropsychobiology 42:5–10

Simpson DL, Rumack BH (1981) Methylenedioxyamphetamine. Clinical description of overdose, death, and review of pharmacology. Arch Intern Med 141:1507–1509

Spencer JP, Jenner P, Daniel SE, Lees AJ, Marsden DC, Halliwell B (1998) Conjugates of catecholamines with cysteine and GSH in Parkinson's disease: possible mechanisms of formation involving reactive oxygen species. J Neurochem 71:2112–2122

van Bladeren PJ (2000) Glutathione conjugation as a bioactivation reaction. Chem Biol Interact 129:61–76

Varela-Rey M, Montiel-Duarte C, Beitia G, Cenarruzabeitia E, Iraburu MJ (1999) 3,4-Methylenedioxymethamphetamine ("ecstasy") stimulates the expression of α1 (I) procollagen mRNA in hepatic stellate cells. Biochem Biophys Res Commun 259:678–682

Walubo A, Seger D (1999) Fatal multi-organ failure after suicidal overdose with MDMA, "ecstasy": case report and review of the literature. Hum Exp Toxicol 18:119–125

Zhang F, Dryhurst G (1994) Effects of L-cysteine on the oxidation chemistry of dopamine: new reaction pathways of potential relevance to idiopathic Parkinson's disease. J Med Chem 37:1084–1098

FACULDADE DE FARMÁCIA DO PORTO BIBLIOTECA

Obtenção e análise de metabolitos e intermediários de síntese
Nuno Jorge da Silva Pereira Milhazes
F.S.596 | Ano: 2006 | 25 Exemplares (1ª Edição) | Produção Gráfica: AJNet | www.ajnet.net

OBTENÇÃO E ANÁLISE DE METABOLITOS E INTERMEDIÁRIOS DE SÍNTESE.

ESTUDOS DE CORRELAÇÃO ENTRE ESTRUTURA, PROPRIEDADES FÍSICO-QUÍMICAS E ACTIVIDADE BIOLÓGICA.

Nuno Jorge da Silva Pereira Milhazes

Abril 2007

ERRATA:

Página	*Localização*	*Onde se lê*	*Deve ler-se*
5	linha 3	relevant physico-chemical and structural	relevant physicochemical and structural
24	linha 16	MDMA, e dos seus intermediários	MDMA, e seus intermediários
24	linha 22	3,4-metilenedioximetanfetamina	3,4-metilenodioximetanfetamina
25	figura 2	entactogénios	estimulantes
25	figura 2	estimulantes	entactogénios
27	linha 10	3,4-metilenedioximetanfetamina	3,4-metilenodioximetanfetamina
31	legenda	3,4-metilenedioximetanfetamina	3,4-metilenodioximetanfetamina
49	legenda	mistura de diastereoisómeros obtida	mistura dos diastereoisómeros *trans* obtida
55	linha 21	com desvio negativos relativamente	com desvios positivos relativamente
76	linha 24	redução aos compostos	redução dos compostos
80	linha 13	glândula suprarrenal de ratinho	glândula supra-renal de ratinho